

Advancing Cell-Free Synthetic Biology: From sustained PURE protein synthesis to an isothermal one-pot DNA replication system

Présentée le 21 juin 2024

Faculté des sciences et techniques de l'ingénieur
Laboratoire de caractérisation du réseau biologique
Programme doctoral en biotechnologie et génie biologique

pour l'obtention du grade de Docteur ès Sciences

par

Laura Sophie GRASEMANN

Acceptée sur proposition du jury

Prof. A. Radenovic, présidente du jury
Prof. S. Maerkl, directeur de thèse
Prof. F. Simmel, rapporteur
Prof. H. Mutschler, rapporteur
Prof. C. Merten, rapporteur

Acknowledgements

First of all, I would like to thank my PhD advisor Sebastian Maerkl for giving me the opportunity to do my PhD in his lab, and for giving me the chance to grow and learn during these five years, not only as a scientist, but also as a person.

Thanks to the members of my thesis committee Christoph Merten, Friedrich Simmel, and Hannes Mutschler for evaluating my PhD work and for the open and encouraging discussion during my PhD defense. A big thanks to my jury president Aleksandra Radenovic, not only for being a great president, but also for the support and for making sure that I am doing well throughout my PhD.

Thanks a lot to my mentor Bart Deplancke and to Bruno Correia, who were always supportive, thereby ensuring that I finished this PhD. I would probably never have embarked on this PhD journey in Lausanne without the recommendation of my Master's thesis' supervisor Petra Schwille. Thanks for encouraging me to get out of my comfort zone and move to this amazing place. I am forever grateful for having had Beatrice Ramm as the best Master's thesis supervisor I can imagine.

The first line of defense against all struggles that arise during a PhD are colleagues and lab members, and I am hugely grateful for all my current and past colleagues at LBNC. I truly appreciate Sebastian's intuition in assembling a diverse and interesting group that goes together so well. I would particularly like to thank Barbora for "adopting" me from the day I joined LBNC, for teaching me, and for becoming a great friend.

I'll forever be grateful for the time I spent sharing the office with amazing colleagues. First Barbora and Fabien: Thanks for all the good laughs, inappropriate jokes, but also for the cheering up when I needed it. I would like to thank Ming, one of the most big-hearted people I have ever met, and Maria and Amogh, who were always there for me, supported me during rough times while simultaneously ensuring that accomplishments were celebrated. Thanks to Julia and Fatemeh, who have become not only great collaborators, but also amazing friends. Thanks to Laura for always being supportive and a great friend, and for embarking on a project with me during probably the toughest time of my PhD. I will forever be grateful for that! Thanks to Fanjun for always being in a good mood and being refreshingly honest, and thanks to Pao-Wan, who I appreciate as much as a person as for his exceptional coffee-making skills. Thanks also to all the current and past LBNC members including Ludovica, Ragu, Zoe, Evan,

Greg, Ivan, Josh, Shiyu, Nadanai, Michael (even though we technically had no actual overlap in the lab), Simone, Moustafa, Daniel, Julian, Nicolas, Alefiya, Mathis, Simon and Lara. Each and every one of you contributed to the success of this thesis. You made PhD life a lot more enjoyable, and I love looking back at all the moments we shared. I would also like to thank my amazing interns Caro, Paula, and Maria Andrea. It was a pleasure to work with you. Thanks for your trust, your motivation, and dedication! Thanks to my collaborator Claudia. It was a pleasure to work with you, and despite circumstances not being in our favor, I think we were a great team and made the best of the situation. Last but not least, I d like to thank Martine for being the best administrative support I can imagine.

Thanks a lot also to the people of the other labs of the 2nd floor of the BM building from LBEN, LANES, CLSE, and people that stick around these labs for so often that you can basically count them as part of those. It was amazing going through this PhD journey with all of you.

The second line of defense are the friends outside of work that have an invaluable contribution towards surviving a PhD. First of all I would like to thank my amazing flatmates Rebekah and Austin with Maria, for being there in good and bad times. Thanks for all the amazing experiences we shared during my time in Lausanne. Thanks also to Pierre, for all the great adventures, for never dropping me off a mountain or a wall, and for being at least partially responsible for the 3 kg I gained during the past years, due to your exceptional cooking and baking skills.

Skiing has always been my big passion, and I am extremely lucky that I moved to a place so close to the mountains and found a lot of friends who share my passion for skiing. Thanks to my skiing friends for making these five years so exceptional. First of all, thanks to my probably oldest friend in Switzerland, Tereza, for sharing so many good and bad moments during the past (must be already close to 20???) years, especially during our common time in Switzerland. Thanks also to Sebastian with Kirsten, Mike, Theo A., Jana and Marine, who took me for the eight longest hours of my life: the Patrouille des Glaciers, Olivier, Coco, and all the others that took me out skiing. A special thanks goes to the coaches I had the chance to work with during my competitive career, especially Harald, who probably knows me best, Frieder, who fuelled my passion not only for skiing but also for science, and Klaus, who is the main reason why skiing became such an important part of my life. Even though I stopped competing, skiing is still a passion, and a good day of skiing can make up for so many bad days in other parts of life. After my retirement from competitive skiing, I found a passion for biking and I would like to acknowledge my biking friends who were always patiently waiting for me, especially Bram and Jimmy.

Climbing and bouldering has been another important activity during the years in Lausanne, and I would like to say thanks to my climbing friends including Fabien, Evan, Amogh, Sebastian, Jana, Laura R., Theo E., Federico with Annie, and of course Rebekah, Austin, Maria, and Pierre.

Thanks also to all the yoga people and especially my favorite yoga teacher Barbora!

Lausanne is such a great place not only due to the surrounding mountains, but also for the lake, and I am extremely grateful that I found a fantastic windsurfing and sailing crew here. A big thanks to the windsurfers and sailors, and the team from the Centre Nautique, especially to

Franck. I can confirm, a good day (or lunchbreak) of windsurfing has nearly the same positive effect on mental health as skiing!

The third line of defense against struggles of a PhD is a solid background of old friends and family. Here, I would like to acknowledge my friends from studies from Munich, especially Anna, Nils, Regina, Magdalena, Jacqueline, Frank, Vivien, and Nikolas. Without you, I would have never been able to even start this PhD, since I wouldn't have stood a chance to finish my Bachelor's and Master's degree. I am extremely grateful that we are still friends despite the geographical distance between us.

A big thanks to my two oldest friends Kira and Julia, and their families. Even when we do not hear from each other in a long time, I know that when we meet, it is always like as if we never spent time apart, and that I can always rely on you, no matter what happens. I love Switzerland, but I miss you.

Thanks to my family, my aunt, uncle, cousins, brothers and sister. You can't choose your family, but if I could, I would choose exactly my family!

A special thanks goes to my parents and my brother Tim, for your unconditional support and love. It is great to know that no matter what comes up, I will always have your back.

Last but not least, I would like to thank Edgar. Thanks for enduring my mental breakdowns and for helping me find solutions to my problems. Thanks for all the adventures we have experienced together, and for always giving me the feeling that I can rely on you.

I

Lausanne, April 2024

Laura Grasemann

¹Parts of this thesis were corrected for grammar and spelling mistakes with the help of ChatGPT and Google Bard/Gemini.

Abstract

One of the goals of synthetic biology is the development of an artificial cell. Building an artificial cell from scratch will provide a deeper understanding of fundamental mechanisms and models in biology and promises to contribute towards building novel platforms that can be leveraged to drive bioengineering innovation. There is ongoing debate on what a synthetic cell looks like in detail; here we define an artificial cell as a system that is able to self-replicate and evolve. Self-replication entails the capability of renewing all of the components of the cellular machinery and replicating its genetic blueprint. If errors in the copying of the genetic blueprint can occur and are propagated, the system is in principle able to undergo Darwinian evolution [1]. One scheme for realizing such an artificial cell is based on transcription-translation (TX-TL). In turn, the most widely-used practical implementation of the TX-TL machinery is the well-defined PURE cell-free system [2], in which case the genetic blueprint is stored in the form of DNA.

Cell-free systems do not only offer a possible foundation for a future synthetic cell, but also provide a powerful platform for innovation in the area of bioengineering. This thesis first reviews and compares existing cell-free platforms, while highlighting opportunities for applications to address a multitude of scientific questions.

Chapter 3 introduces a protocol for setting up a OnePot PURE system that is cost-effective and can be prepared within one week. The OnePot PURE system thereby addresses a key shortcoming of the conventional PURE system: its high cost currently impedes its widespread adoption. Our approach streamlines the process of protein purification of all 36 non-ribosomal proteins to one purification step, thereby saving time and costs.

Chapter 4 details the development of a microfluidic chemostat, augmented with semi-permeable membranes, which addresses a second limitation of the PURE system: its capacity for protein synthesis is at least 25x too low to regenerate all of its components [3]. Implementing dialysis on our chemostat resulted in significantly extended protein synthesis, leading to a 6-fold increase in protein levels at steady-state.

Chapter 5 describes C2CAplus, a one-pot isothermal Circle-to-Circle DNA amplification (C2CA) system. Rolling circle amplification (RCA) is a DNA amplification method that has found widespread usage in biosensing applications and is considered the most promising approach towards developing a DNA replication system for a synthetic cell. However, standard

RCA generates linear, multimeric product from *circular* input DNA, which is not ideal for the construction of an artificial cell. C2CAplus implements a recircularization method employing restriction digest and ligation. The method is highly sensitive and efficient, and the amplified DNA product can be seen with the naked eye, suggesting that C2CAplus also holds promise for use as a biosensor.

Across these chapters, this thesis explores fundamental research into the development of an artificial cell, contributing towards the greater goals of a self-regenerating PURE cell-free system and establishing a robust DNA replication system that can be integrated into a future synthetic cell. Furthermore, it explores opportunities for concrete and timely applications of the systems, which were initially devised for the development of an artificial cell.

Key words: cell-free synthetic biology, self-replication, microfluidics, DNA replication, synthetic cell

Zusammenfassung

Eines der Ziele der synthetischen Biologie ist die Entwicklung einer künstlichen Zelle. Der Bau einer künstlichen Zelle von Grund auf wird ein tieferes Verständnis grundlegender Mechanismen und Modelle in der Biologie ermöglichen und verspricht, zum Aufbau neuartiger Plattformen beizutragen, die Innovationen im Bereich des Bioengineerings vorantreiben können. Es gibt eine anhaltende Debatte darüber, wie eine künstliche Zelle im Detail aussieht; hier definieren wir eine künstliche Zelle als ein System, das die Fähigkeit besitzt, sich selbst zu replizieren und sich zu entwickeln. Selbstreplikation umfasst die Fähigkeit, alle Komponenten der zellulären Maschinerie zu erneuern und ihren genetischen Bauplan zu replizieren. Wenn beim Kopieren des genetischen Bauplans Fehler auftreten können und weitergegeben werden, kann das System prinzipiell Darwinistischer Evolution unterliegen [1].

Ein Schema zur Realisierung einer solchen künstlichen Zelle basiert auf Transkription und Translation (TX-TL). Die am weitesten verbreitete praktische Implementierung der TX-TL-Maschinerie ist wiederum das wohldefinierte zellfreie PURE-System [2], bei dem der genetische Bauplan in Form von DNA gespeichert wird.

Zellfreie Systeme bieten nicht nur eine mögliche Grundlage für eine zukünftige künstliche Zelle, sondern stellen auch eine leistungsstarke Plattform für Innovationen im Bereich des Bioengineerings dar. Diese Arbeit befasst sich zunächst mit der Zusammenfassung und dem Vergleich existierender zellfreier Systeme und hebt dabei die Möglichkeiten der Anwendung zur Beantwortung einer Vielzahl wissenschaftlicher Fragen hervor.

Kapitel 3 stellt ein Protokoll zur Erstellung eines kostengünstigen OnePot-PURE-Systems vor, das innerhalb einer Woche hergestellt werden kann. Das OnePot-PURE-System adressiert damit ein wesentliches Defizit des herkömmlichen PURE-Systems: seine hohen Kosten hindern derzeit eine breite Anwendung. Unser Ansatz rationalisiert den Prozess der Proteinaufreinigung aller 36 nicht-ribosomalen Proteine auf einen Reinigungsschritt, wodurch Zeit und Kosten gespart werden.

Kapitel 4 beschreibt die Entwicklung eines mit semi-permeablen Membranen ausgestatteten mikrofluidischen Chemostats, der eine zweite Einschränkung des PURE-Systems behebt: Die Kapazität des PURE Systems bezüglich der Proteinsynthese ist mindestens 25-fach zu gering, um all seine Komponenten zu regenerieren [3]. Die Implementierung der Dialyse in unserem Chemostat führte zu einer deutlich verlängerten Proteinsynthese, was zu einer

6-fachen Erhöhung des Proteinlevels im stationären Zustand führte.

Stichwörter: Zell-freie synthetische Biologie, Selbstreplikation, Mikrofluidik, DNA Replikation, Synthetische Zelle

Résumé

Un des objectifs de la biologie synthétique est le développement d'une cellule artificielle. Construire une cellule artificielle en partant de zéro permettra une compréhension plus approfondie des mécanismes et modèles fondamentaux en biologie et promet de contribuer à la construction de nouvelles plateformes pouvant être exploitées pour encourager l'innovation en bio-ingénierie. Il existe un débat continu sur ce qui constitue d'une cellule synthétique; ici, nous définissons une cellule artificielle comme un système capable de s'auto-répliquer et d'évoluer. L'autoréplication implique la capacité de renouveler tous les composants de la machinerie cellulaire et de répliquer son code génétique. Si des erreurs dans la copie du code génétique peuvent se produire et se propager, le système est en principe capable de suivre une évolution darwinienne [1].

La technologie pour réaliser une telle cellule artificielle est basé sur la transcription et traduction (TX-TL). Dans ce contexte, la mise en œuvre pratique la plus largement utilisée de la machinerie TX-TL est le système acellulaire PURE bien défini [2], dans lequel le plan génétique est stocké sous forme d'ADN.

Les systèmes acellulaires n'offrent pas seulement une base possible pour une future cellule synthétique, mais fournissent également une plateforme puissante pour l'innovation dans le domaine de la bio-ingénierie. Cette thèse examine et compare d'abord les plateformes acellulaires existantes, tout en soulignant les opportunités d'applications pour répondre à une multitude de questions scientifiques.

Le chapitre 3 introduit un protocole pour mettre en place un système PURE OnePot qui est rentable et peut être préparé en une semaine. Le système PURE OnePot remédie ainsi à une lacune importante du système PURE conventionnel : son coût élevé entrave actuellement son adoption généralisée. Notre approche rationalise le processus de purification de toutes les 36 protéines non ribosomiques en une seule étape de purification, économisant ainsi du temps et de l'argent.

Le chapitre 4 détaille le développement d'un chémostat microfluidique, augmenté avec des membranes semi-perméables, qui répond à une deuxième limitation du système PURE : sa capacité de synthèse de protéines est au moins 25 fois trop faible pour régénérer tous ses composants [3]. La mise en œuvre de la dialyse sur notre chémostat a entraîné une synthèse protéique significativement prolongée, conduisant à une augmentation d'un facteur 6 des

niveaux de protéines à l'état d'équilibre.

Mots clefs : biologie synthétique acellulaire, autoréplication, microfluidique, réplcation d'ADN, cellule synthétique

Contents

Acknowledgements	i
Abstract (English/Français/Deutsch)	v
List of figures	xv
List of tables	xvii
1 Introduction	1
1.1 Towards a synthetic cell	1
1.2 Self-regeneration	3
1.2.1 Self-regeneration of the transcription-translation machinery	3
1.2.2 DNA replication	5
1.2.3 Microfluidics for building a synthetic cell	7
1.3 Overview and objective of this work	8
2 Bottom-Up Construction of Complex Biomolecular Systems With Cell-Free Synthetic Biology	11
2.1 Abstract	12
2.2 Introduction	12
2.3 Deconstructing biology using cell-free systems	13
2.4 Technologies	14
2.4.1 Lysates and reconstituted cell-free systems	14
2.4.2 Microfluidic platforms	21
2.4.3 Compartmentalized cell-free reactions	25
2.5 Scientific opportunities	37
2.5.1 Gene expression regulation	37
2.5.2 Resource constraints as a design feature	38
2.5.3 <i>In vitro</i> DNA replication	40
2.6 Outlook	43
3 One Pot PURE system	45
3.1 Summary	46
3.2 Abstract	46
3.3 Introduction	46

3.4	Protocol	48
3.5	Representative results	62
3.6	Discussion	67
3.7	Supplementary Information	69
3.7.1	Supplementary tables	69
3.8	Annexe	79
4	Improved Cell-Free Transcription–Translation Reactions in Microfluidic Chemostats Augmented with Hydrogel Membranes for Continuous Small Molecule Dialysis	81
4.1	Abstract	82
4.2	Introduction	83
4.3	Results	84
4.3.1	Formulation, Generation, and Characterization of PEG-DA Hydrogel Membranes	84
4.3.2	Batch Cell-Free Expression Augmented with Continuous Dialysis	87
4.3.3	Steady-State Cell-Free Reaction Augmented with Continuous Dialysis	89
4.4	Discussion	90
4.5	Methods	92
4.5.1	Microfluidic Chip Fabrication	92
4.5.2	Chip Silanization and Formation of PEG-DA Hydrogel Membrane	93
4.5.3	Solute Diffusion through the Hydrogel Membranes	94
4.5.4	Energy and Feeding Solution Preparation	94
4.5.5	Device Setup for Cell-Free Expression	94
4.5.6	Data Acquisition and Analysis	94
4.6	Supplementary Information	96
5	C2CAplus: a one-pot isothermal circle-to-circle DNA amplification system	101
5.1	Abstract	102
5.2	Introduction	102
5.3	Results	103
5.3.1	Isothermal restriction and ligation	103
5.3.2	One-Pot C2CAplus	104
5.3.3	C2CAplus is highly sensitive and robust	106
5.4	Discussion	108
5.5	Methods	109
5.5.1	C2CAplus reactions and platereader experiments	110
5.5.2	Image and data processing	111
5.6	Supporting Information	112
5.6.1	DNA sequences	115
6	Conclusion and Outlook	117
6.1	Bottom-Up Construction of Complex Biomolecular Systems With Cell-Free Synthetic Biology	117

6.2	One Pot PURE system	118
6.3	Improved Cell-Free Transcription–Translation Reactions in Microfluidic Chemostats Augmented with Hydrogel Membranes for Continuous Small Molecule Dialysis	120
6.4	C2CAplus: a one-pot isothermal circle-to-circle DNA amplification system . . .	121
6.5	Advances towards a synthetic cell	122

Bibliography	150
---------------------	------------

Curriculum Vitae	
-------------------------	--

List of Figures

2.1	Cell-free lysate systems	17
2.2	Recombinant cell-free systems	21
2.3	Batch and continuous cell-free reaction platforms	24
2.4	Compartmentalized cell-free reactions.	33
2.5	Communication using cell-free transcription translation.	36
2.6	Identifying resource constraints with cell-free gene expression.	39
2.7	Coupling DNA replication and cell-free gene expression.	42
3.1	Representative results for the overexpression test for all expression strains of the PURE system.	64
3.2	OnePot protein purification.	64
3.3	Performance of the prepared systems using the different ribosome variants.	65
3.4	Absorbance spectra at 260 nm during hydrophobic interaction purification of tag-free ribosomes.	66
4.1	Improved Cell-Free Transcription–Translation Reactions in Microfluidic Chemostats Augmented with Hydrogel Membranes for Continuous Small Molecule Dialysis: Graphical Abstract	82
4.2	Microfluidic chemostat augmented with semi-permeable membranes	85
4.3	Solute diffusion through the membrane	87
4.4	Batch cell-free expression augmented with dialysis	88
4.5	Steady-state chemostat reactions augmented with dialysis	91
4.6	Design of the microfluidic device with hydrogel membranes	96
4.7	Time course of in vitro eGFP expression levels in batch with continuous dialysis reactions for different feeding solution concentrations	97
4.8	Chemostat simulations	97
5.1	C2CAplus: Graphical Abstract	102
5.2	Schematic of a C2CAplus amplification scheme, characterization of restriction digest of an amplification product, ligation activity of T3 and T4 ligases.	105
5.3	C2CAplus reactions	107
5.4	BsmBI titration at 30°C and 18 h reaction time.	112
5.5	Non-cropped gel of Figure 5.2C.	113
5.6	Ligase screen.	114

List of Tables

3.1	A daily time-optimized schedule for the preparation of all the OnePot PURE solutions.	69
3.2	PURE protein list	70
3.3	Reagents used in this section	71
3.4	Buffer compositions for protein, tag-free ribosome, and His-tag ribosome purifications as well as the stock solutions.	72
3.5	Amino acid calculations.	73
3.6	Stock solutions for the energy solution	74
3.7	Energy solution.	75
3.8	PCR reactions. The table lists sequences and concentrations of the primers used for the extension PCR and indicates melting temperatures and thermocycler steps	76
3.9	PURE reaction	77
3.10	Materials.	78
4.1	Microfluidic chip operations for batch, batch with static dialysis and batch with continuous dialysis reactions	98
4.2	Microfluidic chip operations for steady-state reactions	99
5.1	Primers used during this work	115

1 Introduction

1.1 Towards a synthetic cell

Can we build a living system, like a cell, from biological building blocks? And: why would we want to do this?

Richard Feynman argued: "What I cannot create, I do not understand" [4]. The ability to construct a synthetic cell from inanimate components represents a profound challenge and extraordinary opportunity. Trying to build an artificial cell from scratch will create a deeper understanding of basic principles in biology and biological system. Furthermore, it promises to provide novel platforms for a variety of applications to address a multitude of scientific problems including biomedical and bioengineering questions [5, 6].

Currently, cells with a genetic background that has evolved for the purpose of survival and fitness in the respective environment are being utilized in biomedical and bioengineering applications. Their application is thus constrained by the inherent biochemical characteristics that have evolved for purposes divergent from the specific objectives we may aim to achieve [1]. This in turn frequently requires reconfiguring metabolic and biochemical pathways [1], circumventing innate cellular mechanisms that we might only partially understand. A synthetic cell, a cell-like entity, or even a lower-order building block of the latter, however, will provide us with a well-understood and defined chassis that can be tailored to specific needs, opening the door to a multitude of opportunities. It needs to be emphasized that not only a finished, ready-to-use synthetic cell will be of great benefit, but also the path of building a synthetic cell will lead to the development of platforms and systems that will be invaluable for bioengineering and biomedical applications.

It is broadly agreed on that building a synthetic cell is one of the greatest challenges in the area of synthetic biology. It is, however, less agreed on that the completion of this task is feasible and within reach [1, 7]. To achieve this visionary goal, it will be necessary to combine engineering approaches with biological and biochemical knowledge and expertise, and some creativity, to assemble inanimate biomolecular building blocks into more complex units and

entities, eventually creating a system that will be able to perform basic tasks of life.

The exact definition of a synthetic cell is still being debated, and there is very little consensus on what it would look like or when it could be considered a true synthetic cell [7]. Here, we define a synthetic cell as an entity capable of performing basic functions of life. As such it would be compartmentalized (whereas the compartment does not necessarily need to be a lipid bilayer, as known from current living organisms) that will be able to self-replicate, adapt to changing environments, and undergo Darwinian evolution [1]. This definition of a minimal approach for a synthetic cell aligns with the concept of the universal automaton proposed by Von Neumann. According to this concept, a self-replicating system possesses a blueprint of its own structure, and the machinery to make a copy of itself and the blueprint, based on the latter. This is under the assumption of unlimited supply of parts [8]. The concept of the universal automaton can be translated to biological systems with the genome being the blueprint and the transcription-translation machinery being the copy machine. The transcription-translation machinery is in principle able to copy itself and the genetic blueprint, using the latter as a template. If errors occur and are propagated, the system can undergo adaptation and ultimately evolution [1].

Two approaches are imaginable to achieve such a form of minimal life: A synthetic cell based on transcription-translation (TX-TL) via DNA as a blueprint molecule, and proteins and ribosomes as copy machine, or an RNA-based approach, where RNA could be used as both, storage molecule and copy machine. Substantial advancements have been achieved in both directions [9]. The RNA-based approach appeals due to its simplicity. RNA can act both as a storage molecule and perform catalytic tasks. The complex central dogma of biology involving the blueprint to be first transcribed and then translated is not needed in RNA based systems. An RNA based system could thus operate on fewer components compared to systems based on transcription and translation. It is due to this simplicity that a common theory for the origin of life claims that early life was based on RNA rather than DNA and proteins [9, 10].

However, given that current living systems operate under the central dogma, we believe that a transcription-translation-based synthetic cell holds the greatest potential. Such a transcription-translation based cell would require a DNA replication system and a transcription-translation machinery capable of reproducing all cellular components including itself and the DNA replication machinery. Utilizing well-defined components will most likely facilitate this task. Additionally, a minimal synthetic cell will most likely also require a simple metabolism to fuel reactions, and a division mechanism would be necessary for cellular reproduction [1, 11].

Implementing all these features in a synthetic cell remains a monumental challenge. If we base a synthetic cell on the PURE TX-TL system, it will have to be capable of regenerating all of its own components plus a DNA replication machinery. While regenerating the DNA replication machinery involves only a few components (see section 1.2.2), it is crucial to emphasize that the most demanding aspect in terms of self-regeneration is the synthesis of the PURE system itself, as this task requires substantial protein production capacities. While

establishing the sub-systems presents a daunting challenge in itself, the orchestration and coordination of all those sub-systems have presented, and will likely continue to present, obstacles and challenges.

1.2 Self-regeneration

1.2.1 Self-regeneration of the transcription-translation machinery

The fully recombinant and, to a significant extent, minimal PURE cell-free transcription-translation (TX-TL) system lies at the heart of our transcription-translation based synthetic cell. Comprising 36 proteins for TX-TL, along with ribosomes, amino acids, tRNAs, and small molecule components that fuel the TX-TL reactions [2], this system is well-defined and thus meets the above mentioned prerequisite as a basis for a self-regenerating synthetic cell. The PURE system has been available for over two decades and has proven to be an indispensable tool for various applications. Chapter 2 provides a comprehensive review of cell-free systems, including the PURE system, offering insights into the scientific challenges that have been or can be addressed using PURE, extending beyond the grand challenge of building an artificial cell.

Regenerating the PURE system will require regenerating 36 non-ribosomal proteins [3, 12–14], ribosomes [15, 16], and tRNAs [17, 18]. While regenerating functional tRNAs and ribosomes present a formidable challenge, here we focus on the self-regeneration of the non-ribosomal protein components of the PURE system. It still needs to be demonstrated if the PURE system is sufficient and capable of generating a copy of itself.

Niwa and co-workers demonstrated the successful synthesis of 70 % of all *E. coli* proteins in PURE [19], suggesting that the synthesis of the *E. coli*-based PURE proteins might indeed be possible. Awai and coworkers reported the synthesis of 19 out of 20 aaRS (aminoacyl-tRNA synthetases) in PURE and confirmed their functionality [20]. A proof-of-concept for the regeneration of PURE components has been demonstrated in our laboratory. Lavickova et al. regenerated up to seven PURE components using a microfluidic chemostat [3]. However, the authors identified limited protein synthesis capacity as a key obstacle hindering the complete regeneration of the PURE system. At its current composition, the protein synthesis capacity of PURE is estimated to be at least 25 times too low to effectively synthesize all 36 non-ribosomal proteins, let alone other essential components like tRNAs, ribosomes, DNA replication factors, and other factors that might be necessary for functional synthesis of the PURE proteins [3, 21]. Libicher and coworkers co-expressed 30 translation factors from multiple plasmids. They furthermore showed that the expressed amounts were too low to regenerate the original amounts of the components in the PURE system, pinpointing a constraint of the PURE system [22]. In a follow-up study the authors demonstrated the functionality of several components including T7 RNAP using a serial transfer experiment [13]. Wei and Endy tested, if all 36 non-ribosomal proteins can be functionally expressed in PURE. Their study verified the functional expression

of 19 components, and revealed that 2-3 in vitro expressed release factors were non-functional, possibly due to a lack of methylation. Interestingly, their study showed no significant decrease in PURE expression efficiency when omitting 13 further PURE components separately, indicating a certain redundancy and robustness in the system [21]. Doerr and coworkers successfully expressed all translation factors and 20 aaRS in PURE from a single plasmid encoding a total of 32 PURE proteins in 30 cistrons. They furthermore showed that functionality of the expressed proteins was greatly impaired by a significant fraction of proteins missing their c-terminal end, revealing a significant bottleneck and challenge for achieving full self-regeneration of the PURE system [12]. Recent work by Hagino and coworkers showed the functional expression of aaRS from a replicated DNA template, successfully linking one round of central dogma. While using PURE in its standard composition led to the successful regeneration of only 5 aaRS, utilizing dialysis enabled them to successfully regenerate 20 aaRS [14].

Current bottlenecks in protein yield of the PURE system include the depletion of energy sources and small molecules including amino acids that are necessary to fuel reactions, as well as the accumulation of inhibitory products [23, 24], impaired processivity of ribosomes [12], or incomplete translation due to ribosome stalling [25].

Significant efforts have been dedicated to enhancing the overall protein synthesis rate of the PURE system, or tailoring its composition to optimize its performance for specific applications by altering its composition or introducing additional components. These efforts are discussed in section 2.4.1. However, while adding components to enhance yield can be beneficial for specific applications, it is not a viable approach to achieve self-regeneration. Replicating these components would further strain the limited synthesis capacity of the PURE system. To improve self-regenerating of the PURE system it may be more constructive to optimize the overall stoichiometric composition of the PURE system and optimize the relative expression levels of each component by minimizing the overall protein concentration while keeping expression levels in an acceptable range. This will lower the overall protein synthesis burden on the system. Another strategy for achieving a higher protein production capacity involves improving the availability of small molecules within the energy solution that fuels the reactions, and removing the inhibitory byproducts, directly addressing the previously identified resource constraints [3, 23, 24, 26].

Living cells address resource availability by active and passive transport of small molecules and metabolites across their membranes. Fresh reagents are taken up from the environment, while metabolic waste products are excreted. Dialysis using semi-permeable membranes lends itself to mimic this exchange of molecules. Large molecules including proteins and ribosomes for instance, will be retained in the reaction compartment, while small molecules and metabolites will be able to freely diffuse across the membrane, constantly fueling the reactions inside the compartments with fresh reagents, at the same time diluting metabolites that might act inhibitory. Dialysis systems have successfully been implemented for PURE reactions and have demonstrated an increase in protein yield [27, 28]. Exchanging metabolites via dialysis membranes offers a significant advantage over protein transport systems by not

requiring energy or imposing a higher protein synthesis burden to the system, rendering them an attractive strategy for developing a self-regenerating synthetic cell. In the above mentioned work by Lavickova and coworkers [3], it was shown that the expression levels at steady-state using a standard chemostat were at least 25-fold too low to regenerate all PURE components. Protein levels at steady-state are highly dependent on dilution rates. Longer intervals between dilution steps at the same expression rate will lead to a higher protein level at steady-state. However, using our current chemostat, increasing the time interval between dilution steps does not increase overall protein levels, due to a decrease in the protein synthesis rate over time. This decrease in synthesis rate results from the exhaustion of small molecules that fuel the reaction. Implementing dialysis in a chemostat promises to enhance the supply of small molecules, keeping reaction rates steady for a longer time interval. This will enable us to prolong dilution cycles and ultimately lead to higher protein levels at steady-state.

1.2.2 DNA replication

The second crucial task a future artificial cell needs to perform is to replicate its own building plan, which, for a transcription-translation based cell, would be encoded in form of DNA. This blueprint serves as the instruction for the cell to create a replica of itself. To generate viable offspring it is of utmost importance that every daughter cell inherits a full set of this building plan. Therefore, a robust DNA replication system is essential.

A DNA replication system for a synthetic cell needs to operate isothermally at ambient temperatures, eliminating the possibility of using PCR. Ideally, the DNA replication system should be designed as simple as possible, minimizing the additional load on the TX-TL system. Finally, it is crucial that the system is compatible with tRNA, ribosome, and protein expression in the PURE system. The latter has proven to be challenging and requires substantial alterations of the standard PURE composition [22, 29, 30].

It is intriguing that conditions optimal for protein expression are not ideal for DNA replication, and conditions suited for DNA replication seem to have a detrimental effect on PURE protein expression [22, 29–31]. Recent work by Seo and coworkers investigates the influence of various components required for transcription, translation, and DNA replication and identifies adverse effects for a multitude of them. For instance, while dNTPs are required for DNA replication, they are detrimental for translation, and tRNAs are crucial for translation, but inhibit transcription and DNA replication. Some components including spermidine improve all three processes, and others like DTT have no effect on either process [32].

This incompatibility highlights a fundamental challenge in building an artificial cell. However, a closer examination of natural systems reveals that it is not uncommon for DNA replication to occur in a different environment than protein expression. Eukaryotic cells, for instance, have developed a sophisticated system that spatially separates DNA replication within the nucleus and temporally through different phases of the cell cycle. Similarly, prokaryotes employ liquid-liquid phase separation to spatially confine and organize membraneless organelles [33].

To implement DNA replication in a PURE environment, two scenarios are possible: either protein expression and DNA replication are spatio-temporally separated, or the PURE system is modified to be compatible with both DNA replication and protein expression. However, such modifications may result in a system that is not ideally suited for either task, despite attempts to enhance the compatibility of the systems by tuning NTP and buffer compositions and concentrations, as well as magnesium concentrations [31, 32].

Most advances towards implementing a DNA replication system for a future synthetic cell are based on the viral phi29 DNA polymerase [14, 22, 29, 30, 34–37]. Advancements towards establishing DNA replication in PURE are reviewed in section 2.5.3. However, it is important to note that since the publication of the review in 2020, further progress has been made in this area, which I will discuss in this section.

While Van Nies and coworkers replicated linear DNA using phi29 DNA polymerase [34], all other studies presented so far utilize rolling circle amplification (RCA) [14, 22, 29, 30, 35–37]. Rolling circle amplification (RCA) begins with the specific recognition and binding of primers (either DNA or mRNA [29]) to a circular template. A DNA polymerase with strand displacement activity then initiates a rolling circle mechanism to replicate the DNA. The product of RCA is long multimeric strands of linear DNA, and as such presents a structural difference to the circular input DNA. DNA can generally be replicated from this linear multimeric DNA product, and continuous DNA replication using an in vitro expressed phi29 DNA polymerase was demonstrated for 10 consecutive rounds of increasing dilution ratios ranging from 2-fold to 100-fold dilutions [36]. However, the inability of DNA polymerases to initiate replication without a priming mechanism results in continuous shortening of the template DNA on the 5' end, when replicating further rounds of the now linear RCA product [36]. This phenomenon is naturally addressed in living organisms through telomeres and enzymes like telomerases, which prevent the critical loss of genes [38].

Recircularization of the linear RCA product is a strategy to keep structural integrity of the synthetic cell genome intact and ensure robust replication and propagation of the genome. Sakatani and coworkers have implemented this strategy via homologous recombination using Cre-recombinase [30]. During their work, they expressed the phi29 DNA polymerase from a circular template that was subsequently replicated using the in vitro expressed phi29 DNA polymerase. A recombinant, commercially available Cre recombinase was utilized to recircularize the product. One major drawback of their system is the inhibitory effect of the cre recombinase on DNA polymerization, which the authors solved by in vitro evolution of the DNA to develop a circular input DNA that was more efficiently replicated in presence of the Cre recombinase. They furthermore evolved the DNA polymerase for higher processivity [35]. Okauchi and coworkers demonstrated 30 rounds of replication/recombination and DNA polymerase expression using this system encapsulated in water-in-oil droplets [37]. These evolutionary rounds resulted in a template with increased replication efficiency due to enhanced polymerase activity, and a decreased inhibitory effect of the Cre recombinase. Recent work from the same group demonstrated the successful replication of a DNA template

encoding a tRNA gene and the subsequent transcription of the tRNA from the replicated template in the PURE system, generating a proof of concept that DNA replication based on RCA and recombination is compatible with tRNA expression [18]. However, one limitation of the Cre-recombinase based RCA/recircularization system is the sequence requirement to avoid Cre recombinase inhibition, which is not ideal in the context of building an artificial cell.

1.2.3 Microfluidics for building a synthetic cell

Microfluidics emerged as a powerful platform for advancements in cell-free synthetic biology, due to its versatility and low volume requirements, which is especially advantageous due to the high cost of cell-free systems. These characteristics empower the development of robust multistep workflows that have the potential to redefine the boundaries of synthetic cell-free biology [39]. Integration of microfluidics with cell-free systems has been explored in various ways, and chapter 2.4.2 offers an in-depth overview of the current advancements and enabling technologies in this area.

In the context of building an artificial cell, prominent choices for microfluidic platforms include droplet-based and compartmentalizing systems, given their inherent resemblance to cellular structures. These systems include for instance polymersomes and liposomes, which compartmentalize an aqueous core of defined size, shape, and composition, and serve as an individual reaction compartment to host biomolecular reactions [40] such as DNA replication, RNA transcription, and cell-free protein expression [41]. Approaches towards compartmentalized cell-free reactions using droplet microfluidics are reviewed in section 2.4.3.

Droplet microfluidic platforms currently face a challenge when used as a platform for a synthetic cell. Most systems are based on water-in-oil systems, and the water-oil interface creates an impermeable barrier between the inside and the outside of the microreactor. This makes it difficult to exchange reagents between the core of the microreactor and the environment. Therefore, the reactor core provides a compartment for a batch reaction that will continue until all resources are exhausted. However, a living system requires reactions to occur at steady-state with an active protein turnover, as this is crucial to implement genetic networks that ultimately form the basis of a living system. This challenge necessitates solutions like integrating functional membrane proteins into the droplets [11].

Microfluidic chemostats enable the implementation of steady-state reactions by controlling the exchange of reactants at predefined dilution rates [42, 43]. This capability allows for the investigation of increasingly complex biological networks, as discussed in detail in section 2.4.2. Therefore, microfluidic chemostats lend themselves as a chassis for research towards establishing a self-regenerating synthetic cell. For instance, Lavickova et al. have recently demonstrated the successful regeneration of up to seven components of the PURE system using a microfluidic chemostat [3].

1.3 Overview and objective of this work

This thesis resides at the intersection of fundamental research in developing an artificial cell, and the practical application of the platforms and systems derived from this research. As elaborated in section 1.1, the development of an artificial cell holds the potential to enhance our understanding of the underlying biological processes, and simultaneously promises to introduce novel platforms that can be applied to address a variety of scientific questions and challenges.

As discussed in section 1.2.1, the fully recombinant PURE system lends itself to be a suitable foundation of a synthetic cell, given its minimal and well-defined nature. The PURE system has proven to not only be a promising chassis for a synthetic cell, but has also shown high potential for diagnostic and therapeutic applications. Chapter 2 provides a comprehensive review of cell-free systems, including the PURE system, offering insights into the scientific challenges that have been or can be addressed using PURE, extending beyond the grand challenge of building an artificial cell. PURE serves as a prime example of how platforms developed for synthetic cells are finding real-world applications today, contributing to the resolution of current challenges, particularly in therapeutic and diagnostic settings.

A major drawback of the PURE system lies in the high cost and limited tunability of commercially available systems. Preparing home-made PURE solutions is laborious, involving the purification of 36 proteins alongside ribosomes, and the preparation of the energy solution. To address this limitation, we present a comprehensive protocol on how to prepare the OnePot PURE system in chapter 3, aiming to enhance accessibility of this powerful tool. Our method streamlines the preparation process by co-cultivating all 36 non-ribosomal proteins, followed by a single His-tag protein purification step. Using our OnePot method, an experienced user can prepare a cost-effective, custom made, versatile PURE system within one week, using standard laboratory equipment.

As detailed in section 1.2.1, a future synthetic cell will need to be able to self-regenerate its own transcription-translation machinery. Advances have been made to achieve self-regeneration of the PURE system. However, it has been reported that the protein synthesis capacity of the PURE system is by far too low to produce all of its components [3]. One way to improve protein levels at steady-state in PURE is by implementing a dialysis system. In chapter 4 we introduce a microfluidic chemostat augmented with semi-permeable membranes that is able to continuously exchange small molecules and metabolites between the reaction compartment and the environment. Using our dialysis chemostat, we were able to significantly increase the protein production capacity in batch mode. The continuous exchange of small molecules via the dialysis membranes enabled a constant protein synthesis rate for a longer time span. This allowed us to increase dilution intervals from 15 to 60 min, thereby increasing protein levels at steady-state by 6-fold, bringing the self-regeneration of PURE closer to realization. We anticipate that the dialysis chemostat will also serve as a promising technological platform for advancing cell-free applications of increasing complexity, particularly those requiring an

enhanced protein synthesis capacity.

The second prerequisite of a transcription-translation based artificial cell is the ability to robustly copy its genome. Current systems for advances towards establishing a DNA replication system for a synthetic cell incorporate RCA and have the disadvantage that the input DNA structure is circular, while the replication product is multimeric and linear. Attempts to recircularize this linear product using Cre-recombinase required the evolution of the underlying DNA to limit inhibitory effects on DNA synthesis by the Cre-recombinase [30]. In chapter 5, we introduce C2CAplus, a fully isothermal, single-step system for robust DNA replication that combines RCA with re-circularization. During C2CAplus, the RCA product is monomerized using a restriction enzyme and recircularized using a ligase. By balancing the ratio of restriction enzyme to ligase, we achieved a one-pot method that robustly and efficiently replicates DNA. C2CAplus incorporates a restriction enzyme and a ligase at a balanced ratio. Not being hindered by inhibiting effects of the utilized components, the only sequence requirement for our system is a unique cutting site for a restriction enzyme. Our C2CAplus system has proven to be robust across ambient temperatures, highly sensitive, and profoundly efficient. White, highly viscous product can be seen in the reaction tube by plain eye. Due to its isothermal one-pot nature and high sensitivity, we anticipate that C2CAplus has a potential as a cost-effective, sensitive biosensor for applications in remote areas.

Throughout this thesis, I hope to convince the reader that pursuing the development of an artificial cell is not merely an ambitious undertaking; it is a visionary endeavour that holds immense promise, not only for the ultimate goal of achieving a well-defined self-sustaining synthetic cell, but also for the multitude of opportunities for groundbreaking discoveries and applications that will emerge along the way.

2 Bottom-Up Construction of Complex Biomolecular Systems With Cell-Free Synthetic Biology

This work was published in *Frontiers in bioengineering and biotechnology*, 2020 [44].

Authors: Nadanai Laohakunakorn, Laura Grasemann, Barbora Lavickova, Grégoire Michielin, Amir Shahein, Zoe Swank, Sebastian J. Maerkl

Reference: Laohakunakorn, Nadanai, et al. "Bottom-up construction of complex biomolecular systems with cell-free synthetic biology." *Frontiers in bioengineering and biotechnology* 8 (2020): 213.

Contribution: LG wrote section 2.5.3. All authors edited the manuscript and approved it for publication.

2.1 Abstract

Cell-free systems offer a promising approach to engineer biology since their open nature allows for well-controlled and characterized reaction conditions. In this review, we discuss the history and recent developments in engineering recombinant and crude extract systems, as well as breakthroughs in enabling technologies, that have facilitated increased throughput, compartmentalization, and spatial control of cell-free protein synthesis reactions. Combined with a deeper understanding of the cell-free systems themselves, these advances improve our ability to address a range of scientific questions. By mastering control of the cell-free platform, we will be in a position to construct increasingly complex biomolecular systems, and approach natural biological complexity in a bottom-up manner.

2.2 Introduction

Synthetic biology promises to transform diverse domains including biomanufacturing, health-care, food production, sustainable energy, and environmental remediation, by applying engineering principles to the design and construction of biological systems [45]. Specifically, this was stipulated to involve abstracting away intricate biological complexity into simpler parts and modules whose behaviour can be quantified [46–48]. The process of ‘building’ thus involves assembling these subsystems together to obtain a required function, while quantitatively characterised components and their interactions ensure that the overall system may be predictively designed.

Practice currently diverges from the ideal framework set out above, due to the fact that we do not yet have a reliable approach to managing biological complexity [49]. While the idea of abstracting the behaviour of a biological process, such as gene expression, into a simple mathematical model may indeed work well for single genes in isolation, as the gene circuit increases in size and complexity, the increased enzymatic and metabolic burden leads to reduced gene expression, changes in host cell state and growth rate, and increasing negative selection pressure. A seemingly modular component naturally loses its modularity as the system becomes more complex, and thus a major bottleneck preventing the current practice of synthetic biology from attaining the ideals outlined above lies in the transition from simple parts and circuits to larger systems [50].

There are several approaches to meet this challenge of reliable engineering of large biological systems, in the face of unknown complexity. One is to take advantage of increasing automation and experimental throughput to arrive at a functional design through screening large libraries of alternative constructs [51]. In order to effectively explore the parameter space, these screens may be guided by techniques such as directed evolution [52]. A more rational approach is to discover designs which are robust to specific uncertainties, as exemplified by control theoretic approaches [53–55]. In this approach, it is not necessarily required to fully characterise the

system, but merely to know which parts of the system are uncharacterized and varying, and therefore need to be buffered by an appropriate architecture.

Finally, a fully bottom-up approach attempts to rationally construct increasingly complex biomolecular systems from basic parts *in vitro* [56–61]. In this approach, the major interactions within the system can in principle be fully quantified and understood. The payoffs from these efforts are well-informed models and understanding of increasingly complex biological systems [62], which may eventually guide fully predictive design in the future.

The rapidly growing field of cell-free synthetic biology [63] brought forth numerous examples where such a constructivist approach has been adopted to elucidate basic principles associated with bottom-up construction of biomolecular complexity. The purpose of this review is to give a historical perspective and present an overview of the current capabilities and challenges facing this particular approach. We begin by giving an overview of the rich scientific history of cell-free gene expression systems and their use in deciphering fundamental biological processes by deconstructing them into their essential components. We then describe the current state of bottom-up cell-free synthetic biology, with a dual focus on both the cell-free systems themselves, as well as emerging technological platforms that enable increasingly complex and sophisticated manipulations of cell-free systems. Finally, we discuss how the construction of additional complexity on top of existing TX-TL systems stimulates the investigation of fundamental biological questions, which include context effects in gene expression, resource management, and possibilities for *in vitro* DNA replication.

Reliable engineering of synthetic biomolecular systems is an ambitious goal, whose success will depend on knowledge and insights gained from many different perspectives. We envision that the bottom-up approach, as exemplified in particular by cell-free synthetic biology, will play a key role in enabling the full potential of synthetic biology.

2.3 Deconstructing biology using cell-free systems

Cell-free systems are created by extracting cellular machinery, and combining them with energetic substrates and cofactors to recapitulate central biological processes such as transcription and translation *in vitro*. While this approach has been in existence since Buchner's 1897 observation of cell-free fermentation in yeast extract [64], it was only during the molecular biology revolution in the 1960s that cell-free systems began to be used in a rational and directed manner to elucidate biological mechanisms.

Early pioneers of cell-free investigations took advantage of two important properties of the system: its simplified biochemical nature, and its open reaction environment. Preparing a cell-free extract strips away much of the complexity of cellular regulation, homeostasis, and growth, revealing the isolated biochemical mechanisms underneath. By reconstituting the basic steps of protein synthesis, *E. coli* cell-free systems were used to demonstrate peptide synthesis from amino acids [65], RNA [66], and finally DNA, via coupled *in vitro* transcription

and translation [67–69], thereby experimentally validating the central dogma of molecular biology. The first full protein synthesised *in vitro* was the coliphage F2 coat protein [70].

The open nature of cell-free systems meant that factors which affected protein synthesis could be isolated and characterised, thus allowing direct study of transcriptional and translational regulation. Well-known examples of this work include the direct demonstration of the lac repressor's effect on peptide synthesis [71], and the identification, isolation, and characterisation of the catabolite activator protein (CAP) [72]. Cell-free systems were subsequently used to identify and elucidate genetic operons in *E. coli* [73].

Another set of cell-free experiments of fundamental importance was the study of translation from synthetic polyribonucleotides by Nirenberg and coworkers. They observed that cell-free extracts loaded with synthetic poly-uracil led to the production of only one type of polypeptide, poly-phenylalanine [74]. Thus, they hypothesised that poly-U must encode for phenylalanine. Over the next few years, the base composition, triplet nature, and eventually the genetic code mapping DNA sequence to amino acids was determined [75].

Over the subsequent few decades, it became a standard approach to use *in vitro* systems to elucidate mechanisms in molecular biology (e.g. RNA replication [76], splicing [77], Golgi trafficking [78], and chemiosmosis [79]). In parallel, the growth of *in vitro* protein synthesis applications drove the development of increasingly efficient cell-free extracts, which achieved greater yields by incorporating more advanced metabolism to energise synthesis and recycle waste products [80]. In the early 2000s, extract engineering merged with the nascent field of synthetic biology, giving rise to the field of cell-free synthetic biology [81], where instead of reconstituting existing biological processes, novel ones were constructed in the cell-free environment. This synthetic approach continues to characterise the field today.

2.4 Technologies

2.4.1 Lysates and reconstituted cell-free systems

In recent years the number of cell-free transcription-translation (TX-TL) systems from different organisms has grown rapidly [82–84]. The most common lysate systems include *E. coli*, insect, yeast, Chinese hamster ovary, rabbit reticulocyte, wheat germ, and human HeLa cells; and newly emerging systems include *B. subtilis* [85, 86], *V. natriegens* [86, 87], and *P. putida* [86, 88], among others [86]. Hybrid systems composed from multiple sources have also recently emerged [86, 89, 90]. Many of these lysate systems are currently commercially available. Concurrent with the expanding set of available lysate systems, there has also been a resurgence of interest in reconstituted recombinant systems, which are composed of mixtures of purified enzyme components. In this review, we will focus on *E. coli* lysate as well as recombinant systems, as they are commonly-used cell-free systems.

***E. coli* lysates**

The preparation and performance of *E. coli* lysate-based TX-TL systems vary tremendously and it is well known that there can be large variability between different batch preparations [91]. For example, a recent study showed variability of more than 40% for TX-TL systems prepared in different laboratories, which resulted mainly from differences in personnel, and reagents used, and significantly, the laboratory in which the measurement was carried out [92]. Fortunately, there is an increasing understanding of the role that each of the preparation steps plays in determining the final extract performance, as well as the factors responsible for reproducibility [93]. Proteomics has been applied to elucidate the dependence of lysate composition and performance on batch variability, preparation methods [94, 95], as well as strain variability [96, 97]. The quest for a deeper understanding is also supported by the use of additional methods such as metabolomics [98], and other techniques as polysome profiling [99], HPLC [100] and gel electrophoresis [101] (Fig. 2.1B). These results raise the exciting prospect that lysates will become an engineerable substrate, where standardized and controlled preparation can result in extracts with a variety of defined behaviours. This approach has been particularly powerful in the context of cell-free metabolic engineering, and has been reviewed extensively by [102, 103]. Here we present an overview of different types of lysate preparation steps (Fig. 2.1A), and their effects on lysate properties. The history of the field, recent advances, as well as the development, optimization, and applications of TX-TL systems are covered in recent reviews [104, 105].

E. coli extracts are prepared from a variety of different strains, whose choice strongly depends on the intended application. The most commonly used strains are BL21-derivatives [92, 106–108], but the use of other strains can also be advantageous. For example, strains lacking DNAase, RNAase, and other *E. coli* enzymes can be used to enhance protein yield [107, 109], for biosensing applications [108], or for circuit prototyping [110].

Different media such as 2×YT [111], 2×YTP [95, 106] or 2×YTPG [107], as well as different temperatures and volumes can be used, which will influence the bacterial proteome and thus the composition of the lysate. For example, adding phosphate and glucose has suppressive effects on phosphatase activity [112]. Bacteria can also be harvested at different time points during exponential or stationary phases. Surprisingly, this appears to have very little effect on lysate performance [95, 107].

Cell lysis is a major and variable step of the overall lysate preparation, and different methods result in varying cost, scalability, and ease of use. Bacterial cells can be lysed by sonication [107], high-pressure homogenization [109], bead-beating [106], or enzymatic auto-lysis [108]. Production yield between systems were shown to be comparable [106, 107]. However, other factors should also be considered. For example, the formation of inverted membrane vesicles is favored in lysates prepared with high-pressure homogenizers, and their preservation is essential for processes such as oxidative phosphorylation [113] and glycosylation [101]. Subsequent lysate clarification usually involves centrifugation at 30000×g for S30 lysates or 12000×g

for S12 lysates, which leads to different lysate clarity as distinct components sediment at different speeds, making the S30 lysate less viscous and opaque. For many applications no significant difference was observed between S30 and S12 lysates [111]; however S12 lysates contain more inverted membrane vesicles which can support oxidative phosphorylation, and hence may be desirable for certain applications.

To reduce preparation time and simplify the process, some steps have been omitted in recent studies. Among these are run-off reaction and/or dialysis [107, 114]. Omitting these has minimal influence on final yield in T7 RNAP based systems [107, 111] and might even be beneficial for retention of co-factors, amino acids, and tRNAs [115, 116]. However, the omission of both run-off reaction and dialysis has a profound effect when native transcriptional machinery is used [93, 107].

Another important difference between systems is related to the energy regeneration approaches used (Fig. 2.1B). The first systems based on substrates containing high-energy phosphate bonds (phosphoenolpyruvate, acetyl phosphate, creatine phosphate) were expensive and inefficient because of their fast degradation by nonspecific phosphatases, and formation of inhibitory inorganic phosphate molecules. Over the last twenty years, a large amount of work has focused on yield improvement and price reduction. Most current energy regeneration systems are based on the native metabolic pathways of *E. coli*. These use either a part of—PANOx [117], 3-PGA [106]—or the entire *E. coli* glycolysis pathway—glucose [24], maltose [117], maltodextrin [118, 119], and starch [120]). These approaches have decreased the price per mg of synthesised protein to under one U.S. dollar. Nevertheless, we still lack systematic studies on the influence of these different energy regeneration methods on lysate properties other than simple protein yield. In particular, for prototyping and characterization of circuits, it is known that resource competition leading to improperly balanced energy usage [121, 122], efficiency of energy sources and small molecule replenishment [121, 123], changes in binding kinetics due to magnesium ion concentration changes [124], and pH variability [24] are all dependent on the energy system used and are expected to have profound influence on circuit behavior.

Finally, lysates can be directly supplemented with additives such as liposomes, polymers, and detergents to facilitate folding of membrane proteins [125, 126]. Enzymes such as gamS [127] or short DNA decoy sequences [128] can be added to prevent linear DNA degradation. The ease of adding functionality to lysates is a major advantage facilitated by the open nature of cell-free reactions.

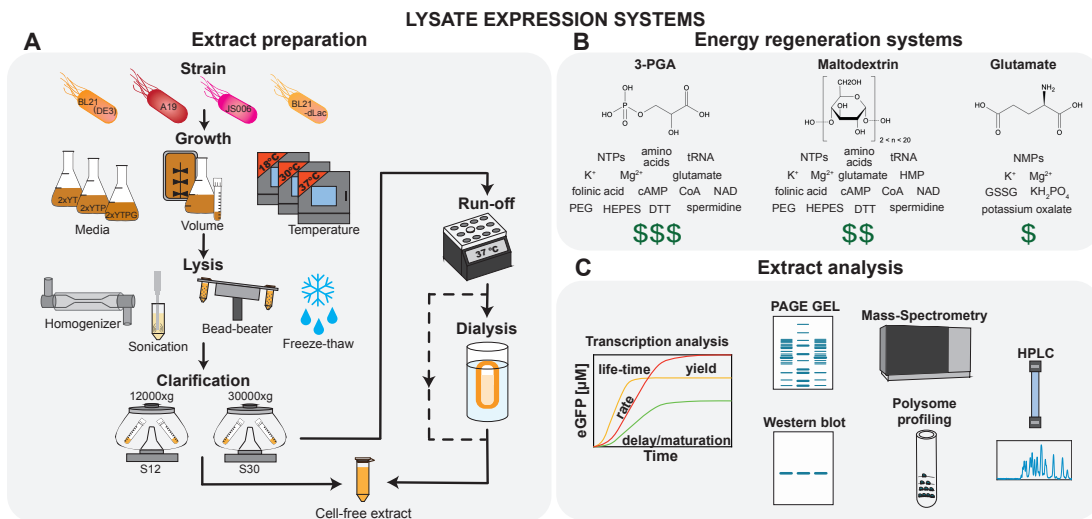


Figure 2.1: **Cell-free lysate systems.** (A) The major steps in lysate preparation include growth, lysis, and clarification; however there exists a number of variables and options at each step, which can be adjusted to influence the final extract performance. (B) Examples of three energy regeneration systems are shown, which offer different cost-performance tradeoffs. (C) The final extract composition and performance may be analysed using techniques such as protein expression analysis, PAGE gel, Western blot, mass-spectrometry, polysome profiling, and HPLC.

Recombinant systems

Lysate systems contain essentially all cytoplasmic components, which is advantageous for recapitulating cellular processes. However, this makes their composition ill-defined, leading to challenges in basic science and engineering. To address these difficulties, efforts were made to generate fully recombinant cell-free systems from a small number of purified enzyme components, whose composition can be defined exactly. Such defined systems are especially important for bottom-up synthetic biology for three main reasons. The first is that their use supports research into minimal cellular systems, as ‘minimality’ of components and pathways can be directly tested. Secondly, the composition of the recombinant system is known much more precisely than for extract-based systems. This property is highly beneficial for modeling, optimization, troubleshooting, and mechanistic understanding of engineered pathways. Thirdly, the use of recombinant cell-free systems presents a viable approach towards the development of *de-novo* constructed synthetic cells.

Almost half a century ago, Weissbach’s group developed the first such systems from recombinant *E. coli* proteins [129], but observed very low protein yield. About 25 years later, thanks to the advent of His-tag purification as well as the addition of a creatine-phosphate-based energy regeneration system, Shimizu *et al.* [2] developed a very similar system called PURE (protein synthesis using recombinant elements) but with markedly higher protein synthesis yield (Fig. 2.2A, B). Currently, there are three commercially available versions of this system: PUREfrex 2.0 (GeneFrontier), PURExpress (NEB) [130], and Magic PURE system (Creative Biolabs). Although highly popular, these systems are more expensive (\$0.6–\$2/ μ L) than lysate systems (\$0.3–\$0.5/ μ L). Moreover, despite the fact that the commercial systems are all based on the original PURE system, their exact composition is proprietary, and functional differences can be observed between them in terms of batch to batch variability, system yield, translation rate, lifespan of the reaction, and shelf-life [131].

Cost-effective and modular PURE systems with user-defined compositions can be prepared in the laboratory [132, 133], but the labour-intensive protocol requires ~36 medium to large scale His-tag and ribosome purification steps (Fig. 2.2A). Thus, different approaches to simplify the protocol have been developed, including His-tagging of *in vivo* enzyme pathways [134], microbial consortia [135], and bacterial artificial chromosomes [136]. The first two systems achieved a 10–20% protein yield compared to the commercial PURExpress (NEB). Although the third approach reached protein synthesis levels comparable to PUREfrex, in all three of these approaches it is not possible to rapidly modify protein levels or omit proteins. We recently demonstrated that all proteins, except ribosomes, can be prepared from individual strains in a single co-culture and purification step called the OnePot PURE system, which achieves a similar protein synthesis yield as commercial PURExpress [137] (Fig. 2.2A).

Much work has been carried out to improve existing recombinant systems, particularly focusing on the protein expression yield: in addition to increasing the versatility of the system, this has also resulted in a better understanding of the system itself. Improved yield, lower cost,

and the ability to adjust the system composition opens up many possibilities for applications such as the development of defined artificial cells, gene network engineering, biosensors, and protein engineering. Here we separated the various approaches into two distinct types: the first includes experimental and theoretical approaches which aim to find an optimal composition of the system, while the second involves supplementing the existing system with factors that augment its behaviour.

One direction for optimizing recombinant systems for protein synthesis yield is focused on finding optimal concentrations of the basic system components such as proteins, energy sources, small molecules, and salts [25, 27, 131, 138] (Fig. 2.2C). Important work to improve our understanding of the system was done by Matsuura *et al.*, who performed titrations of all protein components [139]. These studies showed that although the system is composed of a relatively small number of components, its behaviour is complex, and its analysis requires multivariate optimisation. One of the most important parameters in the system is the magnesium ion concentration, which influences ribosome function. It is difficult to control the concentration of magnesium ions as they can be chelated by negatively charged molecules such as NTPs, creatine phosphates, and pyrophosphates [25, 138]. Studies focused on protein component concentrations showed that the performance of the system is mostly influenced by the concentration of ribosomes and translation factors. Increased yield depended strongly on high concentrations of EF-Tu, which often forms more than 50% of the non-ribosomal protein content *in vivo*. Moreover, finding optimal concentrations is essential for release factors and initiation factors, as an inhibitory effect was shown for these components when higher-than-optimal concentrations were used [27, 138, 139]. Finally, the optimal composition of the system will vary depending on the application. As an example, high concentrations of components such as NTPs enhance transcription and translation, while inhibiting DNA replication [29].

To better understand the system behaviour and to identify limiting factors, computational models of the PURE system have been developed. This includes coarse-grained ordinary differential equation (ODE) models containing effective lumped parameters and a small number of reactions [131, 140, 141], as well as more complex models based on modelling of a large number of elementary reactions, which can provide more detailed mechanistic insights but whose connection to experimental data as well as parameter inference is challenging [142, 143]. These models show that a number of steps involving ribosomes could potentially become rate-limiting: these include slow elongation rates, peptide release, and ribosome dissociation; qualitatively similar results were observed experimentally [25, 131, 144].

As in the case of lysates, a second approach is based on augmenting the system with additional components such as proteins [145], crowding agents, and liposomes. For example, yields can be slightly increased by adding proteins such as EF-4 [138], EF-P [25], Pth [27], and HrpA [145]. Recently, an energy regeneration system originally based on three kinases was replaced by one featuring a single polyphosphate kinase. This improvement lowers the price of the energy source and simplifies the energy regeneration process [146]. While the original PURE system

only contains T7 RNA polymerase, with its limited capability for transcriptional regulation, *E. coli* σ -factor based transcription has been successfully demonstrated, albeit with low efficiency with certain promoters, which can be enhanced by adding purified *E. coli* polymerase alone or in combination with transcription elongation factors [147] (Fig. 2.2D).

Protein folding can be improved by incorporating chaperones such as a trigger factor, DnaK / DnaJ / GrpE, and chaperonin GroEL / GroES (Fig. 5.3E). Likewise, Niwa *et al.* showed that the solubility of 800 aggregation-prone *E. coli* cytoplasmic proteins can be enhanced if chaperones are added [148]. Furthermore, an oxidising environment and a disulfide bond isomerase are essential for the expression of proteins containing disulfide bonds [149] (Fig. 2.2G). The addition of liposomes [150, 151] together with diblock copolymers [152] is important for membrane-protein synthesis (Fig. 2.2F). Finally, the concentration of components in the cell-free system is up to 100 times lower than the native *E. coli* cytoplasm. Crowding agents such as bovine serum albumin (BSA) [138], Ficoll [153], polyethylene glycol (PEG) [138, 153], or osmolites [154] can help mimic the *E. coli* cytosol [153], but they affect both transcription, translation [155], and the final synthesised proteins [151] in a complex way. Further studies will be needed to decipher the various physico-chemical effects of crowding on gene expression. Lastly, it was shown that temperature optimization is a key factor for chaperone-free assembly of protein complexes such as DNA polymerase [156].

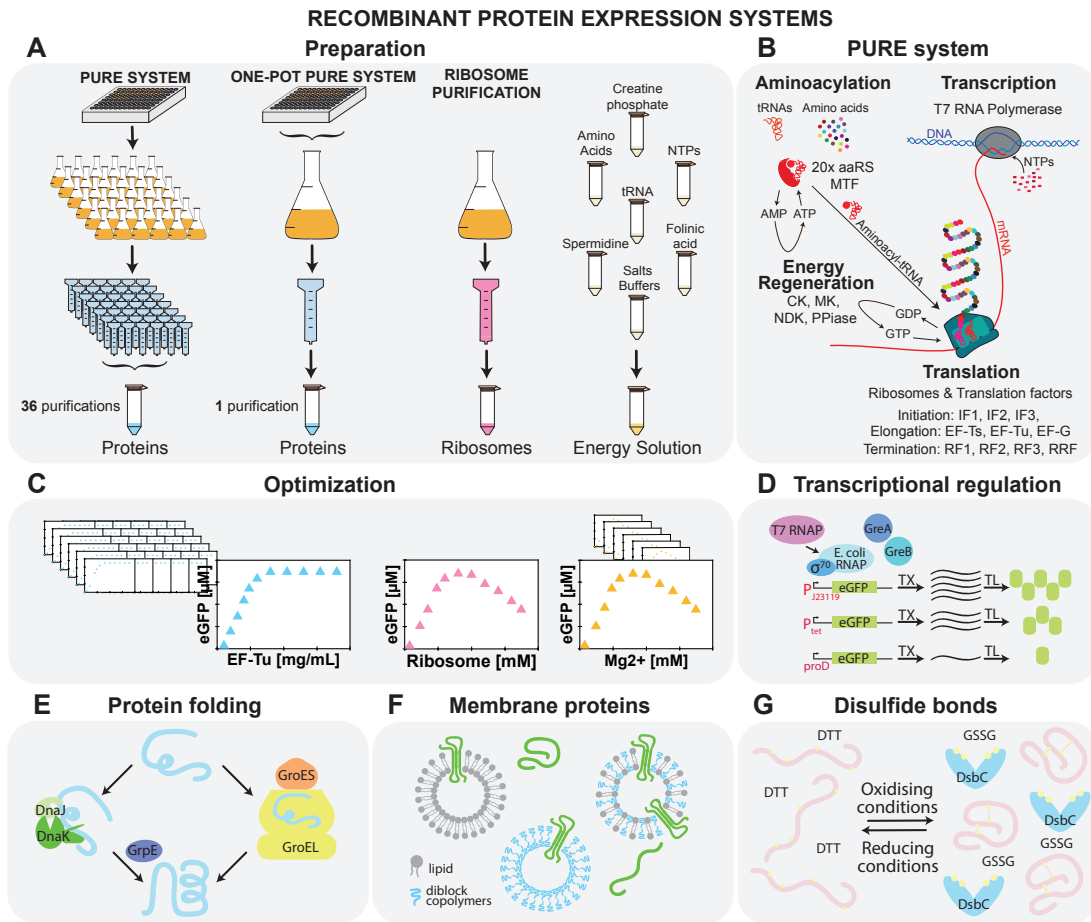


Figure 2.2: **Recombinant cell-free systems.** (A) Schematic of the preparation of the three elements constituting the PURE system: proteins, ribosomes, and energy solution. (B) The four major reactions, aminoacylation, transcription, translation, and energy regeneration occurring during cell-free protein synthesis in the PURE system are shown along with a list of the components involved. (C) Optimization of the system can be carried out by adjusting both protein and energy solution components. Potential system modifications are shown: (D) supplementation with *E. coli* RNAP allows for more complex transcription regulation [147]; (E) addition of chaperones aids protein folding [148]; (F) vesicles enable membrane protein folding and assembly [150, 152, 157]; and (G) oxidising conditions allow for disulfide bond formation [149].

2.4.2 Microfluidic platforms

While cell-free reactions can be carried out successfully in a simple test tube, the complexity and sophistication of experiments can be dramatically augmented by coupling them to the appropriate technological platform. There have been numerous technological advancements with respect to cell-free gene expression over the past few decades, leveraging advances in microarraying, automation, and in particular, microfluidics. Offering reductions of orders

of magnitude in sample volume, concomitant low cost, small device footprint, quantitative detection methods, and precise sample manipulation, microfluidic technology has offered tremendous improvements in control and throughput of cell-free reactions [158, 159]. We will focus on recent platforms enabling increased control over batch and, importantly, steady-state reactions, as well as describe recent work in the area of compartmentalization.

Increased throughput and spatial control of batch reactions

Early high-throughput methods of spatially confined cell-free batch reactions were applied to the generation of protein arrays. In 2004, Ramachandran *et al.* showed that a plasmid array spotted on a glass slide could be transformed into a protein array by submersing the entire slide in a cell-free reaction. mRNA and proteins were locally transcribed and translated from the spotted plasmid DNA and proximally captured by surface bound antibodies [160, 161]. The *in situ* generated protein array could then be interrogated with a protein of interest. A similar concept was later integrated into a microfluidic device for the automated mapping of protein-protein interactions [162]. Here linear expression DNA templates are spotted on a glass slide in pairs. The DNA array is then aligned to a MITOMI microfluidic device [163] so that each pair of linear templates is enclosed by a reaction chamber. Loading of the device with cell-free reaction solution synthesizes the bait and prey proteins, which are then assayed for interaction using the MITOMI method. A similar approach was used to generate large numbers of defined bHLH (basic helix-loop-helix) transcription factor mutants to assess the evolutionary accessible DNA binding specificity repertoire of these transcription factors [164]. Martin *et al.* used the method to generate an RNA array for protein-RNA interaction studies [165]. More recently, hundreds of full-length *Drosophila* transcription factors spanning a size range of 37–231 kDa were expressed on-chip using a wheat germ cell-free system [166]. Such approaches are becoming appealing for protein engineering, especially with the rapid decrease in synthetic DNA cost. In 2015, we demonstrated that over 400 synthetic zinc-finger transcription factors could be synthesized and characterized *in vitro* using this approach [167].

As synthetic gene networks began to emerge, the advantages of cell-free protein expression were adopted to rapidly screen large libraries of functional DNA parts, avoiding *in vivo* cloning steps, and speeding up the design-build-test cycle ([121, 168]). The advent of acoustic liquid handling robots has enabled cell-free reactions to be carried out in standard microwell plate systems with increased throughput and precision, while simultaneously reducing reagent usage. This was recently demonstrated and coupled with a Bayesian modeling approach, which offered a fast route to characterizing regulatory elements from a non-model microbial host [169]. With their rapid and automated method the authors were able to infer previously unknown transcription factor binding affinities as well as quantify resource competition in cell-free reactions (Figure 2.3A). Cell-free systems are particularly amenable to mechanistic modeling, and Bayesian inference of model parameters, which benefits from the possibility to perturb the composition of open cell-free reactions. Bayesian approaches uses probability distributions to quantify the degree of belief and uncertainty in the model, and can be deployed

to quantitatively compare a number of models as well as determining parameter uncertainty. Automated acoustic liquid handling was also used to test serine integrase recombination dynamics [170]. A Python package built to model and simulate biological circuits was then applied to the cell-free prototyping data to carry out Bayesian parameter inference.

Microfluidic platforms applied to cell-free TX-TL have also enabled the exploration of larger design spaces at faster time scales. For example, droplet microfluidics was used to rapidly generate a library of distinct combinations of DNA templates, inducer molecules, and cell-free extract concentrations, with the possibility of generating millions of parameter combinations per hour [171]. Together with a dye labelling scheme, it was possible to create a detailed map of biocircuit expression versus parameter combination (Figure 2.3A). Sharing a common goal of characterizing gene network parameters, an alternative microfluidic platform was developed to carry out cell-free TX-TL in high-throughput, using different combinations of surface immobilised DNA as the reaction templates [172]. Functional repression assays and quantitative affinity measurements [163] were used to characterize a library of synthetic transcription factors, enabling gene regulatory networks to be built from purely synthetic parts *de novo* (Figure 2.3A). Another quantitative and multi-dimensional study of genetic promoters was carried out using parallel piezoelectric cantilever beams that were able to generate an array of droplets containing cell-free TX-TL reaction mixtures with highly accurate concentration gradients [173] (Figure 2.3A).

Setting aside high-throughput techniques, there exist many other innovative technologies for cell-free gene expression, including methods that have sought to introduce spatial organization. In particular, a chip was developed to separate transcription and translation into different compartments [174]. Multi-compartment vesicles were used to predefine regions in which different proteins would be synthesized *in vitro* [175]. Furthermore, Jiao *et al.* fabricated a microfluidic device for the encapsulation of plasmid integrated clay microgels [176]. The incorporation of magnetic beads in the microgels permitted their recovery and re-use in subsequent cell-free TX-TL reactions. A bead-based approach was also used to express and capture recombinant proteins in a hydrogel matrix [177]. Lastly, surface-bound DNA microarrays were aligned with a hydrogel matrix embedding protein synthesis machinery enabling localized protein synthesis [178]. These studies will be discussed in more detail in section 2.4.3.

Steady-state cell-free reactions

While cell-free batch reactions provide a means to characterize gene circuits, parts, and devices, the complexity of biological networks that can be implemented is constrained as the systems quickly reach chemical equilibrium. As discussed in Section 2.4.1, batch cell-free reactions quickly equilibrate or reach a state of non-productivity for a number of reasons, such as byproduct or cofactor accumulation and subsequent drift from the initial reaction composition (e.g. inorganic phosphate, Mg²⁺, H⁺); denaturation or degradation of protein components; and simple exhaustion of substrate molecules. This has motivated the development of *in vitro*

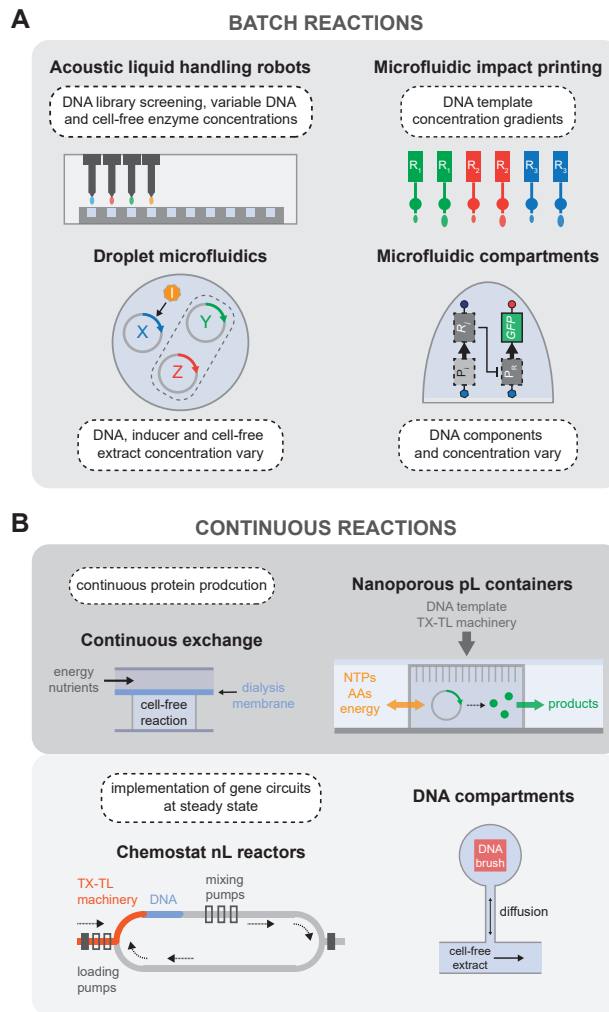


Figure 2.3: **Batch and continuous cell-free reaction platforms.** (A) Overview of the technologies used to carry out high-throughput batch reactions, including the possibilities to vary the concentration of many reaction components in addition to exploring the sequence space of DNA templates. (B) Devices developed for continuous cell-free reactions, separated into two categories: continuous protein production, and steady-state reactors that enabled the implementation of genetic oscillatory circuits.

systems that can exchange reagents over time, maintaining the reaction in a non-equilibrium steady state, and mimicking the dilution and regeneration of cellular components during cell growth. Over 30 years ago there was interest in prolonging cell-free TX-TL reactions by providing a continuous flow of amino acids and energy sources to a reaction chamber from which synthesized proteins and by-products could be removed across an ultrafiltration membrane [179]. Successive work aimed to improve protein synthesis yield for cell-free TX-TL reactions by using a dialysis membrane to separate the reaction from the feeding solution of amino acids and energy sources, leading to a semi-continuous reaction [180, 181]. This

idea was then extended to be compatible with standard micro-well plate systems that could be used for higher throughput applications [182–185]. Following upon the same principles of continuous exchange cell-free reactions, a passive PDMS microreactor was built which separated the feeding and reaction chambers with a dialysis membrane, enabling protein synthesis for up to 15 hours [186] (Figure 2.3B).

Recent improvements in implementing continuous cell-free TX-TL reactions came in the form of novel microfluidic devices. For instance, continuous protein synthesis was demonstrated in an array of cell-sized nanoporous silicon containers that could exchange energy components and materials with the surrounding microfluidic environment [187]. In 2013, Niederholtmeyer *et al.* reported a two-layer PDMS device with 8 independent nano-reactors that exchanged reagents at dilution rates similar to those of growing bacteria. Using this device, steady-state TX-TL reactions could be maintained for up to 30 hours, enabling the first *in vitro* implementation of genetic oscillator circuits [188, 189] (Figure 2.3B). Using the same device, Yelleswerapu *et al.* recently demonstrated the construction of synthetic oscillating networks using sigma-factor-based regulation of native RNAP in *E. coli* lysate [190]. In 2014, Karzbrun *et al.* demonstrated two-dimensional DNA compartments capable of creating oscillating protein expression patterns and protein gradients. Each DNA compartment was linked to a supply channel by a small capillary channel for continuous diffusion of nutrients and products into and out of the compartment [191] (Figure 2.3B). The geometry of the compartments determined the dilution rate of the reaction, giving rise to different observed reaction kinetics. Using high frequency localized electric field gradients, the same group was able to push the TX-TL machinery away from the DNA brush, thereby arresting transcription and translation. They showed that different biomolecules can be manipulated efficiently depending on the applied voltage and obtained sustained oscillation of gene expression from controlled ON/OFF switching of the TX-TL reaction [192].

2.4.3 Compartmentalized cell-free reactions

Compartmentalizing cell-free reactions spatially segregates a bulk reaction into smaller units. In addition to being a fundamental requirement in the construction of artificial cells, compartmentalized TX-TL opens up a number of scientific and practical opportunities, such as increased throughput for screening, *in vitro* directed evolution, distributed computation, and programmable communication. As discussed in sections 2.4.2-2.4.2, microwell plates with reaction volumes as low as 0.5 μL [207], and microfluidic devices with volumes down to femtoliters [208], have been used to compartmentalize cell-free reactions.

Below, we will cover different types of compartmentalization including emulsions that allow for the rapid generation of multiple small volume compartments; liquid-liquid phase separation which can recapitulate naturally occurring crowded environments; hydrogels of natural or synthetic origin that immobilize DNA or proteinaceous factors and similarly provide a favorable crowded environment; liposomes which can provide a good starting point in

the bottom-up assembly of synthetic cells by encapsulating a gene expression system; and other membrane-enclosed compartments with shells composed of polymers or protein-based materials that will expand the repertoire of physicochemical properties and functionalities.

Emulsion-based compartments

Emulsion-based compartmentalization allows for the rapid production of reaction vessels with volumes as low as femtoliters [209]. *In vitro* compartmentalization of TX-TL was first described in the context of *in vitro* evolution when Tawfik *et al.* [210] encapsulated a TX-TL system together with a DNA library of genes coding for an enzyme. Single copies of DNA templates were compartmentalized in $\sim 2 \mu\text{m}$ aqueous droplets dispersed in mineral oil, creating the crucial genotype-phenotype linkage [211] which is required for selection and enrichment of improved enzymes. This eventually allowed a complete cycle of directed evolution of phosphotriesterases to be carried out [212].

One major drawback of emulsions produced by bulk methods is the size polydispersity of the obtained compartments (Figure 2.4A). This leads to enzymatic activity being convolved with noise resulting from variation in droplet size, making it difficult to select droplets containing improved enzymes. Dittrich *et al.* overcame this limitation using droplet microfluidics to generate monodispersed water-in-oil (W/O) droplets (Figure 2.4A) containing a TX-TL reaction expressing GFP. However, their setup did not allow for the production of droplets containing single DNA copies that gave rise to detectable signals, as would be required for *in vitro* evolution. Using a more efficient TX-TL system and stabilized W/O droplets, Courtois *et al.* were able to obtain efficient transcription and translation from a single DNA copy [213], opening the door for high throughput quantitative evolution experiments in droplets generated by microfluidics. Examples of these include multiple screening rounds to enrich for active hydrogenase [214] and beta-galactosidase enzymes [215].

The use of fluorogenic substrates in enzymatic assays can be problematic in surfactant stabilized emulsions as transport of fluorophores can occur between droplets both in single [216] and double emulsions [217]. Woronoff *et al.* demonstrated an alternative methodology where a proteinogenic amino acid is released after enzymatic turnover and then incorporated in the translation of a reporter protein [218]. Using this approach, they were able to screen for active penicillin acylase enzymes in single gene droplets. The literature contains fewer examples of compartmentalized *in vitro* assays to screen for protein binders. However, two-hybrid and three-hybrid systems have been developed in PURExpress supplemented with *E. coli* core RNAP enzyme [219]. Cui *et al.* used such an *in vitro* two-hybrid system encapsulated in single-emulsion droplets to screen a library of 105 peptide binders in a single day [220].

Recent work using droplets has diversified beyond the high-throughput screening studies discussed in the previous paragraphs to encompass physical effects such as the influence of crowding [221] or droplet size [222–224] on protein expression. Schwarz-Schilling *et al.* used W/O droplets to compartmentalize streptavidin-coated magnetic beads which act as

a scaffold on which complex RNA-protein nanostructures can be built using TX-TL [225]. The high-throughput generation of such compartments is also attractive for the extensive parameter space mapping for genetic network prototyping, as exemplified by the work of Hori *et al.* discussed in section 2.4.2 [171].

Liquid-liquid phase separation

Liquid-liquid phase separation occurs when a water-soluble molecule, generally a polymer, is mixed with another aqueous solution containing either a high salt concentration or another water-soluble polymer. Under certain conditions, the first polymer cannot dissolve in the second solution, and a separation into two distinct phases occurs. The resulting 'aqueous two-phase system' (ATPS) can form microscale, membrane-less compartments. The recent discovery that ATPS are ubiquitous in cells has attracted much attention to better understand their role in cell physiology [226]. Recreating cell-free transcription-translation reactions in these systems could help elucidate the properties of such condensates.

Torre *et al.* prepared ATPS of dextran/poly(ethylene glycol) or three-phase systems (A3PS) of dextran/poly(ethylene glycol)/ficoll containing TX-TL by vortexing in mineral oil [193] (Figure 2.4B). In the ATPS, expression of the reporter protein indicated preferential partitioning of the TX-TL machinery to the dextran phase in the ATPS. The A3PS, on the other hand, exhibited lower expression, which was attributed to separation of TX-TL machinery into the different dextran and Ficoll phases, suggesting that different liquid phases could differentially partition TX-TL components.

When a liquid-liquid phase separated compartment consists of a condensate of biological polymers, it is most commonly referred to as a coacervate (Figure 2.4B). These coacervates are characterized by a high degree of macromolecular crowding, exhibiting protein concentrations of up to 272 g/L [227], similar to the *E. coli* cytosol. Such crowding can profoundly influence gene expression. Sokolova *et al.* used a microfluidic device to osmotically concentrate droplets containing lysate, and observed the formation of coacervates in lysate containing 2% PEG-8000 [228]. The resultant reporter gene expression was higher in coacervates than in single phase droplets. The work demonstrated that transcription rates were enhanced in the crowded environment of coacervates, offsetting the lower translation rate. Such observations are in agreement with previous studies in bulk cell-free reactions where macromolecular crowding enhances transcription and impairs translation [153]. To generate monodisperse coacervates in high throughput, Tang *et al.* [229] produced coacervates using a microfluidic device [230] starting from a mixture of carboxymethyl-dextran/polylysine and TX-TL. However, they observed lower gene expression in coacervates compared to the bulk reaction, with results suggesting charge-induced precipitation of the reporter protein after its production. This again indicates that protein expression is sensitive to the partitioning of the TX-TL machinery and that the charge of the coacervate and crowded environment can have opposite effects on yields.

Hydrogels

Similar environments to coacervates are found in hydrogels, where a highly porous hydrated network provides a crowded environment. Forming gel micropads by cross-linking X-shaped DNA entrapping plasmid DNA, or P-gel, Park *et al.* obtained an up to 94-fold increase in protein production compared to a standard batch reaction [194, 195] (Figure 2.4C). They explained the increase in expression by an enhanced transcription rate due to the higher proximity of gene templates in the crowded DNA gel environment. The P-gel has also been prepared in a microdroplet format [231] and the microgel format was modified with Ni^{2+} -NTA to allow the immobilization of the expressed protein on the surface of the microgel [232].

The same group showed that TX-TL was also increased in the presence of a clay hydrogel, which spontaneously forms when mixing hydrated clay in the presence of an ionic solution [196] (Figure 2.4C). DNA and RNA molecules localize to the clay hydrogel and are protected from enzymatic degradation by nucleases. The clay-DNA hydrogels were also formulated into microgels containing magnetic nanoparticles allowing for multiple successive TX-TL reactions after recovery of the magnetic microgel and refreshing of the TX-TL mixture [176]. Finally, clay-DNA microgels have been used as artificial nuclei inside W/O emulsions [176] or inside permeable polymeric capsules [206].

Thiele *et al.* prepared hyaluronic acid functionalized with DNA template and produced porous hydrogel microparticles, which were further encapsulated in droplets containing TX-TL [197] (Figure 2.4C). They observed efficient GFP protein expression proportional to the number of encapsulated DNA hydrogel beads, with the fluorescent protein diffusing inside the droplet. By using mRNA molecular beacons, they show that the transcribed mRNA remains trapped in the hyaluronic acid/DNA hydrogel, suggesting that transcription and translation both take place inside the hydrogel.

Aufinger *et al.* prepared agarose functionalized with alkynes and coupled to azide-modified DNA, and used it to prepare hydrogel-DNA 'organelles' [198] (Figure 2.4C). Transcription organelles contained template DNA coding for mVenus with a toehold switch on the 5' end of the mRNA, whereas the translation organelles were functionalized with the corresponding toehold trigger. These organelles were re-encapsulated in W/O droplets containing TX-TL, and mVenus expression was observed only in droplets containing both the transcription and translation organelles. As these organelles can offer spatial organization of complex reactions while providing continuous exchange with the environment, they are useful for building more complex modular systems.

Whereas the previous studies focused on immobilizing the DNA template inside hydrogels, Zhou *et al.* immobilized the complete set of PURExpress His-tagged proteins on a polyacrylamide gel functionalized with Ni^{2+} -NTA [199] or an anti-His-tag aptamer [233] (Figure 2.4C). The His-tagged proteins, ribosomes, and template plasmids are placed on pre-dried hydrogel particles, which effectively traps the ribosomes and plasmids in the hydrogel network by convection when rehydrated. Sustained gene expression is observed for as long as 11 days

when the cell mimics are constantly supplied with fresh feeding buffer.

Liposomes

Liposomes are compartments encapsulated by a lipid bilayer similar to a cell membrane, making them attractive for the encapsulation of cell-free systems. Liposome technology has been recently reviewed by Stano [234]. Early studies used a film hydration method, where the reaction mix rehydrates a dried lipid film to produce liposomes encapsulating TX-TL (Figure 2.4D). This was deployed to translate peptides [235], proteins [236–238], and finally a more complex genetic cascade [239]. Noireaux and Libchaber [200] presented a more convenient method of liposome production called droplet transfer, where a lipid stabilized emulsion of the reaction is first formed in oil and then layered on top of the feeding solution (Figure 2.4D). Liposomal vesicles are subsequently formed by centrifugation. By producing α -hemolysin *in situ*, which assembled to form pores in the liposome membrane, they were able to constantly supply feeding buffer to the encapsulated reaction and increase the duration of expression up to almost 100 hours.

An interesting improvement in the lipid film rehydration method was presented by Nourian *et al.* where they dried the lipid films on 200 μm glass beads and rehydrated them with PURExpress [240]. This allowed them to use low reaction volumes to produce liposomes in high yield and with high encapsulation efficiency. Moreover, they used phospholipids with shorter acyl chains to produce semi-permeable liposomes and incorporated biotinylated lipids for efficient immobilization of the vesicles on microscope slides.

Droplet microfluidics allows for the generation of double emulsions with ultrathin shells where the middle phase contains dissolved lipids and forms unilamellar vesicles after evaporation of the solvent [241] (Figure 2.4D). Ho *et al.* used this technology to encapsulate a mammalian cell-free system with very high encapsulation efficiency, and observe expression of GFP in the interior of the vesicles as well as expression and assembly of a trans-membrane protein [201]. However, they observed in a consequent study that the surfactant necessary for double emulsion led to aggregation of the mammalian cell-free system [202].

By using triblock copolymer surfactants, Deng *et al.* could control the dewetting of the inner water drop from the middle organic phase thus forming perfectly unilamellar and uniform liposomes, in addition to solvent droplets that could be easily separated [242]. A hierarchical assembly of liposomes inside other liposomes, or vesosomes, through multiple successive encapsulation and dewetting was also demonstrated [243]. *In vitro* transcription of Spinach RNA was carried out in the interior ‘nucleus’ liposome and translation of mRFP in the surrounding ‘cytoplasm’ liposome, showing great potential towards bottom-up assembly of complex biomolecular structures, even though controlled transfer of mRNA from the interior to the surrounding liposome remains to be implemented. Finally, a similar method called octanol-assisted liposome assembly (OLA) was developed where the middle phase alkane solvents are replaced by octanol containing lipids and undergo rapid dewetting, which could

further increase the efficiency and biocompatibility of the encapsulation method [203, 204] (Figure 2.4D).

Other membrane compartments

Other types of membrane compartments have also been used for cell-free protein expression, such as polymersomes, protein-based membranes, and polymeric shells (Figure 2.4E). Although there exist many different strategies and materials to make capsules [244], the conditions necessary for their production often prevent encapsulating cell-free systems. Martino *et al.* [245] used a microfluidic capillary device to generate template double-emulsion for the direct encapsulation of a cell-free expression system inside polymersomes composed of PEG-*b*-PLA copolymer and PLA homopolymer to increase their stability. They successfully expressed an MreB protein which formed patches inside the aqueous core and also adhered to the membrane.

Vogele *et al.* used a film rehydration method similar to the one used for liposome production but with amphiphilic elastin-like peptides as building blocks, which formed vesicles upon rehydration with a TX-TL system [205] (Figure 2.4E). They demonstrate that the expression of the elastin-like peptide led to its successful integration into the membrane and an increase in the size of the vesicles after a few hours of expression. Schreiber *et al.* also used amphiphilic peptides to form vesicles and encapsulate a cell-free expression system, and show the production and incorporation of amphiphilic peptide in the membrane [246]. It will be interesting to see in future studies if pore-forming proteins can be incorporated in these 'growing' protein-based membranes, which might allow for prolonged and higher protein expression, as was observed for cell-free protein expression in liposomes. By encapsulating a cell-free extract in millimeter-sized alginate beads coated with polycationic chitosan [247], silica [248], or polyethyleneimine [249], researchers could show continuous expression of eGFP (Figure 2.4E). However, the core of the capsules presented in the previous studies is in a gel format and it is difficult to assess how well the capsules perform as no absolute quantification of the protein levels was provided.

To our knowledge, the only example to date where cell-free protein expression was demonstrated in liquid core-solid shell polymeric capsules was by Niederholtmeyer *et al.* where they produced porous polyacrylate capsules containing a DNA-clay hydrogel nucleus [206] (Figure 2.4E). The capsules' pores are large enough to allow access by large macromolecules including ribosomes. Transcription-translation from the template DNA immobilized in the clay-DNA hydrogel 'nucleus' can be achieved by immersing the capsules in a cell-free expression system. But, as the shell material leads to adsorption of proteins on the capsule surface and the pores are too large to retain the TX-TL machinery, the direct encapsulation of cell-free systems inside polymeric capsules remains to be demonstrated. Such direct encapsulation in synthetic polymeric capsules would be valuable as they could present attractive properties such as high mechanical and chemical stability, as well as tunable porosity, based on the type of shell material and the fabrication method used.

Physical effects of compartmentalization

The effect of the compartment size and interface composition can have notable effects on gene expression. Initial work in Yomo's group showed that expression in sub-picoliter PDMS compartments severely hampered GFP synthesis, whereas quartz glass microcompartments passivated with amino acids showed expression as high as 41% of the test tube reaction with no dependence on compartment volume in a range from 40 fL to 7 pL [250]. They later showed that synthesis of β -glucuronidase (GUS) with fourth-order reaction kinetics was favored in smaller compartments while GUS substrate depletion was rapidly occurring, pointing to an ideal compartment volume [222, 251].

No size dependence on GFP synthesis was observed in a range from 1 to 100 μm in liposomes composed of a mixture of different phosphatidylcholine (PC) or phosphatidylglycerol (PG) lipids and cholesterol [252], in contradiction to previous reports where PG had inhibitory effect on protein synthesis [253]. In lipid stabilised droplets, the charge of the lipid used could also influence the synthesis rate, but in this case the relatively more negative PG lipid was favoured over phosphatidylethanolamine (PE) or PC [224]. Sakamoto et al. [223] proposed a model with three regimes where there could be activation, no regulation, or repression at the surface. In droplets stabilized by PC lipids, they observed protein expression that did not scale with the droplet volume R^3 , but with R^4 for droplets with radii below 17 μm , suggesting surface repression in their system. Other effects could explain variations in fluorescence intensity, such as the exchange of solutes between droplets which is influenced by the composition of the carrier oil, lipid or surfactant, as well as the radius of the droplets [217].

The compartmentalization of biochemical reactions in smaller volumes increases the gene expression stochasticity as only a few molecules are present in each compartment. Hansen et al. [221] suggest that such randomness can be explained by extrinsic noise, which results from the Poisson distribution of encapsulated reagents of the cell-free system, and intrinsic noise, which results from molecular crowding and other parameters such as the stochasticity of the gene expression reactions or relative plasmid distributions. They co-encapsulated CFP and YFP plasmids in droplets with varying levels of crowding, and observed an increase in intrinsic noise with increased levels of crowding. Intrinsic noise in gene expression can also arise from the stochastic partitioning as was strikingly observed in liposomes prepared in dilute solutions of transcription-translation system [254]. A small number of compartments (< 0.5%) displayed detectable eGFP gene expression, whereas no expression occurred in free solution raising interesting questions about the mechanism of loading of the solute mixture.

High variability in gene expression was also observed in liposomes prepared in PURE solutions of normal concentration and interestingly gave rise to some compartments displaying particularly high or long lasting gene expression [255]. These large variations due to stochastic partitioning are interesting as a mechanism to generate diversity in the population, as recently discussed in a review by Altamura *et al.* [256]. Understanding and harnessing these physical effects of compartmentalization potentially offers yet another way of controlling cell-free gene

expression.

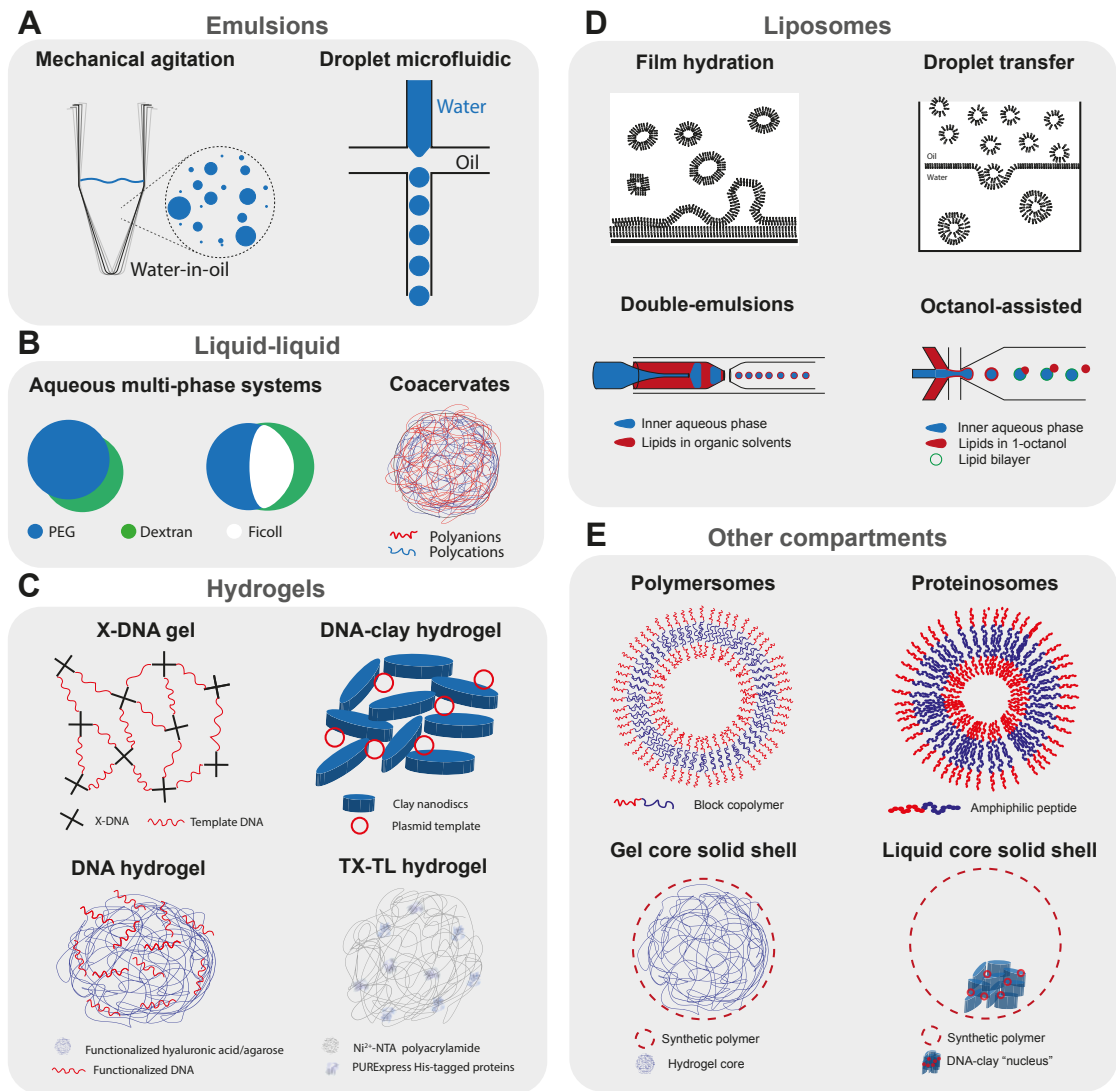


Figure 2.4: **Compartmentalized cell-free reactions.** Schematic representation of the different strategies used to compartmentalize cell-free transcription translation reactions. **(A)** Emulsion-based compartments: polydisperse water-in-oil droplets obtained by mechanical agitation, and microfluidic production of monodisperse droplets. **(B)** Liquid-liquid phase separation: aqueous multiphase systems containing cell-free transcription translation machinery [193], and representation of a complex coacervate. **(C)** Hydrogels: X-DNA linking template DNA and forming a DNA hydrogel [194, 195], a DNA-clay hydrogel [196], hyaluronic acid [197] or agarose [198] functionalized with DNA template, polyacrylamide hydrogel functionalized with Ni²⁺-NTA binding PURExpress His-tagged proteins [199]. **(D)** Liposomes: rehydration of lipid films with an aqueous solution containing TX-TL, droplet transfer method where a lipid-stabilized W/O emulsion is layered on top of a feeding buffer and liposomes transferred to the bottom by centrifugation [200], double-emulsions with ultrathin shells containing lipids in organic solvent [201, 202], and octanol-assisted assembly [203, 204]. **(E)** Other compartments: polymersomes with membrane formed by amphiphilic polymers, proteinosomes with amphiphilic peptides [205], alginate hydrogel coated with various polymers, artificial cells with polymeric shell and liquid core containing a DNA-clay ‘nucleus’ [206].

Communication

Cellular communication is fundamental in biology and responsible for many processes ranging from development to tissue homeostasis. Following the successful developments in compartmentalizing cell-free systems, the next logical challenge consists of engineering inter-compartment communication. On-chip artificial cells consisting of DNA brushes (described in section 2.4.2) were interconnected in series by microfluidic channels, and communication is achieved by diffusion of molecules, which can be tuned by adjusting channel geometry [257] (Figure 2.5A). Diffusion of a σ^{28} activator from one compartment to the next led to sequential switching of a bistable genetic circuit. In a follow-up study, Tayar *et al.* used a non-linear activator-repressor oscillator in compartments coupled by diffusion and observed that the oscillators could be synchronized and tuned by geometric control of diffusion [265]. A key demonstration was that such reaction-diffusion systems could spontaneously form spatial patterns in good agreement with theory.

Moving away from microfluidic chips could potentially allow for the engineering of more complex, dynamic consortia of communicating compartments or even tissue-like assemblies. Schwarz-Schilling *et al.* used capillaries to align W/O droplets encapsulating cell-free extracts as well as *E. coli* cells [258] (Figure 2.5B, top). The bacteria and cell-free systems contained either an AND gate circuit expressing GFP in response to isopropyl β -D-1-thiogalactopyranoside (IPTG) and acyl homoserine lactone (AHL), or a sender circuit producing AHL in response to IPTG. Communication could be established between sender droplets and droplets containing the AND gate, in a cell-free-to-bacteria or bacteria-to-cell-free direction.

Dupin *et al.* used a micromanipulator to arrange multiple directly adjacent W/O droplets in a lipid-in-oil bath, forming a lipid bilayer interface between the compartments [259] (Figure 2.5B, bottom). They show direct communication between sender droplets containing arabinose (ARA) or AHL and droplets containing a responder circuit. By using an incoherent feed-forward loop genelet circuit containing an RNA binding to 3,5-difluoro-4-hydroxybenzylidene imidazolone (DFHBI), they observe the propagation of the DFHBI signal along multiple successive interconnected droplets. Finally, by encapsulating a positive feedback circuit expressing α -hemolysin in response to ARA, they observe an increased variability in protein expression levels among droplets, which they describe as ‘a primitive form of cellular differentiation’.

Liposomes can more closely recapitulate cellular systems. Lentini *et al.* rehydrated liposomes containing a genetic circuit using a riboswitch responding to theophylline to express α -hemolysin and release co-encapsulated IPTG (Figure 2.5C). By incubating *E. coli* with these liposomes acting as signal translators, the bacteria could effectively respond to theophylline in the medium [266]. They later demonstrated that two-way communication is possible between the artificial cells and bacteria by responding to and secreting different AHLs [264] (Figure 2.5C). They even devised a ‘cellular Turing test’ where they compare the expression of quorum sensing genes of *V. fischeri* in the presence of either artificial cells or in a consortium of bacteria. They measure that the artificial cells would be 39% ‘life-like’, but warn that this esti-

mation does not consider that the artificial cells are not fully genetically encoded. Rampioni *et al.* [267] developed synthetic cells which could send quorum sensing molecule C4-HSL to the pathogenic *P. aeruginosa*. Such synthetic cells could have interesting theranostic applications once equipped with additional sensing capabilities such as those discussed in this section.

Two-way communication has been implemented in various contexts, from buffer conditions ideal for artificial cells, to more simple environments such as water or PBS [268]. Other communication modalities have also been explored, such as osmoregulation using a mechanosensitive MscL channel incorporated into liposomes, which opens due to membrane stress in hypotonic environments [261, 262]. Impressively, Berhanu *et al.* encapsulated proteoliposomes containing ATP synthase and bacteriorhodopsin inside liposomes [263] (Figure 2.5C). The artificial cells were able to convert photons to a proton gradient inside the proteoliposomes and drive the synthesis of ATP by ATP synthase, fueling the TX-TL system, effectively making these artificial cells capable of light sensing and even photosynthetic activity.

More complex communication between liposomes was presented by Adamala *et al.*, where they use artificial cells containing either bacterial or mammalian TX-TL systems and use small molecules to communicate between the prokaryotic and eukaryotic artificial cells containing different genetic circuits and cascades [269]. However, the sensing of small molecules is limited to known transcriptional regulators or the theophylline riboswitch. Dwidar *et al.* engineered a riboswitch for the biologically relevant small molecule histamine into liposome-based artificial cells, which could respond to the presence of histamine in a variety of programmed ways [260] (Figure 2.5C). Finally, liposome-based artificial cells expressing *Pseudomonas* exotoxin A were injected *in vivo* inside mice tumors and an increase in caspase activity was shown [270], suggesting their potential use in therapeutic or diagnostic applications.

One major limitation of liposomes is the difficulty in implementing signaling mediated by protein factors, as only small signalling molecules can cross the lipid bilayer with the help of the α -hemolysin pore. The polymeric capsules presented by Niederholtmeyer *et al.* (as discussed in section 2.4.3) are permeabilized by 200–300 nm pores, allowing for the exchange of polymerases and even ribosomes [206]. The authors show a basic form of quorum sensing where the reporter expression increases sharply at a threshold of 400 cell-mimics per 4.5 μ L droplet of TX-TL.

Models have been recently proposed to help understand and implement communication using cell-free systems. These include studies of quorum sensing [271] and the design of spatially distributed compartments [272]. More complex spatial assemblies of compartments capable of communication [273], combined with computation by cell-free TX-TL genetic circuits or other *in vitro* computation methods (such as DNA strand displacement reactions [274], the Polymerase-Exonuclease-Nickase (PEN) DNA toolbox [275], or transcriptional ‘genelet’ circuits [276]), and integration with orthogonal technologies such as electronics [277] may one day allow for the bottom-up engineering of programmable tissues with distributed functional capabilities.

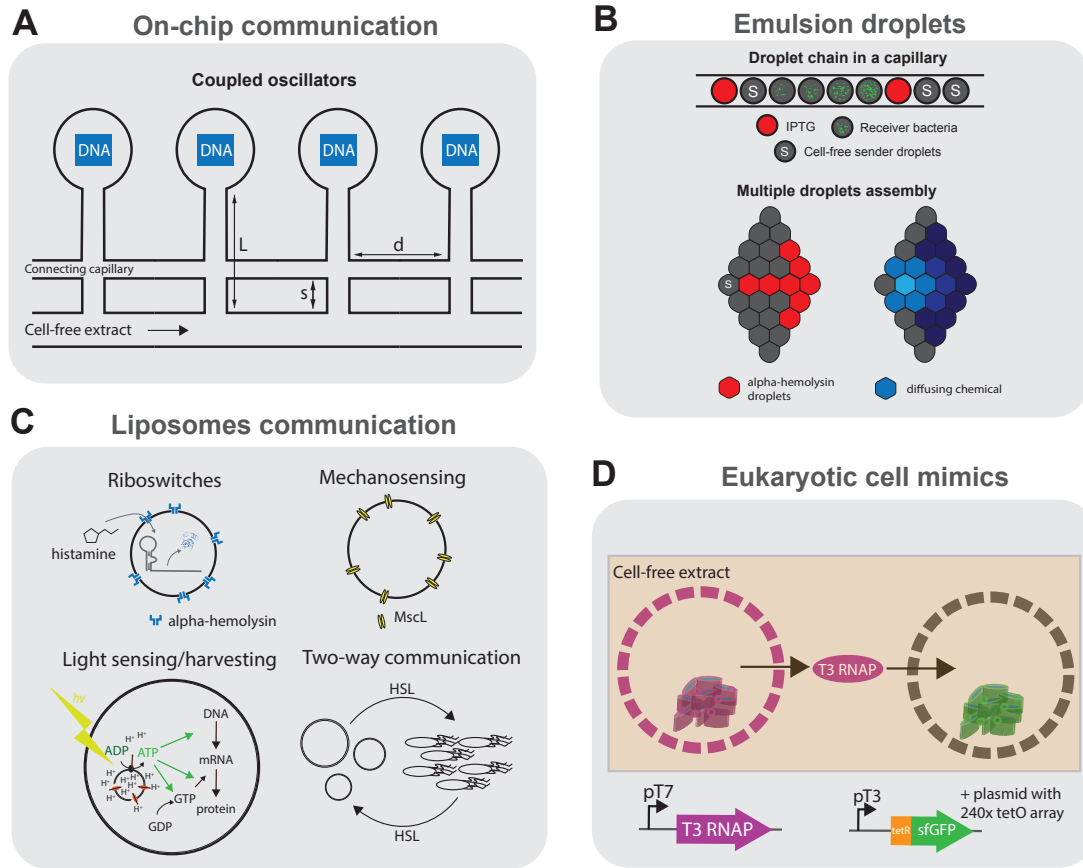


Figure 2.5: **Communication using cell-free transcription translation.** Schematic representation of the different platforms using cell-free transcription translation reactions for communication. **(A)** Artificial cells on chip: DNA compartments are connected to a cell-free reaction feeding channel and interconnected by another capillary allowing the coupling of the compartments [257]. **(B)** Emulsion droplets: top, water-in-oil droplets containing small molecule activators, bacteria or cell-free genetic circuits arranged in a glass capillary [258]; bottom, multiple lipid-stabilized droplets assembled with a micromanipulator with some droplets containing pore forming α -hemolysin [259]. **(C)** Sensing and communication with liposomes: liposomes encapsulating histamine-sensitive riboswitches [260], mechanosensing using MscL pores [261, 262], light-driven ATP synthesis using bacteriorhodopsin and ATP synthase [263], and two-way communication between liposomes and bacteria using various AHLs [264]. **(D)** Eukaryotic cell mimics: microporous polymeric capsules containing a DNA-clay hydrogel 'nucleus' are immersed in cell-free transcription translation. The expressed T3 polymerase can diffuse and activate transcription-translation in another compartment.

2.5 Scientific opportunities

The technical achievements described above have given rise to new research directions involving cell-free gene expression systems. While the pioneering scientific applications of cell-free systems have been the deconstruction and elucidation of molecular biological pathways, today the research landscape is much more varied. Of the numerous active research directions (including biosensing; biomanufacturing; diagnostics; screening; minimal, semi-synthetic, synthetic, and artificial cells; education; and genetic, metabolic, and protein engineering), here we highlight three topics which are particularly relevant in the context of bottom-up construction using cell free systems.

2.5.1 Gene expression regulation

We still lack a complete appreciation for how cells encode, execute, and regulate gene expression [278], which restricts our ability to predictively design new gene regulatory networks or efficiently compose existing modules. Ever since cell-free systems were used to uncover the central dogma, they have contributed profoundly to our understanding of gene expression [73]. In this line of research, PURE and extract systems bring complementary advantages. The PURE system is based on the core components required by the central dogma, and accordingly, can serve as the foundation from which we can build-to-understand basic aspects of gene expression. Extract-based systems serve as environments more similar to their *in vivo* counterparts, but lacking endogenous mRNA and DNA, effectively decoupling them from host processes that can convolute design implementation and data interpretation [121]. This section will highlight recent work that has advanced our understanding of gene expression using cell-free systems to operate at the fertile interface between *in vitro* biochemistry and *in vivo* cell biology.

Biology employs promoters to process input logic and initiate informed transcriptional output [279], an operation believed to lie at the heart of cellular decision-making, yet for which we still possess an incomplete understanding. In investigations of transcriptional regulation, cell-free biology has the benefit of combining complex functional assays with controlled and accessible environments. In contrast to purely *in vitro* research of promoter DNA and transcription factor interactions, cell-free systems have the potential to bridge the divide between promoter occupancy and mRNA production, and help to improve our understanding of the factors that drive transcription. Research from our laboratory by Swank *et al.* [172] used cell-free extract to study the interaction between promoters and the largest family of transcription factors, zinc-fingers. They leveraged the compatibility of cell-free systems with high-throughput assays to quantify the binding-energy landscapes of several synthetic zinc-finger regulators [167]. The precise tuning of repression strength was demonstrated, by mutating the consensus sequence or flanking regions to create small changes in binding affinity. This control facilitated the engineering of gene circuits; adjusting individual binding-site affinities was crucial for optimizing logic gate function for example. By fusing interaction

domains to repressors, cooperativity was engineered between different regulators binding to promoters possessing two binding sites. With the appropriate placement of binding sites, it was shown that cooperativity greatly increased fold-repression and response non-linearity. Notably, the optimal spacing between cooperative repressors was tied to the helical twist of DNA. The repression strength was greatest if the spacing was such that both repressors would bind to the same face of DNA, while repression decayed to match the non-cooperative level as the spacing changed to place the repressors on opposing sides of the DNA. The combination of predictable cooperative interactions and tunable binding affinity guided the engineering of NAND, AND, and OR gates.

Moving away from intragenic composition, intergenic compositional context effects (referring to the position and orientation of entire genes relative to each other on DNA) have also been shown to influence transcriptional regulation [280–283]. Yeung *et al.* arranged genes in convergent, divergent, and tandem orientations, and modelled the relationships (based on torsional stress) between supercoiling and transcription, to support a picture of how supercoiling mediates transcriptional coupling between physically connected genes [283]. Cell-free experimentation served as an important part of the toolkit used to validate their hypotheses and provide evidence for their model. Using cell-free systems, the authors were able to adjust gyrase expression freely, to relax supercoiling and observe the impact on reporter-gene transcription, while avoiding any interference by host-mediated effects. Running cell-free experiments also allowed the authors to control against possible effects coming from plasmid replication. Furthermore, by employing the common practice of expressing linear DNA in cell-free systems [127], Yeung *et al.* were able to investigate the outcome of dissipating peripheral torsional stress, since the ends of linear DNA can rotate freely in response to transcription. Using their insights, the authors leverage supercoiling to build a convergently-oriented toggle switch, which shows a sharper threshold for switching between stable states than the original toggle switch with divergent genes [284].

2.5.2 Resource constraints as a design feature

A current focal point in synthetic biology research is understanding the failure of synthetic biomolecular circuitry due to the coupling of individual circuit components through their competition for the same gene expression resource, and the added coupling with host processes seen in *in vivo* implementations [285–287]. This category of problems, along with other context dependencies, leads to a reduction in design composability, worsening in proportion to circuit size. In recent years, cell-free systems have served as an important research tool to deepen our understanding of resource constraints. Siegal-Gaskins *et al.* exploited the freedom with which DNA concentrations can be varied in cell-free systems to independently quantify the levels of transcriptional and translational cross-talk in cell-free extract [121] (Figure 2.6). They show that increasing the concentration of a second load construct in their reaction results in a decrease in the transcription and translation of the original reporter construct (Figure 2.6B). Loading was largely abolished when the second construct lacked a ribosome binding site

(Figure 2.6C), suggesting that the resource bottleneck was caused primarily through increased protein translation. This result was later found to generalize to *E. coli*. [288]. The effect of an increase in load DNA concentration on reporter protein translation is dependent on the total DNA concentration in the system. At higher total DNA concentrations, translational coupling between genes increases. This was observed experimentally by Siegal-Gaskins *et al.*, where increasing the load DNA in the cell-free system has a greater impact on reporter protein expression when the system contains higher reporter DNA concentrations (Figure 2.6A). In contrast, the way an increase in load DNA concentration affects transcription was found to be independent of DNA for a larger range of concentration values. This result highlights a limiting translation (but not transcription) capacity, which above a certain level of load, causes a simple resource trade-off between proteins being produced.

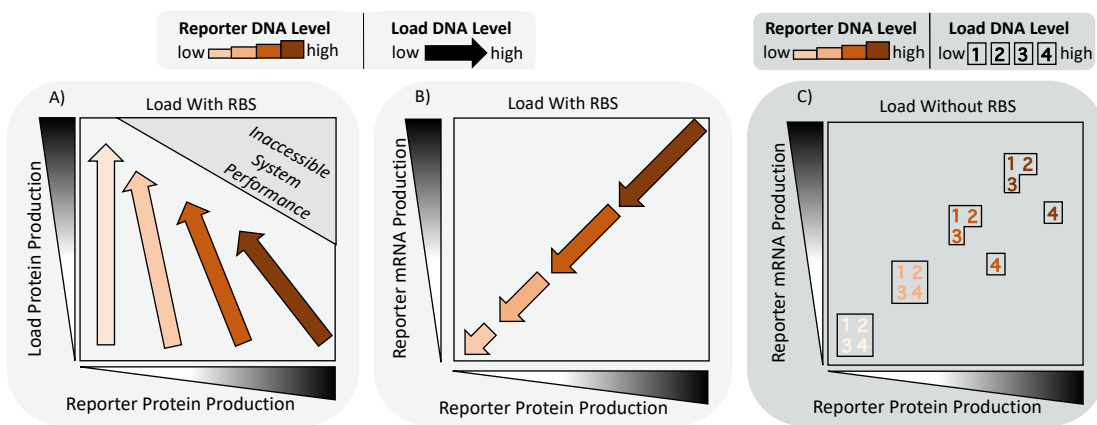


Figure 2.6: **Identifying resource constraints with cell-free gene expression.** Schematic summary of results obtained by Siegal-Gaskins *et al.* [121] (A) The authors observed that at greater reporter DNA concentrations, a given load imposed on the system will produce a larger decrease in reporter protein expression. (B) Loading decreased both transcriptional and translational output from cell-free extract. (C) When the load DNA lacked a ribosome binding site, loading had no effect, except for at the highest combined load and reporter DNA concentrations, suggesting that the bulk of the imposed load is realized through translational processes. In the figure, the relative positioning of numbers in a given box is arbitrary.

A promising direction to improve predictability when composing synthetic parts, in light of resource problems, is to take the primary resources into account in mathematical models, thereby considering non-regulatory interactions between components through resource sequestration [287–289]. Gyorgy *et al.* developed a model that used the previous cell-free extract data obtained by Siegal-Gaskins *et al.* to account for resource competition between genes [290]. They were able to successfully predict expression profiles of multiple co-expressed parts, from data where these parts were characterized individually.

Ceroni *et al.* developed a 'resource capacity monitor' assay implemented in *E. coli* [291], designed to obtain a measure of load imposed on the host by synthetic circuits. They genomically integrated a GFP gene whose output was used to infer the load imposed by synthetic circuitry,

from the relative decrease in GFP when the load is expressed in the host. In a subsequent paper, the same group established a similar approach but using cell-free extract [123], with the reasoning that this avoids growth-dependencies, which cause results to be difficult to interpret since the burden affects growth rate and promotes mutations. They feed the resource-impact data generated from cell-free experiments into a computational model to estimate the resource cost that would be imposed on cells expressing synthetic circuitry employing the proteins they characterized. This strategy could be integrated with cell-free prototyping workflows, to improve the transfer of circuit design from cell-free to *in vivo*, by creating the opportunity to reject resource-demanding implementations. Furthermore, it is imaginable that cell-free extract systems could be adjusted to be resource-constrained in ways that better emulate a given host in order to improve predictive capacity.

Yelleswarapu *et al.* developed a clever oscillator design in cell-free extract that employs resource competition as a functional feature [190]. Their delayed negative feedback topology leverages asymmetric competition between different sigma factors for core RNAP. Studies in this vein can help to improve our understanding of resource competition. By making resource sequestration a design element, circuit failure due to any ‘cross-talk’ through this resource can be reframed as a problem of robust design. By learning design strategies that exhibit the desired behavior over large areas of parameter space, and by figuring out what models properly describe such circuits, we can learn to operate with, and perhaps around, the resource constraints in our biological systems. Even if such a circuit could be implemented successfully *in vivo* using an orthogonal RNAP and sigma-factor system, it would be difficult to untangle the signal of interest from the effects of the asymmetric load that would be imposed on the host. It would be interesting to investigate other resource-related phenomena, like modes of resource coupling or circuit failure following system overloading, using microfluidic chemostats (section 2.4.2), where reaction resources can be varied in a dynamic yet controllable manner.

One interesting strategy to alleviate the resource demands of translation is to implement transcriptional regulation with nucleic-acid hybridization interactions in cell-free systems [292]. Chou *et al.* were able to do this by functionalizing T7 RNAP with single-stranded DNA, so that it can interact with cis-regulatory ssDNA domains on promoters, in a way that is dependent on nucleic-acid assemblies acting analogously to transcription factors. Although this may not directly advance our understanding of how biology encodes native promoters, making the link between gene regulatory networks and DNA strand-displacement reactions could reduce the cost of scaling up computation in genetic circuits, in order to fast-track the investigation of more sophisticated phenomena.

2.5.3 *In vitro* DNA replication

Replication and propagation of genetic material is a key feature of life and is distributed among all living systems, and a robust *in vitro* implementation is crucial in particular for efforts in bottom-up construction of synthetic cells. While self-replicating systems including

autocatalytic peptides, ribozyme replication, or RNA replicators have been established in the past [9], it is crucial to develop a DNA replication system with regard to a transcription-translation based synthetic cell. Here we will focus on efforts to reconstitute DNA replication processes using cell-free TX-TL.

Organisms have evolved a great variety of mechanisms to replicate their DNA, with a broad range of complexity ranging from the eukaryotic replication machinery (consisting of at least five components some of which are further subdivided into complexes [293]), bacterial chromosome and plasmid replication, to simpler bacterial and viral replication strategies. Efforts to achieve *in vitro* reconstitution of DNA replication have focused mostly on the simpler systems.

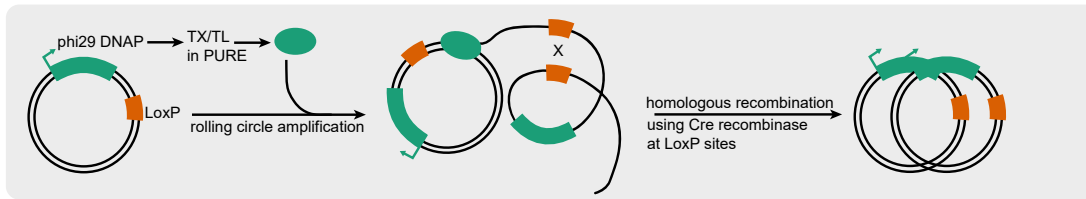
In the 1980s, researchers reported *in vitro* DNA replication in crude cell extract of infected or transfected cells, including replication of plasmid RSF1010 in *P. aeruginosa* and *E. coli* [294], and SV40 virus in monkey and human cell extract [295–297]. By the end of the decade, *in vitro* amplification of DNA became routine with the development of the polymerase chain reaction (PCR). Originally using the Klenow fragment of *E. coli* DNA Polymerase I, which was added anew after each hybridization step [298], the PCR method eventually adopted thermostable polymerases enabling continuous thermal cycling. However, repeated thermal cycling is not ideal for future applications involving synthetic cells, and so work on developing isothermal DNA replication methods remains of interest in this context.

Successful reconstitution of these isothermal machineries was eventually achieved *in vitro*, using partially or entirely recombinantly expressed and purified elements. Examples of these include the *E. coli* replication machinery [299, 300], RSF1010 replication [301], and viral replication systems including the phi29 [302], T7 [303], T4 [304], or SV40 [305] replication machineries.

The establishment of the PURE transcription-translation system has paved the way towards coupling *in vitro* protein expression with DNA replication, with the ultimate aim of reconstituting a self-sustaining system. Sakatani and co-workers expressed the phi29 DNA polymerase (DNAP) in PURE from a circular DNA template, which was then able to replicate the latter via a rolling circle amplification [29]. The same group further developed their system based on a concept proposed by Forster and Church [306], introducing recombinantly expressed Cre recombinase, that re-circularized an evolved form of the DNA template at the lox sites [30]. They took advantage of the tunability of their home made PURE system by optimizing the NTP concentration, which is necessary for protein expression, yet was shown to inhibit DNA replication. Van Nies and co-workers reported that PURE-expressed phi29 DNAP and terminal protein (TP) were able to amplify a linear DNA template encoding both proteins, in presence of recombinantly expressed single stranded and double stranded binding proteins (SSB, DSB) [34]. Those four proteins were shown to be necessary and sufficient for DNA replication of the phi29 bacteriophage [302, 307].

Fujiwara and coworkers implemented an *in vitro* DNA replication machinery by mimicking

A: DNA replication using rolling circle amplification and homologous recombination



B: DNA replication of a linear template DNA



C: DNA replication by *in vitro* expressed *E.coli* DNA Pol III

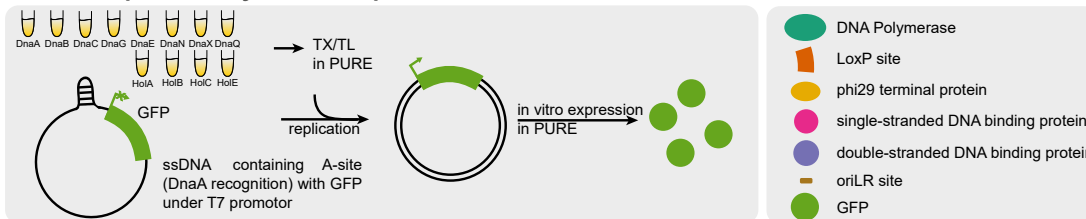


Figure 2.7: Coupling DNA replication and cell-free gene expression. Schematic representation of methods to couple *in vitro* transcription-translation to DNA replication. **(A)** Sakatani and coworkers [29, 30] coupled *in vitro* expression of phi29 DNAP to rolling circle amplification of circular DNA and finally concluded their round of replication by re-circularizing the replicated DNA using homologous recombination by Cre recombinase at LoxP sites. **(B)** Van Nies and coworkers [34] reconstituted the native phi29 life cycle by replicating a linear DNA template flanked by oriLR sites expressing phi29 DNAP and TP *in vitro*, and adding recombinant SSB and DSB to the reaction. **(C)** Fujiwara and coworkers [156] expressed the *E.coli* DNA Pol III holoenzyme *in vitro*. The enzyme was shown to replicate the second strand of a single stranded linear template containing an A-site; the resulting duplex DNA enables GFP expression.

E. coli DNA replication. Using the PURE system, they expressed the machinery consisting of initiator (DnaA), helicase and helicase loader (DnaB and DnaC), DNA primase (DnaG), and the DNA polymerase III holoenzyme consisting of 9 different proteins. By achieving the correct assembly of the holoenzyme in PURE, they furthermore showed the possibility to assemble a complex holoenzyme in the absence of chaperones by decreasing the cell-free expression temperature. The *in vitro*-expressed proteins were able to replicate an artificial gene circuit which expressed GFP in the PURE reaction system [156].

Despite these advances, one major challenge on the way to implementing a self-sustaining DNA replication system remains to be addressed. Current approaches couple gene expression with DNA replication using only a couple of consecutive batch reactions. To ensure continuous replication in a future synthetic cell, it will be necessary to achieve continuous, multi-round replication, which could be explored for instance, in microfluidic chemostats as described in section 2.4.2. It has yet to be demonstrated that DNA replication can be achieved over many consecutive cycles, which may prove to be rather challenging as it appears that current DNA replication methods are rather inefficient and produce DNA in low-quantities [30, 34].

During long term replication, mutations will appear, among which some will enable the mutated DNA template to replicate faster than the original template, due to length or altered codon usage. This parasitic DNA may eventually out-compete the original DNA template, if no selection pressure is applied. Compartmentalization, as discussed above in section 2.4.3, may be a method to address this challenge, as discussed in [9]. Furthermore, implementation of a stable, continuous platform for *in vitro* DNA replication would enable the study of the evolutionary dynamics of molecular replicators, as the system is well-defined, simple, tunable, and does not rely on life-sustaining processes. This may additionally be linked with compartmentalization, where *in vitro* evolution of DNA polymerase using an error prone PCR approach has already been reported [308].

In vitro coupling of transcription-translation with DNA replication is just at the beginning of its development, and it will be interesting to see what the limitations of the systems are. To our knowledge, only phi29 genomic DNA and plasmids have been replicated using coupled *in vitro* expression/replication systems to date. Successful determination of limits such as size, accuracy, and energetic requirements to carry out *in vitro* replication may eventually enable the self-replication of all genes required to sustain a synthetic cell.

2.6 Outlook

The bottom-up approach is but one way of addressing the formidable challenge of reliably building complex synthetic biological systems, and it will necessarily be combined with other complementary methods. However, the key principle of building to understand is undoubtedly a powerful motivation, and cell-free systems represent perhaps one of the best examples where this is currently being put into practice. While cell-free systems have historically been used to deconstruct biology, allowing its core processes to be elucidated, recent advances have led to

its increasing application to construct biological systems.

Today, basic cell-free lysate systems are less of a black-box, and better characterization of their properties and preparation methods has made them an increasingly engineerable, and maybe more importantly, accessible tool. Recombinant systems have been the focus of increasing investigation as users demand more modularity and cost-effectiveness. Technological innovation in automation, microfluidics, and materials science have enabled increased throughput, dynamic control of steady-state reactions, and sophisticated compartmentalization strategies, while at the same time becoming accessible to more labs around the world.

However, there are also clear challenges ahead. Compartmentalizing cell-free reactions has exposed important physical effects, such as crowding and differential partitioning, which, while complex, may one day be harnessed to control the microscale spatial organisation of gene expression. This level of fine control, exhibited by all cells, currently eludes us. Cell-free gene expression studies have unveiled a number of effects such as physical properties of promoters, supercoiling and compositional context dependencies, and the ever-present resource burden of heterologous gene circuits. Replication studies have pointed out to the difficulty of achieving efficient DNA replication and protein synthesis in a cell-free reaction. And while increasingly complex communication systems have been implemented, the field is still in a nascent stage.

A common theme in constructing complex systems is emergence: as the system grows in size, effects appear which cannot be predicted by assessing the parts independently. In synthetic biology, these confounding effects currently stymie many efforts. But it is exactly because cell-free studies allow us to work at the interface between simple and complex systems that they are well-poised to address these issues. Ultimately, a thorough understanding of these effects will allow us to turn what are currently viewed as design constraints into design features, thereby expanding the scope and potential of synthetic biology.

3 One Pot PURE system

This work was published in the Journal of Visualized Experiments (JoVE), 2021 [309]. The corresponding video can be found here: DOI: 10.3791/62625-v

Reference: Grasmann, L. *, Lavickova, B. *, Elizondo-Cantu, M. C., & Maerkl, S. J. (2021). OnePot PURE cell-free system. *JoVE (Journal of Visualized Experiments)*, (172), e62625.

Contribution: L.G. and B.L. are shared first authors. L.G., B.L., and M.C.E. performed the experiments. L.G., B.L., and S.J.M. wrote the manuscript. The work is based on and adapted from the following publication: Lavickova, B., & Maerkl, S. J. (2019). A simple, robust, and low-cost method to produce the PURE cell-free system. *ACS synthetic biology*, 8(2), 455-462.

3.1 Summary

We present a fast and cost-effective method to produce the recombinant PURE cell-free TX-TL system using standard laboratory equipment.

3.2 Abstract

The defined PURE (protein synthesis using recombinant elements) transcription-translation system provides an appealing chassis for cell-free synthetic biology. Unfortunately, commercially available systems are costly, and their tunability is limited. In comparison, a home-made approach can be customized based on user needs. However, the preparation of home-made systems is time-consuming and arduous due to the need for ribosomes as well as 36 medium scale protein purifications. Streamlining protein purification by coculturing and co-purification allows for minimizing time and labor requirements. Here, we present an easy, adjustable, time- and cost-effective method to produce all PURE system components within 1 week, using standard laboratory equipment. Moreover, the performance of the OnePot PURE is comparable to commercially available systems. The OnePot PURE preparation method expands the accessibility of the PURE system to more laboratories due to its simplicity and cost-effectiveness.

3.3 Introduction

Cell-free transcription-translation (TX-TL) systems constitute a promising platform for investigating and engineering biological systems. They provide simplified and tunable reaction conditions, as they no longer rely on life-sustaining processes, including growth, homeostasis, or regulatory mechanisms [44]. Thus, it is anticipated that cell-free systems will contribute to the investigation of biomolecular systems, offer a framework to test rational biodesign strategies [310], and provide a chassis for a future synthetic cell [311, 312]. The fully recombinant PURE system offers an especially appealing chassis due to its defined and minimal composition, as well as its adjustability and tuneability [2].

Since the first functional, fully recombinant PURE system was established in 2001 [2], efforts have been made to expand the system limits and optimize the system's composition to improve the system yields [25, 27, 138] allow for transcriptional regulation [147], membrane[150, 152] and secretory protein synthesis [149], and to facilitate protein folding [148, 151]. Nowadays, there are three commercially available systems: PUREflex (GeneFrontier), PURExpress (NEB), and Magic PURE (Creative Biolabs). However, those systems are costly, their exact composition is proprietary and thus unknown, and adaptability is limited.

PURE systems prepared in-house proved to be the most cost-effective and tunable option

[132, 313]. However, the required 37 purification steps for protein and ribosome fractions are time-consuming and tedious. Several attempts have been made to improve the efficiency of the PURE system preparation [134–136]. We recently demonstrated that it is possible to coculture and co-purify all required non-ribosomal proteins present in the PURE system. This OnePot method has proved to be cost-effective and time-efficient, cutting down preparation time from several weeks to 3 working days. The approach generates a PURE system with a protein production capacity comparable to the commercially available PURExpress system [137]. Contrary to the previous approaches to simplify the PURE preparation [134–136], in the OnePot approach all proteins are still expressed in separate strains. This enables the user to tune the composition of the OnePot PURE system by merely omitting or adding specific strains or adjusting the inoculation volumes, thus generating dropout PURE systems or altering the final protein ratios, respectively.

The protocol presented here provides a detailed method for creating the OnePot PURE system as described previously [137], although β -mercaptoethanol was replaced with tris(2-carboxyethyl)phosphine (TCEP). Moreover, two methods for ribosome purification are described: traditional tag-free ribosome purification using hydrophobic interaction and sucrose cushion, adapted from Shimizu et al. [132], and Ni-NTA ribosome purification based on Wang et al. [134] and Ederth et al. [314], but significantly modified. The latter method further facilitates the preparation of the PURE system and makes it accessible to more laboratories, as only standard laboratory equipment is required.

The experimental protocol summarizes the preparation of a versatile PURE cell-free TX-TL system to provide a simple, tunable, cost-effective cell-free platform, which can be prepared using standard laboratory equipment within a week. Besides introducing the standard PURE composition, we indicate how and where it can be adjusted, with a primary focus on critical steps in the protocol to ensure the system's functionality.

3.4 Protocol

NOTE: This protocol describes the preparation of cell-free TX-TL system from recombinant components. For convenience, the work is separated into five parts. The first part describes preparation steps, which should be done before starting the protocol. The second part describes the preparation of the OnePot protein solution. The third part describes ribosome purifications, the fourth part details the preparation of the energy solution, and the last part provides a manual for setting up a PURE reaction. For convenience, the protocols are divided into days and summarized in daily schedules in 3.1. Following the schedule, the whole system can be prepared in 1 week by one person.

1. Preliminary work

- 1) Prepare the bacterial culture media and media supplements as described in Supplementary Table 3.3. Prepare and sterilize the materials required, including pipette tips, 96 deep-well plates.
- 2) Strain preparation
 - 1) Transform the expression strains indicated in Table 3.2 2 with the corresponding expression vectors using the heat shock method.
 - 1) Add purified plasmid to the chemically competent bacteria and incubate on ice for 20-30 min.
 - 2) Place the mixture at 42 °C for 30 s (heat shock) and then place it back on ice for 2 min.
 - 3) Pipette 20 µL of the bacteria directly onto agar plates containing ampicillin (AMP) and incubate at 37 °C overnight. Store the plates at 4 °C for up to 1 week.
 - 4) Inoculate 3 mL of LB media containing AMP with a single colony of bacteria from the agar plates. Incubate at 37 °C while shaking at 260 rpm overnight.
 - 5) Mix 250 µL of the culture with 250 µL of 50% (v/v) glycerol and store at -80 °C.
NOTE: For faster preparation in the future, store the strains in a 96-well plate as glycerol stocks.
 - 2) Confirm all vector transformations by colony PCR and sequencing. Sequence the gene, promoter region, and ribosome binding site.
- 3) Expression test
 - 1) Inoculate 300 µL of LB media containing AMP with around 1 µL of the prepared glycerol stocks in a 1.3 mL deep-well plate. Seal the plate with a breathable membrane and then incubate at 37 °C while shaking at 260 rpm overnight.
NOTE: All expressions are done separately at this point.

- 2) Inoculate 300 μ L of fresh LB media containing AMP with 1 μ L of the overnight cultures. Incubate at 37 °C while shaking at 260 rpm overnight. After 2 h, induce the cells with 100 μ M of Isopropyl β -D-1-thiogalactopyranoside (IPTG) and grow for an additional 3 h.
- 3) Mix 10 μ L of the culture with 10 μ L of 2x Laemmli buffer and heat to 95 °C for 10 min. Spin the samples for 1 min using a table centrifuge and load 10 μ L of the supernatant on a PAGE gel. Run the gel in Tris/Glycine/SDS buffer at 200 V for 30 min. Rinse it well with deionized water. Cover the gel with a Coomassie protein stain and incubate for 1 h. Destain the gel in water if necessary (representative results for the expression test in Figure 3.1).

NOTE: Use gradient (4%-15% or 4%-20%) PAGE gels to achieve a good separation.

4) IMAC Sepharose resin restoration and cleaning

1) Column preparation.

- 1) Mix the Sepharose resin well by vortexing.
- 2) Pipette the required amount of resin into an empty gravity flow column.
NOTE: The amount of resin required varies between His-ribosome purification and protein purification and is specified in the respective sections.
- 3) Wash the resin with 30 mL of deionized water.
- 4) Proceed with column re-charge as specified in section 1.4.4.
NOTE: Always let all the liquid pass through the column before continuing with the next step. However, make sure that the column never runs dry. Whenever running any liquid through the column, ensure to stop the flow or continue to the next step as soon as the liquid reaches the resin.

2) Restoration.

- 1) Wash the column with 30 mL of deionized water.
- 2) Apply 10 mL of a 0.2 M EDTA and 0.5 M NaCl solution.
- 3) Add 30 mL of a 0.5 M NaCl solution.
- 4) Wash the column with 50 mL of deionized water.
- 5) Store in 20% (v/v) ethanol at 4 °C or continue with the next step.

3) Cleaning.

CAUTION: Wear protective equipment.

- 1) Wash the column with 30 mL of 0.5 M NaOH.
- 2) Wash the column with 30 mL of deionized water.
- 3) Wash the column with 30 mL of 0.1 M acetic acid.
- 4) Wash the column with 30 mL of deionized water.
- 5) Wash the column with 30 mL of 70% (v/v) ethanol.
- 6) Wash the column with 50 mL of deionized water.
- 7) Store in 20% (v/v) ethanol at 4 °C or continue with the next step.

- 4) Re-charging.
 - 1) Add 10 mL of 0.1 M nickel sulfate solution to the column.
CAUTION: Nickel sulfate is toxic. Nickel sulfate waste needs to be discarded with the precautions indicated by the supplier.
 - 2) Wash the column with 50 mL of deionized water.
 - 3) Store in 20% ((v/v)) ethanol at 4 °C or continue with the column equilibration.
NOTE: If the column is stored in ethanol between steps, make sure to remove all traces of ethanol by washing the column with water.

2. OnePot protein solution expression and purification

NOTE: The protocol consists of three parts divided into days (Figure 3.2). An ideal preparation procedure produces 1.5 mL of 13.5 mg/mL OnePot protein solution, which corresponds to more than one thousand 10 μ L PURE reactions. However, the amount and the ideal concentration of the solution will vary from batch to batch. Experienced users can perform multiple OnePot PURE preparations at a time.

Day 1:

- 1) Prepare bacterial culture media and media supplements as described in Supplementary Table 3.3.
- 2) Prepare and sterilize the required materials, including pipette tips, two 96 deep-well plates, and one 1 L baffled Erlenmeyer flask.
- 3) Prepare buffers and supplements as described in Supplementary Table 3.4. Filter sterilize all buffers using bottle top filters (0.45 μ m) and store them at 4 °C. Supplement all the buffers with 1 mM TCEP right before use, unless indicated otherwise.
- 4) Use 2 mL of sepharose resin for the OnePot protein purification. Prepare the column as described in section 1.4.
- 5) To prepare the starter cultures, combine 20 mL of LB media with 20 μ L of AMP. In a sterile 96, 1.3 mL deep-well plate, add 300 μ L of the media into 35 wells. Inoculate each of them with its respective strain, except elongation factor thermo unstable (EF-Tu), and seal the plate with a breathable membrane.
NOTE: Inoculate the plate using a 96-well replicator (see Table 3.10). The well volume of the deep-well plate and the volume of the starter culture are essential. Larger media volumes or smaller well volumes will lead to a different bacterial density due to aeration inconsistencies.

- 6) For the EF-Tu culture, inoculate 3 mL of LB media in a 14 mL culture tube with a snap cap. A single 3 mL of culture for EF-Tu is sufficient for one OnePot expression culture.
- 7) Incubate at 37 °C while shaking at 260 rpm overnight.

Day 2:

NOTE: Perform all the steps at room temperature unless indicated otherwise.

- 8) Transfer 500 mL of LB media and 500 µL of AMP into the sterile baffled flask.
- 9) Inoculate the OnePot PURE culture with 1675 µL of the EF-Tu culture and 55 µL of each of the cultures from the deep-well plate (Table 3.2).
NOTE: During this step, the overall protein composition can be adjusted by tuning the inoculation ratios. Make sure that the overall inoculation volume remains constant at 3.6 mL.
OPTIONAL: To confirm that all strains have grown overnight, measure the optical density of the overnight cultures at 600 nm (OD₆₀₀) in a 96-well plate using a plate-reader. Use a dilution of 10x for the optical density measurement.
- 10) Incubate the culture for 2 h at 37 °C with a shaking of 260 rpm, or until the OD₆₀₀ of the culture reaches 0.2-0.3.
- 11) Induce the culture with 500 µL of 0.1 mM IPTG and grow for an additional 3 h.
- 12) Harvest the cells by centrifugation at 4 °C and 3220 x g for 10 min and store the cell pellet at -80 °C until further use.
NOTE: To optimize the timing, prepare the energy solution described in section 4 during the incubation times on day 2 (Table 3.1).

Day 3:

- 13) Measure the amounts of buffers needed for the purification described in the steps below and add TCEP to all of them as indicated in Supplementary Table 3.2. Store the remaining buffers without TCEP at 4 °C for future purifications.
- 14) Equilibrate the charged column (section 2.4) with 30 mL of buffer A. After 25 mL of buffer A have passed through, close the column from the bottom. In parallel, continue with steps 2.15-2.17.
- 15) Thaw the cells and use a serological pipette to resuspend the cell pellet in 7.5 mL of buffer A.
- 16) Lyse the cells using a 130-watt probe sonicator (see Table 3.10, probe tip diameter: 6 mm) with the following parameters: 4 x 20 s pulse on, 20 s pulse off, 70% amplitude. If sonication is successful, the solution will turn darker (Figure 3.2).

NOTE: Make sure to keep the cells on ice during sonication. Place the probe deep enough into the solution without touching the tube. If a large amount of foam is generated, the energy transfer will be damped. In that case, let the foam settle, lower the probe deeper into the solution, and extend the sonication time.

- 17) Remove the cell debris by centrifugation at 21130 x g for 20 min at 4 °C immediately after sonication. Keep the lysate on ice.
- 18) Add the supernatant to the equilibrated column. Close the column from the top and make sure there is no leakage. Incubate the column for 3 h at 4 °C under rotation using a tube rotator.
- 19) Elute unbound components from the column and wash with 25 mL of buffer A.
- 20) Wash the column with 25 mL of 25 mM imidazole buffer (23.95 mL of buffer A and 1.25 mL of buffer B).
- 21) Elute the proteins with 5 mL of 450 mM imidazole buffer (0.5 mL of buffer A and 4.5 mL of buffer B). Keep the eluted proteins on ice at all times.
- 22) Dilute the eluate with 25 mL of HT buffer, keep the mixture on ice. Add 15 mL to a 15 mL centrifugal filter and concentrate to a volume of 1.5 mL. Add the remaining 15 mL to the filter with the concentrated solution and concentrate to 1.5 mL once more.
- 23) Add 10 mL of HT buffer to the concentrated sample and concentrate to 1 mL. Add an equal amount of stock buffer B and store at -80 °C until further use
NOTE: One round of exchange/concentration takes about 60 min spinning at 3220 x g at 4 °C.
- 24) During the buffer exchange, restore the column as specified in section 1.4.

Day 4:

- 25) Measure the protein concentration using the Bradford assay as described by the supplier. Concentrate the sample with a 0.5 mL of 3 kDa cutoff centrifugal filter to 20 mg/mL.
NOTE: Dilute the protein solution 25-fold or 50-fold before the concentration measurements to avoid oversaturating the Bradford assay.
- 26) To establish the ideal protein concentration, perform an expression test at this stage (section 5.2) with different concentrations of the protein solution. To perform the titration, keep the total volume of the solution constant and pipette the OnePot protein solution, including stock buffer B, at five different ratios (Supplementary Table 3.9).
- 27) Verify the OnePot PURE protein composition using SDS-PAGE (Figure 3.3A). Dilute 2.5 µL of the sample with 7.5 µL of water, mix with 10 µL of 2x Laemmli buffer and

then load 5 μ L and 2.5 μ L of the samples to the gel. Run the SDS-PAGE as specified in section 1.3.3.

- 28) Aliquot the protein solution into 50 μ L aliquots after verifying the expression and adjusting the concentration. Store the OnePot PURE protein solution at -80 °C until further use.

NOTE: If a protein component is suspected not to be present, or is present in a lower-than-expected concentration in the OnePot PURE, perform the following steps.

- 29) Check whether the overnight culture of the respective strain has grown at a comparable rate to the other cultures by performing optical density measurements (OD_{600}) of all cultures.
- 30) Perform an additional expression test of the specific strain to verify the expression of the suspect protein.

3. Ribosome solution

NOTE: Two different ribosome purification strategies are introduced, one for hexahistidine-tagged and one for non-tagged ribosomes. The major advantage of the purification method using His-purification on a standard affinity Ni-NTA gravity flow column is that the purification is easy, fast, and does not require additional laboratory equipment, such as a FPLC system and an ultracentrifuge. However, the protein production capacity in OnePot PURE reactions is around one-third compared to tag-free ribosomes. Therefore, choose the method for ribosome production based on whether a high yield is important for the given application.

1) His-tagged ribosome purification

NOTE: This protocol utilizes the E. coli RB1 strain, a gift from Professor Wang (Columbia University, USA) [134]. This strain has a genomic insertion of a hexahistidine tag on the C terminus of 50S ribosomal protein (L7/L12), allowing for purification using a Ni-NTA gravity-flow column. The usual yield is around 0.5 mL of 3.45 μ M ribosomes, which is sufficient for more than five hundred 10 μ L PURE reactions.

Day 1:

- 1) Prepare bacterial culture media and media supplements as described in Supplementary Table 3.3.
- 2) Prepare and sterilize the required materials, including pipette tips, two 96 deep-well plates, and one 1 L baffled Erlenmeyer flask.
- 3) Prepare buffers and supplements as described in Supplementary Table 3.4. Filter sterilize all buffers using bottle top filters (0.45 μ m) and store them at

4 °C.

Day 2:

- 4) Pipette 5 mL of resin to a column and prepare the column as specified in section 1.4.

NOTE: Due to the higher volume of the resin, the restoration and purification take significantly longer. Use a different column for ribosome purification to avoid cross-contamination and thoroughly clean it before the purification.

- 5) Prepare an overnight culture of E. coli RB1 strain by inoculating 35 mL of LB media in a 100 mL Erlenmeyer flask. Incubate at 37 °C while shaking at 260 rpm.

Day 3:

NOTE: Perform all the steps at room temperature unless indicated otherwise.

- 6) Add 2 L of LB media into a 5 L sterile flask, inoculate with 12 mL of the overnight culture, and then incubate for 3-4 h at 37 °C while shaking at 260 rpm.

NOTE: Alternatively, perform bacterial culturing in 4 x 500 mL of cultures in 1 L baffled flasks.

- 7) Pellet the cells by centrifugation for 10 min at 3220 x g and 4 °C. Store at -80 °C until further use.

Day 4:

- 8) Equilibrate the column prepared in step 3.1.4. with 30 mL of lysis buffer.
- 9) Resuspend the pellet in 20 mL of lysis buffer using a serological pipette.
- 10) Lyse the cells with a 130-watt probe sonicator (see Table 3.10, probe tip diameter: 6 mm) on ice with the following parameters: 11 x 20 s pulse on; 20 s pulse off, 70% amplitude (see step 2.16 for procedure details).
- 11) Immediately after sonication, remove the cell debris by centrifugation for 20 min at 21130 x g at 4 °C. Keep the lysate on ice.
- 12) Load the supernatant to the columns and let it pass through.
- 13) Wash the column with the following mixtures of lysis and elution buffers.
 - 1) Wash 0: use 30 mL of lysis buffer.
 - 2) Wash 1: use 30 mL of 5 mM imidazole (29 mL of lysis buffer, 1 mL of elution buffer).
 - 3) Wash 2: use 60 mL of 25 mM imidazole (50 mL of lysis buffer, 10 mL of elution buffer).

- 4) Wash 3: use 30 mL of 40 mM imidazole (22 mL of lysis buffer, 8 mL of elution buffer).
- 5) Wash 4: use 30 mL of 60 mM imidazole (18 mL of lysis buffer, 12 mL of elution buffer).
- 14) Elute the ribosomes with 7.5 mL of the elution buffer. Keep the eluted proteins on ice at all times.
- 15) Add 22 μ L of pure *beta*-mercaptoethanol to 45 mL of ribosome buffer.
CAUTION: *beta*-mercaptoethanol is toxic. Take safety precautions and work in a fume hood.
- 16) Add the eluate to a 15 mL centrifugal filter and concentrate to 1 mL.
- 17) Add 15 mL of ribosome buffer to the concentrated sample and concentrate again to 1 mL.
NOTE: Repeat the previous step twice.
- 18) Store at -80 °C until further use.
NOTE: One round of exchange/concentration takes about 60 min of centrifugation at 3220 x g at 4 °C.
- 19) During the buffer exchange, restore the column as specified in section 1.4.

Day 5:

- 20) Determine the ribosome concentration by measuring the absorbance at 260 nM of a sample diluted 1:100 in ribosome buffer. An absorbance value of 10 of the diluted solution corresponds to 23 μ M of undiluted solution as previously described [315].
- 21) Implement a final stock concentration of 3.45 μ M. To adjust the concentration, dilute the ribosomes with ribosome buffer or concentrate them further by centrifugation at 14000 x g in a 3 kDa 0.5 mL centrifugal filter at 4 °C.
NOTE: To achieve optimal system expression, perform a ribosome concentration titration (section 5.2, Supplementary Table 3.9).
- 22) Verify the ribosome composition using SDS-PAGE (Figure 3.3A) as specified in section 1.3.3. Dilute 2.5 μ L of the sample with 7.5 μ L of water, mix with 10 μ L of 2x Laemmli buffer, and then load 5 μ L and 2.5 μ L of the samples onto the gel.

2) Tag-free ribosome purification

NOTE: Tag-free ribosome purification is performed using a FPLC system (Table 3.10) and is based on hydrophobic interaction chromatography using 2 x 5 mL Butyl columns (Table 3.10). Although ribosomes may be purified from any strain, using the E. coli A19 (E. coli Genetic Resources at Yale CGSC) strain is advantageous due to its RNase I deletion [315]. Perform the purification at 4 °C in either a cold room or a cooling cabinet. The usual yield is around 0.5 mL of 10 μ M ribosomes,

which corresponds to more than five hundred 10 μ L PURE reactions.

Day 1:

- 1) Prepare bacterial culture media and media supplements as described in Supplementary Table 3.3.
- 2) Prepare and sterilize the required materials, including pipette tips, 5 L Erlenmeyer flask, and 100 mL Erlenmeyer flask.
- 3) Prepare buffers and supplements as described in Supplementary Table 3.4. Filter sterilize all the buffers using bottle top filters (0.45 μ m) and store them at 4 °C.

Day 2:

- 4) To prepare an overnight culture of the E. coli A19 strain, inoculate 35 mL of LB media in a 100 mL Erlenmeyer flask. Incubate at 37 °C while shaking at 260 rpm.

Day 3:

- 5) Transfer 2 L of LB media into the 5 L sterile baffled flask, inoculate with 30 mL of the overnight culture, and then incubate for 3-4 h at 37 °C while shaking at 200 rpm.
- 6) Pellet the cells by centrifugation at 4000 x g for 15 min at 4 °C. Resuspend the pellet in 25 mL of suspension buffer and store at -80 °C until further use.

Day 4:

- 7) Perform steps 3.2.8-3.2.12 in parallel with steps 3.2.13-3.2.19.
- 8) Thaw and lyse the cells using a 130-watt probe sonicator (see Table 3.10 and probe tip diameter: 6 mm) on ice with the following parameters: 12 x 20 s pulse on; 20 s pulse off, 70% amplitude (see step 2.16 procedure details).
- 9) Immediately remove the cell debris by centrifugation at 20000 x g for 20 min at 4 °C.
- 10) Aspirate the supernatant and measure the volume. Add an equal volume of suspension buffer (high salt) to adjust the final concentration of ammonium sulfate to 1.5 M and mix well.
- 11) Remove the precipitate by centrifugation at 20000 x g for 20 min at 4 °C.

- 12) Filter the supernatant using a 0.45 μm polyethersulfone membrane syringe filter before FPLC purification and collect the filtrate in a 100 mL glass bottle. Keep the supernatant at 4 °C at all times.
- 13) Set up the FPLC system for hydrophobic-interaction chromatography purification using a double Butyl column (2 x 5 mL) as follows. For this setup, one column volume (CV) refers to a volume of 10 mL.
- 14) Three inlets will be needed: two as buffer lines and one as the sample line. Due to the default settings of the purifier, it is convenient to choose lines A1 and B1 for buffer C and buffer D, respectively, and line A2 as the sample line. Apply a default flow rate of 4 mL/min, except for pump washes (10 mL/min) or unless indicated otherwise.
NOTE: As TCEP is a costly reagent, add the corresponding amount to buffers C and D only after the equilibration step.
- 15) Perform a system pump wash in 20% ((v/v)) ethanol to clean the system and remove potential contamination from previous purifications. Manually set a flow rate of 0.2 mL/min and mount the column. Stop the flow.
- 16) Execute a system pump wash with water. Wash the column with 3 CV of water.
- 17) Equilibration: place inlets A1 and A2 in buffer C and inlet B1 in buffer D without TCEP. Execute a pump wash and equilibrate the column with 4 CV of buffer C.
- 18) Add TCEP to buffers C and D.
- 19) Prepare 15 mL tubes or clear round fraction collector tubes to the fraction collector to collect 4-5 mL elution fractions.
- 20) Loading: Place the inlet A2 into the bottle with the filtered sample. Load approximately 90% of the sample volume onto the column. Dilute the sample with 20 mL of TCEP-containing buffer C, and load 10 mL of the sample onto the column. Repeat the dilution step at least twice and load as much sample onto the column as possible. It is critical to ensure that no air is sucked into the machine.
- 21) Washing step 1: wash with 3 CV of buffer C to remove the unbound components.
- 22) Washing step 2: wash with 5 CV of 80% buffer C and 20% buffer D.
- 23) Elution: elute the product by applying 50% of buffer C and 50% of buffer D, with a total elution volume of 5 CV. Collect this fraction in the collector tubes.
- 24) Washing step 3: Elute all strongly interacting contaminants using 100% buffer D with a total volume of 5 CV.
- 25) Analyze the absorption spectrum of the sample fraction at 260 or 280 nm (Figure 3.4). The first peak shows the non-absorbed proteins eluted during loading and the first washing step; the second peak shows contaminants that have been eluted during the second washing step. The third peak monitors

the final product, and the last peak shows the strongly interacting contaminants. Pool all sample fractions corresponding to the third peak for further processing. Keep the eluted proteins on ice at all times.

- 26) Gently overlay the recovered fraction onto 15 mL of the cushion buffer in four polycarbonate ultracentrifugation tubes. Add a maximum of 15 mL of the sample to 15 mL of the cushion buffer. Make sure to balance the weight of the tube well. Pellet the ribosomes by ultracentrifugation at 100000 x g at 4 °C for 16 h.

NOTE: Ensure that no cracks are present in the ultracentrifugation tubes.

- 27) Clean and reset the column as follows. A flow rate of 5 mL/min works well. Place all the inlets into the water and execute a pump wash. Wash the column with 2 CV of water.
- 1) Place the inlet into a 0.5 M NaOH solution, perform a pump wash, and subsequently wash the column with 3 CV of NaOH.
 - 2) Place the inlet into water, perform a pump wash, and then wash the column in 2 CV of water.
 - 3) Place the inlet to a 0.1 M acetic acid solution, perform a pump wash, and subsequently wash the column with 3 CV of acetic acid solution.
 - 4) Pump wash and wash the column with 2 CV of water.
 - 5) Place all inlets into 20% ((v/v)) ethanol, execute a pump wash step, and store the column in 20% ((v/v)) ethanol by washing it with 3 CV of a 20% ((v/v)) ethanol solution.

NOTE: Ensure that the system never runs dry or sucks in air. Never apply buffer directly to ethanol, or ethanol to buffer. Always add a water washing step in between, as otherwise there is a risk of precipitates clogging the column. Make sure to add enough sample collection tubes.

Day 5:

- 28) Discard the supernatant and carefully, without disturbing the translucent pellet, wash each pellet with 0.5 mL of ice-cold ribosome buffer. Repeat this step twice.
- 29) Resuspend each of the clear pellets in 100 µL of ribosome buffer on ice using a magnetic stir bar (3 mM diameter, 10 mM length) on a magnetic stirrer using the lowest possible speed. Collect the resuspended ribosomes and wash the tubes with an additional 50 µL of ribosome buffer.
- NOTE: The translucent pellet is difficult to see. Therefore, carefully wash the pellet from the sides of the tube.
- 30) Determine the ribosome concentration by measuring the absorbance at 260 nM of the sample diluted at a ratio of 1:100 in ribosome buffer. An absorbance

of 10 of the diluted solution corresponds to 23 μM of undiluted solution as previously described [313].

- 31) Implement a final stock concentration of 10 μM . To adjust the concentration, dilute the ribosomes with ribosome buffer or concentrate them further by centrifugation at 14000 x g in a 3 kDa centrifugal filter at 4 °C.

NOTE: To achieve optimal system expression, perform ribosome titration (section 5.2, Supplementary Table 3.9).

- 32) Verify the ribosome composition with SDS-PAGE (Figure 3.3A) as specified in section 1.3.3. Dilute 2.5 μL of the sample with 7.5 μL of water, mix with 10 μL of 2x Laemmli buffer, and then load 5 μL and 2.5 μL of the samples to the gel.

4. Energy solution

NOTE: The composition for the 2.5x energy solution introduced here is an example of a solution that worked well for a standard TX-TL reaction. To optimize the timing, prepare the energy solution during day 2. The preparation of the amino acid solution is explained in detail, followed by the final preparation procedure.

1) Amino acid solution

NOTE: Prepare the amino acid solution in bulk. Preparing the amount of amino acid stock solutions required for a final volume of at least 2000 μL will reduce the weighing error for the otherwise very small amounts. The overall concentration of the amino acid solution is limited by the solubility of the amino acids and the respective stock solution concentrations. For the standard PURE system, prepare a solution with a final concentration of 3.25 mM. Use the amino acid solution calculation table (Supplementary Table 3.5) as a template. Use cysteine in the salt form to ensure sufficient solubility. Avoid using KOH-based amino acid preparation methods. It is possible to directly weigh the exact amounts of amino acids into the final amino acid solution without preparing stock solution for all the amino acids. However, this is more challenging and less precise.

- 1) Prepare stock solutions for each amino acid as described in Supplementary Table 3.5, except for Tyrosine.

NOTE: Due to the different solubilities of the amino acids in water, the respective suggested concentrations of the stock solution differ.

- 2) Minimal mass [mg] provides the approximate minimum mass required to obtain a sufficient amount of stock solution for the target overall volume, as a reference.

NOTE: The minimal mass is calculated with a surplus of 10%.

- 3) For an easier preparation of the solutions, do not weigh the exact amount of amino acid, but instead, for the mass at hand, adjust the amount of water to

achieve the desired concentration. Calculate the amount of deionized water (Water to add [μL]) needed, based on the actual mass filled in (light yellow cells) and the desired concentration using the spreadsheet in Supplementary Table 3.5.

- 4) Solubilize the amino acid stock solutions by vortexing until all precipitate has dissolved. The individual amino acid stock solutions can be stored at $-20\text{ }^{\circ}\text{C}$ for several weeks.

NOTE: Some amino acids are difficult to dissolve in water; the process may take some time.

- 5) Weigh the exact amount of tyrosine required to obtain a final concentration of 3.25 mM directly into the tube for the amino acid solution.

NOTE: Tyrosine is very difficult to dissolve in water. Add it directly instead of preparing a stock solution.

- 6) Add the corresponding amounts of amino acid stock solutions and water as indicated in the Final volume to add [μL] column (light blue cells) and vortex the solution well. Store the completed amino acid solution at $-80\text{ }^{\circ}\text{C}$ until further use.

2) Preparation of the energy solution

NOTE: In total, the 2.5x energy solution contains 0.75 mM of each amino acid, 29.5 mM of magnesium acetate, 250 mM of potassium glutamate, 5 mM of ATP and GTP each, 2.5 mM of CTP, UTP, and TCEP, respectively, 8.75 mg/mL of tRNA from *E. coli* MRE 600, 50 mM of creatine phosphate, 0.05 mM of folinic acid, 5 mM of spermidine, and 125 mM of HEPES. First-time users prepare the energy solution in small batches of $200\text{ }\mu\text{L}$. Store the individual solutions prepared according to Supplementary Table 3.6 at $-20\text{ }^{\circ}\text{C}$ or $-80\text{ }^{\circ}\text{C}$ for later use.

- 1) Thaw all aqueous solutions mentioned in the Supplementary Table 3.7 on ice.
- 2) Meanwhile, prepare the stock solutions for the remaining components listed in Supplementary Table 3.6. Keep all the solutions on ice after preparation.
NOTE: Add $500\text{ }\mu\text{L}$ of RNase and DNase-free water directly to the vial to dissolve the lyophilized tRNAs. Mix well by gentle vortexing; limit pipetting to avoid introducing RNases.
- 3) Add the calculated volumes (Supplementary Table 3.7) of stock solutions and water and mix well using a vortex. Keep the solution on ice at all times.
- 4) Measure the pH of the solution by pipetting $1\text{ }\mu\text{L}$ onto a pH strip, to ensure that the pH of the solution is neutral.
- 5) Aliquot the energy solution at $50\text{-}100\text{ }\mu\text{L}$ per tube on ice and store at $-80\text{ }^{\circ}\text{C}$ until further use. While aliquoting, vortex the main stock frequently to prevent the components from precipitating.

NOTE: Optionally, conduct an activity assay of the newly made energy solution against commercial energy solutions, e.g. Solution A in PURExpress. If

a significantly lower performance of the system with the energy solution is observed, optimizing the ion concentrations, especially magnesium ions, by titration (5-20 mM) may be advantageous.

5. OnePot PURE reaction

1) DNA template

NOTE: Proteins encoded downstream of the T7 promoter can be expressed in PURE from either linear or circular DNA. By generating a linear DNA template using extension PCR, tedious cloning steps can be omitted. The linear templates for this study were generated by PCR as described below, using a high-fidelity DNA polymerase (Table 3.10). Primer sequences, melting temperatures, and the thermocycler settings used in this study are specified in Supplementary Table 3.8. The preparation of the DNA template is not included in the daily schedule.

1) Set up a PCR reaction as recommended by the polymerase supplier.

NOTE: Optimized parameters for a high-fidelity DNA polymerase (Table 3.10) are given in Supplementary Table 3.8.

2) Amplify the target gene (e.g., eGFP) as a linear template from a plasmid or genome using gene-specific primers (500 nM) (for the parameters, see Supplementary Table 3.8).

3) The amplification generates short extensions to provide annealing sequences for the following extension PCR steps.

4) Check the amplicon on an agarose gel for correct size and purity.

5) Use the amplified DNA as a template for the subsequent extension steps. Set up a reaction of at least 50 μ L.

6) Run 10 PCR amplification cycles with the extension primers (2.5 nM). After completing the amplification cycles, immediately add the final primers (500 nM) to the same reaction and run 30 cycles to amplify the extended PCR product. Find the melting temperatures and primer sequences in Supplementary Table 3.8.

7) Purify the DNA fragments using a DNA purification kit and elute the DNA in nuclease-free water instead of EDTA containing elution buffer.

8) Check the linear template on an agarose gel for correct size and purity.

9) Measure the DNA concentration in ng/ μ L using an UV-Vis spectrophotometer.

2) Setting up the PURE reaction

NOTE: The final reaction composition is 1x energy solution, tag-free ribosomes or His-tag ribosomes, OnePot PURE proteins, and DNA template. The reaction volume ratio comprises 40% energy solution, 30 protein and ribosome solution, and 30% DNA and water. Typical reaction volumes vary between 5 μ L and 25 μ L. Quantify the expression of a fluorescent protein continuously on a plate-reader. Use a

Green Lys in vitro Translation Labeling System, which incorporates fluorescently labeled Lysine residue into newly synthesized proteins, to verify the expression of non-fluorescent proteins on a SDS-PAGE gel. An example reaction template is given in Supplementary Table 3.9 to help establish a PURE cell-free expression reaction. Cells in yellow indicate user-input values, and cells in orange indicate additional reagents to be optionally added to the reaction. Keep the volume ratios of the components precise to ensure the correct ion balance. For instance, to achieve a higher protein concentration, increase the OnePot protein solution concentration; however, do not increase the volume of protein solution added to the reaction.

- 1) Perform the following steps for Green Lys labeled samples.
- 2) After the cell-free expression, incubate the sample with 0.16 $\mu\text{g}/\mu\text{L}$ of RNase A for 30 min at 37 °C to remove the fluorescent background of the Green Lys labeling kit.
NOTE: Use RNase A, as other types of RNases do not remove the background sufficiently well.
- 3) Visualize the protein expression by running SDS-PAGE as specified in section 1.3.3. Wash the unstained gel gently in deionized water, and image it on a fluorescent imager using an excitation wavelength of 488 nm.
- 4) Subsequently, stain the gel using conventional Coomassie staining methods. For the suitable parameters see section 1.3.3.
NOTE: Perform a titration of the protein solution with the recommended ribosome concentration and, if required, titrate ribosomes with the optimal OnePot protein concentration afterward. Use the commercial PURExpress Δ Ribosome kit as a positive control. Solution A, Factor Mix, and the ribosome solution correspond to the prepared energy, the OnePot protein solution, and the purified ribosomes, respectively.

3.5 Representative results

The above protocol is designed to facilitate establishing the PURE cell-free TX-TL system in any laboratory. The protocol includes a detailed description of the preparation of the three distinct parts of the PURE system: the OnePot protein, ribosome, and energy solution. A detailed daily schedule, which optimizes the workflow, is shown in Table 3.1. The workflow is optimized for the purification of His-tagged ribosomes, and time frames may differ slightly if tag-free ribosome purification is performed. One preparation provides a sufficient amount of PURE for a minimum of five hundred 10 μL reactions. Moreover, the prepared solutions are stable for more than a year at -80 °C and can withstand multiple freeze-thaw cycles.

Adequate overexpression levels for all strains are crucial for the functionality of the final protein solution. Figure 3.1 shows successful overexpression in all 36 individual strains used

subsequently for the OnePot protein preparation. Variation in the over-expressed proteins' band intensities occurred most probably due to a bias in loading volumes onto the SDS-PAGE gel. The expected protein sizes are summarized in Table 3.2. GlyRS and PheRS consist of two subunits of various molecular weights; the remaining 34 proteins consist of a single subunit. Key to this protocol's simplicity and time-effectiveness is the coculturing and co-purification step (Figure 3.2). The OnePot protein solution was prepared by increasing the ratio of EF-Tu strain with respect to all the other expression strains. The overall composition of the final proteins was analyzed by SDS-PAGE (Figure 3.3A). From the gels (lanes 2, 3), it is noticeable that EF-Tu (43.3 kDa) is present in a higher concentration compared to the other proteins, as expected. While the gel provides a good first indication of protein expression ratios, it is difficult to determine whether and at which level each individual protein was expressed. Therefore, it is highly recommended to confirm the overexpression in each strain before coculturing, as shown above.

The *E. coli* ribosome is a complex molecular machine composed of over 50 individual protein subunits [316]. A representative absorption spectrum at 260 nm for tag-free ribosome purification is shown in Figure 3.4; the third peak is characteristic of successful ribosome elution. For both ribosome purification methods, the expected running pattern on the SDS-PAGE gel (Figure 3.3A)[134] was observed. We did observe contaminations for both purifications, albeit in small quantities (<10%). Notably, different contaminants were present in the tag-free (lanes 5, 6) and His-tagged (lanes 11, 12) ribosomes due to the variation in the method. For user reference, the SDS-PAGE gels for the combined systems are also included (lanes 8, 9, and 14, 15).

Lastly, the performance of the prepared systems (Figure 3.3) using the different ribosome variants are compared. The time courses of in vitro eGFP expression show that both PURE systems are functional and produce fluorescent eGFP. However, the OnePot protein solution combined with the His-tagged ribosomes, using the ribosome concentration optimized by titration, yielded only one-third of the expression level of the non-tagged ribosome version (Figure 3.3B). Similar results were observed when three proteins of different sizes were expressed and labeled using the Green Lys tRNA in vitro labeling system (Figure 3.3C). As seen on the fluorescent gel, full-length products were successfully expressed in both systems; however, only around half of the expression level was achieved with the His-tag ribosome system. In addition to the fluorescence labeling, the expected bands for all three proteins are distinguishable on a Coomassie-stained gel (Figure 3.3D). The results show that the introduced expression system, which can be prepared within a week in a laboratory with standard equipment, can be used for the in vitro expression of proteins encoded downstream of the T7 promoter from linear templates.

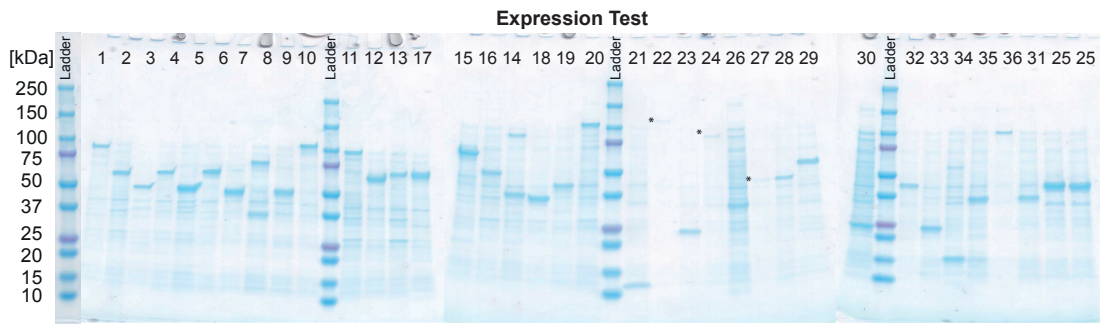


Figure 3.1: **Representative results for the overexpression test for all expression strains of the PURE system.** PURE protein numbers and sizes are summarized in Table 3.2. Protein numbers 21, 24, and 27 are marked with a star for better visualization.

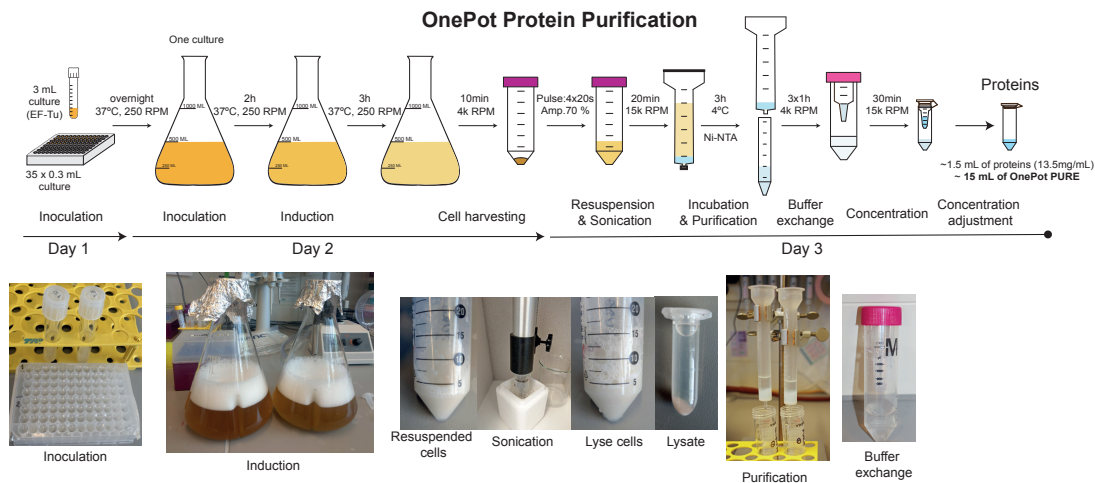


Figure 3.2: **OnePot protein purification.** The schematic depiction and corresponding photographs of all steps involved in the production of the OnePot protein solution.

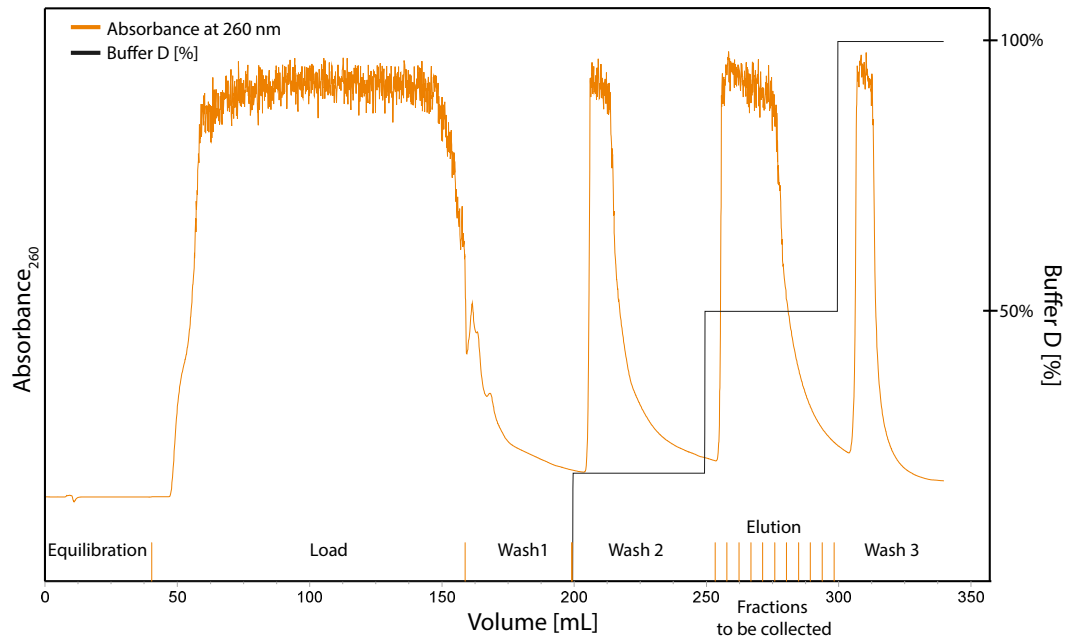


Figure 3.3: **Performance of the prepared systems using the different ribosome variants.** (A) Coomassie blue stained SDS-PAGE gels of the OnePot protein solution (lanes 2, 3), tag-free ribosomes without protein solution (lanes 5, 6) and with protein solution (lanes 8, 9), His-tagged ribosomes without protein solution (lanes 11, 12) and with protein solution (lanes 14, 15). Two different concentrations were loaded per sample. (B) Comparison of eGFP expression of His-tagged ribosomes and tag-free ribosomes. The fluorescence intensity of in vitro eGFP expression is monitored over time for a PURE reaction using tag-free ribosomes (1.8 μM , blue) and His-tagged ribosomes (0.62 μM , red). The concentrations of the linear template and the OnePot protein solution were 4 nM and 2 mg/mL, respectively. Panels (C) and (D) show the SDS-PAGE gel of proteins synthesized in OnePot with tag-free (1.8 μM , blue, lanes 3, 4, 5) and His-tag ribosomes (0.62 μM , red, lanes 6, 7, 8) labeled with a GreenLys in vitro labeling kit (C) and stained with Coomassie blue (D), respectively. The black arrows indicate the expected bands of synthesized proteins: eGFP (26.9 kDa), ArgRS (64.7 kDa), T7 RNAP (98.9 kDa). The linear template and OnePot protein solution concentrations were 4 nM and 1.6 mg/mL, respectively.

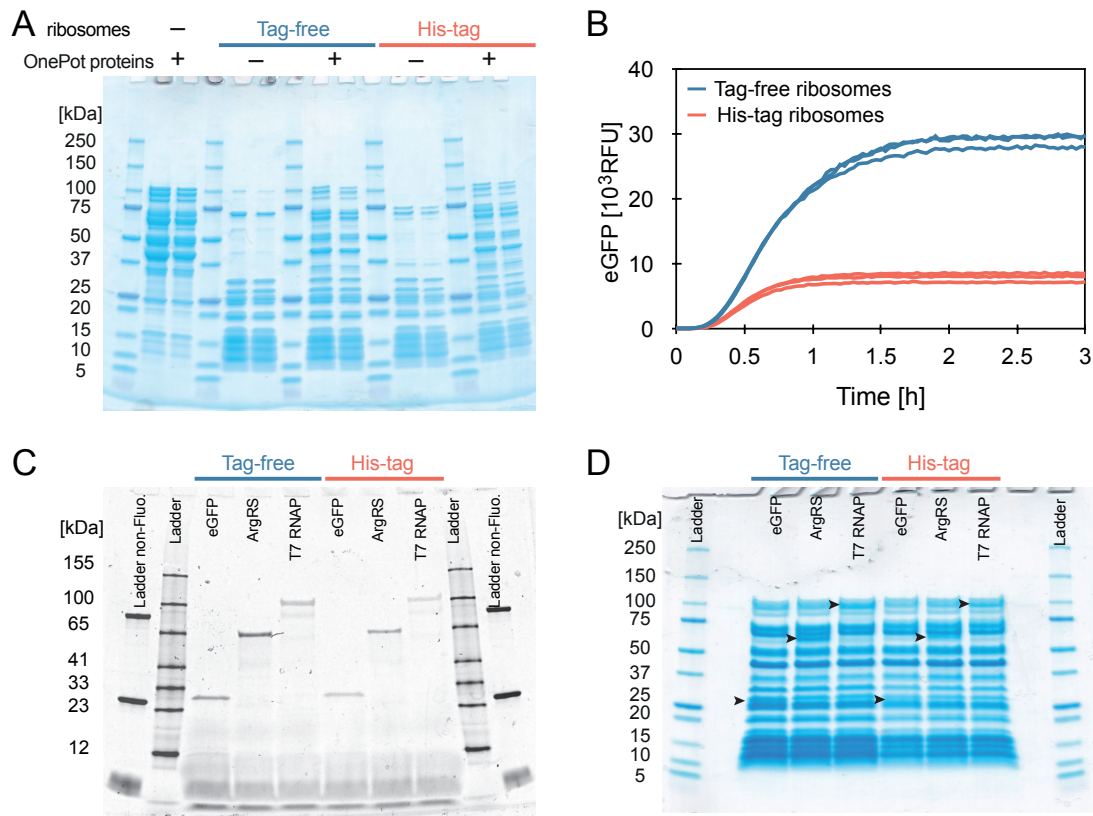


Figure 3.4: **Absorbance spectra at 260 nm.** Representative results of absorbance spectra at 260 nm during hydrophobic interaction purification of tag-free ribosomes.

3.6 Discussion

The protocol presented here describes a simple, time- and cost-effective method to prepare a versatile PURE expression system [137] based on the standard composition [132]. By utilizing the protocol together with the supplied daily schedules (Table 3.1), all components can be prepared in 1 week and yield amounts sufficient for up to five hundred 10 μ L PURE reactions. Since the proteins used in this protocol are overexpressed from high copy plasmids and have low toxicity to *E. coli*, good expression levels are observed for all the required proteins (Figure 3.1). This allows for the easy adjustment of strains, and therefore also protein composition in cocultures, simply by modifying the ratios of the inoculation strains [137]. Besides the ribosomal proteins, the concentration of EF-Tu showed to be of fundamental importance for expression yields [138]. In contrast, changes in the concentration of the other protein components had a relatively low impact on the robustness of the PURE system [27, 139]. Therefore, by adjusting the inoculation ratio of EF-Tu with regard to all the other components, a comparable composition to the standard PURE composition can be achieved, and a PURE system with a similar yield [137] can be attained. In preparing the protein solution, it is crucial to ensure that all strains grow well and overexpress the encoded protein after induction (Figure 3.1).

Ribosome function is key for the overall performance of the PURE system [139]. In this protocol, two different methods for preparing the ribosome solution are demonstrated, i.e., tag-free and His-tagged ribosome purification. The tag-free ribosome purification is based on hydrophobic interaction chromatography followed by centrifugation with a sucrose cushion, which requires access to a FPLC purification system and an ultracentrifuge [132]. In contrast, the method utilizing His-tagged ribosomes [134] and gravity flow affinity chromatography purification does not require specialized equipment and can be performed in most laboratories. The latter method, therefore, brings advantages such as simplicity and accessibility. However, we observed a significantly lower synthesis yield when using the His-tagged ribosomes in the OnePot PURE compared to the tag-free variant (Figure 3.3). Based on the type of application, this lower yield may be acceptable.

The energy solution provides the low molecular weight components and tRNAs required to fuel in vitro TX-TL reactions. This protocol provides a recipe for a typical energy solution, which can be easily adjusted based on user needs. Together with tRNA, NTP, and creatine phosphate, the abundance and concentration of Mg²⁺ ions have been crucial for the overall performance of the PURE system [25], as they are critical cofactors for transcription and translation. In some cases, the titration of ions can, therefore, greatly enhance the overall PURE performance. DNA integrity is crucial for PURE performance. Thus, sequence verifying the promoter region, ribosome binding site, and target gene and ensuring that an adequate DNA concentration (<2 nM) will help troubleshoot issues that may arise while setting up a PURE reaction.

The PURE system is a minimal TX-TL system, and specific applications may thus require

additional adjustments [22]. These may include incorporating different RNA polymerases [42, 147], chaperones [148], and protein factors such as EF-P or ArfA [25]. Although the expression strains for these proteins can be included in the cocultures, adding them separately to the prepared system may provide better control of the required protein levels. Furthermore, the inclusion of vesicles is essential to the production of membrane proteins [150, 152]. Oxidizing rather than reducing environments and a disulfide bond isomerase facilitate proper disulfide bond formation, which are, for example, required for secretory proteins [149].

It is essential to ensure that any additional components do not interfere with the reaction. The most important factors to pay attention to when setting up a reaction or adding other components are listed below. Ensure that neither incompatible buffers are used nor the ion concentrations are disturbed. Avoid solutions containing glycerol, high concentrations of potassium, magnesium, calcium ions, osmolytes, pyrophosphate, antibiotics, or EDTA, as much as possible. For example, replacing an elution buffer with water during DNA purification can be beneficial as EDTA is a common additive in this buffer. Supplying the solutions with additional negatively charged molecules such as NTP or dNTP requires adjusting the magnesium concentration [25], as the negatively charged molecules behave as chelating agents and bind positively charged molecules. A neutral pH is ideal for the reaction. Accordingly, all components should be buffered to the corresponding pH; this is especially important for highly acidic or basic molecules such as NTPs. Lastly, temperature and volume are key parameters for the reaction. To achieve a good yield, one should implement a temperature around 37 °C, as temperatures below 34 °C will significantly reduce the yield [3].

It is relevant to note that before preparing the OnePot PURE, one should consider the target application and the associated requirements, such as volume, purity, ease of modification, and inclusion or omission of components. For many applications, the system will be an excellent choice, but others may require yields, adjustability, and other factors, which the OnePot system cannot provide. Irrespectively, the introduced protocol will be beneficial for the preparation of any home-made system, as all critical steps for such preparation are summarized here.

One of the main advantages of the OnePot system is its compatibility with the commercially available PURExpress system, which provides the possibility of testing the functionality and integrity of all components separately by sequentially replacing each PURExpress component with its OnePot equivalent. The advantages of the OnePot PURE system, such as tunability and easy, fast, and cost-effective preparation, will make cell-free TX-TL accessible to more laboratories worldwide and contribute to expanding the implementation of this powerful platform in cell-free synthetic biology.

3.7 Supplementary Information

3.7.1 Supplementary tables

The interactive excel files of the following supplementary tables can be downloaded from the publication website. Tables 3.8 and 3.9 have been slightly modified to fit the format of this thesis.

Table 3.1: A daily time-optimized schedule for the preparation of all the OnePot PURE solutions.

DAILY SCHEDULE						
Time	Mon	Tue	Wed	Thu	Fri	
8:00 AM	Preparation LB media/ autoclave	Inoculation		Inoculation		
8:30 AM			Cell resuspension, lysis, centrifugation			
9:00 AM		Cell growth	Column preparation	Cell resuspension, lysis, centrifugation	Column preparation	
9:30 AM						Concentration adjustment (or ribosome resuspension)
10:00 AM	Buffer preparation					
10:30 AM		Induction		Cell harvest		
11:00 AM			Incubation on column			
11:30 AM		Other components				
12:00 PM	Buffer preparation	Protein expression		Purification	SDS-PAGE gel	SDS-PAGE gel
12:30 PM		Components mixing				
1:00 PM			Purification			
1:30 PM		Cell harvest				
2:00 PM			Column regeneration			
2:30 PM						Expression test
3:00 PM	Column preparation & resin cleaning	Column preparation & Resin cleaning (only for Ni-NTA purification)	Buffer exchange and concentration	Buffer exchange and concentration (or ultracentrifugation)	Column regeneration	
3:30 PM						
4:00 PM						
4:30 PM						
5:00 PM	Starter culture	Starter culture		Concentration adjustment		
5:30 PM						
6:00 PM						

Active time	Energy solution
Active time	Protein solution
Passive time	
Active time	Ribosome solution
Passive time	

Table 3.2: PURE protein list

#Addgene	Number	Protein	Protein name	Size [kDa]	Vector	Strain	Induction volume [μ L]	Note
#124103	1	AlaRS	Alanyl-tRNA synthetase	96.0	pQE30	M15	55	
#124104	2	ArgRS	Arginyl-tRNA synthetase	64.7	pET16b	BL21(DE3)	55	
#124105	3	AsnRS	Asparaginyl-tRNA synthetase	52.6	pQE30	M15	55	
#124106	4	AspRS	Aspartate-tRNA synthetase	65.9	pET21a	BL21(DE3)	55	
#124107	5	CysRS	Cysteiny-tRNA synthetase	52.2	pET21a	BL21(DE3)	55	
#124108	6	GlnRS	Glutaminy-tRNA synthetase	63.5	pET21a	BL21(DE3)	55	
#124109	7	GluRS	Glutamyl-tRNA synthetase	53.8	pET21a	BL21(DE3)	55	
#124110	8	GlyRS	Glycyl-tRNA synthetase	34.8 & 76.8	pET21a	BL21(DE3)	55	2 subunits
#124111	9	HisRS	Histidyl-tRNA synthetase	47.0	pET21a	BL21(DE3)	55	
#124112	10	IleRS	Isoleucyl-tRNA synthetase	104.3	pET21a	BL21(DE3)	55	
#124113	11	LeuRS	Leucyl-tRNA synthetase	97.2	pET21a	BL21(DE3)	55	
#124114	12	LysRS	Lysyl-tRNA synthetase	57.8	pET21a	BL21(DE3)	55	
#124115	13	MetRS	Methionine-tRNA ligase	76.3	pET21a	BL21(DE3)	55	
#124116	14	PheRS	Phenylalanyl-tRNA synthetase	36.8 & 87.4	pQE30	M15	55	2 subunits
#124117	15	ProRS	Prolyl-tRNA synthetase	63.7	pET21a	BL21(DE3)	55	
#124118	16	SerRS	Seryl-tRNA synthetase	48.4	pET21a	BL21(DE3)	55	
#124119	17	ThrRS	Threonyl-tRNA synthetase	74.0	pQE30	M15	55	
#124120	18	TrpRS	Tryptophanyl-tRNA synthetase	37.4	pET21a	BL21(DE3)	55	
#124121	19	TyrRS	Tyrosyl-tRNA synthetase	47.5	pET21a	BL21(DE3)	55	
#124122	20	ValRS	Valyl-tRNA synthetase	108.2	pET21a	BL21(DE3)	55	
#124123	21	IF1	Initiation factor 1	8.3	pQE30	M15	55	
#124124	22	IF2	Initiation factor 2	97.4	pQE30	M15	55	
#124125	23	IF3	Initiation factor 3	20.6	pQE30	M15	55	
#124126	24	EF-G	Elongation factor G	77.6	pQE60	M15	55	
#124127	25	EF-Tu	Elongation factor Tu	43.3	pQE60	M15	1675	
#124128	26	EF-Ts	Elongation factor Ts	30.4	pQE60	M15	55	
#124129	27	RF1	Release factor 1	40.5	pQE30	M15	55	
#124130	28	RF2	Release factor 2	41.2	pET15b	BL21(DE3)	55	
#124131	29	RF3	Release factor 3	59.6	pQE30	M15	55	
#124132	30	RRF	Ribosome recycling factor	20.6	pQE60	M15	55	
#124133	31	MTF	Methionyl-tRNA formyltransferase	34.2	pET21a	BL21(DE3)	55	
#124134	32	CK	Creatine kinase	37.1	pQE30	M15	55	
#118977	33	MK	Adenylyate kinase (Myokinase)	21.7	pET21a	BL21(DE3)	55	
#124136	34	NDK	Nucleotide diphosphate kinase	15.5	pQE30	M15	55	
#118978	35	PPiase	Inorganic pyrophosphatase	32.3	pET21a	BL21(DE3)	55	
#124138	36	T7 RNAP	T7 RNA polymerase	98.9	pQE30	M15	55	

Table 3.3: **Reagents.** The table lists concentrations, volumes, and other specific details of the reagents and components used during this study

Compound	Concentration	Volume	Sterilization	Note
Lysozyme broth (LB) media	25 g/L	3 L	Autoclave	2 L for ribosome solution preparation, 0.5 L for OnePot PURE, 0.5 L surplus
Ampicilin (AMP)	100 mg/mL in 50% (v/v) ethanol	2 mL	Filter sterilize (0.22 µM)	Can be made in larger volumes and stored at -20 °C for later use.
50 % Glycerol	50% (v/v)	100 mL	Autoclave	
Isopropyl β-D-1-thiogalactopyranoside (IPTG)	100 mM (23.8 mg/mL)	2 mL	Filter sterilize (0.22 µM)	Can be made in larger volumes and stored at -20 °C for later use.
Nickel sulfate	0.1 M	0.5 L		Dilute 100 mL of 0.5 M nickel sulfate in 400 mL water.
EDTA buffer	0.2 M EDTA, 0.5 M NaCl	1 L		Weigh 29.22 g of NaCl, 58.4 g of EDTA and add 700 mL water. EDTA will not dissolve completely at this pH. Adjust to pH = 7 with NaOH to dissolve EDTA, then add water to 1 L.
NaCl	0.5 M	1 L		Prepare 29.22 g of NaCl and add water to 1 L.
Acetic acid	0.1 M	1 L		Add 5.72 mL of glacial acetic acid to 994.3 mL of water. Caution: Add acid to water, not in the opposite order.
NaOH	0.5 M	1 L		Dissolve 20 g of NaOH in 800 mL water on ice and add water to 1 L
20% Ethanol	20% (v/v)	1 L		
70% Ethanol	70% (v/v)	1 L		

Table 3.4: **Buffers.** The spreadsheet lists the exact buffer compositions for protein, tag-free ribosome, and His-tag ribosome purifications, as well as the concentrations of the stock solutions used for their preparation. In addition, it calculates the required amounts of components based on the buffer volume.

Stock solutions		Stock solution				Notes	
MW [g/mol]	Concentration [M]	Volume [L]	Mass [g]				
214.45	1	0.25	53.6				Add the required mass, fill with water to the required volume. Filter sterile and store at 4°C.
74.55	2	1	149.1				Add the required mass, fill with water to the required volume.
53.49	1	1	53.5				Add the required mass, fill with water to the required volume.
68.08	1	1	68.1				Add the required mass, fill with water to 80%, adjust the pH to 7 with HCl, and fill with water to the required volume.
121.136	1	0.5	60.6				Add the required mass of Trisbase, fill with water to 80%, adjust the pH to 7.6 with HCl, and fill with water to the required volume.

Protein solution purification components	Stock solution		Buffer A		Buffer B		Buffer HT		Stock buffer A		Stock buffer B	
	MW [g/mol]	Concentration [M]	concentration	volume	concentration	volume	concentration	volume	concentration	volume	concentration	volume
HEPES**		1	50	25	50	25	50	10	50	5	50	5
Ammonium chloride*	53.49	1	1000	26.7	10	5	10	2	10	10	10	1
Potassium chloride	74.55	2	10	5	10	5	10	2	10	10	10	1
Potassium chloride	74.55	2	10	5	10	5	10	2	10	10	10	1
Imidazole (pH7)	68.08	1			500	250			30%	100	30	5
Cl ₂ CCP**									30%	100	30	5
TECP**		0.5	1	1	1	1	1	0.4	1	1	1	0.20
total buffer volume				500		500		200		100		300

Ribosome purification components	Stock solution		Suspension buffer		Suspension buffer (high salt)		Buffer C		Buffer D		Cushion buffer		Ribosome buffer	
	MW [g/mol]	Concentration [M]	concentration	volume	concentration	volume	concentration	volume	concentration	volume	concentration	volume	concentration	volume
HEPES**		1	10	2.5	10	1	20	10	20	6	20	5	20	5
Magnesium acetate	214.45	1	10	2.5	10	1	10	10	10	3	10	2.5	10	1.5
Potassium chloride	74.55	2	50	1.25	50	2.5	50	5	50	3	50	0	30	3.75
Ammonium chloride	53.49	1			3000	39.6	1500	99.1			30	7.5		
Ammonium sulfate*	132.14	1												
Sodium acetate	82.03	1												
TECP**		0.5	1	0.50	1	0.20	1	1.00	1	1	1	0.50	1	0.50
total buffer volume				250		100		500		300		250		250

His-ribosome purification components	Stock solution		Lysis buffer		Elution buffer		Ribosome buffer	
	MW [g/mol]	Concentration [M]	concentration	volume	concentration	volume	concentration	volume
HEPES**		1					20	5
TrisHCl (pH7.6)	121.136	1	20	20	20	20	20	5
Ammonium chloride	53.49	1	30	30	30	30	6	1.5
Magnesium chloride	214.45	1	10	10	10	10	6	1.5
Magnesium chloride	74.55	2	150	75	150	75	30	3.75
Potassium chloride	68.08	1			150	150	7	0.12
Imidazole (pH7)								
Glycerol								
P-mercaptoethanol**		14.3						
total buffer volume				3000		3000		250

* weighed directly to the buffer without preparing a prior stock solution

** add just before use

Table 3.5: **Amino acid calculations.** The spreadsheet lists the amino acids and their recommended stock solution concentrations required for the energy solution. It calculates the amount of water to be added to each amino acid based on the actual weighed mass, and also calculates the volume of the amino acid solution to be added to the final amino acids' mixture.

Amino acid	Density [g/mL]	MW [g/mol]	Stock concentration [mM]	Minimal required mass [mg]	Actual weighed mass [mg]	Water to add [μ L]	Final volume to add [μ L]	
Ala	1.42	89.1	168	0.7		0	38.7	
Arg	1.42	210.66	500	1.6		0	13.0	
Asn	1.54	132.1	100	1		0	65.0	
Asp	1.7	133.1	12.5	1		0	520.0	
Cys	1.54	157.62	200	1.2		0	32.5	
Glu	1.46	147.1	25	1.1		0	260.0	
Gln	1.47	146.2	100	1.1		0	65.0	
Gly	1.61	75.1	500	0.6		0	13.0	
His	1.49	209.63	500	1.5		0	13.0	
Ile	1.23	131.2	100	1		0	65.0	
Leu	1.17	131.2	150	1		0	43.3	
Lys	1.1	182.65	500	1.4		0	13.0	
Met	1.34	149.2	250	1.1		0	26.0	
Phe	1.34	165.2	100	1.2		0	65.0	
Pro	1.38	115.1	200	0.9		0	32.5	
Ser	1.6	105.1	500	0.8		0	13.0	
Thr	1.3	119.1	100	0.9		0	65.0	
Trp	1.4	204.2	12.5	1.5		0	520.0	
Tyr	1.46	181.2	3.25		1.18			
Val	1.32	117.1	200	0.9		0	32.5	
H2O							104.5	
Amino acid solution total							final concentration	final volume
							3.25	2000

Table 3.6: **Stock solutions for the energy solution.** The table lists the concentrations and volumes of stock solutions needed for the energy solution and indicates further details, including storage conditions.

Compound	Stock solution					Note
	Mw [mol/g]	Concentration [M]	Volume [mL]	Mass [g]		
Magnesium acetate	214.45	2	50	21.4	Filter sterilize, Store at -20 °C	
Potassium glutamate	203.23	2	50	20.3	Filter sterilize, Store at -20 °C	
Creatine phosphate	327.14	1	1	0.327	Store at -20 °C	
Folic acid	511.50	0.034	1	0.017	Store at -20 °C	
Spermidine	145.25	0.5	0.5	0.036	Warm to 34 °C, pipette 39.5 µL of spermidine and fill to 500 µL with water. Store at -20 °C	
tRNA			0.5	0.100	Add water directly to the vial and vortex gently. Store at -20 °C	

Table 3.7: **Energy solution.** The table lists the energy solution components and their recommended concentrations. In addition, it calculates their required volumes to be added to the final solution based on their stock solution concentrations and the volume of the energy solution.

Component	Stock concentration [mM]	Concentration of components in reaction [mM]	Concentration in Energy solution [mM]	Final volume to add [μ L]
HEPES	1000	50	125	625.0
Potassium glutamate	2000	100	250	625.0
Magnesium acetate	2000	11.8	29.5	73.8
ATP*	100	2	5	250.0
GTP*	100	2	5	250.0
CTP	100	1	2.5	125.0
UTP	100	1	2.5	125.0
tRNA [mg/mL]	200	3.5	8.75	218.8
Creatine phosphate	1000	20	50	250.0
TCEP	500	1	2.5	25.0
Folinic acid	34	0.02	0.05	7.4
Spermidine	500	2	5	50.0
Amino Acid solution	3.25	0.3	0.75	1153.8
Water				1221.3

Energy solution total	Final concentration [fold]	Final volume
	2.5	5000

*For energy solutions volumes above 5 mL order double the amount of these components

Table 3.8: **PCR.** The table lists sequences and concentrations of the primers used for the extension PCR and indicates melting temperatures and thermocycler steps optimized for a high-fidelity DNA polymerase.

Primer name	Primer sequence	Primer working concentration	Melting temperature	Notes	Thermocycler setting		
					Step 1	Step 2	Step 3
5' flucI	5' GATCTTAAGGCTAGAGTAC 3'	500 nM	47 °C		1x	30x	1x
3' flucI	5' CAAAACCCCTCAAGAC 3'	500 nM	47 °C		98 °C, 180 s	98 °C, 20 s - 47 °C, 30 s - 72 °C, 30 s per 1 kb	72 °C, 420 s
5' extension	5' GATCTTAAGGCTAGAGTACTAATACGA CTCACTA TAGG GAGACACAA CGGTTT CCCCTGAGAATAATTTTGGTTAAC 3'	2.5 nM	58 °C	T7 promoter	1x	10x	1x
3' extension	5' CAAACCCCTCAAGACCGTTTA GAGCCCAAGGGTTATGCTA GTTT GTAG CAGCCTGAGTCC 3'	2.5 nM	58 °C	T7 terminator	98 °C, 30 s	98 °C, 8 s - 58 °C, 20 s - 72 °C, 30 s per 1 kb	72 °C, 420 s
5' Gene specific	5' CCTGAGAAATAA TTTGTTTAACTTAAGAGGAGGAAAAAAA NNNNNNNNNNNNNNNNNNNNNNNN 3'	500 nM	Tm*	RBS; Modify based on 5'-terminus of the target gene	1x	30x	1x
3' Gene specific	5' GTAGAGCCTGAGTCTTA TTTANNNNNNNNNNNNNNNNNNNNNNN 3'	500 nM	Tm*	Modify based on 3'-terminus of the target gene	98 °C, 180 s	98 °C, 20 s - Tm °C, 30 s - 72 °C, 30 s per 1 kb	72 °C, 420 s

* determine by user

Table 3.9: **PURE reaction.** The spreadsheet shows an example setup of a PURE reaction. It lists the used concentrations and volumes of the components for a PURE reaction using tag-free ribosomes or His-tag ribosomes. Moreover, it calculates the volume ratios for protein and ribosome titrations.

PURE reaction setup for Tag-free ribosomes					
Component	Input concentration	Unit	Final concentration	Unit	Volume for one reaction [μL]
Energy solution 2.5x	2.50	x	1	x	4.00
Protein solution**		mg/mL		mg/mL	1.20
Ribosome solution ***	10	μM	1.8	μM	1.80
DNA 1	100	ng/μL	4	nM	0.26
DNA 2	100	ng/μL	0	nM	0.00
tRNA Lys*	25	x		x	0.00
Additional components					
Water					2.74
Total volume [μL]					
10					
Calculation for DNA concentration					
DNA length [bp]	Unit	Avg. MW of bp	Unit		
eGFP	990	bp	650	g/mol	
		bp	650	g/mol	

** determine the optimal protein concentration by titration
 *** ribosome concentration can be optimised by titration
 * use at final concentration 1x

PURE reaction setup for His-Taged ribosomes					
Component	Input concentration	Unit	Final concentration	Unit	Volume for one reaction [μL]
Energy solution 2.5x	2.50	x	1	x	4.00
Protein solution**		mg/mL		mg/mL	1.20
Ribosome solution (His-tag)***	3.45	μM	0.6	μM	1.80
DNA 1	100	ng/μL	4	nM	0.26
DNA 2	100	ng/μL		nM	0.00
tRNA Lys*	25	x		x	0.00
Additional components					
water					2.74
Total volume [μL]					
10					
Calculation for DNA concentration					
DNA length [bp]	Unit	Avg. MW of bp	Unit		
eGFP	990	bp	650	g/mol	
		bp	650	g/mol	

** determine the optimal protein concentration by titration
 *** ribosome concentration can be optimised by titration
 * use at final concentration 1x

Protein solution titration **					
Input proteins concentration (determined by Bradford assay):	20	mg/mL			
Final protein concentration [mg/mL]	2.4	2.1	1.8	1.5	1.2
Protein solution [μL]	1.20	1.05	0.90	0.75	0.60
Stock buffer B [μL]	0.00	0.15	0.30	0.45	0.60

Total concentration of protein solution and stock buffer B is kept constant

Optional: Ribosome solution titration (Tag-free)***					
Input ribosome concentration:	15	μM			
Final ribosome concentration [mg/mL]	2.7	2.25	1.8	1.35	0.9
Ribosome solution [μL]	1.80	1.50	1.20	0.90	0.60
Ribosom buffer [μL]	0.00	0.30	0.60	0.90	1.20

Optional: Ribosome solution titration (His-tag)***					
Input ribosome concentration:	10	μM			
Final ribosome concentration [mg/mL]	1.8	1.4	1	0.6	0.3
Ribosome solution [μL]	1.80	1.40	1.00	0.60	0.30
Ribosom buffer [μL]	0.00	0.40	0.80	1.20	1.50

Table 3.10: Materials.

Material / Equipment	Supplier	Catalog Number	Comments
384-well Black Assay Plates	Corning	3544	
Sodium hydroxide	Sigma-Aldrich	6203	
Ampicillin	Condalab	6801	
Creatine phosphate	Sigma-Aldrich	27920	
Potassium glutamate	Sigma-Aldrich	49601	
Sucrose	Sigma-Aldrich	84097	
96-Well Polypropylene DeepWell plate	Nunc	260252	
Falcon® 14 mL Round Bottom Polystyrene Test Tube, with Snap Cap	Falcon	352051	
Centrifuge tubes polycarbonate	Beckman	355631	purification of tag free ribosomes
Thickwall Polycarbonate Tube	Beckman	355631	
10x Tris/Glycine/SDS buffer	Bio-Rad Laboratories	1610732	
4-20% Mini-PROTEANRTM TGXTM Precast Protein Gels	Bio-Rad Laboratories	4561096	
Quick Start™ Bradford 1x Dye Reagent	Bio-Rad Laboratories	5000205	
Econo-Pac Chromatography Columns	Bio-Rad Laboratories	7321010	
Flasks, baffled 1000 mL 4 baffles, borosilicate glass	Scilabware	9141173	
Nickel Sulfate	Alfa Aesar	15414469	
HiTrap Butyl HP Column	GE Healthcare	28411005	purification of tag free ribosomes
Acetic acid, 99.8 %	Acros	222140010	
tRNA	Roche	10109541001	
EDTA (Ethylenediaminetetraacetic acid)	Sigma-Aldrich	03609-250G	
Ammonium chloride	Sigma-Aldrich	09718-250G	
HEPES	Gibco	15630-056	
IMAC Sepharose® 6 Fast Flow	GE Healthcare	17-0921-07	
Eppendorf Protein LoBind microcentrifuge tubes	VWR International / Eppendorf	525-0133	
50 mL centrifuge tubes	VWR International	525-0304	
15 mL centrifuge tubes	VWR International	525-0309	
Thermo Scientific™ Nalgene™ Rapid-Flow™ Sterile Single Use Bottle Top Filters	ThermoFisher	10319590	
Magnesium chloride	Honeywell Fluka	63020-1L	
TCEP (Tris(2-carboxyethyl)phosphin -hydrochlorid)	Sigma-Aldrich	646547-10X1mL	
Lysozyme broth (LB) media	AppliChem	A0954	
Ammonium sulfate	Sigma-Aldrich	A4418	
RNaseA solution	Promega	A7973	
IPTG (Isopropyl-beta-D-thiogalactoside)	Alfa Aesar	B21149.03	
Tris base	ThermoFisher	BP152-500	

3.8 Annexe

In 2022/2023 the supply of the specified tRNAs by Roche was discontinued. Adding tRNAs from different suppliers failed to function in the PURE environment. We therefore developed a protocol for tRNA purification based on work published by Cayama and coworkers [317], which was further adjusted by Matt Cummins, ETHZ, and refined by our laboratory.

1. Grow a culture of *E. coli* BL21 and harvest the cells after around 6 h
2. Cells can be aliquoted and stored at -80 °C until further use
3. Weigh cell pellet, the weight in g, typically between 4-8 g, will subsequently be referred to as X.
4. Equilibrate at least 7 x X of equilibrated phenol once in resuspension buffer (10 mM HEPES, 10 mM MgCl₂, pH 7.2)
5. Resuspend cells in 5x X mL of resuspension buffer
6. Add 5x X mL of equilibrated phenol to achieve a 1:1 v/v mixture
7. Mix well and incubate for 30 min at 4 °C rotating.
8. Separate the phases by spinning for 10 min at 4000 x g.
9. Remove the aqueous phase (top) with a serological pipette and transfer it to a new tube
10. Add ultrapure Isopropanol to be 1:1 v/v or slightly more. If the reagent freezes at -20°C add more Isopropanol
11. incubate at -20°C at least over night
12. Precipitate nucleic acids by centrifugation for 10 min at 4000 x g and 4°C. Discard the supernatant
13. Resuspend the pellet in X mL of Lithium buffer (0.8 M LiCl and 0.8 M NaCl)
14. Precipitate the DNA and transfer the supernatant to a new tube
15. Add X mL of Isopropanol to reach a v/v ratio of 1:1
16. Precipitate the RNA and discard the supernatant
17. Wash the pellet three times with ultrapure Ethanol by dissolving the pellet in Ethanol and subsequently precipitating by centrifugation for 10 min at 4000 x g and 4 °C
18. Dry the pellet with Nitrogen

19. Dissolve the pellet in resuspension buffer (50 mM NaCl, 10 mM HEPES in ultrapure water)
20. tRNAs can be stored at -80°C. Adding RNase inhibitor will increase tRNA stability during storage

4 Improved Cell-Free Transcription–Translation Reactions in Microfluidic Chemostats Augmented with Hydrogel Membranes for Continuous Small Molecule Dialysis

This work was published in *ACS Synthetic Biology*, 2022. Reprinted with permission from [318]. Copyright 2022 American Chemical Society.

Reference: Lavickova, B., Grasmann, L. & Maerkl, S. J. (2022). Improved Cell-Free Transcription–Translation Reactions in Microfluidic Chemostats Augmented with Hydrogel Membranes for Continuous Small Molecule Dialysis. *ACS Synthetic Biology*, 11(12), 4134-4141.

Contribution: B.L. and L.G. performed experiments. B.L., L.G., and S.J.M. designed experiments, analyzed data, and wrote the manuscript.

4.1 Abstract

Increasing the protein production capacity of the PURE cell-free transcription–translation (TX-TL) system will be key to implementing complex synthetic biological circuits, and to establishing a fully self-regenerating system as a basis for the development of a synthetic cell. Under steady-state conditions, the protein synthesis capacity of the PURE system is likely at least one order of magnitude too low to express sufficient quantities of all PURE protein components. This is in part due to the fact that protein synthesis cannot be sustained during the entire dilution cycle, especially at low dilution rates. We developed a microfluidic chemostat augmented with semipermeable membranes that combines steady-state reactions and continuous dialysis as a possible solution to enhance protein synthesis at steady-state. In batch operation, the continuous dialysis of low molecular weight components via the membranes extended protein synthesis by over an order of magnitude from 2 h to over 30 h, leading to a 7-fold increase in protein yield. In chemostat operation, continuous dialysis enabled sustained protein synthesis during the entire dilution cycle even for low dilution rates, leading to 6-fold higher protein levels at steady state. The possibility to combine and independently manipulate continuous dialysis and chemostat operation renders our dialysis chemostat a promising technological basis for complex cell-free synthetic biology applications that require enhanced protein synthesis capacity.

KEYWORDS: cell-free transcription and translation microfluidics nonequilibrium reactions synthetic biology dialysis

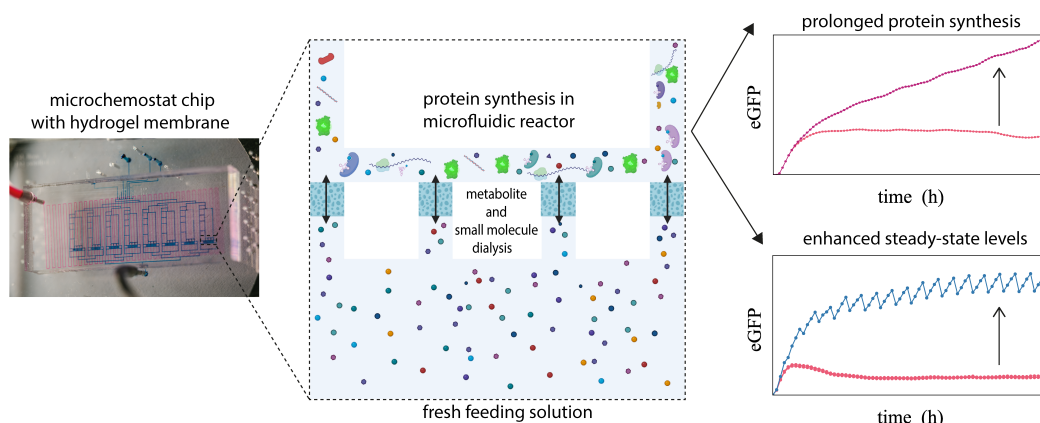


Figure 4.1: Graphical Abstract

4.2 Introduction

A reconstituted cell-free transcription–translation (TX-TL) system such as the PURE system is a viable chassis for constructing a synthetic cell [44]. However, one critical requirement that remains a major challenge is achieving a sufficiently high protein synthesis rate to regenerate all PURE proteins simultaneously in order to achieve sustained self-regeneration. We recently demonstrated that several proteins of the PURE system could be sustainably self-regenerated in a microfluidic-based synthetic cell-like system [3]. However, the synthesis rate and yield in the recombinant cell-free system are currently predicted to be orders of magnitude below what would be required to regenerate all of its nonribosomal protein components, which is a limitation not only for advances in constructing a synthetic cell, but also for prototyping of complex synthetic systems.

Cell-free reactions can be classified into equilibrium and nonequilibrium reactions [44]. Standard batch experiments are classified as equilibrium reactions. All components are combined at the outset, after which they undergo reactions with no further external input, until chemical equilibrium is reached. A standard cell-free protein synthesis system in batch configuration ceases to function mainly due to the rapid depletion of critical small molecular weight components such as NTPs [44]. This, however, does not mimic biological systems, which operate far from chemical equilibrium. Therefore, continuous *in vitro* systems, where reagents are exchanged over time, have been developed.

These nonequilibrium reactions can be further separated into two subcategories: batch reactions with continuous dialysis, and reactions in chemostat reactors. During batch reactions with dialysis, replenishment is achieved by passive, diffusion driven exchange based on dialysis, which allows the exchange of small molecules with the environment, while retaining the TX-TL machinery within a defined reaction compartment [319]. This approach permits protein synthesis to last for up to several days, leading to a total protein synthesis yield in the range of mg/mL [27]. Batch reactions with continuous dialysis have previously been realized using standard tube-based dialysis [27], a microwell plate with integrated dialysis membranes, [28, 183], or a passive PDMS microreactor [186]. In comparison, reactions in chemostat reactors overcome equilibrium by diluting all reaction components with fresh components; this allows for replenishment of both small molecules and the enzymatic machinery, allowing an efficient protein turnover rate and thus implementation of complex genetic networks [42, 191, 320]. Therefore, combining both approaches by replenishing small molecules by dialysis and replenishing the enzymatic machinery by dilution is likely crucial to achieve adequate synthesis rates required for self-replicating systems.

In this work, we designed a microfluidic device with 8 independent microfluidic chemostat reactors with integrated PEG-DA dialysis membranes. Our device enables the implementation of steady-state reactions in combination with small molecule feeding by continuous dialysis. We describe a simple silanization protocol that does not require either the use of oxygen plasma or organic solvents, and a technique for simple PEG-DA hydrogel membrane patterning, using

pneumatic valves in an oxygen-free environment. Additionally, we describe how different membrane permeabilities can be generated to achieve an ideal molecular weight cutoff for a continuous dialysis TX-TL reaction. Furthermore, we report a simple way to avoid water evaporation from PDMS at low environmental humidity by adding a PDMS hydration layer. We show that implementing continuous dialysis protein synthesis in our steady-state chemostat reactor with semipermeable membranes extended protein synthesis to at least 30 h, leading to a 7-fold increase in the synthesis yield compared to batch reactions. Moreover, by combining the chemostat TX-TL reaction with continuous dialysis, we achieved a 6-fold increase in steady-state protein synthesis levels while maintaining active protein turnover.

4.3 Results

4.3.1 Formulation, Generation, and Characterization of PEG-DA Hydrogel Membranes

To achieve continuous dialysis of small molecules, several methods and designs have been proposed [28, 183, 186], with most of them suffering from the drawback that they are difficult to implement and manufacture. We adapted a method to manufacture PEG-DA semipermeable membranes inside of a microfluidic device utilized for protein crystallization [321]. PEG-DA is ideal for this purpose due to several advantages including biocompatibility [322], tunable pore sizes [323–326], the possibility to be integrated within PDMS [321], the ability to be introduced as the unpolymerized prepolymer, and to be quickly cured by UV. The reactor uses fluidically hard-coded dilution fractions as described previously [43], and was augmented with a feeding channel for the continuous dialysis of small molecules, and an antievaporation layer on top of the device (Fig 4.6a-f). The feeding channel is linked to the main reactor by four channels, which contain the PEG-DA hydrogel membranes. These PEG-DA membranes form a semipermeable barrier between the reactor and feeding chamber to allow the continuous supply of small molecular weight components while retaining high molecular weight components such as proteins or ribosomes inside the reactor (Figure 4.2a,b 4.6a,b). These linker channels can be controlled by two valves on either end. To generate PEG-DA membranes, the valves facing the reactor ring were closed to prevent any chemical from entering the actual reaction chamber, and the linker channels were addressed via the feeding chamber. The PDMS surface was functionalized with silane as described below, and subsequently PEG-DA was flown into the channels. The valve facing the feeding chamber was actuated to trap the PEG-DA inside the linker channels, and the feeding chamber was thoroughly washed to remove all remaining PEG-DA. The PEG-DA was then cured using a UV lamp generating semipermeable membranes separating the main reactor from the feeding channel. To implement the semipermeable hydrogel membranes for the application of long-term continuous dialysis of small molecular reagents during cell-free expressions, several crucial factors, such as strong anchoring of the membranes to the PDMS and glass surfaces, a correct molecular weight cutoff, and a low evaporation rate of liquids from the reactors had to be achieved.

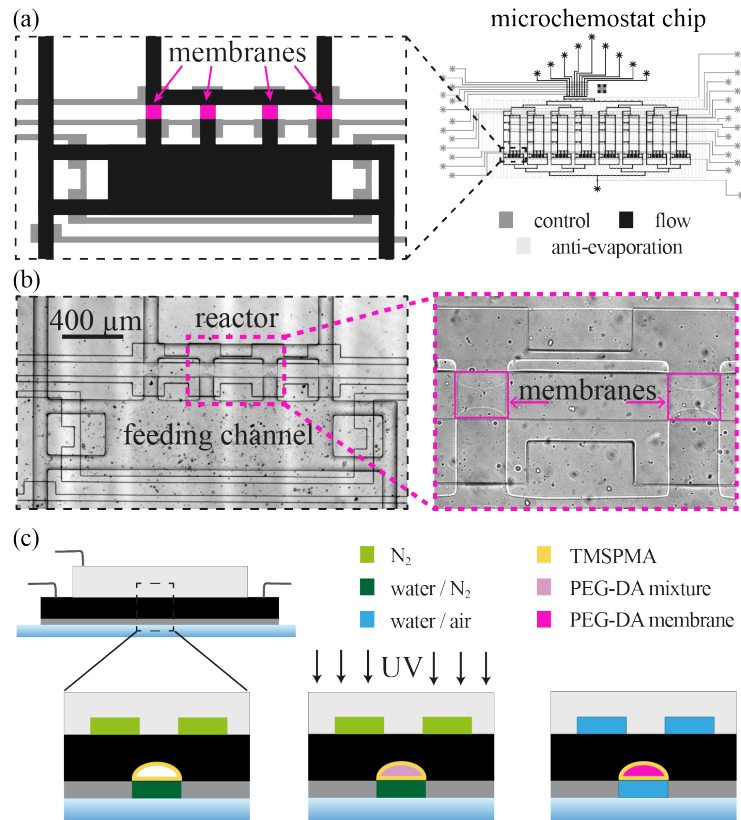


Figure 4.2: (a) Design schematic of the microfluidic device featuring eight individual chemostat reactors and details of a single reactor showing the feeding channel separated from the main reactor by hydrogel membranes. The flow layer is shown in black, the control layer in dark gray, and the antievaporation layer in light gray. Design and functional details are provided in 4.6. (b) Bright-field image of the hydrogel membranes between the reactor and feeding channel. (c) Schematic protocol for preparing hydrogel membranes. First the PDMS channels were functionalized with TMSPMA, subsequently PEG-DA prepolymer was flown and polymerized inside of the membrane channels, and the formed membranes were washed overnight with water before conducting on-chip cell-free TX-TL reactions.

In our device, pressure on the membranes is imposed over extended periods due to the osmotic pressure generated by the differences in composition of the feeding solution and the PURE TX-TL solution, as well as during the pressure-driven loading phase, and as a result of volume displacement arising from the pneumatic valve actuation. Therefore, strong anchoring of the membranes to PDMS is crucial. To anchor the membranes, the addition of vinyl groups to the PDMS surface by silanization with silane-containing acrylate or methacrylate [327] was essential. Here we report a simple and fast (<1 h) silanization protocol based on hydrochloric acid/hydrogen peroxide treatment [328, 329] and TMSPMA hydrolyzed in acidic conditions [330], without the use of organic solvents, which can support strong PEG-DA anchoring and is compatible with PDMS valves (Figure 4.2c). Polymerization of PEG-DA membranes has to be performed in an oxygen-free environment, as the presence of oxygen leads to a thin oxidized layer that is not able to cross-link with the PDMS [321]. To deplete oxygen, the hydrogel-forming valves controlling the connection of the feeding channel with the ring, and the antievaporation layer were pressurized with nitrogen instead of air (Figure 4.2c). The resulting channel functionalization and formation of hydrogel membranes was highly reproducible, and the membranes were stable against rupture and could withstand the imposed transmembrane pressure for more than 2 days.

To achieve continuous cell-free expression, membranes of the correct molecular weight cutoff have to be implemented on the device. The ideal molecular weight cutoff level for cell-free continuous dialysis reactions is around 10 kDa [321], which allows small molecules to diffuse between feeding and reaction chamber, while retaining protein components inside the reaction chamber. One of the main advantages of utilizing hydrogel membranes as dialysis membranes is their tunable pore size. In particular PEG-DA hydrogels have been shown to be tunable from nm pores [331] to μm [324–326] pores, allowing molecular weight cutoffs from small molecules to large proteins. The porosity depends mostly on the molecular size of the PEG-DA polymer [324] and porogen [325, 331] used during the polymerization reaction. To achieve the desired permeability of our membrane and low hydrogel swelling [332, 333], we decided to use PEG-DA M_n 700 g/mol (average M_n) with photoinitiator 2-hydroxy-2-methylpropio-phenone [321]. The main advantage of using M_n 700 g/mol PEG-DA prepolymer is its solubility in water, in contrast to M_n 250 g/mol PEG-DA prepolymer for example, which is insoluble in water. This significantly simplifies prepolymer manipulation within the microfluidic chip, as any remaining unpolymerized prepolymer can easily be washed away. Moreover, water simultaneously acts as a porogen during hydrogel polymerization; therefore, the hydrogel permeability can be tuned by modifying the PEG-DA/water ratio.

We initially prepared two aqueous formulations of different PEG-DA/water ratios (33% and 42% w/w PEG-DA/water), and examined the diffusion of different molecular weight solutes through the formed membranes from the feeding channels to the chemostat reactor (Figure 4.3a,b). While the small molecular weight methylene blue dye (Figure 4.3c) diffused rapidly into the reactor for both tested PEG-DA formulations, 10 kDa (Figure 4.3d) and 40 kDa (Figure 4.3e) fluorescently labeled dextrans were mainly retained in the feeding channel and diffused into the reactor at a much slower rate. In particular for the membrane formulation of 42%

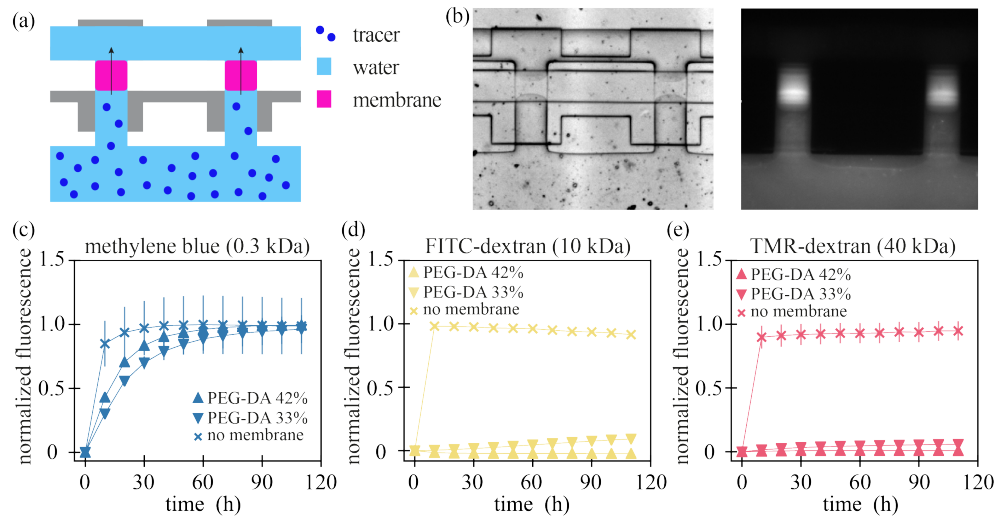


Figure 4.3: Solute diffusion through the membrane: (a) Schematic of a hydrogel permeability experiment. The feeding chamber (bottom) and the reaction ring (top) are separated by semipermeable membranes (pink) which allow small molecules to diffuse freely, while retaining molecules above the respective molecular weight cutoff. (b) Bright field and fluorescent images of the semipermeable membrane and the feeding channel loaded with methylene blue dye. Diffusion of solutes of different molecular weight from the enclosed feeding channel to the reactor chamber through the membrane over time: (c) methylene blue, (d) 10 kDa FITC-dextran, (e) 40 kDa TMR-dextran. The fluorescence of methylene blue was normalized to the maximum level attained in each experiment. For 10 kDa FITC-dextran and 40 kDa TMR-dextran, the fluorescence was normalized to the maximum level attained in reactors without membrane.

w/w PEG-DA/water, there was no observable diffusion into the reactor ring for the 10 kDa or the 40 kDa dextran in the time frame of the experiment. This renders both formulations ideal candidates to be utilized for membranes for continuous dialysis protein synthesis, and we decided to implement the 33% w/w PEG-DA/water formulation for subsequent experiments.

4.3.2 Batch Cell-Free Expression Augmented with Continuous Dialysis

We first tested if our microfluidic device with integrated membranes could be used for batch cell-free protein synthesis and whether the dialysis membranes have a noticeable effect on protein synthesis. To be able to sustain long-term protein synthesis we implemented an anti-evaporation layer to prevent evaporation of water through the PDMS. In a PDMS device during a batch reaction (environmental humidity and 34 °C), evaporation can be observed after 2 h, if no evaporation prevention is applied (Supplementary figure 4.6g). The anti-evaporation layer features a dead-end serpentine channel covering the reactors, and is bonded on top of the chip using oxygen plasma (Supplementary Figure 4.6c-f. During the experiment, the channel is connected to a pressurized, water-filled tube to sustain a constant water supply

Improved Cell-Free Transcription–Translation Reactions in Microfluidic Chemostats 4 Augmented with Hydrogel Membranes for Continuous Small Molecule Dialysis

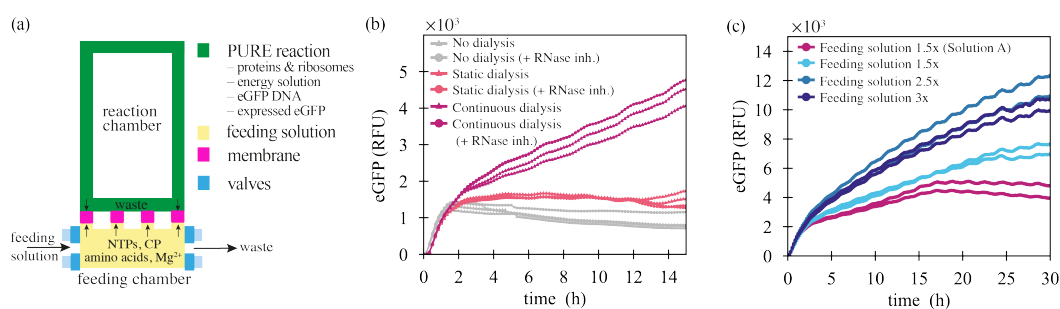


Figure 4.4: Batch cell-free expression augmented with dialysis: (a) Schematic of a continuous dialysis reaction of a single chemostat reactor augmented with a hydrogel membrane. (b) Time course of in vitro eGFP expression in batch, batch with static dialysis, and batch with continuous dialysis reactions. A concentration of 1.5× of the feeding solution based on solution A was used for batch with static dialysis and batch with continuous dialysis reactions. Each curve represents a technical replicate. (c) Time course of in vitro eGFP expression levels in batch with continuous dialysis reactions for different feeding solution concentrations based on the commercial solution A (PURExpress) or homemade energy solution. Each curve represents a technical replicate.

in the anti-evaporation layer. With the anti-evaporation layer, no discernible evaporation was observed after 16 h (Supplementary Figure 4.6g). Compared to previously reported anti-evaporation methods [334–337], our design is easy to fabricate, assemble, and can be applied to most standard double-layer microfluidic designs without the need of additional hardware.

For cell-free expression experiments, the chemostat reactors were filled with the PURExpress components in a ratio of 2:2:1 for solution A (2.5×, energy solution), solution B (2.5×, protein/ribosome), and DNA solution (5×), respectively. The feeding channel was loaded with a 1.5× feeding solution (1.5× solution A and PURE buffer (see Methods 4.5), either once in the beginning of the experiment for the batch with static dialysis reaction, or every 10 min for the continuous dialysis experiments (Figure 4.4a). The batch reaction was run as previously described [3] using a traditional chemostat device without a feeding chamber, but augmented with the anti-evaporation layer. The experimental procedures and parameters of the batch, batch with static dialysis, and batch with continuous dialysis experiments are detailed in Supplementary Table 4.6.

There was no significant difference between the batch reaction and batch with static dialysis reaction, as the feeding channel was filled only once at the beginning of the reaction, therefore supplying only a limited amount of additional energy components. For both reactions, protein synthesis ceased after around 2 h. However, continuous eGFP synthesis was observed for the batch reaction with continuous dialysis, when the feeding solution was replenished every 10 min, which resulted in a 3-fold increase in the reaction yield after 15 h compared to the batch reaction with static dialysis (Figure 4.4b). In addition, we explored the importance of an RNase inhibitor to prevent the degradation of RNA based components, but did not observe any difference between the reactions with and without RNase inhibitors for any conditions

tested (Figure 4.4b).

We tested different concentrations of the feeding solution to further increase protein synthesis (Figure 4.4c, Supplementary Figure 4.7). We prepared different concentrations of feeding solutions, with energy solutions prepared based on previously published protocols [309], and compared them to the feeding solution based on the commercially available solution A of the PURExpress system. We achieved a similar expression level comparing our homemade 1.5× solution to the 1.5× concentrated PURExpress solution A for up to 15 h. However, in contrast to the homemade solution, which exhibited steady protein expression during the entire experiment duration of 30 h, we observed a cessation of eGFP expression after 15 h when using the commercial solution. This effect is potentially due to the use of the more stable TCEP as a reducing agent in the homemade solution instead of DTT that is used in the commercial solution. The relatively constant expression rate throughout the experiment timeline indicates low degradation of ribosomes and other macromolecules. Although we did not study the stability of the various components in detail, this observation is in accordance with literature and our previous results, where long-term stability of macromolecules at 34 °C was observed [3]. This is probably a result of low amounts of proteases and RNases present in the PURE system and the use of a temperature-stable reducing agent as mentioned above.

Increasing feeding solution concentration to 2.5× led to an increase in synthesis rates and overall higher yield by around 2-fold compared to the 1.5× feeding solution concentration. After 30 h, we achieved a 7-fold increase of protein yield without observing any cessation of protein synthesis. Further increasing the concentration (3×) did not increase synthesis rate or yield compared to the 2.5× feeding solution.

4.3.3 Steady-State Cell-Free Reaction Augmented with Continuous Dialysis

A system that is designed to implement complex biological networks needs to be able to exchange reagents and operate at steady-state. We have previously shown that a microfluidic chemostat can achieve steady-state transcription and translation [3, 42, 320]. However, a remaining challenge is obtaining adequate protein synthesis at steady-state to implement larger and more complex biological circuits and to establish a self-replicating system for a future synthetic cell. Steady-state is achieved when the synthesis rate matches the combined dilution and degradation rate. Hence, at a given synthesis rate, faster dilutions lead to lower steady-state levels, and vice versa. In the experiments described in this work, the fraction of the ring being exchanged is held constant at 20%, and the dilution rate is determined solely by the dilution frequency. In silico models of the chemostat show that in the ideal case, where the synthesis rate remains constant throughout the time interval between dilution steps, steady-state levels are inversely proportional to dilution rates (Supplementary Figure 4.8a). For instance, a dilution interval of 60 min should lead to a 4-fold increase in steady-state GFP level compared to a 15 min dilution interval. However, if the supply of small molecules is limiting (Supplementary Figure 4.8b) or inhibitory byproducts accumulate, the synthesis rate

4 Improved Cell-Free Transcription–Translation Reactions in Microfluidic Chemostats Augmented with Hydrogel Membranes for Continuous Small Molecule Dialysis

between dilution steps may not be constant and decrease or cease entirely, and hence lower dilution rates will not lead to proportionally increased steady-state protein levels.

To test whether resource supply might be a limiting factor, as we hypothesized in our previous work [3], we investigated steady-state expression at different dilution rates. The chemostat reactors were loaded with PURExpress components in a ratio of 2:2:1 (v/v/v) for energy solution (2.5×, energy components), solution B (2.5×, proteins/ribosomes), and DNA solution. Subsequently, to investigate steady-state expression levels at different dilution rates, 20% of the reactor volume was exchanged with fresh components using the same ratio every 15, 30, or 60 min (Supplementary Table 4.7). We observed similar steady-state levels for all dilution frequencies, with the lowest steady-state level for the 60 min dilution interval. This indicates that the synthesis rate averaged over one cycle is the lowest for the 60 min dilution interval. As it can be seen in 4.5a, the synthesis rate in fact decreases during the cycle, probably due to insufficient supply of energy components. As lower dilution rates mean less components being replenished per unit time, and the 20% volume replacement every 60 min is apparently insufficient to supply enough small molecules to sustain a constant synthesis rate during the 60 min reaction, a lower steady-state protein level is achieved.

We thus combined the chemostat reaction with a continuous dialysis reaction to overcome the insufficient supply of small molecular components at lower dilution rates (Figure 4.5b). For continuous dialysis reactions, the chemostat reactors were filled and diluted as described above for the standard chemostat reactions. In addition, the feeding channel was loaded with a 3× feeding solution (3× energy solution and PURE buffer, see Methods 4.5, which was exchanged every 15 min, if not indicated otherwise (Figure 4.5b). Surprisingly, we already observed a significantly enhanced eGFP synthesis rate (4-fold) when continuously exchanging the feeding solution for the 15 min dilution interval, indicating that even our highest dilution rate is already resource limited. By lowering the dilution rates, we further increased the steady-state level eGFP fluorescence level by 6-fold compared to the reaction without continuous dialysis. In contrast to the traditional chemostat reactor, we did not observe any significant decrease in synthesis rate during each dilution cycle even for the longest dilution interval (60 min), indicating a sufficient supply of small molecules through the membranes to sustain protein expression. However, the average synthesis rate for the 60 min interval was lower than the average synthesis rate at an interval of 15 min, suggesting that further optimization might be possible.

4.4 Discussion

In this work, we augmented a microfluidic reactor with hydrogel-based semipermeable dialysis membranes to combine chemostat operation with continuous dialysis. For standard batch reactions, augmenting the reaction chambers with semipermeable membranes led to a prolongation of protein synthesis from approximately 2 to at least 30 h, increasing total protein yield by 7-fold. For chemostat operation we showed that combining steady-state protein

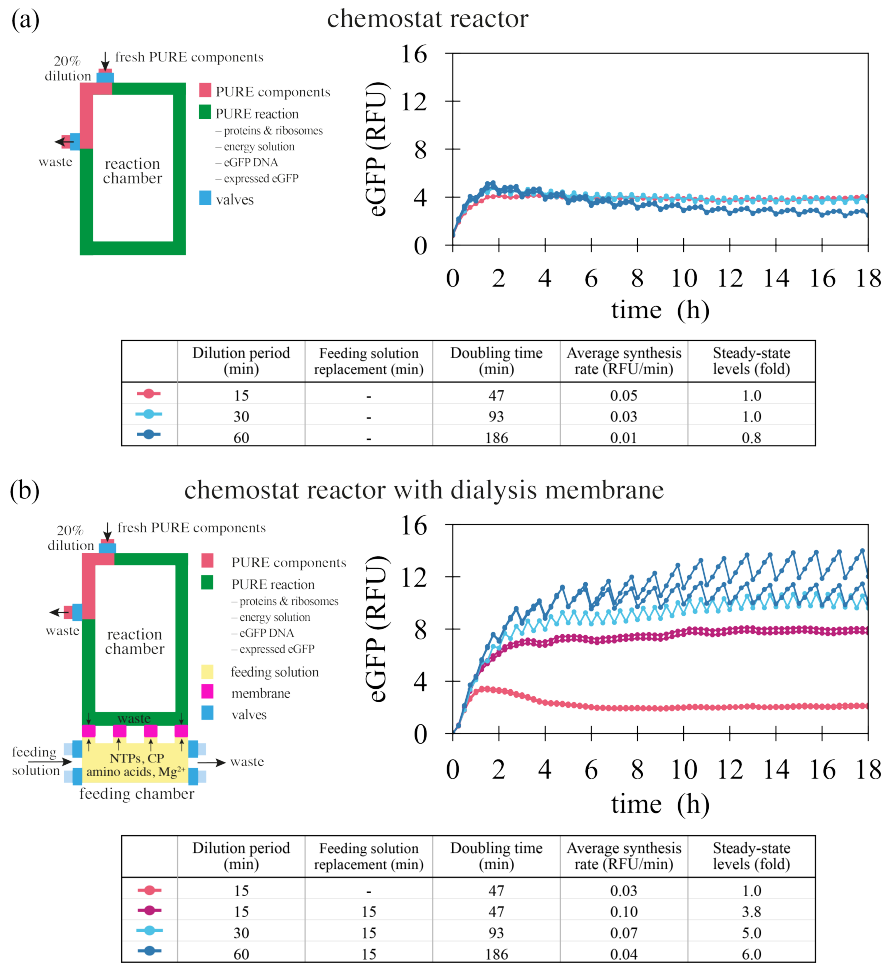


Figure 4.5: Steady-state chemostat reactions. (a) eGFP steady-state levels on a traditional chemostat reactor as previously described (30) for different dilution rates. 20% of the chemostat reactor volume was diluted with energy solution, solution B (PUREExpress), and DNA at different time intervals of 15, 30, and 60 min. Each curve represents a technical replicate. (b) eGFP steady-state levels for chemostat reactors augmented with hydrogel membranes for different dilution rates. 20% of the chemostat reactor volume was diluted with energy solution, solution B (PUREExpress), and DNA at different time intervals of 15, 30, and 60 min. The feeding solution (3×) was replaced as specified in the table. Each curve represents a technical replicate. Doubling time $t_d = \ln(2)\mu^{-1}$ was calculated from the dilution rate $\mu = -\ln(C_t/C_0)t^{-1}$. The average synthesis rate for each dilution period was calculated from the steady-state levels (average during 5–18 h) based on the percentage of dilution and the dilution period.

synthesis with continuous dialysis led to a 6-fold increase in protein levels at steady-state. By decoupling small molecule supply from TX-TL machinery replenishment and dilution, we more closely mimic the dilution and regeneration of cellular components during cell growth. In a living cell, small molecules are taken up from the outside to fuel reactions inside the cell, providing a supply of small metabolites that is decoupled from growth and thus dilution. Large biomolecules including proteins and DNA are synthesized inside the cell and diluted (or rather kept constant) by growth and degradation. Likewise, our chemostat exchanges small molecules with the feeding chamber to fuel the reactions inside, while keeping proteins and DNA inside the reactor subject to exchange by dilution. To our knowledge, this is the first device that combines chemostat operation and continuous dialysis cell-free protein expression.

The increase in the protein production capacity at steady-state is a key step toward achieving adequate protein synthesis likely required when building a synthetic cell based on the PURE cell-free expression system. We anticipate that further optimizing and tuning the system, for instance by increasing protein concentration in the reactor, omitting glycerol [27], or further optimizing the exact composition of the feeding solution [28], will render even higher protein production rates possible.

Although this specific microfluidic device is designed to study systems requiring nonequilibrium conditions such as synthetic cells and biomolecular oscillators that operate out-of-equilibrium, the methods described here could also be expanded to be used for applications that would benefit from a higher protein synthesis yield, including for instance continuous dialysis protein synthesis combined with on-chip purification [338, 339] or protein crystallization [321]. Besides, the simplicity and time-efficiency of the silanization protocol and method to prepare PEG-DA hydrogel membranes by utilizing pneumatic valves presented here also suggests itself for the implementation of other applications that involve hydrogels [339, 340] in-double-layer microfluidic devices, such as on-chip concentration gradient generator- and separation devices [339].

4.5 Methods

4.5.1 Microfluidic Chip Fabrication

The device with 8 reactors and 9 fluid inputs (Figure 4.2 Supplementary Figure 4.6) is based on a previous design [3, 43]. Molds for the control, the flow layer, and the anti-evaporation layer were fabricated on separate wafers by standard photolithography techniques. The positive photoresist AZ 10XT-60 (Merck) with a height of 14 μm was used to generate the flow channel features. For the control layer and the anti-evaporation layer, SU-8 photoresist (Microchem 3025, Kayaku Advanced Materials) was used to generate the channel features with a height of 40 μm . Subsequently, each of the wafers was treated with trimethylchlorosilane. For the flow and the anti-evaporation layers, PDMS with an elastomer to cross-linker ratio of 5:1

was prepared and poured over the wafers. The wafers coated with PDMS were placed in a desiccator for 40 min prior to baking. For the control layer, PDMS with a 20:1 elastomer to cross-linker ratio was spin-coated at 1400 rpm onto the wafer and left to relax for 40 min prior to baking. The flow and control layers were partially cured at 80 °C for 20 min. The flow layer was then cut out and aligned onto the control layer. The aligned devices were placed back in the oven at 80 °C for 90 min. The anti-evaporation layer was cured at 80 °C for 90 min. After the curing, the devices and the anti-evaporation layers were removed from the wafer and the inlets were punched. The aligned devices were plasma bonded to a glass slide and subsequently the evaporation layer was plasma bonded on top of the chip.

4.5.2 Chip Silanization and Formation of PEG-DA Hydrogel Membrane

To prime the chip, control lines were filled with water and pressurized with air at 1.38 bar, except for the hydrogel-forming valves, which were pressurized with nitrogen at 1.38 bar. The inner walls of the flow channels, except for the reactors, were oxidized by flowing freshly prepared solution of H₂O:H₂O₂(30% (v/v)):HCl(36%) solution in a ratio of 5:1:1 v/v for 10 min, followed by a washing step with Milli-Q water for 4 min. The silanization solution was freshly prepared by mixing Milli-Q water with 0.4% (v/v) 3-(trimethoxysilyl)propyl methacrylate (TMSPMA, Sigma) and 0.4% (v/v) glacial acetic acid (VWR) and let flow for 20 min through the oxidized channels. Subsequently, the channels were washed with Milli-Q water for 15 min.

Meanwhile, an aqueous solution for the polymerization of the hydrogel membrane was prepared. First, the PEG-DA (Mn 700 g/mol, Sigma) was mixed with photoinitiator 2-hydroxy-2-methylpropio-phenone (Sigma) (90/10% w/w). Subsequently, different volumes of UltraPure water (Invitrogen) were added to the mixture, as specified in section 4.3.1 Formulation, Generation, and Characterization of PEG-DA Hydrogel Membranes. The solution was perfused with nitrogen gas for up to 20 min to remove oxygen. However, we found that shorter times of less than 1 min are sufficient for the hydrogel formation. After the silanization process, the anti-evaporation layer was pressurized with nitrogen at 1.38 bar to deplete oxygen from the chip. The PEG-DA solution was injected into the feeding chamber for 10 min, after which the hydrogel-forming valves were closed, and the remaining PEG-DA was removed by washing with water. The remaining PEG-DA was polymerized for 2 × 30 s using an Omnicure S1500 200 W UV curing lamp with a standard filter (320–500 nm). After the formation of the membranes, the hydrogel forming valves and the anti-evaporation layer were disconnected from the nitrogen source. The anti-evaporation layer was primed with water, and the formed membranes were washed with UltraPure water for 20 h and subsequently passivated with bovine serum albumin (1%, Sigma-Aldrich) in 50 mM HEPES, 100 mM potassium chloride, 10 mM magnesium chloride for 1–3 h, and finally primed with a wash buffer (50 mM HEPES, 100 mM potassium glutamate, 11.8 mM magnesium acetate).

4.5.3 Solute Diffusion through the Hydrogel Membranes

The reactors were thoroughly washed and filled with the wash buffer, while the feeding channel was loaded with either 10 µg/mL of methylene blue, fluorescein isothiocyanate-dextran (FITC-dextran, 10 kDa), or tetramethylrhodamine-dextran (TMR-dextran, 40 kDa) solutes. The peristaltic pump was actuated at 20 Hz to mix the solutions inside the reactor. The reactor was imaged every 10 min.

4.5.4 Energy and Feeding Solution Preparation

The energy solutions were prepared as described previously [309] although at a higher final concentration (4×). The 4× energy solution contained 1.2 mM of each amino acid, 47.2 mM magnesium acetate, 400 mM potassium glutamate, 8 mM ATP and GTP, 4 mM CTP, UTP, and TCEP (tris(2-carboxyethyl)phosphine hydrochloride), 14 mg/mL tRNA, 80 mM creatine phosphate, 0.08 mM folinic acid, 8 mM spermidine, and 200 mM HEPES. The prepared energy solution was then diluted to 2.5× working concentration, or used in a feeding solution. The feeding solutions were prepared by combining the energy solution or Solution A (PURExpress) at the desired concentrations with PURE buffer (final concentration in the feeding solution: 13 mM HEPES, 1.4 mM magnesium acetate, 1.7 mM magnesium chloride, 7 mM potassium glutamate, 4.2 mM potassium chloride, 4 mM TCEP, 2.8 mM 2-mercaptoethanol).

4.5.5 Device Setup for Cell-Free Expression

PURExpress solution B supplemented with RNase inhibitor (2 U/µL), mScarlet, and TCEP (10 mM), PURExpress solution A or energy solution 2.5×, and DNA solutions were mixed in the microfluidic reactors on the microfluidic chip in a 2:2:1 v/v ratio. The DNA solution at five times its final concentration was prepared by mixing 10 nM eGFP linear templates and 6.25 µM Chi DNA as described previously [3].

For continuous dialysis batch experiments, the reactor was imaged every 10 min and the feeding channel solution was replenished if indicated. For chemostat experiments, the reactor was imaged every 15 min, a 20% fraction of the reactor volume was replaced with fresh components with the same 2:2:1 ratio every 15, 30, or 60 min, while the feeding channel solution was replenished every 15 min, if indicated. Details on the operation of the microfluidic chip can be found in Supplementary Tables 4.1 and 4.2.

4.5.6 Data Acquisition and Analysis

Solenoid valves, microscope, and camera were controlled by a custom Matlab and LabVIEW program. The chip and microscope stage were enclosed in an environmental chamber at 34 °C. The fluorescence was monitored over time on an automated inverted fluorescence microscope (Nikon), using 20× magnification and FITC/Cy5/mCherry filters. The microscope

hardware details are as described previously [43]. Fluorescence images were analyzed using a custom Python script.

4.6 Supplementary Information

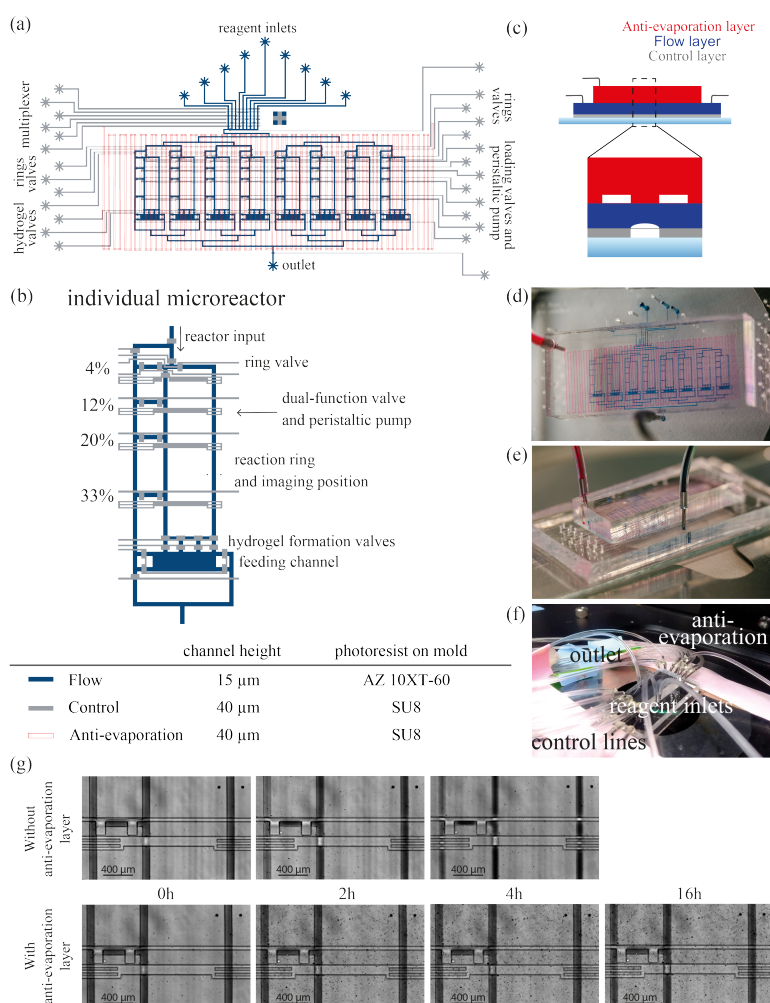


Figure 4.6: Design of the microfluidic device with hydrogel membranes: (a) Design schematic of the microfluidic device. The control layer is shown in gray, the flow layer in blue, and the anti-evaporation layer in red. The device features eight chemostat reactors. (b) Close-up of a microfluidic reactor and table of channel heights and corresponding photoresists used during mold fabrication. Each reactor has four outlets corresponding to four different dilution fractions. Four Control lines serve dual-functions as valves and peristaltic pumps. The width of a flow channel is 100 μm . (c) Schematic depiction (not to scale) of the microfluidic chip cross-section. Image of the microfluidic chip from the top (d) and from the side (e), for visualization the flow channels and the anti-evaporation channel are filled with blue and red dye, respectively. (f) Image of microfluidic chip connected to the control lines, reagent inputs and outlet. (g) Comparison of the water evaporation in the chip with and without the anti-evaporation layer at different times at 34°C. The flow channels were filled with blue dye for better visualization.

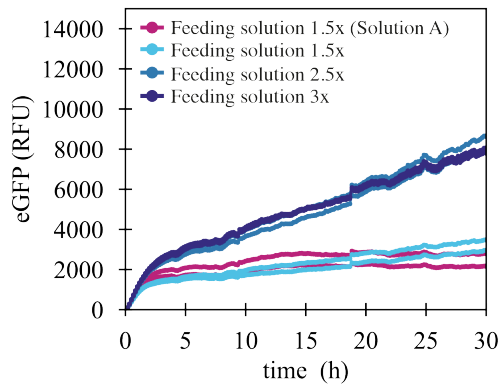


Figure 4.7: Time course of in vitro eGFP expression levels in batch with continuous dialysis reactions for different feeding solution concentrations based on the commercial solution A (PURExpress) or home-made energy solution. Each curve represents a technical replicate.

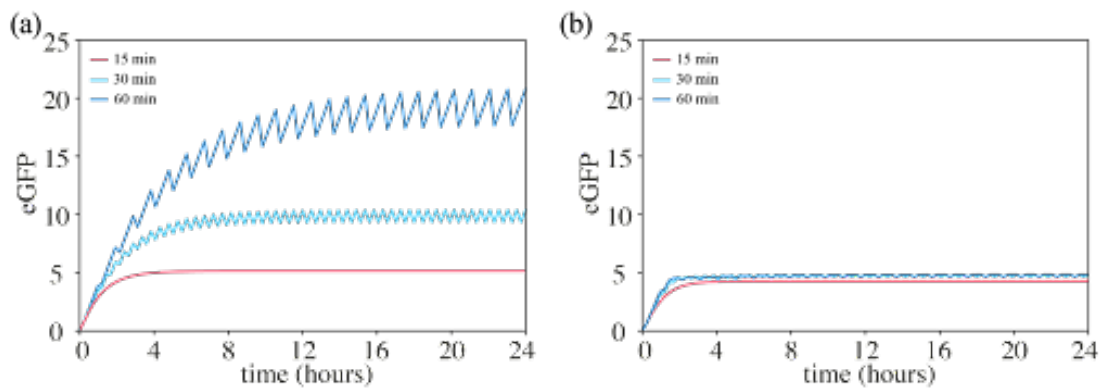


Figure 4.8: Chemostat simulations: The chemostat was simulated using a minimal resource-dependent TX-TL model [3] periodically diluting and replenishing species and solving ODEs every 15 min to match the experimental measurements. The resource R_0 was chosen so: (a) the resource depletion is not rate limiting ($R_0 = 1000$), (b) the resource depletion is rate limiting ($R_0 = 30$). 20% of the chemostat reactor volume was diluted at different time intervals of 15, 30, and 60 min. Parameter conditions $\alpha = 0.7$, $\beta = 0.07$, $K = 1$ and initial conditions $pT = 10$, $dG = 2$, with all other species set to zero.

Improved Cell-Free Transcription–Translation Reactions in Microfluidic Chemostats 4 Augmented with Hydrogel Membranes for Continuous Small Molecule Dialysis

Table 4.1: Microfluidic chip operations for batch, batch with static dialysis and batch with continuous dialysis reactions

Batch reaction		
<i>Step</i>	<i>Operation</i>	<i>Solution</i>
0A	Initial fill	
	Flush rings	PURE solution
	Load 20% (Flush through outlet 20%)	eGFP DNA
0B	Mix	

Extended batch reaction		
<i>Step</i>	<i>Operation</i>	<i>Solution</i>
0A	Initial fill	
	Flush rings	PURE solution
	Load 20% (Flush through outlet 20%)	eGFP DNA
0B	Feeding chamber fill	
	Load feeding chamber	Feeding solution
0C	Mix	

Continuous exchange reaction		
<i>Step</i>	<i>Operation</i>	<i>Solution</i>
0A	Initial fill	
	Flush rings	PURE solution
	Load 20% (Flush through outlet 20%)	eGFP DNA
0B	Feeding chamber fill	
	Load feeding chamber	Feeding solution
0C	Mix	
	Repeat the following steps every 10 min	
1A	Feeding chamber fill	
	Load feeding chamber	Feeding solution

Table 4.2: Microfluidic chip operations for steady-state reactions

Steady-state reaction			Steady-state reaction augmented with continuous exchange		
Step	Operation	Solution	Step	Operation	Solution
Initial fill			Initial fill		
0A	Reactor fill		0A	Reactor fill	
	Flush rings	PURE solution		Flush rings	PURE solution
	Load 20% (Flush through outlet 20%)	eGFP DNA		Load 20% (Flush through outlet 20%)	eGFP DNA
0B	Mix		0B	Feeding chamber fill	
				Load feeding chamber	Feeding solution
			0C	Mix	
Dilution steps			Dilution steps		
Repeat the following steps every 15 min			Repeat the following steps every 15 min		
1A	Image each reactor		1A	Image each reactor	
Repeat the following steps every 15, 30 or 60 min			Repeat the following steps every 15, 30 or 60 min		
1B	Replace 20% of the ring content		1B	Feeding chamber fill	
	Load 8% (Flush through outlet 20%)	Energy solution		Load feeding chamber	Feeding solution
	Load 8% (Flush through outlet 12%)	Solution B			
	Load 4% (Flush through outlet 4%)	eGFP DNA	Repeat the following steps every 15, 30 or 60 min		
1C	Mix		1C	Replace 20% of the ring content	
				Load 8% (Flush through outlet 20%)	Energy solution
				Load 8% (Flush through outlet 12%)	Solution B
				Load 4% (Flush through outlet 4%)	eGFP DNA
			1D	Mix	
Repeat from the step 1A-C			Repeat from the step 1A-D		

5 C2CAplus: a one-pot isothermal circle-to-circle DNA amplification system

This work was published in ACS Synthetic Biology, 2023. Reprinted with permission from [341]. Copyright 2023 American Chemical Society.

Reference: Grasmann, L., Thiel Pizarro, P. & Maerkl, S. J. (2023). C2CAplus: a one-pot isothermal circle-to-circle DNA amplification system. ACS Synthetic Biology, 12(10), 3137-3142.

Contribution: L.G. and P.T. performed experiments. L.G., P.T., and S.J.M. designed experiments. L.G. and S.J.M analyzed data, and wrote the manuscript.

5.1 Abstract

Rolling circle amplification (RCA) is a widely used DNA amplification method that uses circular template DNA as input and produces multimeric, linear single or double stranded DNA. Circle-to-circle amplification (C2CA) has further expanded this method by implementing product re-circularization using restriction and ligation, leading to a higher amplification yield, and enabling the generation of circular products. However, C2CA is a multistep, non-isothermal method, requiring multiple fluid manipulations and thereby compromises several advantages of RCA. Here, we improved C2CA to implement a one-pot, single step, isothermal reaction at temperatures ranging from 25 to 37°C. Our C2CAplus method is simple, robust, and produces large quantities of product DNA that can be seen with the naked eye.

keywords: synthetic biology, DNA replication, circle-to-circle amplification, cell-free synthetic biology, phi29, rolling circle amplification

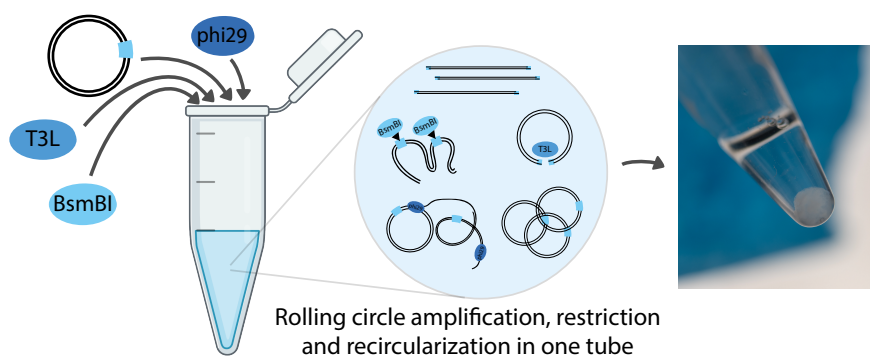


Figure 5.1: Graphical Abstract

5.2 Introduction

RCA is a robust DNA amplification method that has become increasingly popular with a broad range of applications [342]. RCA requires a circular template. Sequence specific primers bind to this template and subsequently a polymerase with strand displacement activity, mainly bacteriophage phi29 DNA polymerase [343], will replicate the DNA in a rolling circle fashion, producing long multimeric strands of linear DNA. In contrast to PCR, no thermal cycling is required, which offers a multitude of advantages. DNA amplification using RCA is cost-effective, simple, and at the same time can be highly specific [344]. RCA has shown great potential for the use in diagnostics and as a biosensor, and various biologically relevant targets have been detected using RCA [345–347]. Hence, it is not surprising that isothermal systems such as RCA are anticipated to be used for on site testing in remote areas and poorly equipped healthcare settings [345]. Besides being used in biosensing, RCA is currently one of the most promising DNA replication methods for the construction of a synthetic cell [22, 29, 30, 36, 37].

To that end, however, a major drawback is that the output DNA structure of a RCA reaction is different to the input structure, that is linear instead of circular DNA.

Circle-to-circle-amplification (C2CA) was originally developed to improve RCA for the use in biosensing [348]. In a first step, padlock probes specific to the tested single-stranded DNA sequence and a ligase are used to generate a circular target DNA, which can then be amplified using standard RCA [349, 350]. In C2CA, the linear, single-stranded, multimeric RCA product is then digested by restriction digest and re-circularized in combination with a second primer by ligation generating circular monomeric products. These circles can then enter a consecutive round of RCA amplification, leading to circles of the opposite polarity, followed by another round of restriction, and ligation. The repetitive amplification, restriction, and ligation of template DNA during C2CA yielded 100x higher amounts of DNA than PCR [346]. Recent work has successfully demonstrated the detection of the Zika virus using padlock probes and C2CA combined with microfluidic affinity chromatography enrichment of the amplification product [351]. Martin and coworkers developed a biosensor to detect the antibiotic resistance gene *sul1* for sulfonamide resistance using padlock probes. They furthermore developed a readout method that was visible by the naked eye using functionalized magnetic nanoparticles that aggregate with the C2CA product [352].

While RCA has the advantage that the process is simple, isothermal and is functional at ambient temperatures, current C2CA methods lost these advantages, as different temperatures are required for restriction and ligation, additional heat inactivation steps are necessary, and multiple reagent additions are needed in each round of amplification. C2CA therefore requires considerable user interaction or the use of liquid handling robotic platforms. We thus set out to develop an isothermal C2CA system that contains all components in a single tube, creating an isothermal C2CA method that requires no user interaction or complex automation. Our C2CAplus method is more sensitive than standard RCA, and produces large quantities of DNA that can be seen by naked eye. C2CAplus functions robustly in a temperature range between 25-37°C and produces circular DNA products that can be transformed. We anticipate that C2CAplus will pave the way towards lower-cost, and easier-to-use RCA based biosensing methods, and could form the basis of a DNA replication system in a synthetic cell.

5.3 Results

5.3.1 Isothermal restriction and ligation

In RCA one or more primers bind to a circular target DNA. A strand displacing DNA polymerase elongates these primers in a rolling circle manner producing long, multimeric, initially single-stranded DNA products. If an anti-directional primer is added, double-stranded, multimeric DNA can be generated. In C2CA and C2CAplus a restriction enzyme is then used to monomerize this double-stranded DNA, and subsequently a ligase ligates the ends, thus re-circularizing the initially linear product (Figure 5.2A).

To develop an isothermal one-pot C2CAplus system, one thus requires a restriction enzyme and ligase that operate under isothermal conditions, ideally around 30°C. We used the enzyme BsmBI v2 (NEB) to cut the sequence of our target plasmid exactly once to monomerize the double-stranded product, as can be seen by the single band in Figure 5.2B. The non-digested high-molecular weight product in the gel loading pocket is most likely single-stranded DNA that can't be cut by BsmBI, but can be digested by P1, a nuclease that specifically degrades ssDNA and RNA (Figure 5.2B). Adding both P1 and BsmBI produced a single band at around 5 kbp (Figure 5.2B), which is presumably monomeric, double-stranded DNA. Albeit optimal conditions for BsmBI v2 include NEB buffer 3.1 and incubation at 55°C, BsmBI activity at 30°C in an RCA reaction environment is sufficient to monomerize all product DNA after 18 h of incubation at 30°C using a concentration of around 0.5 - 0.2 U/μL (Supplementary Figure 5.4).

In the next step we digested an RCA product using BsmBI and screened several commercially available ligases including T4 DNA ligase, Taq DNA ligase, T3 DNA ligase, T7 DNA ligase, and *E. coli* DNA ligase, under their respective optimal conditions. When transforming the ligation product into 10-beta competent *E. coli* cells, we observed a significant increase in colonies for T4 DNA ligase, T3 DNA ligase, and *E. coli* DNA ligase treated samples compared to the BsmBI digested control and the plain RCA product (Supplementary Figure 5.6). As the optimal temperatures for T3 and T4 ligases of 25°C are already close to our target temperature of 30°C, and *E. coli* DNA ligase optimally operates at 16°C, we focused on T3 and T4 ligase.

Optimal ligation conditions for both T3 and T4 ligases include the above mentioned ligation temperature of 25°C, addition of a reaction buffer, and dilution of the restricted RCA product. We set out to investigate the performance of both ligases under non-optimal conditions. We added the ligases to the non-diluted restricted RCA product and omitted the respective reaction buffer. Both ligases retained activity under these conditions (Figure 5.2C). In a second experiment we increased the ligation temperature from the optimal 25°C to 30°C. Both, T3 and T4 DNA ligases ligated the restricted product at 30°C in absence of ligase buffer at both temperatures, rendering them promising candidates for an isothermal one-pot C2CA system.

5.3.2 One-Pot C2CAplus

The development of a one-pot C2CAplus system requires a careful balance of restriction enzyme to ligase ratio (Figure 5.3A). If too little restriction enzyme is present, most product will remain multimeric, rendering re-circularization inefficient. If too much restriction enzyme is present, the restriction enzyme will linearize all DNA including newly ligated circular DNA. As RCA only works on circular DNA, the presence of only linear template will not lead to an improved DNA amplification. We thus tested concentrations between 0 - 0.15 U/μL of BsmBI which were below the 0.2 U/μL used above and which digested all RCA product during the time course of a RCA reaction. As T3 out-performed T4 ligase in our initial characterization (Figure 5.2C), we chose to test different concentrations of T3 DNA ligase between 0-120 U/μL. To develop our one-pot C2CAplus reaction, we investigated a combinatoric space of BsmBI-to-T3

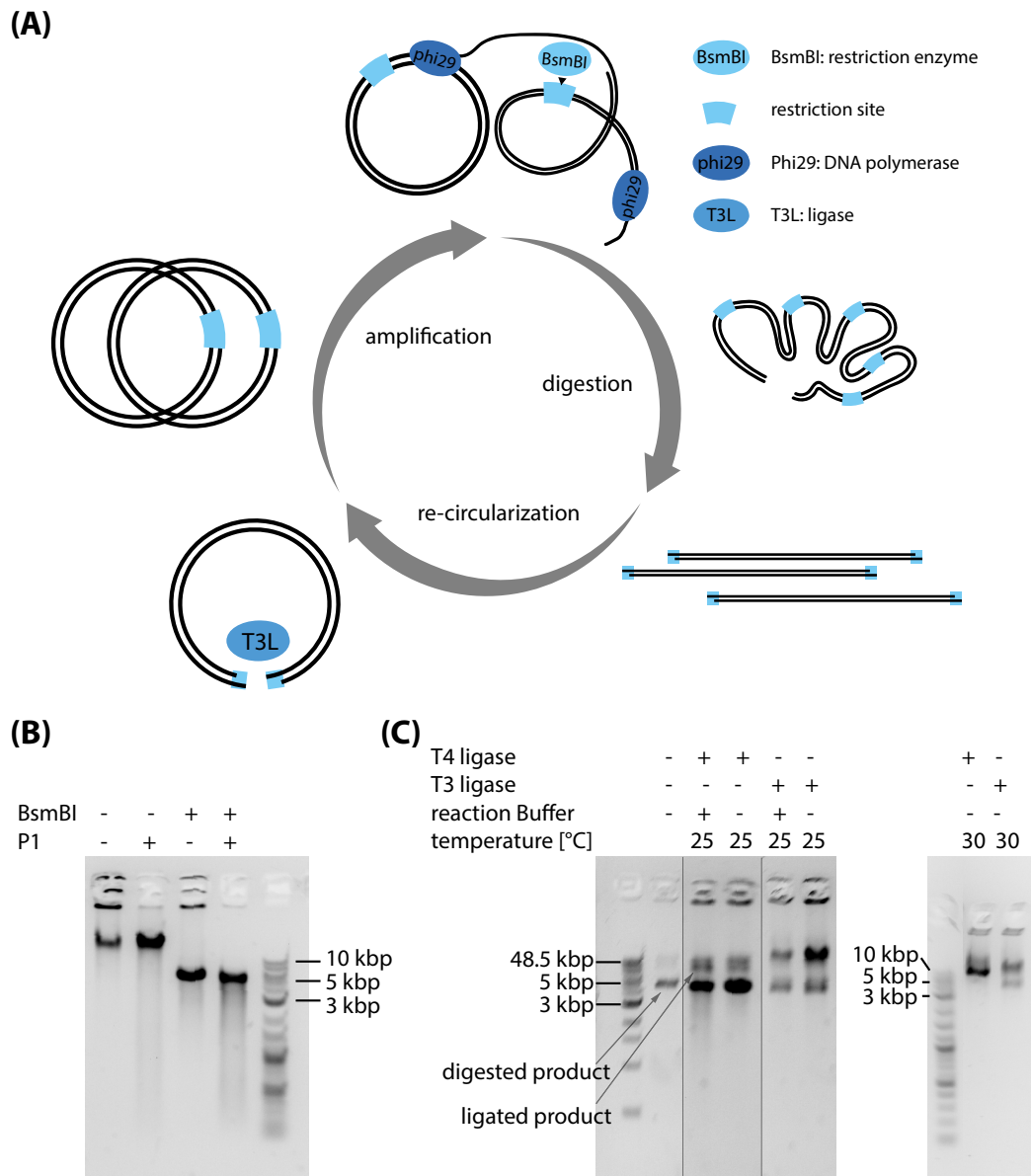


Figure 5.2: **(A)** Schematic of a C2CAplus amplification scheme that integrates DNA amplification, restriction, and re-circularization. DNA amplification by Phi29 DNA polymerase produces multimeric double-stranded DNA that can be monomerized using a restriction enzyme. These monomers are subsequently ligated and thus circularized using a ligase. **(B)** Characterization of restriction digestion of an amplification product. The left band shows the untreated reaction with product in the pocket and a distinct band at a running length greater than the uppermost band of 48.5 kbp of the 1kb Extend Ladder. The product in the pocket can be digested by exonuclease P1 (5 U/ μ L), which is specific for ssDNA. The band at > 48.5 kbp can be cut by BsmBI (0.67 U/ μ L) to a length of around 5 kbp, which is the monomeric length of our input plasmid, indicating that this band is multimeric dsDNA.

Figure 5.2: (C) Ligation activity of T4 and T3 DNA ligases (both 0.5 μL in a total reaction volume of 10 μL) after an initial BsmBI digest (0.67 U/ μL) with and without reaction buffer, at 25°C and 30°C. The dashed lines indicate where different lanes were pasted together in the left gel. A non-cropped version of that gel is shown in Supplementary Figure 5.5.

concentrations (Figure 5.3B).

The tested BsmBI concentrations were indeed low enough to not drastically affect amplification (Figure 5.3B). However, without the addition of T3 ligase, amplification efficiency was decreased compared to the control lacking T3 ligase and BsmBI (Figure 5.3B, first band). The sole addition of T3 ligase did not change amplification efficiency considerably (Figure 5.3B, bands e, i, m). However, if both BsmBI and T3 ligase were added together, amplification efficiency was increased (Figure 5.3B, bands f-h, j-l, n-p).

Amplification was generally so efficient that the solution in the reaction tube became highly viscous and was difficult to be applied to an agarose gel. Amplification was so large with optimal combinations of BsmBI and T3 ligase that a white, highly viscous precipitate formed in the reaction tubes, which became more pronounced after a freeze - thaw cycle (Figure 5.3C). Precipitate formation could be seen for all reactions containing both BsmBI and T3 ligase, indicating that C2CAplus is robust over the tested range of restriction enzyme-to-ligase ratios. However, a concentration of 0.1 U/ μL BsmBI with T3 ligase at 30, 60, and 120 U/ μL , seemed to be especially advantageous for precipitate formation, with a qualitative optimum at 0.1 U/ μL BsmBI and 30 U/ μL T3 ligase (Figure 5.3C panels g, k, o). Precipitate formation is less pronounced at lower and higher BsmBI concentrations, indicating that BsmBI concentration is critical for DNA amplification efficiency. It should be mentioned that although the precipitate can be seen directly after the reaction, precipitate becomes even more prominent after freeze-thawing the reaction tubes. We subsequently validated DNA sequence integrity by transforming 10-beta *E. coli* cells with the C2CAplus product, isolated the plasmid via Miniprep, and sequence verified the plasmid.

5.3.3 C2CAplus is highly sensitive and robust

We tested the sensitivity of C2CAplus by titrating input plasmid concentrations between 1.6 pM and 0.16 nM (0.005 ng/ μL and 0.5 ng/ μL) to an RCA and a C2CAplus reaction supplemented with EvaGreen DNA stain and measured fluorescence over time (Figure 5.3D). While plain RCA produced an increase in fluorescence for input plasmid concentrations of 0.5 and 0.1 ng/ μL (Figure 5.3D), C2CAplus amplified plasmid DNA for all tested input DNA concentrations including 0.005 ng/ μL (Figure 5.3E). C2CAplus also generated a significantly higher fluorescent signal compared to plain RCA. The curves for C2CAplus were exponential, in contrast to the linear curves obtained for plain RCA, indicating that the restriction enzyme and ligase indeed circularize a significant amount of the RCA product, which can subsequently serve as a circular input template for further rounds of replication leading to an exponential amplification.

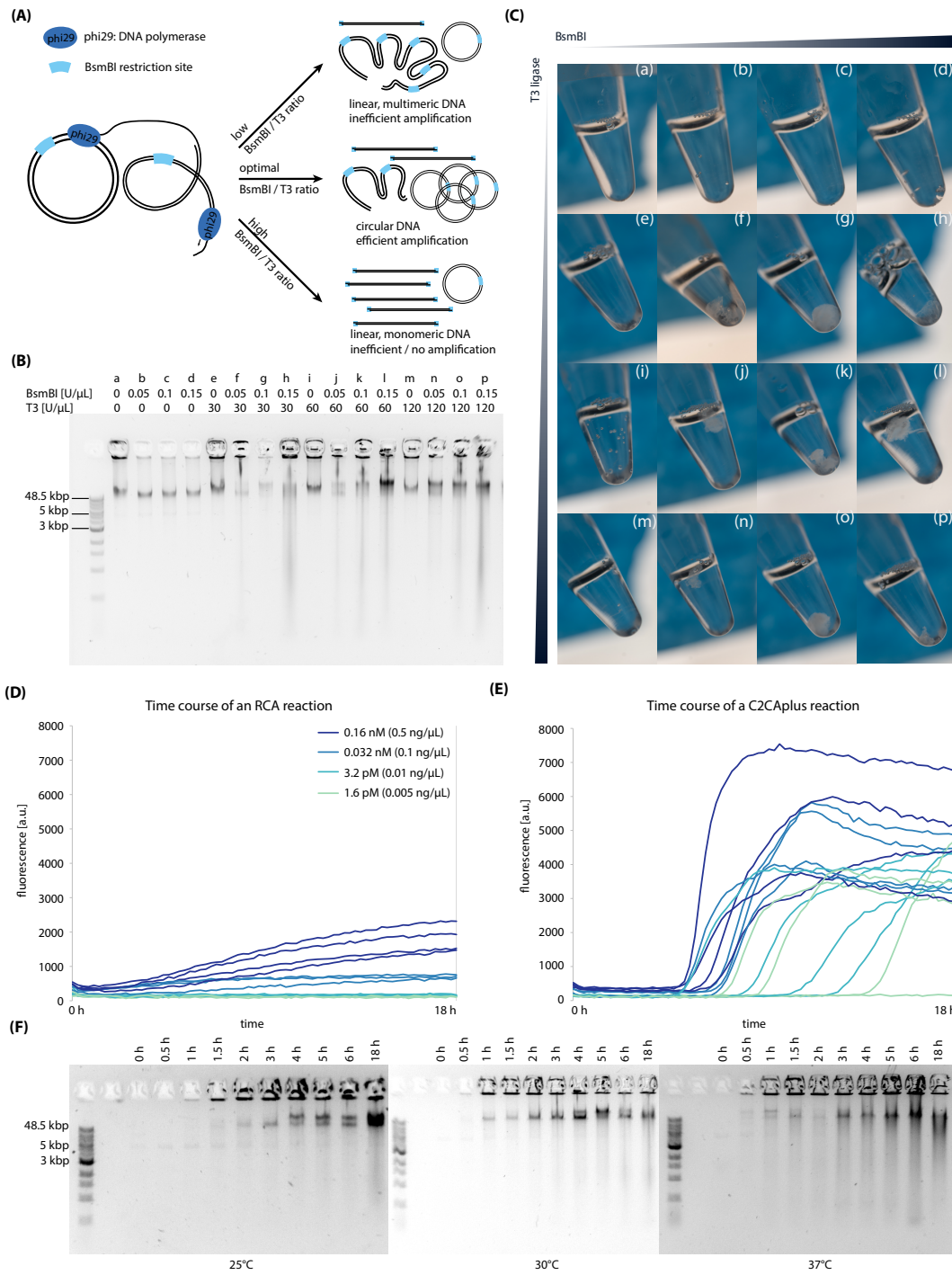


Figure 5.3: Caption next page.

Figure 5.3: **(A)** Schematic overview of all potential outcomes of C2CAplus reactions. If the BsmBI to T3 ligase ratio is too low, most of the RCA product will remain multimeric leading to inefficient amplification. If the ratio is too high, the restriction enzyme will monomerize the majority of the product and input DNA, which will reduce amplification. Therefore, an optimal ratio is required to facilitate efficient re-circularization of the digested products present in the reaction. If the BsmBI to ligase ratio is optimal, more circular product will be generated, which serves as an efficient template for further rounds of replication, thus generating a high amplification rate. **(B)** Agarose gel showing the products of C2CAplus reactions with different concentrations of BsmBI and T3 DNA ligase **(C)** Pictures of the reaction tubes from (B). **(D)**, **(E)** RCA (D) and C2CA (E) reaction curves measured on a platereader using different input plasmid concentrations. C2CAplus successfully amplifies lower DNA input concentration than RCA. **(F)** Agarose gels of a time course of C2CAplus using different reaction temperatures.

If used as a biosensor or in a synthetic cell, a tolerance to reaction temperatures is ideal. We therefore compared the performance of C2CAplus at 30°C to its performance at 25°C and 37°C. Figure 5.3F shows the time course of C2CAplus reactions at 25°C, 30°C, and 37°C. Despite the reaction at 25°C being delayed by about 30 min compared to the reactions at higher temperatures, no differences are observed between the general amplification levels, indicating that C2CAplus performs robustly in the tested temperature range of 25 to 37°C.

5.4 Discussion

In this work we developed a fully isothermal one-pot C2CA method called C2CAplus using the restriction enzyme BsmBI to cut the linear multimeric DNA produced by phi29 DNA polymerase, and T3 DNA ligase to re-ligate the monomers to form circular DNA. As the only sequence requirement for C2CAplus is a single unique restriction site, the method promises to be versatile and broadly applicable for various purposes. Although the system has so far only been tested with BsmBI as restriction enzyme, we anticipate that after optimization other restriction enzymes that are active at ambient temperatures could be used for C2CAplus, as well. This might be necessary when sequence restrictions limit the use of BsmBI, especially if long or multiple DNA fragments are replicated. C2CAplus combines the main advantage of standard RCA by being able to operate in isothermal conditions, with the advantages of C2CA of a higher amplification rate and the ability to generate circular DNA products.

C2CAplus successfully amplified DNA with input concentrations of 0.005 ng/ μ L (1.6pM). The exponential amplification produces large quantities of DNA and generates precipitate that is visible to the naked eye. We anticipate that a simple readout based on precipitate formation could facilitate the use of C2CAplus as a biosensor in remote areas, rendering readout independent of sophisticated laboratory equipment. However, comparable to LAMP and other highly sensitive DNA amplification methods that exponentially amplify DNA, C2CAplus is also prone to producing false-positives and care must be taken to avoid DNA contamination when used as a biosensor, or highly specific primers need to be developed.

DNA hydrogels have become popular due to characteristics that render them advantageous especially in biomedical applications and biosensing [353]. Recently, Song and coworkers demonstrated the fabrication of a DNA hydrogel in 24 h, using multiple primed RCA reactions [354]. As our C2CAplus method produces large quantities of DNA that precipitates in the tube to a white, viscous, gel-like structure, we expect that C2CAplus could also be helpful in efficiently producing DNA for use in biomaterials.

Lastly, we see potential for C2CAplus to be used as a DNA replication mechanism in a synthetic cell. Thus far, endeavours have mainly focused on implementing standard RCA in cell-free transcription/translation systems [22, 29, 36] and Van Nies and coworker implemented a method that replicates DNA from a linear template [34]. One main challenge of using RCA as a replication method is the structural difference of DNA produced by RCA: while the input DNA structure is circular, the output structure is linear, entangled, and multimeric. Although Okauchi and coworkers successfully demonstrated the replication of short (100-200 basepair) multimeric DNA sequences using the RCA method, RCA is generally more efficient for circular templates of longer DNA sequences [36].

Sakatani and coworkers [30], as well as Okauchi and coworkers in a subsequent publication [37] attempted to solve this issue by implementing a re-circularization mechanism using cre recombinase. However, cre recombinase seemed to inhibit DNA replication. Okauchi [37] solved this by evolving the DNA. Yet, in the larger context of eventually building an artificial cell, sequence restrictions to avoid inhibition by a cre recombinase may be problematic. We therefore suggest that implementing re-circularization by restriction and re-ligation may be a viable path towards achieving integrated DNA replication in a cell-free transcription - translation system. It needs to be mentioned that both re-circularization mechanisms using cre-recombinase and C2CAplus produce a significant amount of linear, entangled, and multimeric DNA side products [29, 37], but the main advantage of re-circularization systems is that they do regenerate some circular product that will amplify efficiently and therefore has a better chance of sustaining a long-term DNA replication system.

5.5 Methods

Stand-alone RCA, restriction, and ligation reactions

A standard RCA reaction was performed using 0.1 U/ μ L phi29 DNA polymerase (ThermoFisher Scientific, stock: 10 U/ μ L) supplemented with 1x reaction buffer, 1 μ M 3' final primer and 1 μ M 5' final primer, (sequences in Supplementary Table 5.1), 0.5 mM dNTP mix (ThermoFisher Scientific), and an input plasmid (sequence in Supplementary Information) concentration of 0.5 ng/ μ L (0.16 nM) unless indicated otherwise.

Nuclease P1 (NEB) treatment was performed as recommended by the supplier in a reaction volume of 10 μ L, by supplementing 8.5 μ L of RCA product with 1 μ L NEB 1.1 reaction buffer (final concentration: 1x) and 0.5 μ L P1 nuclease (final concentration: 5 U/ μ L). Restriction

digest using BsmBI v2 (NEB, stock concentration 10 000 U/mL) was performed at a BsmBI-v2 concentration of 0.67 U/ μ L. The restriction was performed in undiluted RCA product omitting any additional buffer at 55°C for 1 h, followed by heat inactivation at 80°C, unless indicated otherwise.

All ligases (T3, T4, *E.coli*, T7, Taq) used during this work were obtained from NEB. Ligations were performed as indicated by the supplier. For the transformation experiments in Supplementary Figure 5.6, 1 μ L of BsmBI digested RCA product was supplemented with 0.5 μ L of each ligase in 1x reaction buffer in a total reaction volume of 10 μ L. Incubation times and temperatures are as follows: T4 ligase was incubated at 25°C for 2 h, followed by heat inactivation at 65°C for 10 min; T3 and T7 ligases were incubated at 25°C for 30 min without heat inactivation; Taq ligase was incubated at 45°C for 15 min; *E. coli* ligase was incubated at 16°C for 30 min, followed by heat inactivation at 65°C for 20 min.

For transformation reactions, 5 μ L of the respective ligated product was added to one vial (50 μ L) of NEB 10-beta competent *E. coli* cells. Non-ligated RCA and BsmBI products were diluted 1:10 in MiliQ water prior to transformation, to obtain the same dilution factor as the ligated product.

For the ligation tests of T3 and T4 ligases in Figure 5.2C, 4.5 μ L of BsmBI digested RCA product was added to the reactions containing reaction buffer, and 9.5 μ L of BsmBI digested RCA product was added to the reactions without reaction buffer. Reaction temperatures and times are as indicated above, unless specified otherwise.

Gel electrophoresis was performed using 1 % agarose gels and the ladders used were either Quick-Load 1 kb Extend DNA Ladder (NEB), or Quick-Load Purple 1 kb plus DNA Ladder (NEB).

5.5.1 C2CAplus reactions and platereader experiments

C2CAplus reactions were performed in a total reaction volume of 20 μ L or 50 μ L. 0.1 U/ μ L phi29 DNA polymerase was supplemented with 1x reaction buffer, 0.5 mM dNTP mix, 1 μ M 3'final primer, and 1 μ M 5'final primer (Supplementary Table 5.1). The reaction was additionally supplemented with 120 U/ μ L T3 ligase, and 0.1 U/ μ L BsmBI, unless indicated otherwise. It should be noted that T3 DNA ligase is ATP dependent. No ATP is present in the RCA reaction buffer, and by omitting the T3 ligase buffer, we do not add any ATP to the reaction. However, it is known that T3 ligase ligates DNA efficiently in presence of dATP as well [355]. The C2CAplus reaction was incubated in a thermocycler for 18 h at 30°C. The highly viscous product was subsequently applied to a 1% agarose gel for analysis. It needs to be noted that due to the high viscosity of the product, the application to a gel was challenging. For the analysis of precipitate formation in Figure 5.3B, the product was freeze-thawed once before imaging. Here, the total reaction volume was 50 μ L. All platereader experiments were performed with 20 μ L volumes and the reactions were further supplemented with 2% BSA and 0.25x EvaGreen (Biotium, stock:

20x in H₂O) in an optical, black, flat bottom 384 well-plate (Thermo Scientific). It should be noted that EvaGreen inhibits the reaction if applied at higher concentrations, and the addition of BSA is crucial in platereader experiments. Samples were sealed using a SealPlate film (Excel Scientific). Fluorescence was measured every 10 min at 500 / 530 nm ex/em for 18 h at 30°C, and during every 10 min interval, the plate was shaken for 10 s.

5.5.2 Image and data processing

Gel images were cropped using Adobe Photoshop and labeled in Adobe Illustrator. Plate images in Figure 5.6 were adjusted in brightness and contrast for better visibility of the colonies using Fiji.

5.6 Supporting Information

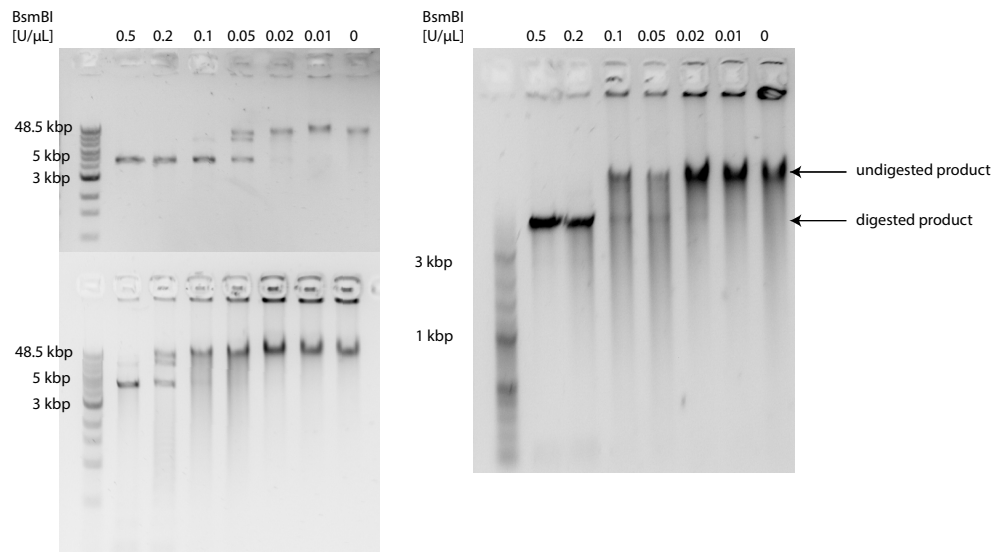


Figure 5.4: BsmBI titration at 30°C and 18 h reaction time. Three independent replicates were performed. A concentration of 0.5 to 0.2 U/μL digests most of the RCA product in the given conditions.

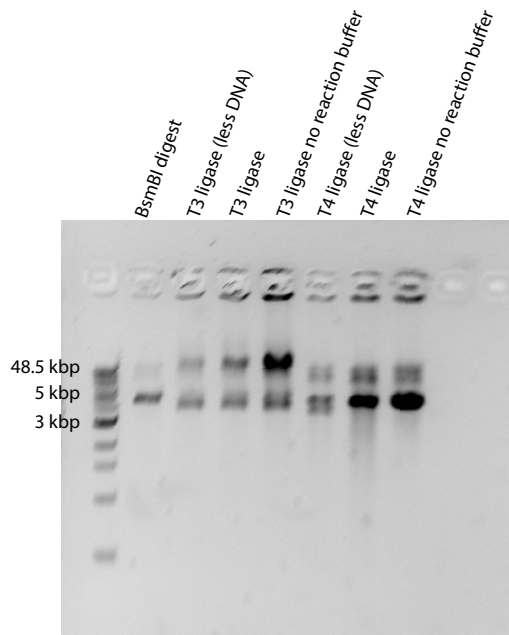


Figure 5.5: Non-cropped gel of 5.2C. The first lane is a BsmBI digested product as shown in Figure 1C. The second lane is a T3 ligase ligation reaction with less DNA (3 μ L in a total volume of 10 μ L), not included in Figure 1C. The following two lanes are again included in Figure 1C, and show the T3 ligation with and without reaction buffer. The 5th lane, T4 ligase (less DNA) is not included in Figure 1C, and shows the T4 ligation with 3 μ L of DNA in a total volume of 10 μ L. The last two lanes are again included in Figure 1C, and show the T4 ligation reaction with and without reaction buffer.

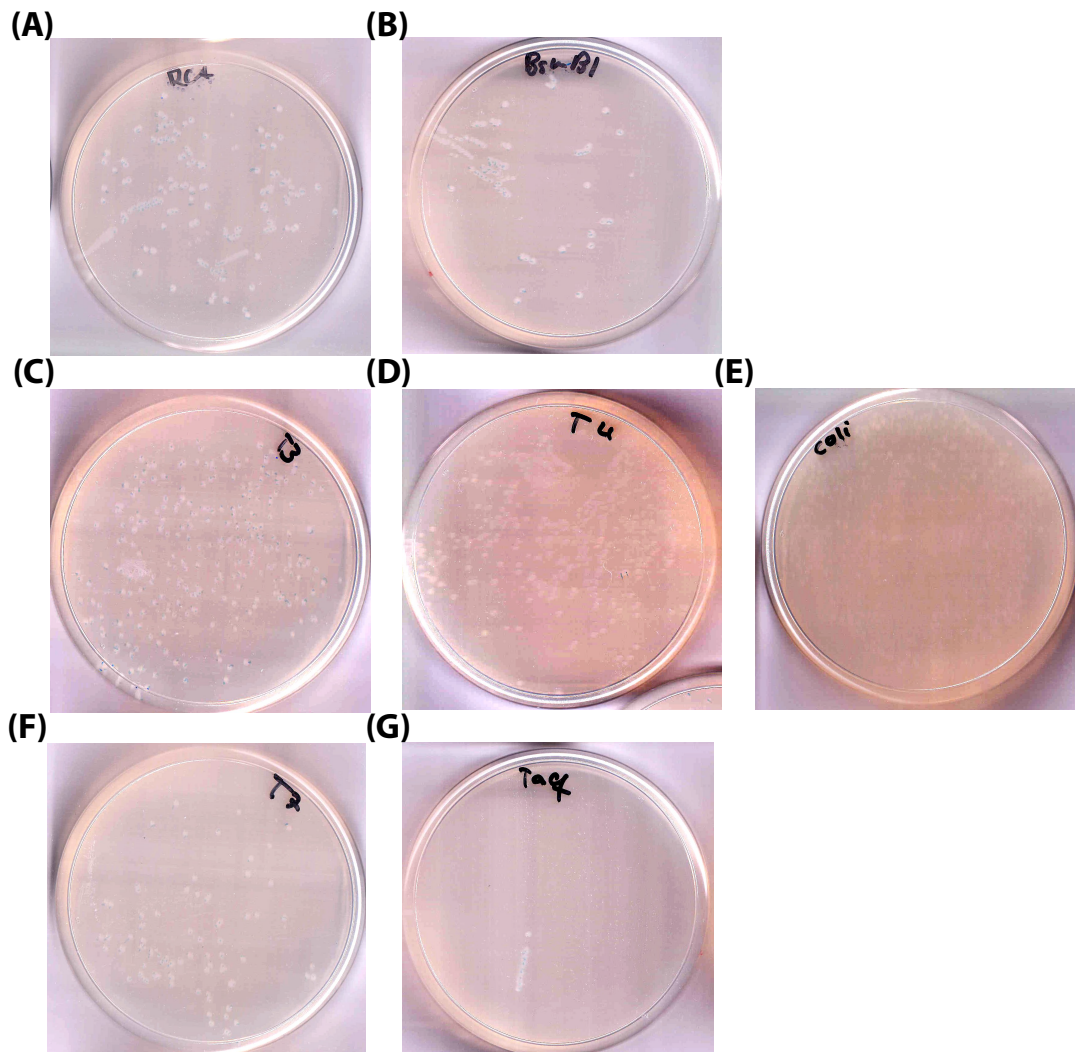


Figure 5.6: Ligase screen. Transformation results of: (A) non-treated RCA product, (B) BsmBI digested RCA product, T3 (C) T3 ligase, T4 (D) T4 ligase, (E) *E. coli* ligase, (F) T7 ligase, (G) Taq ligase.

5.6.1 DNA sequences

Primer sequences

The primers used in this work were:

Table 5.1: Primers used during this work

5' final	GATCTTAAGGCTAGAGTAC
3' final	CAAAAAACCCCTCAAGAC

Plasmid sequence

The plasmid used in this work is a pSTBlue plasmid encoding Kanamycin and Ampicillin resistance as well as an EGFP gene. The BsmBI restriction site is located inside the Kanamycin resistance gene. The complete plasmid sequence is:

```

CTCAGGCGCAATCACGAATGAATAACGGTTTGGTTGATGCGAGTGATTTTGATGACGAGCGTAATGGCTGGCCTGTTGAACAAGTCTGAAAGAAATGCATAAACTTTTGCCA
TTCTCACCGGATTACAGTCGCACTCATGGTGATTTCTCACTTGATAACCTTATTTTGACGAGGGGAAATTAATAGGTTGATTGATGTTGGACGAGTCGGAATCGCAGACCGA
TACCAGGATCTTGCCATCCTATGGAATGCCTCGGTGAGTTTTCTCCTTCATTACAGAAACGGCTTTTTCAAAAATATGGTATTGATAATCCTGATATGAATAAATTCAGTTC
ATTTGATGCTCGATGAGTTTTTCTAAGAATTAATTATGACCAAAATCCCTTAACGTGAGTTTTTCGTTCCACTGAGCGTCAGACCCCGTAGAAAAGATCAAAGGATCTTCTTGA
GATCCTTTTTTCTGCGCGTAATCTGCTGCTGCAAAACAAAAACCCAGCTACACGCGTGGTTTGGTTCGCGGATCAAGAGTACCAACTCTTTTTCCGAAGGTAACGTGG
CTTCAGCAGAGCGCAGATACCAAACTGTCCTTCTAGTGTAGCCGTAGTTAGGCCACCCTCAAGAAGTCTGTAGCACCGCTACATACCTCGCTGCTAATCCTGTTAC
CAGTGGCTGCTGCCAGTGGCGATAAGTGTCTTACCAGGTTGACTCAAGACGATAGTTACCAGGATAAGGCGCAGCGGTCGGGCTGAACGGGGGGTTCGTGCACACAGC
CCAGCTTGAGGCGAACGACCTACACCGAATGAGATACCTACAGCGTGAGCTATGAGAAAGCGCCACGCTTCCCGAAGGGAGAAAGGCGGACAGGTATCCGGTAAGCGGCA
GGGTCGGAACAGGAGAGCGCACGAGGAGCTTCCAGGGGAAACGCCCTGATCTTTATAGTCTGTGGGTTTCGCCACCTCTGACTTGAGCGTCGATTTTTGTGATGCTC
GTCAGGGGGCGGAGCCTATGAAAAACGCCAGCAACGCGCCCTTTTACGGTTCCTGGCCCTTTTGTGCTTTCGCTCATGTTCTTCTGCTTATCCCCTGATTCT
GTGGATAACCGTATTACCCTTTGAGTGAGCTGATACCGCTCGCCGACGCGAACGACGAGCGCAGCGAGTCAGTGAGCGAGGAAGCGGAAGCGCCCAATACGCAAA
CCGCTCTCCCGCGCGTTGGCCGATTCAATATGACAGTGGCAGCAGGTTTCCCGACTGGAAAGCGGGCAGTGAGCGCAACGCAATTAATGTGAGTGTAGCTCACTCATT
AGGCACCCAGGCTTACACTTTATGCTTCCGGCTCGATGTTGTGTTGAAATTTGAGCGGATAACAATTTACACAGGAAACAGCTATGACCATGATTACGCCAAGCTCTAAT
ACGACTCACTATAGGAAAGCTCGGTACCACGATGCTGCAGACGCGTTACGTATCGGATCCAGAATTCGTGATGATCTTAAGGCTAGAGTACTAATACGACTCACTATAGGG
AGACCACAACGGTTTCCCTAGAAATAATTTGTTAACTTAAGAAGGAGGAAAAAAATGTCTAAAGGTGAAGAATTATCACTGGTGTGTGCCAATTTGGTTGAATTAG
ATGGTGATGTTAATGGTCACAAATTTCTGTCTCCGGTGAAGTGAAGGTGATGCTACTTACGGTAAATGACCTTAAAAATTTATTTGACTACTGGTAAATGGCAGTCCAT
GGCAACCTTAGTCACTACTTTAACTTATGGTGTCAATGTTTTCTAGATACCCAGATCATATGAAACAACATGACTTTTTCAAGTCTGCCATGCCAGAAGGTTATGTTCAAGA
AAGAACTATTTTTTCAAAGATGACGGTAACTACAAGACCAGAGCTGAAGTCAAGTTTGAAGGTGATACCTTAGTAAATAGAATCGAATTAAGGATTTGATTTAAAGAGAT
GGTAACATTTTAGTCACAAAATGGAATACAATACTCTCAATGTTTACATCATGGCTGACAAACAAAAGAAATGGTATCAAAGTTAACTTCAAAATTAGACACAACATTG
AAGATGGTCTGTCAATTAGCTGACCATTATCAACAAAATACTCCAATGGTGTGGTCCAGTCTTGTACCAGACAACCACTTATCCACTCAATCTGCCCTTATCCAAAGA
TCCAAACGAAAAGAGACCATGTTCTGTTAGAATTTGTTACTGCTGCTGATTACCCATGGTATGGATGAATTTGACAAATAAATACGACTCAGGCTGCTACGCGCTGTG
TACTGAAAACAAAACAAAACAAAACAAAACAAAACAAAACAAAACAAAACAAAACAAAACAAAACAAAACAAAACAAAACAAAACAAAACAAAACAAAACAAAACAAAAC
GGGGCTCTAAACGGGCTTGTAGGGGTTTTGATCTGAATTCGTGCAGAACGCTTCGAGCCTAGGCTAGCTTAGACCACACGCTGTGGGGCCCGAGCTCGCGCGCGCT
GTATTTCTATAGTGCACCTAAATGGCCGACAAATCACTGGCGTCTGTTTACAACGCTGCTGACTGGGAAAACCTGGCGTTACCCAATTAATCGCCTTGACGACATCCCC
CTTTCCAGCTGGCGTAATAGCGAAGAGGCCCGCACCGATCGCCCTCCCAACAGTTGCGCAGCCTGAATGGCGAATGGAATTTGAAGCGTTAATATTTGTTAAATTCG
CGTAAATTTTTGTTAAATCAGCTCATTTTTAACCAATAGGCCGAAATCGGCAAAATCCCTTATAAATCAAAGAATAGACCGAGATAGGGTTGAGTGTGTTCCAGTTTGGAA

```

CAAGAGTCCACTATTAAGAACGTGGACTCCAACGCTCAAAGGGCGAAAAACCGTCTATCAGGGCGATGGCCACTACGTGAACCATCACCTAATCAAGTTTTTTGGGGTCGA
GGTGCCGTAAAGCACTAAATCGGAACCTAAAGGGAGCCCCGATTTAGAGCTTGACGGGGAAAGCCGGCGAACGTGGCGAGAAAGGAAGGGAAGAAAGCGAAAGGAGCGG
GCGCTAGGGCGCTGGCAAGTGTAGCGGTACGCTGCGCGTAACCACCACACCCGCGCGCTTAATGCCCGCTACAGGGCGCGTCAGGTGGCACTTTTCGGGGAAATGTGC
GCGGAACCCCTATTTGTTATTTTCTAAATACATTCAAATATGTATCCGCTCATGAGACAATAACCCTGATAAATGCTTCAATAATATTGAAAAAGGAAGAGTATGAGTATTCA
ACATTTCCGTGTCGCCCTTATTCCTTTTTTTGGCGCATTTTGCCTTCCTGTTTTTGTCTACCCAGAAACGCTGGTAAAAGTAAAAGATGCTGAAGATCAGTTGGGTGCACGAGT
GGGTTACATCGAACTGGATCTCAACAGCGGTAAGATCCTTGAGAGTTTTCGCCCCGAAGAACGTTTTCCAATGATGAGCACTTTTAAAGTTCTGCTATGTGGCGCGGTATTAT
CCCGTATTGACGCCGGCAAGAGCAACTCGGTGCGCGCATACTATTCTCAGAATGACTTGGTTGAGTACTCACCAGTCACAGAAAAGCATCTTACGGATGGCATGACAGTA
AGAGAATTATGCAGTGTGCCATAACCATGAGTGATAACACTGCGGCCAACTTACTTCTGACAACGATCGGAGGACCGAAGGAGCTAACCGCTTTTTTGCAACATGGGGGA
TCATGTAACTCGCCCTTGATCGTTGGGAACCGGAGCTGAATGAAGCCATACCAAACGACGAGCGTGACACCACGATGCCTGTAGCAATGGCAACAACGTTGCGCAAACATTAA
CTGGCGAACTACTTACTCTAGCTTCCCGGCAACAATTAATAGACTGGATGGAGGCGGATAAAGTTGCAGGACCACCTTCTGCGCTCGGCCCTTCCGGCTGGCTGGTTATTGC
TGATAAATCTGGAGCCGGTGAGCGTGGGTCTCGCGGTATCATTGCAGCACTGGGGCCAGATGGTAAGCCCTCCCGTATCGTAGTTATCTACACGACGGGAGTCAGGCAACT
ATGGATGAACGAAATAGACAGATCGCTGAGATAGGTGCCTCACTGATTAAGCATTGGTAACTGTGACACCAAGTTTACTCATATATACTTTAGATTGATTTAAAACTTCATTTTT
AATTTAAAAGGATCTAGGTGAAGATCCTTTTTGATAATCTCATGAACAATAAACTGTCTGCTTACATAAACAGTAATAACAAGGGGTGTTATGAGCCATATTCAACGGGAAACGT
CTTGCTCTAGGCCGCGATTAATTCACATGGATGCTGATTTATATGGGTATAAATGGGCTCGCGATAATGTCGGGCAATCAGGTGCGACAATCTATCGATTGTATGGGAAG
CCCGATGCGCCAGAGTTGTTCTGAAACATGGCAAAGTAGCGTTGCCAATGATGTTACAGATGAGATGGTCAGACTAAACTGGCTGACGGAATTTATGCCTCTTCCGACCAT
CAAGCATTTTATCCGTACTCTGATGATGCATGGTTACTCACCCTGCGATCCCGGGAAAAACAGCATTCCAGGTATTAGAAGAATATCCTGATTGAGGTGAAAAATTTGTTGA
TGGCTGGCAGTGTCTGCGCCGGTTCATTGATTCCTGTTGTAATTGTCTTTTAAACAGGATCGCGTATTTTCGTCTCG

6 Conclusion and Outlook

Building a synthetic cell from scratch is one of the goals of synthetic biology. Research and advances during the past decades have contributed to a greater understanding of biochemical and biological processes. Synthetic biology leverages engineering principles and methodologies to apply this knowledge, making the ambitious goal of creating a synthetic cell more attainable [1]. However, despite being able to build and assemble building blocks of increasing complexity, we are not at the finish line yet, and a multitude of components still remain to be established and compiled.

The work presented in this thesis contributes towards the advancement of synthetic cell development and the practical application of platforms designed for this purpose. This section provides a summary of the results presented in the preceding chapters, discusses limitations encountered, and offers insights into potential future steps and opportunities.

6.1 Bottom-Up Construction of Complex Biomolecular Systems With Cell-Free Synthetic Biology

Chapter 2 discusses different cell-free systems, enabling platforms, and highlights scientific opportunities. Cell-free systems provide a unique chassis for engineering biomolecular systems and pathways due to their versatile, open, and well-defined nature. It is thus not surprising that they are expected to transform a variety of different areas including bioengineering, healthcare, environmental remediation, or food production [45]. In the review presented, we start by discussing the history of cell-free systems and give examples of milestone experiments that utilized cell-free systems and revolutionized our understanding of biology. We continue by introducing and comparing the two versions of cell-free systems: lysates, and the fully recombinant PURE system. We show advantages and limitations of either system and highlight preparation methods and examples to tailor the respective systems. In the next section we introduce microfluidics as an enabling platform and provide examples illustrating how microfluidics has increased the complexity and sophistication of experiments involving

cell-free systems. These include high-throughput platforms and spatially controlled batch reactions, devices enabling experiments at steady-state, and platforms for compartmentalized cell-free reactions. We furthermore discuss emergent scientific opportunities, starting with research towards gene expression regulation using cell-free systems, and finishing with current advances towards DNA replication methods in the context of cell-free systems and the development of an artificial cell. The review was published in 2020 and since then, advances have been made.

Arguably the greatest advantages of cell-free systems are their open nature and versatility, and the fact that they do not depend on life-sustaining processes. This allows for the easy expression of a great variety of proteins that would otherwise require sophisticated expression and purification methods. This includes toxic proteins, proteins requiring liposomes or detergents, multiprotein complexes, or proteins requiring disulfide bonds, which may for instance be harnessed for pharmaceutical applications [356]. Prominent examples are the plasminogen activator which contains disulfide bonds, multidomain proteins such as malaria vaccines, the toxic microtubule binding protein (MID1), or G-protein coupled receptors (GPCRs) as membrane proteins [356]. Another great advantage of cell-free systems, especially the PURE system is the possibility to express from linear templates, which renders cell-free protein expression considerably faster than protein expression in cells.

Ongoing work in our lab leverages several of the above mentioned advantages to identify, which mutational patterns of the omicron variant of SARS CoV-2 have permitted it to evade antibody binding. Using the commercially available PUREfrex 2.1 kit with its DsbC disulfide kit, we expressed 519 variants of the SARS CoV-2 spike protein receptor binding domain (RBD) between the wild type and omicron variants (Grasemann et al., unpublished data). The variants were expressed from non-purified linear templates, which were previously generated by assembly PCR using a liquid handling system. The ability to avoid cloning, transformation and purification steps for 519 variants saved significant amounts of time and costs. More importantly, using our PURE kit complemented with the disulfide bond enhancing kit enabled us to correctly express and fold the RBDs. In other expression systems the correct expression and folding of RBDs is complicated by the critical importance of the correct formation of disulfide bonds [357]. We have since measured the binding affinities of the variants against therapeutically relevant antibodies using a high throughput microfluidic chip [163] and are currently finalizing the analysis thereof.

6.2 One Pot PURE system

As outlined previously, the PURE cell-free system presents an attractive platform for cell-free synthetic biology. However, its usage is restricted due to the high cost and limited customization options of commercially available systems, as well as the laborious and time-consuming preparation of home-made solutions. In chapter 3, we present a protocol for the preparation of

a OnePot PURE system. The protocol streamlines the purification of all 36 non-ribosomal proteins to a single purification by co-culturing all 36 protein-encoding strains. We provide two detailed protocols for ribosome purification. Purifying tag-free ribosomes requires access to an Akta purifier, which we consider to be beyond the scope of standard laboratory equipment. To expand the accessibility of PURE to users with standard laboratory equipment, we also provide a protocol for purifying His-tagged ribosomes. Although easier to purify, His-tagged ribosomes exhibit a decreased protein production rate compared to tag-free ribosomes. Next, we introduce a protocol to prepare the energy solution. Finally, we guide the user through setting up a PURE experiment. Using our protocol, an experienced user can synthesize a custom-made PURE system within one week. This protocol is adaptable, allowing the PURE system to be tailored to specific needs and applications. Unfortunately, the supply of tRNAs from Roche was discontinued in 2023, and tRNAs from other sources were not compatible with the PURE system. As a result, we have purified tRNAs in our laboratory. The protocol for tRNA purification is described in section 3.8.

For the fall semester 2022/23, we established a synthetic biology student lab course with the aim of producing a functional OnePot PURE system including His-tagged ribosomes and energy solution. The successful realization of the PURE system by the students in the fall semesters 2022/23 and 2023/24 underlines the robustness of the method and indicates that the OnePot PURE system can be successfully prepared by users with varying levels of experience.

In its current state the OnePot PURE system still has notable limitations, but also potential for further improvement and tailoring to specific applications. The first notable limitation of OnePot compared to home-made PURE is that after protein expression the OnePot PURE protein composition can only be modified by adding components. Another drawback of the co-culturing and co-purification of all 36 non-ribosomal strains is that the exact concentrations of the single components in the PURE system are unknown and may vary from batch to batch. While protein expression using OnePot PURE is insensitive to slight changes of system composition, this might limit the application of the OnePot PURE in cases where the composition must be carefully adjusted and tuned. An example application where the exact composition may be critical is the full self-regeneration of the PURE system, as discussed in section 6.3. It is worth noting that the ratio and composition of the OnePot PURE components can be altered and controlled by adjusting the inoculation volumes of the strains [137]. However, further work is required to define optimal inoculation volumes for specific applications. A possible direction could be to tailor the protein composition match the concentrations and ratios proposed by Kazuta and coworkers, who increased protein yield by tuning the concentrations of the components of the PURE system [27].

Adding further components to the OnePot PURE could open the door towards a broader range of applications. For instance, the addition of chaperones could be interesting to enhance folding for aggregation prone proteins [148]. Meanwhile, the addition of disulfide bond isomerases [149] such as DsbC could be implemented to express and fold proteins containing disulfide bonds. However, experimental investigations are still required to confirm that adding these

components to the OnePot co-culturing / co-purification process have the desired effects.

6.3 Improved Cell-Free Transcription–Translation Reactions in Microfluidic Chemostats Augmented with Hydrogel Membranes for Continuous Small Molecule Dialysis

Achieving self-regeneration of the PURE system is a formidable task. Current efforts towards achieving a full regeneration of the system are hindered by the limited protein production capacity of the PURE system, which is at least 25x too low to replicate all 36 non-ribosomal proteins, let alone further components that may need to be added for functional protein synthesis [21, 137]. To overcome this limitation, we implemented dialysis membranes in a microfluidic chemostat (chapter 4). This resulted in a seven fold increase of the overall protein yield and a six-fold increase in protein levels at steady-state. Additionally, our platform was able to sustain continuous protein synthesis by an order of magnitude longer, from two to over 30 h. During our work we demonstrated the increase in protein production yield for a GFP reporter protein. A next step would be to probe self-regeneration on the dialysis chemostat to investigate new limitations in self-regeneration.

However, despite achieving these noteworthy improvements, our dialysis chemostat alone will most likely not produce enough protein to fully regenerate the PURE system in its standard composition. One potential point for further optimizing the dialysis chemostat is to increase the dialysis surface. The area for dialysis in the current chip is small compared to the overall surface and volume of the microchemostat. Increasing the surface area could improve the exchange of small molecules, rendering the energy supply of the reactions inside the reactor more efficient. However, this might be a challenging endeavour, as it would likely impede the physical stability of the microfluidic chip.

Given how far away we are still from reaching a more than 25-fold increase in protein production rate to achieve full regeneration, it will be essential to enhance the efficiency of the system by further optimizing the system itself. Ribosome stalling and impeded translation efficiencies lead to wasted protein production capacities on non-functional proteins. This bottleneck will need to be addressed to generate a more efficient PURE system [12, 25].

Further improvement could be achieved by adjusting the composition and stoichiometry of the PURE system, which has already shown to be not optimal [27, 138, 139]. Ongoing efforts in our laboratory are directed towards synthesizing a more minimal and thus more efficient PURE system (Bava Ganesh et al., unpublished data). Currently, the PURE system is composed in a way to achieve maximal protein production capacity, rather than optimal protein production capacity. By minimizing the protein concentration of the PURE system while keeping protein expression at an acceptable level, the protein production burden could be significantly decreased, bringing us one step further towards full regeneration of the PURE

system.

Dialysis offers an attractive approach to enhance protein yield and the reaction span of cell-free reactions, while maintaining an open reaction environment which is one of the key advantages of cell-free reactions for applied scientific questions, extending beyond the scope of building an artificial cell [44]. The most costly or laborious components of the PURE system are proteins and ribosomes. Dialysis systems effectively increase the yield while minimizing the consumption of these components. Most reported dialysis systems utilize microfluidic chips [233, 318, 358, 359] or complex microscale dialyzer plates [27, 28]. These systems require access to sophisticated equipment and thus limit the usage to well-equipped laboratories. Ongoing research in our lab thus focuses on developing a user-friendly DIY dialysis system to enhance protein yield in PURE reactions at medium scale. Our system was able to sustain protein synthesis in PURE for at least 12 days and produce up to 1 mg/mL of EGFP, outperforming a lysate system with the same dialysis system. We achieved this yield using a standard, commercially available PURE system and home-made energy solution (Grasemann, L.*, Roset Julia, L.* et al., unpublished data). We anticipate that this system could be utilized to produce proteins at medium scale for biomedical or bioengineering applications that benefit from the open nature and versatility of cell-free systems.

6.4 C2CAplus: a one-pot isothermal circle-to-circle DNA amplification system

A robust DNA replication system is key to developing an artificial cell. Existing DNA replication systems for this purpose are based on RCA, which has the drawback that the resulting product is linear and multimeric, while the input structure is circular. We developed a recircularization system that employs restriction digest using a restriction enzyme that cuts the sequence exactly once, and religation of the monomers using a ligase. The concept of circle-to-circle amplification (C2CA) was previously introduced by Dahl et al. [348] for biosensor applications. However, their method requires multiple steps and thermal cycling, making it unsuitable for a synthetic cell. Our C2CAplus system improves this approach by employing a balanced ratio of restriction enzyme to ligase to enable a single-step isothermal process that operates at ambient temperature. C2CAplus has demonstrated high sensitivity, efficiency, and robustness across a temperature range of 25-37°C. Due to the exponential amplification of DNA achieved by C2CAplus, high amounts of product are generated, making them observable to the naked eye. We therefore anticipate that C2CAplus could also be used as a platform to develop low-cost and user friendly RCA-based biosensors.

A next step towards utilizing C2CAplus for a synthetic cell is to couple the system to in vitro expression of the respective components using PURE. The PURErep system developed by Libicher and coworkers [22] based on the PURE composition proposed by Sakatani and coworkers [29] proposes itself for this application. A major challenge will be to tune the

expression levels of the ligase and restriction enzyme to meet a ratio that enables C2CAplus. This could for instance be achieved by implementing partial repression of the restriction enzyme, or tuning the promoter strengths of both components. Another challenge is the proprietary sequence of the utilized BsmBI v2 restriction enzyme [360]. While the sequence of the original BsmBI version 1 is publicly available [361], it still needs to be demonstrated that C2CAplus functions with BsmBI v1. Lastly, it needs to be demonstrated that T3 ligase and BsmBI can be functionally expressed in PURE.

A current challenge of utilizing C2CAplus as a biosensor is its susceptibility to producing false-positives. Nonspecific amplification is a well-recognized challenge for isothermal DNA replication methods, like for instance loop-mediated isothermal amplification (LAMP) [362, 363]. Sources for nonspecific amplification include unintended interactions between a template and the polymerase, partial hybridization of a non-target DNA molecule to a primer, or the formation of primer dimers. A multitude of strategies have been developed to minimize these false-positives by for instance developing methods to degrade carryover contaminations [363].

We are confident that further exploration of these strategies within the context of C2CAplus will improve the specificity of the system, thereby increasing its potential as a cost-effective and sensitive biosensor. The ability of C2CAplus to operate at temperatures between 25-37°C is a notable advantage over methods like LAMP, which require a higher temperature. This suggests that a simple water bath or even room temperature might be sufficient for utilizing a C2CAplus-based sensor.

Droplet microfluidics has shown to be compatible with C2CA [364], so it is likely that C2CAplus could be encapsulated, too. Encapsulating C2CAplus could take us one step further towards developing an artificial cell, and could be utilized to increase throughput in a biosensing format. Encapsulation of a highly sensitive isothermal DNA amplification method has already been used to detect cancer markers or pathogens including a variety of bacteria and viruses (reviewed in [41]). We thus anticipate that encapsulated C2CAplus could be utilized as a powerful platform to address both biosensing and synthetic cell applications.

6.5 Advances towards a synthetic cell

Can we build an artificial cell from scratch? I think the answer to this question is yes, but the successful implementation and assembly of all biological building blocks to form a living system remains a distant prospect, and there is still a multitude of challenges ahead of us. This thesis contributes to pushing the boundaries of self-replicating the PURE system, and developing a sustainable, robust DNA replication system. Nonetheless, it is evident that numerous obstacles lie ahead, particularly considering the interplay between subsystems that will need to be integrated into a synthetic cell. A striking example of challenges posed by assembling parts into increasingly complex systems is the surprising incompatibility of the

PURE system with DNA replication, which continues to demand innovative solutions [32].

Why do we want to address this grand challenge of building this artificial cell, especially given the unpredictable hurdles that lie ahead? First, building to understand promises to provide a deeper understanding of the fundamental principles of life, of the interactions of specific subsystems, of how life might have originated, and many more. Second, developing an artificial cell requires the convergence of engineering approaches with biological and biochemical expertise. This convergence promises to drive innovation and introduce powerful tools to address a multitude of bioengineering challenges. A notable example is the PURE cell-free system, which has proven to be a versatile platform for a broad range of applications, as discussed in chapter 2. Another, much more modest example is our C2CAplus system, a DNA replication system initially developed for synthetic cell applications but also exhibiting potential as a cost-effective and user-friendly biosensor applicable in remote areas.

I am confident that the path towards building an artificial cell will be a path of innovation that will contribute to addressing some of today's most emergent problems.

Bibliography

- ¹S. J. Maerkl, “On biochemical constructors and synthetic cells”, *Interface Focus* **13** (2023).
- ²Y. Shimizu, A. Inoue, Y. Tomari, T. Suzuki, T. Yokogawa, K. Nishikawa, and T. Ueda, “Cell-free translation reconstituted with purified components”, *Nature Biotechnology* **19**, 751–755 (2001).
- ³B. Lavickova, N. Laohakunakorn, and S. J. Maerkl, “A partially self-regenerating synthetic cell”, *Nature Communications* **11**, 6340 (2020).
- ⁴S. Hawking, *The universe in a nutshell* (Bantam Books, 2001).
- ⁵L. Olivi, M. Berger, R. N. Creyghton, N. De Franceschi, C. Dekker, B. M. Mulder, N. J. Claassens, P. R. ten Wolde, and J. van der Oost, “Towards a synthetic cell cycle”, *Nature Communications* **12**, 1–11 (2021).
- ⁶Z. Abil and C. Danelon, “Roadmap to Building a Cell: An Evolutionary Approach”, *Frontiers in Bioengineering and Biotechnology* **8**, 927 (2020).
- ⁷K. P. Adamala, M. Dogterom, Y. Elani, P. Schwille, M. Takinoue, and T. Y. Tang, “Present and future of synthetic cell development”, *Nature Reviews Molecular Cell Biology* 2023, 1–6 (2023).
- ⁸J. von Neumann, “Theory of self-reproducing automata”, University of Illinois Press (1966).
- ⁹N. Ichihashi, “What can we learn from the construction of in vitro replication systems?”, *Annals of the New York Academy of Sciences* **1447**, 144–156 (2019).
- ¹⁰N. Ichihashi and T. Yomo, “Constructive Approaches for Understanding the Origin of Self-Replication and Evolution”, *Life* **6**, 26 (2016).
- ¹¹K. Yue, Y. Li, M. Cao, L. Shen, J. Gu, and L. Kai, “Bottom-Up Synthetic Biology Using Cell-Free Protein Synthesis”, in *Advances in biochemical engineering/biotechnology*, Vol. 185 (Springer Science and Business Media Deutschland GmbH, 2023), pp. 1–20.
- ¹²A. Doerr, D. Foschepoth, A. C. Forster, and C. Danelon, “In vitro synthesis of 32 translation-factor proteins from a single template reveals impaired ribosomal processivity”, *Scientific Reports* **11**, 1898 (2021).
- ¹³K. Libicher and H. Mutschler, “Probing self-regeneration of essential protein factors required for: In vitro translation activity by serial transfer”, *Chemical Communications* **56**, 15426–15429 (2020).

- ¹⁴K. Hagino and N. Ichihashi, “In Vitro Transcription/Translation-Coupled DNA Replication through Partial Regeneration of 20 Aminoacyl-tRNA Synthetases”, *ACS Synthetic Biology* **12**, 1252–1263 (2023).
- ¹⁵M. C. Jewett, B. R. Fritz, L. E. Timmerman, and G. M. Church, “In vitro integration of ribosomal RNA synthesis, ribosome assembly, and translation”, *Molecular Systems Biology* **9**, 678 (2013).
- ¹⁶R. Aoyama, K. Masuda, M. Shimojo, T. Kanamori, T. Ueda, and Y. Shimizu, “In vitro reconstitution of the Escherichia coli 70S ribosome with a full set of recombinant ribosomal proteins”, *The Journal of Biochemistry* **171**, 227–237 (2022).
- ¹⁷K. Hibi, K. Amikura, N. Sugiura, K. Masuda, S. Ohno, T. Yokogawa, T. Ueda, and Y. Shimizu, “Reconstituted cell-free protein synthesis using in vitro transcribed tRNAs”, *Communications Biology* **3**, 30 (2020).
- ¹⁸R. Miyachi, Y. Shimizu, and N. Ichihashi, “Transfer RNA Synthesis-Coupled Translation and DNA Replication in a Reconstituted Transcription/Translation System”, *ACS Synthetic Biology* **11**, 2791–2799 (2022).
- ¹⁹T. Niwa, B. W. Ying, K. Saito, W. Jin, S. Takada, T. Ueda, and H. Taguchi, “Bimodal protein solubility distribution revealed by an aggregation analysis of the entire ensemble of Escherichia coli proteins”, *Proceedings of the National Academy of Sciences of the United States of America* **106**, 4201–4206 (2009).
- ²⁰T. Awai, N. Ichihashi, and T. Yomo, “Activities of 20 aminoacyl-tRNA synthetases expressed in a reconstituted translation system in Escherichia coli”, *Biochemistry and Biophysics Reports* **3**, 140–143 (2015).
- ²¹E. Wei and D. Endy, “Experimental tests of functional molecular regeneration via a standard framework for coordinating synthetic cell building”, *bioRxiv*, 433818 (2021).
- ²²K. Libicher, R. Hornberger, M. Heymann, and H. Mutschler, “In vitro self-replication and multicistronic expression of large synthetic genomes”, *Nature Communications* **11** (2020).
- ²³M. C. Jewett and J. R. Swartz, “Mimicking the Escherichia coli Cytoplasmic Environment Activates Long-Lived and Efficient Cell-Free Protein Synthesis”, *Biotechnology and Bioengineering* **86**, 19–26 (2004).
- ²⁴K. A. Calhoun and J. R. Swartz, “Energizing cell-free protein synthesis with glucose metabolism”, *Biotechnology and bioengineering* **90**, 606–613 (2005).
- ²⁵J. Li, C. Zhang, P. Huang, E. Kuru, E. T. C. Forster-Benson, T. Li, and G. M. Church, “Dissecting limiting factors of the Protein synthesis Using Recombinant Elements (PURE) system”, *Translation* **5**, e1327006 (2017).
- ²⁶D.-M. Kim and J. R. Swartz, “Prolonging Cell-Free Protein Synthesis by Selective Reagent Additions”, *Biotechnology Progress* **16**, 385–390 (2000).
- ²⁷Y. Kazuta, T. Matsuura, N. Ichihashi, and T. Yomo, “Synthesis of milligram quantities of proteins using a reconstituted in vitro protein synthesis system”, *Journal of Bioscience and Bioengineering* **118**, 554–557 (2014).

- ²⁸K. Jackson, T. Kanamori, T. Ueda, and Z. H. Fan, “Protein synthesis yield increased 72 times in the cell-free PURE system”, *Integrative Biology* **6**, 781–788 (2014).
- ²⁹Y. Sakatani, N. Ichihashi, Y. Kazuta, and T. Yomo, “A transcription and translation-coupled DNA replication system using rolling-circle replication”, *Scientific Reports* **5**, 10404 (2015).
- ³⁰Y. Sakatani, T. Yomo, and N. Ichihashi, “Self-replication of circular DNA by a self-encoded DNA polymerase through rolling-circle replication and recombination”, *Scientific Reports* **8**, 13089 (2018).
- ³¹F. Han, B. Xu, N. Lu, A. Caliarì, H. Lu, Y. Xia, M. Su’etsugu, J. Xu, and T. Yomo, “Optimization and compartmentalization of a cell-free mixture of DNA amplification and protein translation”, *Applied Microbiology and Biotechnology* **106**, 8139–8149 (2022).
- ³²K. Seo and N. Ichihashi, “Investigation of Compatibility between DNA Replication, Transcription, and Translation for in Vitro Central Dogma”, *ACS Synthetic Biology* **12**, 1813–1822 (2023).
- ³³C. A. Azaldegui, A. G. Vecchiarelli, and J. S. Biteen, “The emergence of phase separation as an organizing principle in bacteria”, *Biophysical Journal* **120**, 1123–1138 (2021).
- ³⁴P. van Nies, I. Westerlaken, D. Blanken, M. Salas, M. Mencía, and C. Danelon, “Self-replication of DNA by its encoded proteins in liposome-based synthetic cells”, *Nature Communications* **9**, 1583 (2018).
- ³⁵Y. Sakatani, R. Mizuuchi, and N. Ichihashi, “In vitro evolution of phi29 DNA polymerases through compartmentalized gene expression and rolling-circle replication”, *Protein Engineering, Design and Selection* **32**, 481–487 (2019).
- ³⁶H. Okauchi, Y. Sakatani, K. Otsuka, and N. Ichihashi, “Minimization of Elements for Isothermal DNA Replication by an Evolutionary Approach”, *ACS Synthetic Biology* **9**, 1771–1780 (2020).
- ³⁷H. Okauchi and N. Ichihashi, “Continuous Cell-Free Replication and Evolution of Artificial Genomic DNA in a Compartmentalized Gene Expression System”, *ACS Synthetic Biology* **10**, 3507–3517 (2021).
- ³⁸J. Nosek, P. Kosa, and L. Tomaska, “On the origin of telomeres: A glimpse at the pre-telomerase world”, *BioEssays* **28**, 182–190 (2006).
- ³⁹A. K. Baranwal and S. J. Maerkl, “Microfluidic approaches for cell-free synthetic biology”, in preparation (2024).
- ⁴⁰H. Seo and H. Lee, *Recent developments in microfluidic synthesis of artificial cell-like polymersomes and liposomes for functional bioreactors*, Vol. 15, 2 (American Institute of Physics Inc., 2021), p. 21301.
- ⁴¹R. Sieskind, A. L. Cortajarena, and A. Manteca, “Cell-Free Production Systems in Droplet Microfluidics”, in *Advances in biochemical engineering/biotechnology*, Vol. 185 (Springer Science and Business Media Deutschland GmbH, 2023), pp. 91–127.

- ⁴²H. Niederholtmeyer, V. Stepanova, and S. J. Maerkl, “Implementation of cell-free biological networks at steady state”, *Proceedings of the National Academy of Sciences of the United States of America* **110**, 15985–15990 (2013).
- ⁴³N. Laohakunakorn, B. Lavickova, Z. Swank, J. Laurent, and S. J. Maerkl, “Steady-State Cell-Free Gene Expression with Microfluidic Chemostats”, in *Methods in molecular biology*, Vol. 2229 (Humana Press Inc., 2021), pp. 189–203.
- ⁴⁴N. Laohakunakorn, L. Grasemann, B. Lavickova, G. Michielin, A. Shahein, Z. Swank, and S. J. Maerkl, “Bottom-up construction of complex biomolecular systems with cell-free synthetic biology”, *Frontiers in Bioengineering and Biotechnology* **8**, 213 (2020).
- ⁴⁵D. Endy, “Foundations for engineering biology”, *Nature* **438**, 449–453 (2005).
- ⁴⁶A. Arkin, “Setting the standard in synthetic biology”, *Nature Biotechnology* **26**, 771–774 (2008).
- ⁴⁷B. Canton, A. Labno, and D. Endy, “Refinement and standardization of synthetic biological parts and devices”, *Nature Biotechnology* **26**, 787–793 (2008).
- ⁴⁸M. Heinemann and S. Panke, “Synthetic biology - Putting engineering into biology”, *Bioinformatics* **22**, 2790–2799 (2006).
- ⁴⁹R. Kwok, “Five hard truths for synthetic biology”, *Nature* **463**, 288–290 (2010).
- ⁵⁰P. E. Purnick and R. Weiss, “The second wave of synthetic biology: From modules to systems”, *Nature Reviews Molecular Cell Biology* **10**, 410–422 (2009).
- ⁵¹N. Hillson, M. Caddick, Y. Cai, J. A. Carrasco, M. W. Chang, N. C. Curach, D. J. Bell, R. L. Feuvre, D. C. Friedman, X. Fu, N. D. Gold, M. J. Herrgård, M. B. Holowko, J. R. Johnson, R. A. Johnson, J. D. Keasling, R. I. Kitney, A. Kondo, C. Liu, V. J. J. Martin, F. Menolascina, C. Ogino, N. J. Patron, and M. Pavan, “Building a global alliance of biofoundries”, *Nature Communications* **10**, 1–4 (2019).
- ⁵²J. J. Agresti, E. Antipov, A. R. Abate, K. Ahn, A. C. Rowat, J.-C. Baret, M. Marquez, A. M. Klibanov, A. D. Griffiths, and D. A. Weitz, “Ultrahigh-throughput screening in drop-based microfluidics for directed evolution”, *Proceedings of the National Academy of Sciences of the United States of America* **107**, 4004–4009 (2010).
- ⁵³V. Hsiao, A. Swaminathan, and R. M. Murray, “Control Theory for Synthetic Biology: Recent Advances in System Characterization, Control Design, and Controller Implementation for Synthetic Biology”, *IEEE Control Systems* **38**, 32–62 (2018).
- ⁵⁴M. Khammash, “An engineering viewpoint on biological robustness”, *BMC Biology* **14**, 22 (2016).
- ⁵⁵D. D. Vecchio, A. J. Dy, and Y. Qian, “Control theory meets system biology”, *Journal of the Royal Society Interfac* **13**, 20160380 (2016).
- ⁵⁶A. P. Liu, “The rise of bottom-up synthetic biology and cell-free biology”, *Physical Biology* **16**, 040201 (2019).

- ⁵⁷P. Schwille, J. Spatz, K. Landfester, S. Herminghaus, V. Sourjik, T. J. Erb, P. Bastiaens, A. Hyman, P. Dabrock, J.-C. Baret, T. Vidakovic-Koch, P. Bieling, R. Dimova, H. Mutschler, T. Robinson, T.-Y. D. Tang, S. Wegner, and K. Sundmacher, “MaxSynBio: Avenues Towards Creating Cells from the Bottom Up”, *Angewandte Chemie - International Edition* **57**, 13382–13392 (2018).
- ⁵⁸K. Göpfrich, I. Platzman, and J. P. Spatz, “Mastering Complexity: Towards Bottom-up Construction of Multifunctional Eukaryotic Synthetic Cells”, *Trends in Biotechnology* **36**, 938–951 (2018).
- ⁵⁹F. Caschera and V. Noireaux, “Integration of biological parts toward the synthesis of a minimal cell”, *Current opinion in chemical biology* **22**, 85–91 (2014).
- ⁶⁰A. P. Liu and D. A. Fletcher, “Biology under construction: in vitro reconstitution of cellular function”, *Nature Reviews Molecular Cell Biology* **10**, 644–650 (2009).
- ⁶¹K. A. Ganzinger and P. Schwille, “More from less – bottom-up reconstitution of cell biology”, *J Cell Sci* **132**, jcs227488 (2019).
- ⁶²M. Elowitz and W. A. Lim, “Build life to understand it”, *Nature* **468**, 889–890 (2010).
- ⁶³D. Garenne and V. Noireaux, “Cell-free transcription–translation: engineering biology from the nanometer to the millimeter scale”, *Current Opinion in Biotechnology* **58**, 19–27 (2019).
- ⁶⁴E. Buchner, “Alkoholische Gärung ohne Hefezellen”, *Berichte der deutschen chemischen Gesellschaft* **30**, 1110–1113 (1897).
- ⁶⁵M. R. Lamborg and P. C. Zamecnik, “Amino acid incorporation into protein by extracts of *E. coli*”, *Biochimica et Biophysica Acta* **42**, 206–211 (1960).
- ⁶⁶M. W. Nirenberg and J. H. Matthaei, “The dependence of cell-free protein synthesis in *E. coli* upon naturally occurring or synthetic polyribonucleotides.”, *Proceedings of the National Academy of Sciences* **47**, 1588–602 (1961).
- ⁶⁷W. B. Wood and P. Berg, “the Effect of Enzymatically Synthesized Ribonucleic Acid on Amino Acid Incorporation By a Soluble Protein-Ribosome System From *Escherichia Coli*”, *Proceedings of the National Academy of Sciences* **48**, 94–104 (1962).
- ⁶⁸M. Lederman and G. Zubay, “DNA-directed peptide synthesis I. A comparison of T2 and *Escherichia coli* DNA-directed peptide synthesis in two cell-free systems”, *Biochimica et Biophysica Acta* **149**, 253–258 (1967).
- ⁶⁹J. K. DeVries and G. Zubay, “DNA-directed peptide synthesis II. The synthesis of the alpha-fragment of the enzyme beta-galactosidase”, *Proceedings of the National Academy of Sciences* (1967).
- ⁷⁰D. Nathans, G. Notani, J. H. Schwartz, and N. D. Zinder, “Biosynthesis of the coat protein of coliphage F2 by *E. coli* extracts”, *Proceedings of the National Academy of Sciences* **48**, 1424–1431 (1962).
- ⁷¹G. Zubay, M. Lederman, and J. K. DeVries, “DNA-directed peptide synthesis, III. Repression of beta-galactosidase synthesis and inhibition of repressor by inducer in a cell-free system”, *Proceedings of the National Academy of Sciences* **58**, 1669–1675 (1967).

- ⁷²G. Zubay, D. Schwartz, and J. Beckwith, "Mechanism of Activation of Catabolite-Sensitive Genes: A Positive Control System", *Proceedings of the National Academy of Sciences* **66**, 104–110 (1970).
- ⁷³G. Zubay, "In Vitro Synthesis of Protein in Microbial Systems", *Annual Review of Genetics* **7**, 267–287 (1973).
- ⁷⁴M. Nirenberg and P. Leder, "RNA codewords and protein synthesis", *Science* **145**, 1399–1407 (1964).
- ⁷⁵M. W. Nirenberg, T. Caskey, R. Marshall, R. Brimacombe, D. Kellog, B. Doctor, D. Hatfield, J. Levin, F. Rottman, S. Pestka, M. Wilcox, and F. Anderson, "The RNA Code and Protein Synthesis", *Cold Spring Harbor Symposia on Quantitative Biology* **31**, 11–24 (1966).
- ⁷⁶D. R. Mills, R. L. Peterson, and S. Spiegelman, "An extracellular Darwinian experiment with a self-duplicating nucleic acid molecule.", *Proceedings of the National Academy of Sciences of the United States of America* **58**, 217–224 (1967).
- ⁷⁷K. Kruger, P. J. Grabowski, A. J. Zaug, J. Sands, D. E. Gottschling, and T. R. Cech, "Self-splicing RNA: Autoexcision and autocyclization of the ribosomal RNA intervening sequence of tetrahymena", *Cell* **31**, 147–157 (1982).
- ⁷⁸W. E. Balch, W. G. Dunphy, W. A. Braell, and J. E. Rothman, "Reconstitution of the transport of protein between successive compartments of the golgi measured by the coupled incorporation of N-acetylglucosamine", *Cell* **39**, 405–416 (1984).
- ⁷⁹G. Steinberg-Yfrach, J. L. Rigaud, E. N. Durantini, A. L. Moore, D. Gust, and T. A. Moore, "Light-driven production of ATP catalysed by FOF1-ATP synthase in an artificial photosynthetic membrane", *Nature* **392**, 479–482 (1998).
- ⁸⁰L. Jermutus, L. A. Ryabova, and A. Plückthun, "Recent advances in producing and selecting functional proteins by using cell-free translation", *Current Opinion in Biotechnology* **9**, 534–548 (1998).
- ⁸¹V. Noireaux, R. Bar-Ziv, and A. Libchaber, "Principles of cell-free genetic circuit assembly", *Proceedings of the National Academy of Sciences* **100**, 12672–12677 (2003).
- ⁸²N. E. Gregorio, M. Z. Levine, and J. P. Oza, "A User's Guide to Cell-Free Protein Synthesis", *Methods and Protocols* **2** (2019).
- ⁸³A. Zemella, L. Thoring, C. Hoffmeister, and S. Kubick, "Cell-Free Protein Synthesis: Pros and Cons of Prokaryotic and Eukaryotic Systems", *ChemBioChem* **16**, 2420–2431 (2015).
- ⁸⁴J. G. Perez, J. C. Stark, and M. C. Jewett, "Cell-Free Synthetic Biology: Engineering Beyond the Cell.", *Cold Spring Harbor Perspectives in Biology* **8**, a023853 (2016).
- ⁸⁵R. Kelwick, A. J. Webb, J. T. MacDonald, and P. S. Freemont, "Development of a *Bacillus subtilis* cell-free transcription-translation system for prototyping regulatory elements", *Metabolic Engineering* **38**, 370–381 (2016).

- ⁸⁶S. S. Yim, N. I. Johns, J. Park, A. L. Gomes, R. M. McBee, M. Richardson, C. Ronda, S. P. Chen, D. Garenne, V. Noireaux, and H. H. Wang, “Multiplex transcriptional characterizations across diverse bacterial species using cell-free systems”, *Molecular Systems Biology* **15**, e8875 (2019).
- ⁸⁷J. Failmezger, “Understanding limitations to increased potential of cell-free protein synthesis”, (2018).
- ⁸⁸S. Wang, S. Majumder, N. J. Emery, and A. P. Liu, “Simultaneous monitoring of transcription and translation in mammalian cell-free expression in bulk and in cell-sized droplets”, *Synthetic Biology* **3** (2018).
- ⁸⁹B. Panthu, T. Ohlmann, J. Perrier, U. Schlattner, P. Jalinot, B. Elena-Herrmann, and G. J. P. Rautureau, “Cell-Free Protein Synthesis Enhancement from Real-Time NMR Metabolite Kinetics: Redirecting Energy Fluxes in Hybrid RRL Systems”, *ACS Synthetic Biology* **7**, 218–226 (2018).
- ⁹⁰M. Anastasina, I. Terenin, S. J. Butcher, and D. E. Kainov, “A technique to increase protein yield in a rabbit reticulocyte lysate translation system”, *BioTechniques* **56**, 36–39 (2014).
- ⁹¹M. K. Takahashi, C. A. Hayes, J. Chappell, Z. Z. Sun, R. M. Murray, V. Noireaux, and J. B. Lucks, “Characterizing and prototyping genetic networks with cell-free transcription-translation reactions”, *Methods* **86**, 60–72 (2015).
- ⁹²S. D. Cole, K. Beabout, K. B. Turner, Z. K. Smith, V. L. Funk, S. V. Harbaugh, A. T. Liem, P. A. Roth, B. A. Geier, P. A. Emanuel, S. A. Walper, J. L. Chávez, and M. W. Lux, “Quantification of Interlaboratory Cell-Free Protein Synthesis Variability”, *ACS Synthetic Biology* **8**, 2080–2091 (2019).
- ⁹³A. D. Silverman, N. Kelley-Loughnane, J. B. Lucks, and M. C. Jewett, “Deconstructing Cell-Free Extract Preparation for in Vitro Activation of Transcriptional Genetic Circuitry”, *ACS Synthetic Biology* **8**, 403–414 (2019).
- ⁹⁴D. Foshag, E. Henrich, E. Hiller, M. Schäfer, C. Kerger, A. Burger-Kentischer, I. Diaz-Moreno, S. M. García-Mauriño, V. Dötsch, S. Rupp, and F. Bernhard, “The E. coli S30 lysate proteome: A prototype for cell-free protein production”, *New Biotechnology* **40**, 245–260 (2018).
- ⁹⁵J. Failmezger, M. Rauter, R. Nitschel, M. Kraml, and M. Siemann-Herzberg, “Cell-free protein synthesis from non-growing, stressed *Escherichia coli*”, *Scientific Reports* **7**, 16524 (2017).
- ⁹⁶D. Garenne, C. L. Beisel, and V. Noireaux, “Characterization of the all-E. coli transcription-translation system myTXTL by mass spectrometry”, *Rapid Communications in Mass Spectrometry* **33**, 1036–1048 (2019).
- ⁹⁷G. B. Hurst, K. G. Asano, C. J. Doktycz, E. J. Consoli, W. L. Doktycz, C. M. Foster, J. L. Morrell-Falvey, R. F. Standaert, and M. J. Doktycz, “Proteomics-Based Tools for Evaluation of Cell-Free Protein Synthesis”, *Analytical Chemistry* **89**, 11443–11451 (2017).
- ⁹⁸M. Bujara, M. Schümperli, R. Pellaux, M. Heinemann, and S. Panke, “Optimization of a blueprint for in vitro glycolysis by metabolic real-time analysis”, *Nature Chemical Biology* **7**, 271–277 (2011).

- ⁹⁹D. V. Liu, J. F. Zawada, and J. R. Swartz, “Streamlining Escherichia coli S30 extract preparation for economical cell-free protein synthesis”, *Biotechnology Progress* **21**, 460–465 (2005).
- ¹⁰⁰R. W. Martin, B. J. D. Soye, Y.-C. Kwon, J. Kay, R. G. Davis, P. M. Thomas, N. I. Majewska, C. X. Chen, R. D. Marcum, M. G. Weiss, A. E. Stoddart, M. Amiram, A. K. R. Charna, J. R. Patel, F. J. Isaacs, N. L. Kelleher, S. H. Hong, and M. C. Jewett, “Cell-free protein synthesis from genomically recoded bacteria enables multisite incorporation of noncanonical amino acids”, *Nature Communications* **9**, 1–9 (2018).
- ¹⁰¹T. Jaroentomeechai, J. C. Stark, A. Natarajan, C. J. Glasscock, L. E. Yates, K. J. Hsu, M. Mrksich, M. C. Jewett, and M. P. DeLisa, “Single-pot glycoprotein biosynthesis using a cell-free transcription-translation system enriched with glycosylation machinery”, *Nature Communications* **9**, 2686 (2018).
- ¹⁰²A. S. Karim, Q. M. Dudley, and M. C. Jewett, “Cell-Free Synthetic Systems for Metabolic Engineering and Biosynthetic Pathway Prototyping”, *Industrial Biotechnology*, 125–148 (2016).
- ¹⁰³A. S. Karim and M. C. Jewett, “Cell-Free Synthetic Biology for Pathway Prototyping”, *Methods in Enzymology* **608**, 31–57 (2018).
- ¹⁰⁴A. C. Chiao, R. M. Murray, and Z. Z. Sun, “Development of prokaryotic cell-free systems for synthetic biology”, *bioRxiv*, 1–38 (2016).
- ¹⁰⁵A. D. Silverman, A. S. Karim, and M. C. Jewett, “Cell-free gene expression: an expanded repertoire of applications”, *Nature Reviews Genetics* (2019).
- ¹⁰⁶Z. Z. Sun, C. A. Hayes, J. Shin, F. Caschera, R. M. Murray, and V. Noireaux, “Protocols for Implementing an Escherichia coli Based TX-TL Cell-Free Expression System for Synthetic Biology”, *Journal of Visualized Experiments*, 1–15 (2013).
- ¹⁰⁷Y.-C. Kwon and M. C. Jewett, “High-throughput preparation methods of crude extract for robust cell-free protein synthesis”, *Scientific Reports* **5**, 8663 (2015).
- ¹⁰⁸A. Didovyk, T. Tonooka, L. Tsimring, and J. Hasty, “Rapid and Scalable Preparation of Bacterial Lysates for Cell-Free Gene Expression”, *ACS Synthetic Biology* **6**, 2198–2208 (2017).
- ¹⁰⁹S. H. Hong, Y.-C. Kwon, R. W. Martin, B. J. Des Soye, A. M. de Paz, K. N. Swonger, I. Ntai, N. L. Kelleher, and M. C. Jewett, “Improving Cell-Free Protein Synthesis through Genome Engineering of Escherichia coli Lacking Release Factor 1”, *Chembiochem : a European journal of chemical biology* **16**, 844–853 (2015).
- ¹¹⁰H. Niederholtmeyer, Z. Z. Sun, Y. Hori, E. Yeung, A. Verpoorte, R. M. Murray, and S. J. Maerkl, “Rapid cell-free forward engineering of novel genetic ring oscillators”, *eLife* **4**, edited by F. Simmel, e09771 (2015).
- ¹¹¹T.-W. Kim, J.-W. Keum, I.-S. Oh, C.-Y. Choi, C.-G. Park, and D.-M. Kim, “Simple procedures for the construction of a robust and cost-effective cell-free protein synthesis system”, *Journal of Biotechnology* **126**, 554–561 (2006).
- ¹¹²R. Kim and C. Choi, “Expression-independent consumption of substrates in cell-free expression system from Escherichia coli”, *Journal of Biotechnology* **84**, 27–32 (2000).

- ¹¹³M. C. Jewett, K. A. Calhoun, A. Voloshin, J. J. Wu, and J. R. Swartz, “An integrated cell-free metabolic platform for protein production and synthetic biology”, *Molecular Systems Biology* **4**, 220 (2008).
- ¹¹⁴P. Shrestha, T. M. Holland, and B. C. Bundy, “Streamlined extract preparation for Escherichia coli-based cell-free protein synthesis by sonication or bead vortex mixing”, *BioTechniques* **53**, 163–174 (2012).
- ¹¹⁵Q. Cai, J. A. Hanson, A. R. Steiner, C. Tran, M. R. Masikat, R. Chen, J. F. Zawada, A. K. Sato, T. J. Hallam, and G. Yin, “A simplified and robust protocol for immunoglobulin expression in Escherichia coli cell-free protein synthesis systems”, *Biotechnology Progress* **31**, 823–831 (2015).
- ¹¹⁶K. A. Calhoun and J. R. Swartz, “An Economical Method for Cell-Free Protein Synthesis using Glucose and Nucleoside Monophosphates”, *Biotechnology Progress* **21**, 1146–1153 (2005).
- ¹¹⁷F. Caschera and V. Noireaux, “Synthesis of 2.3 mg/ml of protein with an all Escherichia coli cell-free transcription–translation system”, *Biochimie* **99**, 162–168 (2014).
- ¹¹⁸F. Caschera and V. Noireaux, “A cost-effective polyphosphate-based metabolism fuels an all E. coli cell-free expression system”, *Metabolic Engineering* **27**, 29–37 (2015).
- ¹¹⁹J. Kim and E. Winfree, “Synthetic in vitro transcriptional oscillators”, *Molecular Systems Biology* **7**, 1–15 (2011).
- ¹²⁰H.-C. Kim, T.-W. Kim, and D.-M. Kim, “Prolonged production of proteins in a cell-free protein synthesis system using polymeric carbohydrates as an energy source”, *Process Biochemistry* **46**, 1366–1369 (2011).
- ¹²¹D. Siegal-Gaskins, Z. A. Tuza, J. Kim, V. Noireaux, and R. M. Murray, “Gene circuit performance characterization in a cell-free ‘breadboard’”, *ACS Synthetic Biology*, 1–15 (2014).
- ¹²²M. Koch, J.-L. Faulon, and O. Borkowski, “Models for Cell-Free Synthetic Biology: Make Prototyping Easier, Better, and Faster”, *Frontiers in Bioengineering and Biotechnology* **6**, 1–6 (2018).
- ¹²³O. Borkowski, C. Bricio, M. Murgiano, B. Rothschild-Mancinelli, G.-B. Stan, and T. Ellis, “Cell-free prediction of protein expression costs for growing cells”, *Nature Communications* **9**, 1457 (2018).
- ¹²⁴T.-W. Kim, H.-C. Kim, I.-S. Oh, and D.-M. Kim, “A highly efficient and economical cell-free protein synthesis system using the S12 extract of Escherichia coli”, *Biotechnology and Bioprocess Engineering* **13**, 464–469 (2008).
- ¹²⁵E. Henrich, C. Hein, V. Dötsch, and F. Bernhard, “Membrane protein production in Escherichia coli cell-free lysates”, *FEBS Letters* **589**, 1713–1722 (2015).
- ¹²⁶C. Hein, E. Henrich, E. Orbán, V. Dötsch, and F. Bernhard, “Hydrophobic supplements in cell-free systems: Designing artificial environments for membrane proteins”, *Engineering in Life Sciences* **14**, 365–379 (2014).

- ¹²⁷Z. Z. Sun, E. Yeung, C. A. Hayes, V. Noireaux, and R. M. Murray, “Linear DNA for Rapid Prototyping of Synthetic Biological Circuits in an Escherichia coli Based TX-TL Cell-Free System”, *ACS Synth Biol* **3**, 387–397 (2014).
- ¹²⁸R. Marshall, C. S. Maxwell, S. P. Collins, C. L. Beisel, and V. Noireaux, “Short DNA containing x sites enhances DNA stability and gene expression in E. coli cell-free transcription–translation systems”, *Biotechnology and Bioengineering* **114**, 2137–2141 (2017).
- ¹²⁹H. F. Kung, B. Redfield, B. V. Treadwell, B. Eskin, C. Spears, and H. Weissbach, “DNA-directed in vitro synthesis of beta-galactosidase. Studies with purified factors.”, *Journal of Biological Chemistry* **252**, 6889–6894 (1977).
- ¹³⁰C. Tuckey, H. Asahara, Y. Zhou, and S. Chong, “Protein Synthesis Using A Reconstituted Cell-Free System”, *Current protocols in molecular biology* **108**, 16.31.1–16.31.22 (2014).
- ¹³¹A. Doerr, E. d. Reus, P. v. Nies, M. v. d. Haar, K. Wei, J. Kattan, A. Wahl, and C. Danelon, “Modelling cell-free RNA and protein synthesis with minimal systems”, *Physical Biology* **16**, 025001 (2019).
- ¹³²Y. Shimizu and T. Ueda, “PURE technology.”, *Methods in Molecular biology* **607**, 11–21 (2010).
- ¹³³S. Horiya, J. K. Bailey, and I. J. Krauss, “Chapter Four - Directed Evolution of Glycopeptides Using mRNA Display”, in *Methods in Enzymology*, Vol. 597, Chemical Glycobiology Part A. Synthesis, Manipulation and Applications of Glycans (Academic Press, 2017), pp. 83–141.
- ¹³⁴H. H. Wang, P. Y. Huang, G. Xu, W. Haas, A. Marblestone, J. Li, S. P. Gygi, A. C. Forster, M. C. Jewett, and G. M. Church, “Multiplexed in vivo his-tagging of enzyme pathways for in vitro single-pot multienzyme catalysis”, *ACS Synthetic Biology* **1**, 43–52 (2012).
- ¹³⁵F. Villarreal, L. E. Contreras-Llano, M. Chavez, Y. Ding, J. Fan, T. Pan, and C. Tan, “Synthetic microbial consortia enable rapid assembly of pure translation machinery”, *Nature Chemical Biology* **14**, 29–35 (2018).
- ¹³⁶T. R. Shepherd, L. Du, J. Liljeruhm, Samudyata, J. Wang, M. O. Sjödin, M. Wetterhall, T. Yomo, and A. C. Forster, “De novo design and synthesis of a 30-cistron translation-factor module”, *Nucleic Acids Research* **45**, 10895–10905 (2017).
- ¹³⁷B. Lavickova and S. J. Maerkl, “A Simple, Robust, and Low-Cost Method to Produce the PURE Cell-Free System”, *ACS Synthetic Biology* (2019).
- ¹³⁸J. Li, L. Gu, J. Aach, and G. M. Church, “Improved Cell-Free RNA and Protein Synthesis System”, *PLOS ONE* **9**, e106232 (2014).
- ¹³⁹T. Matsuura, Y. Kazuta, T. Aita, J. Adachi, and T. Yomo, “Quantifying epistatic interactions among the components constituting the protein translation system”, *Molecular Systems Biology* **5**, 297 (2009).
- ¹⁴⁰F. Mavelli, R. Marangoni, and P. Stano, “A Simple Protein Synthesis Model for the PURE System Operation”, *Bulletin of Mathematical Biology* **77**, 1185–1212 (2015).

- ¹⁴¹P. Carrara, E. Altamura, F. D'Angelo, F. Mavelli, and P. Stano, "Measurement and Numerical Modeling of Cell-Free Protein Synthesis: Combinatorial Block-Variants of the PURE System", *Data* **3**, 41 (2018).
- ¹⁴²T. Matsuura, K. Hosoda, and Y. Shimizu, "Robustness of a Reconstituted Escherichia coli Protein Translation System Analyzed by Computational Modeling", *ACS Synthetic Biology* **7**, 1964–1972 (2018).
- ¹⁴³T. Matsuura, N. Tanimura, K. Hosoda, T. Yomo, and Y. Shimizu, "Reaction dynamics analysis of a reconstituted Escherichia coli protein translation system by computational modeling", *Proceedings of the National Academy of Sciences* **114**, E1336–E1344 (2017).
- ¹⁴⁴N. Kempf, C. Remes, R. Ledesch, T. Züchner, H. Höfig, I. Ritter, A. Katranidis, and J. Fitter, "A Novel Method to Evaluate Ribosomal Performance in Cell-Free Protein Synthesis Systems", *Scientific Reports* **7**, 46753 (2017).
- ¹⁴⁵Y. Kazuta, J. Adachi, T. Matsuura, N. Ono, H. Mori, and T. Yomo, "Comprehensive Analysis of the Effects of Escherichia coli ORFs on Protein Translation Reaction", *Molecular & Cellular Proteomics : MCP* **7**, 1530–1540 (2008).
- ¹⁴⁶P.-H. Wang, K. Fujishima, S. Berhanu, Y. Kuruma, T. Z. Jia, A. N. Khusnutdinova, A. F. Yakunin, and S. E. McGlynn, "A Single Polyphosphate Kinase-Based NTP Regeneration System Driving Cell-Free Protein Synthesis", (2019).
- ¹⁴⁷L. L. Maddalena, H. Niederholtmeyer, M. Turtola, Z. N. Swank, G. A. Belogurov, and S. J. Maerkl, "GreA and GreB Enhance Expression of Escherichia coli RNA Polymerase Promoters in a Reconstituted Transcription-Translation System", *ACS Synthetic Biology* **5**, 929–935 (2016).
- ¹⁴⁸T. Niwa, T. Kanamori, T. Ueda, and H. Taguchi, "Global analysis of chaperone effects using a reconstituted cell-free translation system", *Proceedings of the National Academy of Sciences of the United States of America* **109**, 8937–8942 (2012).
- ¹⁴⁹Y. Shimizu, T. Kanamori, and T. Ueda, "Protein synthesis by pure translation systems", *Methods* **36**, 299–304 (2005).
- ¹⁵⁰Y. Kuruma and T. Ueda, "The PURE system for the cell-free synthesis of membrane proteins", *Nature protocols* **10**, 1328–1344 (2015).
- ¹⁵¹T. Niwa, R. Sugimoto, L. Watanabe, S. Nakamura, T. Ueda, and H. Taguchi, "Large-scale analysis of macromolecular crowding effects on protein aggregation using a reconstituted cell-free translation system", *Frontiers in Microbiology* **6** (2015).
- ¹⁵²M. L. Jacobs, M. A. Boyd, and N. P. Kamat, "Diblock copolymers enhance folding of a mechanosensitive membrane protein during cell-free expression", *Proceedings of the National Academy of Sciences* **116**, 4031–4036 (2019).
- ¹⁵³X. Ge, D. Luo, and J. Xu, "Cell-free protein expression under macromolecular crowding conditions", *PLoS ONE* **6** (2011).
- ¹⁵⁴Y. Moriizumi, K. V. Tabata, D. Miyoshi, and H. Noji, "Osmolyte-Enhanced Protein Synthesis Activity of a Reconstituted Translation System", *ACS Synthetic Biology* **8**, 557–567 (2019).

- ¹⁵⁵S. E. Norred, P. M. Caveney, G. Chauhan, L. K. Collier, C. P. Collier, S. M. Abel, and M. L. Simpson, “Macromolecular Crowding Induces Spatial Correlations That Control Gene Expression Bursting Patterns”, *ACS Synthetic Biology* **7**, 1251–1258 (2018).
- ¹⁵⁶K. Fujiwara, T. Katayama, and S. I. M. Nomura, “Cooperative working of bacterial chromosome replication proteins generated by a reconstituted protein expression system”, *Nucleic Acids Research* **41**, 7176–7183 (2013).
- ¹⁵⁷T. Niwa, Y. Sasaki, E. Uemura, S. Nakamura, M. Akiyama, M. Ando, S. Sawada, S. A. Mukai, T. Ueda, H. Taguchi, and K. Akiyoshi, “Comprehensive study of liposome-assisted synthesis of membrane proteins using a reconstituted cell-free translation system.”, *Scientific reports* **5**, 18025–18025 (2015).
- ¹⁵⁸S. Damiati, R. Mhanna, R. Kodzius, E.-K. Ehmoser, S. Damiati, R. Mhanna, R. Kodzius, and E.-K. Ehmoser, “Cell-Free Approaches in Synthetic Biology Utilizing Microfluidics”, *Genes* **9**, 144 (2018).
- ¹⁵⁹E. Dubuc, P. A. Pieters, A. J. van der Linden, J. C. van Hest, W. T. Huck, and T. F. de Greef, “Cell-free microcompartmentalised transcription–translation for the prototyping of synthetic communication networks”, *Current Opinion in Biotechnology* **58**, 72–80 (2019).
- ¹⁶⁰N. Ramachandran, E. Hainsworth, B. Bhullar, S. Eisenstein, B. Rosen, A. Y. Lau, J. C. Walter, and J. LaBaer, “Self-assembling protein microarrays”, *Science (New York, NY)* **305**, 86–90 (2004).
- ¹⁶¹N. Ramachandran, J. V. Raphael, E. Hainsworth, G. Demirkan, M. G. Fuentes, A. Rolfs, Y. Hu, and J. Labaer, “Next-generation high-density self-assembling functional protein arrays.”, *Nature Methods* **5**, 535–538 (2008).
- ¹⁶²D. Gerber, S. J. Maerkl, and S. R. Quake, “An in vitro microfluidic approach to generating protein-interaction networks”, *Nature Methods* **6**, 71–74 (2009).
- ¹⁶³S. J. Maerkl and S. R. Quake, “A systems approach to measuring the binding energy landscapes of transcription factors”, *Science (New York, NY)* **315**, 233–237 (2007).
- ¹⁶⁴S. J. Maerkl and S. R. Quake, “Experimental determination of the evolvability of a transcription factor”, *Proceedings of the National Academy of Sciences of the United States of America* **106**, 18650–18655 (2009).
- ¹⁶⁵L. L. Martin, M. M. Meier, S. M. S. Lyons, R. V. R. Sit, W. F. W. Marzluff, S. R. S. Quake, and H. Y. H. Chang, “Systematic reconstruction of RNA functional motifs with high-throughput microfluidics.”, *Nature Methods* **9**, 1192–1194 (2012).
- ¹⁶⁶S. Rockel, M. Geertz, K. Hens, B. Deplancke, and S. J. Maerkl, “iSLIM: a comprehensive approach to mapping and characterizing gene regulatory networks.”, *Nucleic acids research* **41**, e52 (2013).
- ¹⁶⁷M. C. Blackburn, E. Petrova, B. E. Correia, and S. J. Maerkl, “Integrating gene synthesis and microfluidic protein analysis for rapid protein engineering”, *Nucleic acids research*, 1497 (2015).

- ¹⁶⁸M. K. Takahashi, J. Chappell, C. A. Hayes, Z. Z. Sun, J. Kim, V. Singhal, K. J. Spring, S. Al-Khabouri, C. P. Fall, V. Noireaux, R. M. Murray, and J. B. Lucks, “Rapidly Characterizing the Fast Dynamics of RNA Genetic Circuitry with Cell-Free Transcription–Translation (TX-TL) Systems”, *ACS Synthetic Biology* **4**, 503–515 (2015).
- ¹⁶⁹S. J. Moore, J. T. MacDonald, S. Wienecke, A. Ishwarbhai, A. Tsipa, R. Aw, N. Kylilis, D. J. Bell, D. W. McClymont, K. Jensen, K. M. Polizzi, R. Biedendieck, and P. S. Freemont, “Rapid acquisition and model-based analysis of cell-free transcription–translation reactions from nonmodel bacteria”, *en, Proceedings of the National Academy of Sciences* **115**, E4340–E4349 (2018).
- ¹⁷⁰A. Swaminathan, V. Hsiao, and R. M. Murray, “Quantitative Modeling of Integrase Dynamics Using a Novel Python Toolbox for Parameter Inference in Synthetic Biology”, *en, bioRxiv*, 121152 (2017).
- ¹⁷¹Y. Hori, C. Kantak, R. M. Murray, and A. R. Abate, “Cell-free extract based optimization of biomolecular circuits with droplet microfluidics”, *Lab on a Chip* **17**, 3037–3042 (2017).
- ¹⁷²Z. Swank, N. Laohakunakorn, and S. J. Maerkl, “Cell-free gene-regulatory network engineering with synthetic transcription factors”, *Proceedings of the National Academy of Sciences* **116**, 5892–5901 (2019).
- ¹⁷³J. Fan, F. Villarreal, B. Weyers, Y. Ding, K. H. Tseng, J. Li, B. Li, C. Tan, and T. Pan, “Multi-dimensional studies of synthetic genetic promoters enabled by microfluidic impact printing”, *en, Lab on a Chip* **17**, 2198–2207 (2017).
- ¹⁷⁴V. Georgi, L. Georgi, M. Blechert, M. Bergmeister, M. Zwanzig, D. A. Wüstenhagen, F. F. Bier, E. Jung, and S. Kubick, “On-chip automation of cell-free protein synthesis: new opportunities due to a novel reaction mode”, *en, Lab on a Chip* **16**, 269–281 (2016).
- ¹⁷⁵Y. Elani, R. V. Law, and O. Ces, “Vesicle-based artificial cells as chemical microreactors with spatially segregated reaction pathways”, *en, Nature Communications* **5**, 1–5 (2014).
- ¹⁷⁶Y. Jiao, Y. Liu, D. Luo, W. T. Huck, and D. Yang, “Microfluidic-Assisted Fabrication of Clay Microgels for Cell-Free Protein Synthesis”, *ACS Applied Materials and Interfaces* **10**, 29308–29313 (2018).
- ¹⁷⁷K.-H. Lee, K.-Y. Lee, J.-Y. Byun, B.-G. Kim, and D.-M. Kim, “On-bead expression of recombinant proteins in an agarose gel matrix coated on a glass slide”, *en, Lab on a Chip* **12**, 1605–1610 (2012).
- ¹⁷⁸J.-Y. Byun, K.-H. Lee, K.-Y. Lee, M.-G. Kim, and D.-M. Kim, “In-gel expression and in situ immobilization of proteins for generation of three dimensional protein arrays in a hydrogel matrix”, *en, Lab on a Chip* **13**, 886–891 (2013).
- ¹⁷⁹A. S. Spirin, V. I. Baranov, L. A. Ryabova, S. Y. Ovodov, and Y. B. Alakhov, “A continuous cell-free translation system capable of producing polypeptides in high yield”, *en, Science* **242**, 1162–1164 (1988).
- ¹⁸⁰D.-M. Kim and C.-Y. Choi, “A Semicontinuous Prokaryotic Coupled Transcription/Translation System Using a Dialysis Membrane”, *Biotechnology Progress* **12**, 645–649 (1996).

- ¹⁸¹K. Madin, T. Sawasaki, T. Ogasawara, and Y. Endo, “A Highly Efficient and Robust Cell-Free Protein Synthesis System Prepared from Wheat Embryos: Plants Apparently Contain a Suicide System Directed at Ribosomes”, *Proceedings of the National Academy of Sciences of the United States of America* **97**, 559–564 (2000).
- ¹⁸²Q. Mei, C. K. Fredrickson, W. Lian, S. Jin, and Z. H. Fan, “Ricin Detection by Biological Signal Amplification in a Well-in-a-Well Device”, *Analytical Chemistry* **78**, 7659–7664 (2006).
- ¹⁸³Q. Mei, C. K. Fredrickson, A. Simon, R. Khnouf, and Z. H. Fan, “Cell-free protein synthesis in microfluidic array devices”, *Biotechnology Progress* **23**, 1305–1311 (2007).
- ¹⁸⁴R. Khnouf, D. J. Beebe, and Z. H. Fan, “Cell-free protein expression in a microchannel array with passive pumping”, *en, Lab on a Chip* **9**, 56–61 (2009).
- ¹⁸⁵R. Khnouf, D. Olivero, S. Jin, and Z. H. Fan, “Miniaturized fluid array for high-throughput protein expression”, *en, Biotechnology Progress* **26**, 1590–1596 (2010).
- ¹⁸⁶G.-H. Hahn, A. Asthana, D.-M. Kim, and D. Kim, “A continuous-exchange cell-free protein synthesis system fabricated on a chip”, *Analytical biochemistry* **365**, 280–282 (2007).
- ¹⁸⁷P. Siuti, S. T. Retterer, and M. J. Doktycz, “Continuous protein production in nanoporous, picolitre volume containers”, *en, Lab on a Chip* **11**, 3523–3529 (2011).
- ¹⁸⁸H. Niederholtmeyer, L. Xu, and S. J. Maerkl, “Real-Time mRNA Measurement during an in Vitro Transcription and Translation Reaction Using Binary Probes”, *ACS Synthetic Biology* **2**, 411–417 (2013).
- ¹⁸⁹A. J. van der Linden, M. Yelleswarapu, P. A. Pieters, Z. Swank, W. T. S. Huck, S. J. Maerkl, and T. F. A. de Greef, “A Multilayer Microfluidic Platform for the Conduction of Prolonged Cell-Free Gene Expression”, *Journal of Visualized Experiments*, 1–14 (2019).
- ¹⁹⁰M. Yelleswarapu, A. J. van der Linden, B. van Sluijs, P. A. Pieters, E. Dubuc, T. F. A. de Greef, and W. T. S. Huck, “Sigma Factor-Mediated Tuning of Bacterial Cell-Free Synthetic Genetic Oscillators, Supplementary Information”, *ACS Synthetic Biology* **7**, 2879 (2018).
- ¹⁹¹E. Karzbrun, A. Tayar, V. Noireaux, and R. Bar-Ziv, “Programmable on-chip DNA compartments as artificial cells”, *Science* **345**, 829–832 (2014).
- ¹⁹²Y. Efrat, A. M. Tayar, S. S. Daube, M. Levy, and R. H. Bar-Ziv, “Electric-Field Manipulation of a Compartmentalized Cell-Free Gene Expression Reaction”, *ACS Synthetic Biology* **7**, 1829–1833 (2018).
- ¹⁹³P. Torre, C. D. Keating, and S. S. Mansy, “Multiphase Water-in-Oil Emulsion Droplets for Cell-Free Transcription–Translation”, *Langmuir* **30**, 5695–5699 (2014).
- ¹⁹⁴N. Park, S. H. Um, H. Funabashi, J. Xu, and D. Luo, “A cell-free protein-producing gel”, *Nature Materials* **8**, 432–437 (2009).
- ¹⁹⁵N. Park, J. S. Kahn, E. J. Rice, M. R. Hartman, H. Funabashi, J. Xu, S. H. Um, and D. Luo, “High-yield cell-free protein production from P-gel”, *Nature Protocols* **4**, 1759–1770 (2009).

- ¹⁹⁶D. Yang, S. Peng, M. R. Hartman, T. Gupton-Campolongo, E. J. Rice, A. K. Chang, Z. Gu, G. Q. M. Lu, and D. Luo, “Enhanced transcription and translation in clay hydrogel and implications for early life evolution”, *Scientific Reports* **3**, 27–6 (2013).
- ¹⁹⁷J. Thiele, Y. Ma, D. Foschepoth, M. M. K. Hansen, C. Steffen, H. A. Heus, and W. T. S. Huck, “DNA-functionalized hydrogels for confined membrane-free in vitro transcription/translation”, *Lab Chip* **14**, 2651–6 (2014).
- ¹⁹⁸L. Aufinger and F. C. Simmel, “Artificial Gel-Based Organelles for Spatial Organization of Cell-Free Gene Expression Reactions”, *Angewandte Chemie International Edition* **57**, 17245–17248 (2018).
- ¹⁹⁹X. Zhou, H. Wu, M. Cui, S. N. Lai, and B. Zheng, “Long-lived protein expression in hydrogel particles: towards artificial cells”, *Chemical Science* **9**, 4275–4279 (2018).
- ²⁰⁰V. Noireaux and A. Libchaber, “A vesicle bioreactor as a step toward an artificial cell assembly.”, *Proceedings of the National Academy of Sciences of the United States of America* **101**, 17669–17674 (2004).
- ²⁰¹K. K. Y. Ho, V. L. Murray, and A. P. Liu, “Engineering artificial cells by combining hela-based cell-free expression and ultrathin double emulsion template”, *Methods in cell biology*, 303–318 (2015).
- ²⁰²K. K. Y. Ho, J. W. Lee, G. Durand, S. Majumder, and A. P. Liu, “Protein aggregation with poly(vinyl) alcohol surfactant reduces double emulsion-encapsulated mammalian cell-free expression”, *PLoS ONE* **12**, e0174689–15 (2017).
- ²⁰³S. Deshpande, Y. Caspi, A. E. Meijering, and C. Dekker, “Octanol-assisted liposome assembly on chip”, *Nature Communications* **7**, 1–9 (2016).
- ²⁰⁴S. Deshpande and C. Dekker, “On-chip microfluidic production of cell-sized liposomes”, *Nature Protocols* **13**, 856–874 (2018).
- ²⁰⁵K. Vogele, T. Frank, L. Gasser, M. A. Goetzfried, M. W. Hackl, S. A. Sieber, F. C. Simmel, and T. Pirzer, “Towards synthetic cells using peptide-based reaction compartments”, *Nature Communications* **9**, 1–7 (2018).
- ²⁰⁶H. Niederholtmeyer, C. Chaggan, and N. K. Devaraj, “Communication and quorum sensing in non-living mimics of eukaryotic cells”, *Nature Communications* **9**, 1–8 (2018).
- ²⁰⁷R. Marshall, J. Garamella, V. Noireaux, and A. Pierson, “High-Throughput Microliter-Sized Cell-Free Transcription-Translation Reactions for Synthetic Biology Applications using the Echo 550 Liquid Handler”, *Labcyte Application Note*, App–G124 (2018).
- ²⁰⁸D. K. Karig, S.-Y. Jung, B. Srijanto, C. P. Collier, and M. L. Simpson, “Probing Cell-Free Gene Expression Noise in Femtoliter Volumes”, *ACS Synthetic Biology* **2**, 497–505 (2013).
- ²⁰⁹M. Shojaeian, F.-X. Lehr, H. U. Göringer, and S. Hardt, “On-Demand Production of Femtoliter Drops in Microchannels and Their Use as Biological Reaction Compartments”, *Analytical Chemistry* **91**, 3484–3491 (2019).
- ²¹⁰D. S. Tawfik and A. D. Griffiths, “Man-made cell-like compartments for molecular evolution”, *Nature Biotechnology* **16**, 652–656 (1998).

- ²¹¹L. E. Contreras-Llano and C. Tan, “High-throughput screening of biomolecules using cell-free gene expression systems”, *Synthetic Biology* **3**, 47–13 (2018).
- ²¹²A. D. Griffiths and D. S. Tawfik, “Directed evolution of an extremely fast phosphotriesterase by in vitro compartmentalization”, *Embo Journal* **22**, 24–35 (2003).
- ²¹³F. Courtois, L. F. Olguin, G. Whyte, D. Bratton, W. T. S. Huck, C. Abell, and F. Hollfelder, “An Integrated Device for Monitoring Time-Dependent in vitro Expression From Single Genes in Picolitre Droplets”, *ChemBioChem* **9**, 439–446 (2008).
- ²¹⁴J. A. Stapleton and J. R. Swartz, “Development of an In Vitro Compartmentalization Screen for High-Throughput Directed Evolution of [FeFe] Hydrogenases”, *PLoS ONE* **5**, e15275–8 (2010).
- ²¹⁵A. Fallah-Araghi, J.-C. Baret, M. Ryckelynck, and A. D. Griffiths, “A completely in vitro ultrahigh-throughput droplet-based microfluidic screening system for protein engineering and directed evolution”, *Lab Chip* **12**, 882–11 (2012).
- ²¹⁶P. Gruner, B. Riechers, B. i. t. Semin, J. Lim, A. Johnston, K. Short, and J.-C. Baret, “Controlling molecular transport in minimal emulsions”, *Nature Communications* **7**, 1–9 (2019).
- ²¹⁷G. Etienne, A. Vian, M. Biočanin, B. Deplancke, and E. Amstad, “Cross-talk between emulsion drops: how are hydrophilic reagents transported across oil phases?”, *Lab Chip* **18**, 3903–3912 (2018).
- ²¹⁸G. Woronoff, M. Ryckelynck, J. Wessel, O. Schicke, A. D. Griffiths, and P. Soumillon, “Activity-Fed Translation (AFT) Assay: A New High-Throughput Screening Strategy for Enzymes in Droplets”, *ChemBioChem* **16**, 1343–1349 (2015).
- ²¹⁹Y. Zhou, H. Asahara, N. Schneider, P. Dranchak, J. Inglese, and S. Chong, “Engineering Bacterial Transcription Regulation To Create a Synthetic in Vitro Two-Hybrid System for Protein Interaction Assays”, *Journal of the American Chemical Society* **136**, 14031–14038 (2014).
- ²²⁰N. Cui, H. Zhang, N. Schneider, Y. Tao, H. Asahara, Z. Sun, Y. Cai, S. A. Koehler, T. F. A. de Greef, A. Abbaspourrad, D. A. Weitz, and S. Chong, “A mix-and-read drop-based in vitro two-hybrid method for screening high-affinity peptide binders”, *Scientific Reports* **6**, 1–10 (2016).
- ²²¹M. M. K. Hansen, L. H. H. Meijer, E. Spruijt, R. J. M. Maas, M. V. Rosquelles, J. Groen, H. A. Heus, and W. T. S. Huck, “Macromolecular crowding creates heterogeneous environments of gene expression in picolitre droplets”, *Nature Nanotechnology* **11**, 191–197 (2015).
- ²²²T. Matsuura, K. Hosoda, Y. Kazuta, N. Ichihashi, H. Suzuki, and T. Yomo, “Effects of Compartment Size on the Kinetics of Intracompartamental Multimeric Protein Synthesis”, *ACS Synthetic Biology* **1**, 431–437 (2012).
- ²²³R. Sakamoto, V. Noireaux, and Y. T. Maeda, “Anomalous Scaling of Gene Expression in Confined Cell-Free Reactions.”, *Scientific Reports* **8**, 7364 (2018).

- ²²⁴A. Kato, M. Yanagisawa, Y. T. Sato, K. Fujiwara, and K. Yoshikawa, “Cell-Sized confinement in microspheres accelerates the reaction of gene expression”, *Scientific Reports* **2**, 1172–5 (2012).
- ²²⁵M. Schwarz-Schilling, A. Dupin, F. Chizzolini, S. Krishnan, S. S. Mansy, and F. C. Simmel, “Optimized Assembly of a Multifunctional RNA-Protein Nanostructure in a Cell-Free Gene Expression System”, *Nano Letters* **18**, 2650–2657 (2018).
- ²²⁶S. Alberti, A. Gladfelter, and T. Mittag, “Considerations and Challenges in Studying Liquid-Liquid Phase Separation and Biomolecular Condensates”, *Cell* **176**, 419–434 (2019).
- ²²⁷N.-N. Deng, M. A. Vibhute, L. Zheng, H. Zhao, M. Yelleswarapu, and W. T. S. Huck, “Macromolecularly Crowded Protocells from Reversibly Shrinking Monodisperse Liposomes”, *Journal of the American Chemical Society* **140**, 7399–7402 (2018).
- ²²⁸E. Sokolova, E. Spruijt, M. M. K. Hansen, E. Dubuc, J. Groen, V. Chokkalingam, A. Piruska, H. A. Heus, and W. T. S. Huck, “Enhanced transcription rates in membrane-free protocells formed by coacervation of cell lysate”, *Proceedings of the National Academy of Sciences of the United States of America* **110**, 11692–11697 (2013).
- ²²⁹T. Y. D. Tang, D. van Swaay, A. deMello, J. L. R. Anderson, and S. Mann, “In vitro gene expression within membrane-free coacervate protocells”, *Chemical Communications* **51**, 11429–11432 (2015).
- ²³⁰D. van Swaay, T. Y. D. Tang, S. Mann, and A. de Mello, “Microfluidic Formation of Membrane-Free Aqueous Coacervate Droplets in Water”, *Angewandte Chemie* **127**, 8518–8521 (2015).
- ²³¹R. C. H. Ruiz, P. Kiatwuthinon, J. S. Kahn, Y. H. Roh, and D. Luo, “Cell-Free Protein Expression from DNA-Based Hydrogel (P-Gel) Droplets for Scale-Up Production”, *Industrial Biotechnology* **8**, 372–377 (2012).
- ²³²J. S. Kahn, R. C. H. Ruiz, S. Sureka, S. Peng, T. L. Derrien, D. An, and D. Luo, “DNA Microgels as a Platform for Cell-Free Protein Expression and Display”, *Biomacromolecules* **17**, 2019–2026 (2016).
- ²³³S. N. Lai, X. Zhou, X. Ouyang, H. Zhou, Y. Liang, J. Xia, and B. Zheng, “Artificial Cells Capable of Long-Lived Protein Synthesis by Using Aptamer Grafted Polymer Hydrogel”, *ACS Synthetic Biology* **9**, 76–83 (2020).
- ²³⁴P. Stano, “Gene Expression Inside Liposomes: From Early Studies to Current Protocols”, *Chemistry - A European Journal* **25**, 7798–7814 (2019).
- ²³⁵T. Oberholzer, K. H. Nierhaus, and P. L. Luisi, “Protein expression in liposomes”, *Biochemical and Biophysical Research Communications* **261**, 238–241 (1999).
- ²³⁶W. Yu, K. Sato, M. Wakabayashi, T. Nakaishi, E. P. Ko-Mitamura, Y. Shima, I. Urabe, and T. Yomo, “Synthesis of functional protein in liposome.”, *Journal of Bioscience and Bioengineering* **92**, 590–593 (2001).
- ²³⁷T. Oberholzer and P. L. Luisi, “The use of liposomes for constructing cell models”, *Journal of Biological Physics* **28**, 733–744 (2002).

- ²³⁸S.-i. M. Nomura, K. Tsumoto, T. Hamada, K. Akiyoshi, Y. Nakatani, and K. Yoshikawa, “Gene Expression within Cell-Sized Lipid Vesicles”, *ChemBioChem* **4**, 1172–1175 (2003).
- ²³⁹K. Ishikawa, K. Sato, Y. Shima, I. Urabe, and T. Yomo, “Expression of a cascading genetic network within liposomes”, *FEBS Letters* **576**, 387–390 (2004).
- ²⁴⁰Z. Nourian, W. Roelofsen, and C. Danelon, “Triggered Gene Expression in Fed-Vesicle Microreactors with a Multifunctional Membrane”, *Angewandte Chemie International Edition* **51**, 3114–3118 (2012).
- ²⁴¹L. R. Arriaga, S. S. Datta, S.-H. Kim, E. Amstad, T. E. Kodger, F. Monroy, and D. A. Weitz, “Ul-trathin Shell Double Emulsion Templated Giant Unilamellar Lipid Vesicles with Controlled Microdomain Formation”, *Small* **10**, 950–956 (2013).
- ²⁴²N.-N. Deng, M. Yelleswarapu, and W. T. S. Huck, “Monodisperse Uni- and Multicompart-ment Liposomes”, *Journal of the American Chemical Society* **138**, 7584–7591 (2016).
- ²⁴³N.-N. Deng, M. Yelleswarapu, L. Zheng, and W. T. S. Huck, “Microfluidic Assembly of Monodisperse Vesosomes as Artificial Cell Models”, *Journal of the American Chemical Society* **139**, 587–590 (2017).
- ²⁴⁴F. Cuomo, A. Ceglie, A. De Leonardis, and F. Lopez, “Polymer Capsules for Enzymatic Catalysis in Confined Environments”, *Catalysts* **9**, 1–18 (2019).
- ²⁴⁵C. Martino, S.-H. Kim, L. Horsfall, A. Abbaspourrad, S. J. Rosser, J. Cooper, and D. A. Weitz, “Protein Expression, Aggregation, and Triggered Release from Polymersomes as Artificial Cell-like Structures”, *Angewandte Chemie International Edition* **51**, 6416–6420 (2012).
- ²⁴⁶A. Schreiber, M. C. Huber, and S. M. Schiller, “Prebiotic Protocell Model Based on Dynamic Protein Membranes Accommodating Anabolic Reactions”, *Langmuir* **35**, 9593–9610 (2019).
- ²⁴⁷Y.-C. Kwon, G.-H. Hahn, K. M. Huh, and D.-M. Kim, “Synthesis of functional proteins using *Escherichia coli* extract entrapped in calcium alginate microbeads”, *Analytical Biochemistry* **373**, 192–196 (2008).
- ²⁴⁸S. Y. Lim, K.-O. Kim, D.-M. Kim, and C. B. Park, “Silica-coated alginate beads for in vitro protein synthesis via transcription/translation machinery encapsulation”, *Journal of Biotechnology* **143**, 183–189 (2009).
- ²⁴⁹D. Saeki, S. Sugiura, T. Kanamori, S. Sato, and S. Ichikawa, “Microcompartmentalized cell-free protein synthesis in semipermeable microcapsules composed of polyethylenimine-coated alginate”, *Journal of Bioscience and Bioengineering* **118**, 199–204 (2014).
- ²⁵⁰T. Okano, T. Matsuura, Y. Kazuta, H. Suzuki, and T. Yomo, “Cell-free protein synthesis from a single copy of DNA in a glass microchamber”, *Lab Chip* **12**, 2704–8 (2012).
- ²⁵¹T. Okano, T. Matsuura, H. Suzuki, and T. Yomo, “Cell-free Protein Synthesis in a Microchamber Revealed the Presence of an Optimum Compartment Volume for High-order Reactions”, *ACS Synthetic Biology* **3**, 347–352 (2014).
- ²⁵²K. Nishimura, T. Matsuura, K. Nishimura, T. Sunami, H. Suzuki, and T. Yomo, “Cell-Free Protein Synthesis inside Giant Unilamellar Vesicles Analyzed by Flow Cytometry”, *Langmuir* **28**, 8426–8432 (2012).

- ²⁵³T. Sunami, K. Hosoda, H. Suzuki, T. Matsuura, and T. Yomo, “Cellular Compartment Model for Exploring the Effect of the Lipidic Membrane on the Kinetics of Encapsulated Biochemical Reactions”, *Langmuir* **26**, 8544–8551 (2010).
- ²⁵⁴P. Stano, E. D’Aguanno, J. Bolz, A. Fahr, and P. L. Luisi, “A remarkable self-organization process as the origin of primitive functional cells”, *Angewandte Chemie - International Edition* **52**, 13397–13400 (2013).
- ²⁵⁵D. Blanken, P. van Nies, and C. Danelon, “Quantitative imaging of gene-expressing liposomes reveals rare favorable phenotypes”, *Physical Biology* **16**, 045002–15 (2019).
- ²⁵⁶E. Altamura, P. Carrara, F. D’Angelo, F. Mavelli, and P. Stano, “Extrinsic stochastic factors (solute partition) in gene expression inside lipid vesicles and lipid-stabilized water-in-oil droplets: a review”, *Synthetic Biology* **3**, 1–16 (2018).
- ²⁵⁷A. M. Tayar, E. Karzbrun, V. Noireaux, and R. H. Bar-Ziv, “Propagating gene expression fronts in a one-dimensional coupled system of artificial cells”, *Nature Physics* **11**, 1037–1041 (2015).
- ²⁵⁸M. Schwarz-Schilling, L. Aufinger, A. Mückl, and F. C. Simmel, “Chemical communication between bacteria and cell-free gene expression systems within linear chains of emulsion droplets”, *Integrative Biology* **8**, 564–570 (2016).
- ²⁵⁹A. Dupin and F. C. Simmel, “Signalling and differentiation in emulsion-based multi-compartmentalized in vitro gene circuits”, *Nature Chemistry* **11**, 32–39 (2019).
- ²⁶⁰M. Dwidar, Y. Seike, S. Kobori, C. Whitaker, T. Matsuura, and Y. Yokobayashi, “Programmable Artificial Cells Using Histamine-Responsive Synthetic Riboswitch”, *Journal of the American Chemical Society* **141**, 11103–11114 (2019).
- ²⁶¹S. Majumder, J. Garamella, Y.-L. Wang, M. DeNies, V. Noireaux, and A. P. Liu, “Cell-sized mechanosensitive and biosensing compartment programmed with DNA”, *Chem. Commun.* **53**, 7349–7352 (2017).
- ²⁶²J. Garamella, S. Majumder, A. P. Liu, and V. Noireaux, “An adaptive synthetic cell based on mechanosensing, biosensing, and inducible gene circuits”, *ACS Synthetic Biology*, 9b00204 (2019).
- ²⁶³S. Berhanu, T. Ueda, and Y. Kuruma, “Artificial photosynthetic cell producing energy for protein synthesis.”, *Nature Communications* **10**, 1325–10 (2019).
- ²⁶⁴R. Lentini, N. Y. Martín, M. Forlin, L. Belmonte, J. Fontana, M. Cornella, L. Martini, S. Tamburini, W. E. Bentley, O. Jousson, and S. S. Mansy, “Two-Way Chemical Communication between Artificial and Natural Cells”, *ACS Central Science* **3**, 117–123 (2017).
- ²⁶⁵A. M. Tayar, E. Karzbrun, V. Noireaux, and R. H. Bar-Ziv, “Synchrony and pattern formation of coupled genetic oscillators on a chip of artificial cells.”, *Proceedings of the National Academy of Sciences* **114**, 11609–11614 (2017).

- ²⁶⁶R. Lentini, S. P. Santero, F. Chizzolini, D. Cecchi, J. Fontana, M. Marchioretto, C. Del Bianco, J. L. Terrell, A. C. Spencer, L. Martini, M. Forlin, M. Assfal, M. Dalla Serra, W. E. Bentley, and S. S. Mansy, “Integrating artificial with natural cells to translate chemical messages that direct *E. coli* behaviour.”, *Nature Communications* **5**, 4012 (2014).
- ²⁶⁷G. Rampioni, F. D’Angelo, M. Messina, A. Zennaro, Y. Kuruma, D. Tofani, L. Leoni, and P. Stano, “Synthetic cells produce a quorum sensing chemical signal perceived by: *Pseudomonas aeruginosa*”, *Chemical Communications* **54**, 2090–2093 (2018).
- ²⁶⁸Y. Ding, L. E. Contreras-Llano, E. Morris, M. Mao, and C. Tan, “Minimizing Context Dependency of Gene Networks Using Artificial Cells”, *ACS Applied Materials & Interfaces* **10**, 30137–30146 (2018).
- ²⁶⁹K. P. Adamala, D. A. Martin-Alarcon, K. R. Guthrie-Honea, and E. S. Boyden, “Engineering genetic circuit interactions within and between synthetic minimal cells”, *Nature Chemistry* **9**, 431–439 (2016).
- ²⁷⁰N. Krinsky, M. Kaduri, A. Zinger, J. Shainsky-Roitman, M. Goldfeder, I. Benhar, D. Hershkovitz, and A. Schroeder, “Synthetic Cells Synthesize Therapeutic Proteins inside Tumors”, *Advanced Healthcare Materials* **7**, 1701163–10 (2017).
- ²⁷¹H. Shum and A. C. Balazs, “Synthetic quorum sensing in model microcapsule colonies.”, *Proceedings of the National Academy of Sciences* **114**, 8475–8480 (2017).
- ²⁷²G. Menon and J. Krishnan, “Design Principles for Compartmentalization and Spatial Organization of Synthetic Genetic Circuits”, *ACS Synthetic Biology* **8**, 1601–1619 (2019).
- ²⁷³G. Villar, A. D. Graham, and H. Bayley, “A Tissue-Like Printed Material”, *Science (New York, N.Y.)* **340**, 48–52 (2013).
- ²⁷⁴A. Joesaar, S. Yang, B. B. x. gels, A. Linden, P. Pieters, B. V. V. S. P. Kumar, N. Dalchau, A. Phillips, S. Mann, and T. F. A. Greef, “DNA-based communication in populations of synthetic protocells”, *Nature Nanotechnology* **21**, 1–12 (2019).
- ²⁷⁵A. J. Genot, A. Baccouche, R. Sieskind, N. Aubert-Kato, N. Bredeche, J. F. Bartolo, V. Taly, T. Fujii, and Y. Rondelez, “High-resolution mapping of bifurcations in nonlinear biochemical circuits”, *Nature Chemistry* **8**, 760–767 (2016).
- ²⁷⁶M. Weitz, J. Kim, K. Kapsner, E. Winfree, E. Franco, and F. C. Simmel, “Diversity in the dynamical behaviour of a compartmentalized programmable biochemical oscillator”, *Nature Chemistry* **6**, 295–302 (2014).
- ²⁷⁷J. Selberg, M. Gomez, and M. Rolandi, “The Potential for Convergence between Synthetic Biology and Bioelectronics”, *Cell Systems* **7**, 231–244 (2018).
- ²⁷⁸R. Phillips, N. M. Belliveau, G. Chure, H. G. Garcia, M. Razo-Mejia, and C. Scholes, “Figure 1 Theory Meets Figure 2 Experiments in the Study of Gene Expression”, *Annual Review of Biophysics* **48**, 121–163 (2019).
- ²⁷⁹L. Bintu, N. E. Buchler, H. G. Garcia, U. Gerland, T. Hwa, J. Kondev, and R. Phillips, *Transcriptional regulation by the numbers: Models* (2005).

- ²⁸⁰K. Y. Rhee, M. Opel, E. Ito, S. P. Hung, S. M. Arfin, and G. W. Hatfield, “Transcriptional coupling between the divergent promoters of a prototypic LysR-type regulatory system, the *ilvYC* operon of *Escherichia coli*”, *Proceedings of the National Academy of Sciences of the United States of America* (1999).
- ²⁸¹K. E. Shearwin, B. P. Callen, and J. B. Egan, “Transcriptional interference - A crash course”, *Trends in Genetics* **21**, 339–345 (2005).
- ²⁸²S. Chong, C. Chen, H. Ge, and X. S. Xie, “Mechanism of transcriptional bursting in bacteria”, *Cell* (2014).
- ²⁸³E. Yeung, A. J. Dy, K. B. Martin, A. H. Ng, D. Del Vecchio, J. L. Beck, J. J. Collins, and R. M. Murray, “Biophysical Constraints Arising from Compositional Context in Synthetic Gene Networks”, *Cell Systems* (2017).
- ²⁸⁴T. S. Gardner, C. R. Cantor, and J. J. Collins, “Construction of a genetic toggle switch in *Escherichia coli*”, *Nature* **403**, 339–342 (2000).
- ²⁸⁵S. Cardinale and A. P. Arkin, “Contextualizing context for synthetic biology - identifying causes of failure of synthetic biological systems”, *Biotechnology Journal* **7**, 856–866 (2012).
- ²⁸⁶M. Carbonell-Ballester, E. Garcia-Ramallo, R. Montañez, C. Rodriguez-Caso, and J. Macía, “Dealing with the genetic load in bacterial synthetic biology circuits: Convergences with the Ohm’s law”, *Nucleic Acids Research* (2016).
- ²⁸⁷Y. Qian, H. H. Huang, J. I. Jiménez, and D. Del Vecchio, “Resource Competition Shapes the Response of Genetic Circuits”, *ACS Synthetic Biology* (2017).
- ²⁸⁸A. Gyorgy, J. I. Jiménez, J. Yazbek, H. H. Huang, H. Chung, R. Weiss, and D. Del Vecchio, “Isocost Lines Describe the Cellular Economy of Genetic Circuits”, *Biophysical Journal* (2015).
- ²⁸⁹T. E. Gorochofski, I. Avciilar-Kucukgoze, R. A. Bovenberg, J. A. Roubos, and Z. Ignatova, “A Minimal Model of Ribosome Allocation Dynamics Captures Trade-offs in Expression between Endogenous and Synthetic Genes”, *ACS Synthetic Biology* (2016).
- ²⁹⁰A. Gyorgy and R. M. Murray, “Quantifying resource competition and its effects in the TX-TL system”, in *2016 IEEE 55th Conference on Decision and Control, CDC 2016* (2016).
- ²⁹¹F. Ceroni, R. Algar, G. B. Stan, and T. Ellis, “Quantifying cellular capacity identifies gene expression designs with reduced burden”, *Nature Methods* (2015).
- ²⁹²L. Chou and W. Shih, “Cell-free transcriptional regulation via nucleic-acid-based transcription factors”, *bioRxiv* (2019).
- ²⁹³J. M. Berg, J. L. Tymoczko, and L. Stryer, *Biochemistry* (W.H. Freeman, 2012), p. 48.
- ²⁹⁴R. Diaz and W. L. Staudenbauer, “Replication of the broad host range plasmid RSF1010 in cell-free extracts of *Escherichia coli* and *Pseudomonas aeruginosa*”, *Nucleic Acids Research* **10**, 4687–4702 (1982).
- ²⁹⁵J. J. Li and T. J. Kelly, “Simian virus 40 DNA replication in vitro.”, *Proceedings of the National Academy of Sciences of the United States of America* **81**, 6973–7 (1984).

- ²⁹⁶B. W. Stillman and Y. Gluzman, “Replication and supercoiling of simian virus 40 DNA in cell extracts from human cells.”, *Molecular and cellular biology* **5**, 2051–60 (1985).
- ²⁹⁷C. R. Wobbe, F. Dean, L. Weissbach, and J. Hurwitz, “In vitro replication of duplex circular DNA containing the simian virus 40 DNA origin site.”, *Proceedings of the National Academy of Sciences of the United States of America* **82**, 5710–4 (1985).
- ²⁹⁸K. B. Mullis and F. A. Faloona, “Specific Synthesis of DNA in Vitro via a Polymerase-Catalyzed Chain Reaction”, *Recombinant DNA Methodology*, 189–204 (1987).
- ²⁹⁹J. M. Kaguni and A. Kornberg, “Replication initiated at the origin (oriC) of the E. coli chromosome reconstituted with purified enzymes”, *Cell* **38**, 183–190 (1984).
- ³⁰⁰M. Su’etsugu, H. Takada, T. Katayama, and H. Tsujimoto, “Exponential propagation of large circular DNA by reconstitution of a chromosome-replication cycle”, *Nucleic Acids Research* **45**, 11525–11534 (2017).
- ³⁰¹E. Scherzinger, V. Haring, R. Lurz, and S. Otto, “Plasmid RSF1010 DNA replication in vitro promoted by purified RSF1010 RepA, RepB and RepC proteins”, *Nucleic Acids Research* **19**, 1203–1211 (1991).
- ³⁰²L. Blanco, J. M. Lázaro, M. de Vega, A. Bonnin, and M. Salas, “Terminal protein-primed DNA amplification.”, *Proceedings of the National Academy of Sciences of the United States of America* **91**, 12198–202 (1994).
- ³⁰³D. Hürtgen, J. Mascarenhas, M. Heymann, S. M. Murray, P. Schwille, and V. Sourjik, “Reconstitution and Coupling of DNA Replication and Segregation in a Biomimetic System”, *ChemBioChem*, cbic.201900299 (2019).
- ³⁰⁴Y. Schaerli, V. Stein, M. M. Spiering, S. J. Benkovic, C. Abell, and F. Hollfelder, “Isothermal DNA amplification using the T4 replisome: circular nicking endonuclease-dependent amplification and primase-based whole-genome amplification”, *Nucleic Acids Research* **38**, e201–e201 (2010).
- ³⁰⁵S. Waga, G. Bauer, and B. Stillman, “Reconstitution of Complete SV40 DNA Replication with Purified Replication Factor”, *The Journal of biological chemistry* **3**, 1907–1941 (1994).
- ³⁰⁶A. C. Forster and G. M. Church, “Synthetic biology projects in vitro”, *Genome Research* **17**, 1–6 (2007).
- ³⁰⁷M. Salas, I. Holguera, M. Redrejo-Rodríguez, and M. de Vega, “DNA-Binding Proteins Essential for Protein-Primed Bacteriophage Φ 29 DNA Replication”, *Frontiers in Molecular Biosciences* **3**, 37 (2016).
- ³⁰⁸F. J. Ghadessy, J. L. Ong, and P. Holliger, “Directed evolution of polymerase function by compartmentalized self-replication”, *Proceedings of the National Academy of Sciences* **98**, 4552–4557 (2001).
- ³⁰⁹L. Grasemann, B. Lavickova, M. C. Elizondo-Cantú, and S. J. Maerkl, “Onepot pure cell-free system”, *Journal of Visualized Experiments* **2021**, 62625 (2021).
- ³¹⁰N. Laohakunakorn, “Cell-Free Systems: A Proving Ground for Rational Biodesign”, *Frontiers in Bioengineering and Biotechnology* **8**, 788 (2020).

- ³¹¹E. Cho and Y. Lu, “Compartmentalizing cell-free systems: Toward creating life-like artificial cells and beyond”, *ACS Synthetic Biology* **9**, 2881–2901 (2020).
- ³¹²N. J. Gaut and K. P. Adamala, “Reconstituting Natural Cell Elements in Synthetic Cells”, *Advanced Biology* **5** (2021).
- ³¹³S. Horiya, J. K. Bailey, and I. J. Krauss, “Directed Evolution of Glycopeptides Using mRNA Display”, *Methods in Enzymology* **597**, 83–141 (2017).
- ³¹⁴J. Ederth, C. Mandava, S. Dasgupta, and S. Sanyal, “A single-step method for purification of active His-tagged ribosomes from a genetically engineered *Escherichia coli*”, *Nucleic acids research* **37**, e15–e15 (2009).
- ³¹⁵R. F. Gesteland, “Isolation and characterization of ribonuclease I mutants of *Escherichia coli*”, *Journal of Molecular Biology* **16**, 67–84 (1966).
- ³¹⁶J. Li, W. Haas, K. Jackson, E. Kuru, M. C. Jewett, Z. H. Fan, S. Gygi, and G. M. Church, “Cogenerating Synthetic Parts toward a Self-Replicating System”, *ACS Synthetic Biology* **6**, 1327–1336 (2017).
- ³¹⁷E. Cayama, A. Yépez, F. Rotondo, E. Bandeira, A. Ferreras, and F. Triana-Alonso, “New chromatographic and biochemical strategies for quick preparative isolation of tRNA”, *Nucleic Acids Research* **28**, e64–e64 (2000).
- ³¹⁸B. Lavickova, L. Grasmann, and S. J. Maerkl, “Improved Cell-Free Transcription-Translation Reactions in Microfluidic Chemostats Augmented with Hydrogel Membranes for Continuous Small Molecule Dialysis”, *ACS Synthetic Biology* **11**, 4134–4141 (2022).
- ³¹⁹A. S. Spirin, “Cell-free protein synthesis”, *Cell-Free Translation Systems*, 3–20 (2002).
- ³²⁰Z. Swank and S. J. Maerkl, “CFPU: a cell-free processing unit for high-throughput, automated in vitro circuit characterization in steady-state conditions”, *BioDesign Research* (2021).
- ³²¹H. T. Nguyen, M. Massino, C. Keita, and J. B. Salmon, “Microfluidic dialysis using photo-patterned hydrogel membranes in PDMS chips”, *Lab on a Chip* **20**, 2383–2393 (2020).
- ³²²C. Warr, J. C. Valdoz, B. P. Bickham, C. J. Knight, N. A. Franks, N. Chartrand, P. M. Van Ry, K. A. Christensen, G. P. Nordin, and A. D. Cook, “Biocompatible PEGDA Resin for 3D Printing”, *ACS Applied Bio Materials* **3**, 2239–2244 (2020).
- ³²³J. Decock, M. Schlenk, J. S. .-. L. o. a. Chip, and U. 2018, “In situ photo-patterning of pressure-resistant hydrogel membranes with controlled permeabilities in PEGDA microfluidic channels”, *Lab on a chip* **18**, 1075–1083 (2018).
- ³²⁴S. Lin, N. Sangaj, T. Razafiarison, C. Zhang, and S. Varghese, “Influence of physical properties of biomaterials on cellular behavior”, *Pharmaceutical Research* **28**, 1422–1430 (2011).
- ³²⁵Y.-C. Chiu, J. C. Larson, A. Isom, and E. M. Brey, “Generation of Porous Poly(Ethylene Glycol) Hydrogels by Salt Leaching”, *Tissue Engineering Part C: Methods* **16**, 905–912 (2010).





- ³²⁶S. Orsi, D. Guarnieri, and P. A. Netti, “Design of novel 3D gene activated PEG scaffolds with ordered pore structure”, in *Journal of materials science: materials in medicine*, Vol. 21, 3 (2010), pp. 1013–1020.
- ³²⁷H. Yuk, T. Zhang, S. Lin, G. Parada, and X. Zhao, “Tough bonding of hydrogels to diverse non-porous surfaces”, *Nature materials* **15**, 190–196 (2016).
- ³²⁸L. Yu, C. Li, Y. Liu, J. Gao, W. Wang, and Y. Gan, “Flow-through functionalized PDMS microfluidic channels with dextran derivative for ELISAs”, *Lab on a Chip* **9**, 1243–1247 (2009).
- ³²⁹G. Sui, J. Wang, C. C. Lee, W. Lu, S. P. Lee, J. V. Leyton, A. M. Wu, and H. R. Tseng, “Solution-phase surface modification in intact poly(dimethylsiloxane) microfluidic channels”, *Analytical Chemistry* **78**, 5543–5551 (2006).
- ³³⁰B. Park and S. Song, “Investigation on Coating Methods of a Self-Assembled Monolayer on PDMS (Poly (dimethylsiloxane)) Surface”, *BioChip Journal* **1**, 140–143 (2007).
- ³³¹M. Li, M. Humayun, B. Hughes, J. A. Kozinski, and D. K. Hwang, “A microfluidic approach for the synthesis and assembly of multi-scale porous membranes”, *RSC Advances* **5**, 100024–100029 (2015).
- ³³²M. L. Torres-Mapa, M. Singh, O. Simon, J. L. Mapa, M. Machida, A. Günther, B. Roth, D. Heinemann, M. Terakawa, and A. Heisterkamp, “Fabrication of a Monolithic Lab-on-a-Chip Platform with Integrated Hydrogel Waveguides for Chemical Sensing”, *Sensors* **19**, 4333 (2019).
- ³³³V. Chan, P. Zorlutuna, J. H. Jeong, H. Kong, and R. Bashir, “Three-dimensional photopatterning of hydrogels using stereolithography for long-term cell encapsulation”, *Lab on a Chip* **10**, 2062–2070 (2010).
- ³³⁴B. Zheng, L. S. Roach, and R. F. Ismagilov, “Screening of protein crystallization conditions on a microfluidic chip using nanoliter-size droplets”, *Journal of the American Chemical Society* **125**, 11170–11171 (2003).
- ³³⁵Y. Ning, X. Cui, C. Yang, F. Jing, X. Bian, L. Yi, and G. Li, “A self-digitization chip integrated with hydration layer for low-cost and robust digital PCR”, *Analytica Chimica Acta* **1055**, 65–73 (2019).
- ³³⁶X. Zhou, G. C. Ravichandran, P. Zhang, Y. Yang, and Y. Zeng, “A microfluidic alternating-pull-push active digitization method for sample-loss-free digital PCR”, *Lab on a Chip* **19**, 4104–4116 (2019).
- ³³⁷A. Zambrano, A. S. Zadorin, Y. Rondelez, A. Estévez-Torres, and J. C. Galas, “Pursuit-and-Evasion Reaction-Diffusion Waves in Microreactors with Tailored Geometry”, *Journal of Physical Chemistry B* **119**, 5349–5355 (2015).
- ³³⁸T. W. Murphy, J. Sheng, L. B. Naler, X. Feng, and C. Lu, “On-chip manufacturing of synthetic proteins for point-of-care therapeutics”, *Microsystems and Nanoengineering* **5**, 1–12 (2019).
- ³³⁹C. B. Goy, R. E. Chaile, and R. E. Madrid, “Microfluidics and hydrogel: A powerful combination”, *Reactive and Functional Polymers* **145**, 104314 (2019).

- ³⁴⁰Y. Tabata and M. P. Lutolf, “Multiscale microenvironmental perturbation of pluripotent stem cell fate and self-organization”, *Scientific Reports* **7**, 1–11 (2017).
- ³⁴¹L. Grasemann, P. Thiel Pizarro, and S. J. Maerkl, “C2CAplus: A One-Pot Isothermal Circle-to-Circle DNA Amplification System”, *ACS Synthetic Biology* **12**, 3137–3142 (2023).
- ³⁴²M. G. Mohsen and E. T. Kool, “The Discovery of Rolling Circle Amplification and Rolling Circle Transcription”, *Accounts of Chemical Research* **49**, 2540–2550 (2016).
- ³⁴³L. Blanco, A. Bernad, J. M. Lazaro, G. Martin, C. Garmendia, and M. Salas, “Highly efficient DNA synthesis by the phage phi29 DNA polymerase. Symmetrical mode of DNA replication”, *Journal of Biological Chemistry* **264**, 8935–8940 (1989).
- ³⁴⁴X. Cao, C. Chen, and Q. Zhu, “Biosensors based on functional nucleic acids and isothermal amplification techniques”, *Talanta* **253**, 123977 (2023).
- ³⁴⁵P. Boonbanjong, K. Treeratrakoon, W. Waiwinya, P. Pitikultham, and D. Japrungr, “Isothermal Amplification Technology for Disease Diagnosis”, *Biosensors* **12** (2022).
- ³⁴⁶S. Yue, Y. Li, Z. Qiao, W. Song, and S. Bi, “Rolling Circle Replication for Biosensing, Bioimaging, and Biomedicine”, *Trends in Biotechnology* **39**, 1160–1172 (2021).
- ³⁴⁷H. Deng and Z. Gao, “Bioanalytical applications of isothermal nucleic acid amplification techniques”, *Analytica Chimica Acta* **853**, 30–45 (2015).
- ³⁴⁸F. Dahl, J. Banér, M. Gullberg, M. Mendel-Hartvig, U. Landegren, and M. Nilsson, “Circle-to-circle amplification for precise and sensitive DNA analysis”, *Proceedings of the National Academy of Sciences of the United States of America* **101**, 4548–4553 (2004).
- ³⁴⁹M. Nilsson, H. Malmgren, M. Samiotaki, M. Kwiatkowski, B. P. Chowdhary, and U. Landegren, “Padlock probes: Circularizing oligonucleotides for localized DNA detection”, *Science* **265**, 2085–2088 (1994).
- ³⁵⁰J. Banér, M. Nilsson, M. Mendel-Hartvig, and U. Landegren, “Signal amplification of padlock probes by rolling circle replication”, *Nucleic Acids Research* **26**, 5073–5078 (1998).
- ³⁵¹R. R. Soares, A. Pettke, A. Robles-Remacho, S. Zeebaree, S. Ciftci, M. Tampere, A. Russom, M. R. Puumalainen, M. Nilsson, and N. Madaboosi, “Circle-to-circle amplification coupled with microfluidic affinity chromatography enrichment for in vitro molecular diagnostics of Zika fever and analysis of anti-flaviviral drug efficacy”, *Sensors and Actuators, B: Chemical* **336**, 129723 (2021).
- ³⁵²D. Sánchez Martín, M. Wrande, L. Sandegren, and T. Zardán Gómez de la Torre, “Naked-eye detection of antibiotic resistance gene *sul1* based on aggregation of magnetic nanoparticles and DNA amplification products”, *Biosensors and Bioelectronics: X* **12**, 100277 (2022).
- ³⁵³F. Li, D. Lyu, S. Liu, and W. Guo, “DNA Hydrogels and Microgels for Biosensing and Biomedical Applications”, *Advanced Materials* **32**, 1806538 (2020).
- ³⁵⁴H. Song, Y. Zhang, P. Cheng, X. Chen, Y. Luo, and W. Xu, “A rapidly self-assembling soft-brush DNA hydrogel based on RCA products”, *Chemical Communications* **55**, 5375–5378 (2019).

- ³⁵⁵L. Cai, C. Hu, W. Wang, and W. Huang, "Characterization of Bacteriophage T3 DNA Ligase", *Journal of Biochemistry* **135**, 397–403 (2004).
- ³⁵⁶M. G. Casteleijn, A. Urtti, and S. Sarkhel, "Expression without boundaries: Cell-free protein synthesis in pharmaceutical research", *International Journal of Pharmaceutics* **440**, 39–47 (2013).
- ³⁵⁷A. Grishin, N. Dolgova, S. Landreth, O. F. .-. J. o. M. . . ., and U. 2022, "Disulfide bonds play a critical role in the structure and function of the receptor-binding domain of the SARS-CoV-2 spike antigen", *Journal of Molecular Biology* **434**, 167357 (2022).
- ³⁵⁸X. Zhou, H. Wu, M. Cui, S. Lai, B. Z. .-. C. Science, and U. 2018, "Long-lived protein expression in hydrogel particles: towards artificial cells", *Chemical Science* **9**, 4275–4279 (2018).
- ³⁵⁹X. Ouyang, X. Zhou, S. N. Lai, Q. Liu, and B. Zheng, "Immobilization of Proteins of Cell Extract to Hydrogel Networks Enhances the Longevity of Cell-Free Protein Synthesis and Supports Gene Networks", *ACS Synthetic Biology* **10**, 749–755 (2021).
- ³⁶⁰S.-y. Xu, A. Dore, A. Hume, J. Pelletier, 8. J Zhou - US Patent 6, 764, and U. 2004, *Method for cloning and expression of BsmBI restriction endonuclease and BsmBI methylase in E. coli and purification of BsmBI endonuclease*, 2004.
- ³⁶¹Z. Zhu, J. Samuelson, J. Zhou, A. Dore, S. X. .-. J. of molecular Biology, and U. 2004, "Engineering strand-specific DNA nicking enzymes from the type IIS restriction endonucleases BsaI, BsmBI, and BsmAI", *Journal of molecular biology* **337**, 573–583 (2004).
- ³⁶²X. Zhang, S. B. Lowe, and J. J. Gooding, "Brief review of monitoring methods for loop-mediated isothermal amplification (LAMP)", *Biosensors and Bioelectronics* **61**, 491–499 (2014).
- ³⁶³B. Özay and S. E. McCalla, "A review of reaction enhancement strategies for isothermal nucleic acid amplification reactions", *Sensors and Actuators Reports* **3**, 100033 (2021).
- ³⁶⁴M. Kühnemund, D. Witters, M. Nilsson, and J. Lammertyn, "Lab on a Chip Circle-to-circle amplification on a digital microfluidic chip for amplified single molecule detection", *Lab on a Chip* **14**, 2983 (2014).

Laura Grasmann

 Place de la Gare 8b, CH-1020 Renens
 laura.grasmann@freestyleteam.de
 +41 77 2682809

 30.04.1992, Heidelberg
 German (B-permit)
 laura-grasmann.de
 linkedin.com/laura-grasmann



PhD student in biotechnology and bioengineering working in the intersection between microfluidics, cell-free synthetic biology and life science engineering

EDUCATION

2019 - today
PhD in bioengineering and biotechnology
École Polytechnique Fédérale de Lausanne

2015 - 2018
M.Sc. Molecular Biotechnologies
Technical University of Munich

2011 - 2015
B.Sc. Molecular Biotechnologies
Technical University of Munich

COMPETITIVE SPORTS

2006 - 2020
Member of the German National Team Ski Freestyle Moguls (Freestyleteam Moguls Germany)

- 3rd World Cup Tazawako (JAP) 2018
- 5th World Ski Championships Park City (USA) 2019
- 10th Overall Worldcup 2018/2019
- 9th World Rank List 2017/2018
- 15 top-10 results in Worldcup or World Championships
- 14x German Champion
- Participant of the 2014 Sochi Olympic Winter Games

QUALIFICATION

Unit safety coordinator CoSEC (2021-today)

- communication with the safety and health department
- chemical storage and waste management
- safety introductions

PROFESSIONAL EXPERIENCE

DOCTORAL RESEARCHER

Laboratory of Biological Network Characterization EPFL

- Development of an assay to measure differences in binding affinities of Corona virus spike protein receptor binding domain variants using a high throughput microfluidics platform
 - Development of an isothermal DNA replication system for the use as a biosensor and in a synthetic cell
 - Collaboration to develop a microfluidic chemostat featuring semi-permeable hydrogel membranes to enable continuous exchange of low molecular weight molecules
- main methods: microfluidics, nano-immunoassays on chip, cell-free protein expression, DNA replication

MASTER'S THESIS

Max Planck Institute for Biochemistry, Department for Cellular and Molecular Biophysics

Characterization of self-organizing ParA-type ATPases

- Engineering of the ParA-type ATPase proteins MinD and PomZ for switched matrix affinity
 - investigate the influence of the matrix DNA vs membrane on self-organization properties
- main methods: protein purification, fluorescence microscopy

INTERNSHIP NEUROBIOLOGY

Chair for Neuronal Control of Metabolism, TU Munich

Analysis of serotonergic and serotonergic receptor neurons in the gut-brain-axis

- Behavioral analysis of neurons involved in taste aversion
- Histological analysis of said neurons

main methods: optogenetics, histology, fluorescence microscopy

INTERNSHIP CELL BIOLOGY

Cell biology and Biophysics Unit, EMBL, Heidelberg

Analysis of the subcellular localization of LMAN2L, TMEM130, and SLC30A under cholesterol depleted conditions

- Cholesterol depletion in HeLa cells
- Analysis of the translocation of the above mentioned proteins

main methods: cell culture, fluorescence microscopy

2019 - CURRENT

2018

2017

2016

SKILLS

LABORATORY

BIOCHEMICAL AND BIOLOGICAL METHODS

biochemical methods, protein purification (Äkta), cloning, cell and bacterial cultures, cell-free TX-TL, enzymatic assays

MICROFLUIDICS

Fabrication of single- and double-layer microfluidic devices, fluorescence microscopy, image analysis, assay development

COMMUNICATION AND PROJECT

MANAGEMENT SKILLS

- Keynote speaker: talks about resilience, overcoming challenges and navigating obstacles, high performance, interviews, moderations
- poster presentations for on-site and online conferences
- Athletes' representative Freestyleteam Moguls Germany (2016-2020): Internal coordination, representation of our team in front of stakeholders including the German Ski Federation, National Olympic Comitee, and governmental institutions
- Participation in the workshop: "Preventing and facing conflicts, a toolbox" (2021)
- Lead of the multinational "Team Covid RBD" consisting of one PostDoc, one Technician and one undergraduate student (2022)

TEACHING

- Supervision of three summer internship students
- Teaching of the "Lab on a Chip" experiment and project for the course "Advanced Bioengineering Methods Laboratory"
- set up and teaching of a laboratory course and a synthetic biology course
- supervision of the EPFL iGEM 2020 team (Award: Gold Medal)

LANGUAGES

German	<div style="width: 100%; height: 10px; background-color: black;"></div>
English	<div style="width: 95%; height: 10px; background-color: black;"></div>
French	<div style="width: 70%; height: 10px; background-color: black;"></div>
Spanish	<div style="width: 20%; height: 10px; background-color: black;"></div>

HONORS AND AWARDS

- Stipend of the Willy Robert Pitzer Stiftung (2017-2019)
- Deutsche Bank sport stipend (2012-2017)
- Finalist for the election as the student athlete of the year by Deutsche Bank and Deutsche Sporthilfe 2015 & 2017

PUBLICATIONS

- Grasemann, L. Thiel Pizarro, P. and Sebastian J. Maerkl. "C2CAplus: a one-pot isothermal circle-to-circle DNA amplification system." ACS Synthetic Biology (2023)
- Grasemann, L.*, Lavickova, B.*, Elizondo-Cantú, C. and Sebastian J. Maerkl. "OnePot PURE cell-free system." Jove (2021)
- Lavickova, B., Grasemann, L. and Sebastian J. Maerkl. "Improved cell-free transcription-translation reactions in microfluidic chemostats augmented with hydrogel membranes for continuous small molecule dialysis" ACS Synthetic Biology (2022)
- Laohakunakorn, N., Grasemann, L., et. al "Bottom-up construction of complex biomolecular systems with cell-free synthetic biology." Frontiers in bioengineering and biotechnology (2020)

COMMITMENT

Rider's Alliance member for Protect Our Winters (POW) Germany

- raise awareness for climate warming in the context of outdoor sports
- develop strategies how to be more sustainable in our local ski federation (SVS-Nord)

Member of "Landeslehrteam SVS-Nord"

- teach ski instructors how to approach and teach mogul skiing
- member of the sustainability working group and responsible for the collaboration with POW

Coach in tennis, athletics, trampoline, and skiing for different age groups ranging from kids to seniors

HOBBIES

